Mineral Resource Estimate Update for the Schaft Creek Property, British Columbia, Canada



PRESENTED TO
Copper Fox Metals Inc.

EFFECTIVE DATE: JANUARY 15, 2021
FILE: 219180-00-RPT-001

PREPARED BY:
HASSAN GHAFFARI, M.A.SC., P.ENG.
JIANHUI JOHN HUANG, PH.D., P.ENG.
MICHAEL F. O'BRIEN, P.GEO.

Tetra Tech Canada Inc.
Suite 1000 – 10th Floor, 885 Dunsmuir Street
Vancouver, BC V6C 1N5 CANADA
Tel 604.685.0275 Fax 604.684.6241

TABLE OF CONTENTS

LIST OF TABLES

LIST OF FIGURES

ACRONYMS & ABBREVIATIONS

Acronyms/Abbreviations	Definition
AA	Atomic Absorption
Acme Labs	Acme Analytical Laboratories Ltd.
ADIS	Automated Digital Imaging System
AN	Andesites
AP	Acid Generation Potential
ASARCO	American Smelting and Refining Company
BCEAA	British Columbia Environmental Assessment Act
BQL	Bob Quinn Lake
BV	Bureau Veritas
BWi	Ball Mill Work Index
CEAA	Canadian Environmental Assessment Act
CESL	Cominco Engineering Services Limited
COS	Change of Support
CRM	Certified Reference Material
CWi	Crushing Work Index
DCIP	Direct Current Induced Polarization
DEM	Digital Elevation Model
DTM	Digital Terrain Model
EA	Environmental Assessment
EGL	Effective Grinding Length
GPS	Global Positioning System
Hazen	Hazen Research Inc.
Hecla	Hecla Operating Company
HEL	HYYPPA Engineering, LLC
HPGR	High-pressure Grinding Rolls
ICP-ES	Inductively Coupled Plasma Emission Spectroscopy
ICP-MS	Inductively Coupled Plasma Mass Spectrometry

Acronyms/Abbreviations	Definition
IP	Induced Polarization
JV	Joint Venture
K	Potassium
Liard	Liard Copper Mines Ltd.
LiDAR	Light Detection and Ranging
LOI	Loss-on-Ignition
LRMP	Land and Resource Management Plan
McElhanney	McElhanney Associates
ML-ARD	Metal Leaching / Acid Rock Drainage
MT	Magneto-telluric
MYAB	Multi-year Area Based
N	Normal
NN	Nearest Neighbour
NP	Neutralization Potential
NPI	Net Proceeds Interest
NSR	Net Smelter Returns
NTL	Northwest Transmission Line
NTS	National Topographic System
P	Phosphate
Paramount	Paramount Mining Ltd
Pembrook	Pembrook Mining Corp.
PEX	Potassium Ethyl Xanthate
QA/QC	Quality Assurance and Quality Control
RMZ	Resource Management Zone
RQD	Rock Quality Designation
RWi	Rod Mill Work Index
S(-2)	Sulphide Sulphur
SABC	SAG Mill, Ball Mill, Cone Crushing
Salazar	Guillermo Salazar

Acronyms/Abbreviations	Definition
SAG	Semi-autogenous Grinding
SG	Specific Gravity
SI	International System of Units
Silver Standard	Silver Standard Mines Ltd
SMA	Standard Major Axis
SMC	SAG Mill Comminution
sPOR	Syn-mineral Porphyry Dikes
SRTM	Shuttle Radar Topography Mission
Teck	Teck Resources Limited
The Project	Schaft Creek Project
ZTEM	Z Axis Tipper Electromagnetic

UNITS OF MEASURE

annum (year)	a
billion	B
centimetre	cm
cubic centimetre	cm^3
Coefficients of Variation	CVs
day	d
degree	°
degrees Celsius	°C
dollar (American)	US$
dollar (Canadian)	Cdn$
foot	ft
gigajoule	GJ
gram	g
grams per tonne	g/t
greater than	>
hectare (10,000 m^2)	ha
hour	h
inch	"
kilogram	kg
kilometre	km
kilowatt hour	kWh
kilowatt hours per tonne (metric ton)	kWh/t
less than	<
litre	L
metre	m
metres above sea level	m.a.s.l.
metric ton (tonne)	t
millilitre	mL
millimetre	mm
million tonnes	Mt
minute (plane angle)	'
Neutron	N
ounce	oz
parts per million	ppm
parts per billion	ppb
percent	%
pound(s)	lb
second (plane angle)	"
specific gravity	SG
square kilometre	km^2
square metre	m^2
Three Dimensional	3D
tonnes per day	t/d

GLOSSARY

Throughout the code, certain words are used in a general sense when a more specific meaning may be attached to them by particular commodity groups within the industry. In order to avoid unnecessary duplication, a non-exclusive list of generic terms is tabulated below, together with other terms that may be regarded as synonymous for the purposes of this technical report.

Generic Term	Synonyms and Similar Terms	Intended Generalized Meaning
Tonnage	Quantity, Volume	An expression of the amount of material of interest irrespective of the units of measurement (which should be stated when figures are reported).
Grade	Quality, Assay, Analysis (Value)	Any physical or chemical measurement of the characteristics of the material of interest in samples or product. Note that the term quality has special meaning for diamonds and other gemstones. The units of measurement should be stated when figures are reported.
Metallurgy	Processing, Beneficiation, Preparation, Concentration	Physical and/or chemical separation of constituents of interest from a larger mass of material. Methods employed to prepare a final marketable product from material as mined. Examples include screening, flotation, magnetic separation, leaching, washing, roasting, etc.
Recovery	Yield	The percentage of material of initial interest that is extracted during mining and/or processing. A measure of mining or processing efficiency.
Mineralization	Type of Deposit, Orebody, Style of Mineralization	Any single mineral or combination of minerals occurring in a mass or deposit, of economic interest. The term is intended to cover all forms in which mineralization may occur, whether by class of deposit, mode of occurrence, genesis, or composition.
Mineral Resources	Resources	“Resources” is preferred under the JORC Code but “Mineral Resources” is the recommended term under CIM guidelines and NI43-101 rules.
Cut-off Grade	Product Specifications	The lowest grade or quality of mineralized material that qualifies as economically mineable and available in a given deposit. May be defined on the basis of economic evaluation, or on physical or chemical attributes that define an acceptable product specification.

1.0 SUMMARY

A summary of the consultants responsible for each section of this Mineral Resource Estimate Update Report is detailed in Table 2-1.

1.1 Project Description

The Schaft Creek Project is managed through the Schaft Creek Joint Venture (JV) formed in 2013 between Teck Resources Limited (“Teck”) (75%) and Copper Fox Metals Inc. (“Copper Fox”) (25%) with Teck being the operator.

Schaft Creek is a large copper-molybdenum-gold-silver porphyry deposit located in Tahltan territory in northwestern British Columbia, approximately 60 km south of Telegraph Creek and 37 km northeast of the Galore Creek property. The Schaft Creek Project (the Project) is situated within the traditional territory of the Tahltan Nation, and the nearest villages are Telegraph Creek, Dease Lake, and Iskut. Dease Lake is the centre of government for the Tahltan Nation and is a local supply point for basic goods and medical services. Tahltan Nation Development Corporation (TNDC), along with numerous Tahltan-owned or partnered businesses, can provide a wide range of services in support of the evaluation and potential development of the Project. There is a permanent exploration camp for the Project in the Schaft Creek valley that can accommodate approximately 70 people. There is no power currently available to site. The completion of the Northwest Transmission Line (NTL) from Skeena to Bob Quinn in 2014 brought reliable and sufficient power to within 90 km of the Project. Potable water is currently sourced from wells within the Project site. Process water for any future process plant could be supplied by a combination of pit dewatering wells and reclaim water from the proposed tailings storage facility.

1.2 Mineral Tenure, Surface Rights, Water Rights, Royalties and Agreements

The Project is a 75/25 joint venture (Schaft Creek JV) between Teck and Copper Fox, with Teck holding a 75% interest and acting as the operator. As illustrated in Figure 1-1, the Project is located approximately 60 km south of the village of Telegraph Creek, 120 km southwest of Dease Lake, 45 km due west of Highway 37, 70 km west northwest of Bob Quinn Lake (BQL), and approximately 375 km northwest of Smithers. The Project mineral tenure comprises approximately 56,124 ha encompassing portions of the Schaft Creek and Mess Creek Valleys, and Mount LaCasse situated in the Cassiar/Liard Mining Division of northwestern BC, Canada. Access to the Project is via helicopter and fixed wing aircraft from Dease Lake, BQL, or Smithers.

Figure 1-1: Location Map of the Schaft Creek Project

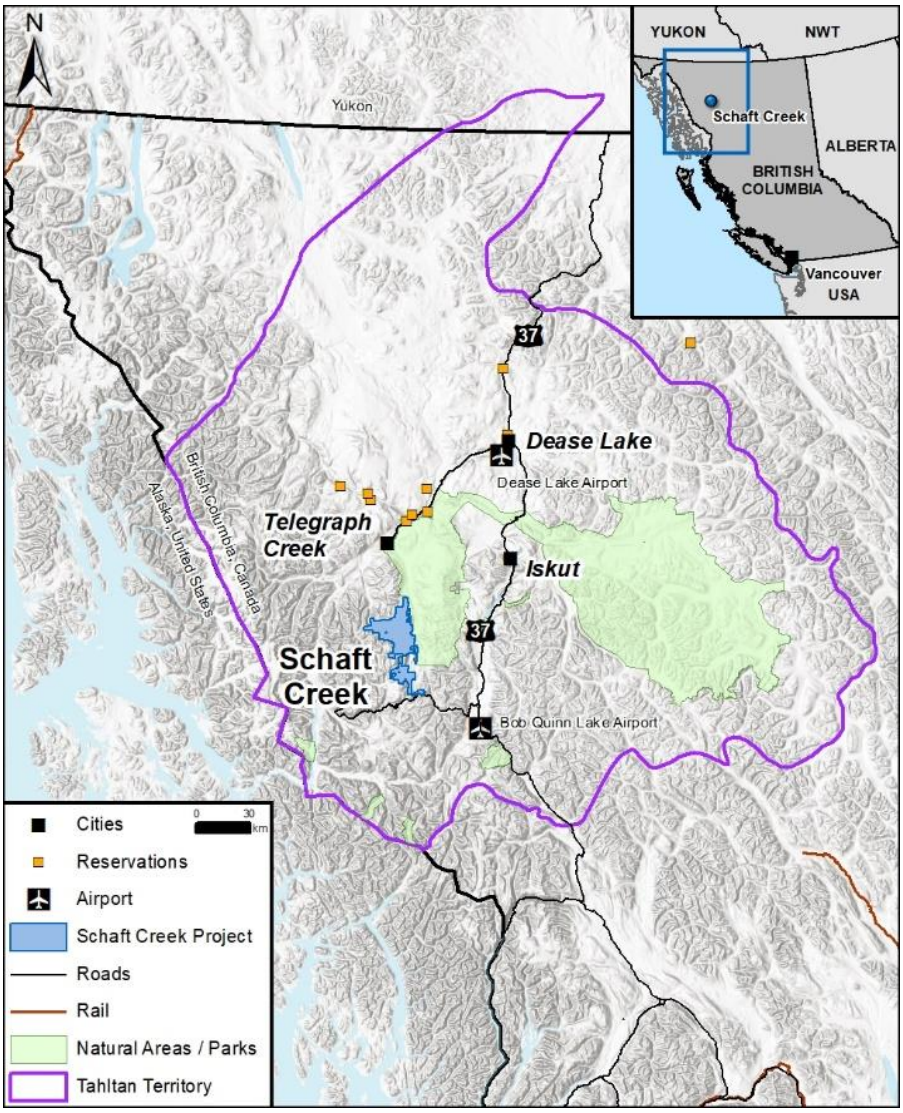

Source: the Schaft Creek JV (2019)

1.3 Geology, Mineralization, Status of Exploration and Mineral Resource Estimate

The Schaft Creek deposit is located within a geological and metallogenic domain called the Stikine Arch. The Stikine Arch is located on the north to northwest margin of the Bowser Basin. Within this region, the Stikine Terrane is intruded by numerous Late Triassic to Jurassic plutons, which comprise several major magmatic suites. Several of these magmatic suites are associated with Cu-Au ± Mo ± Ag porphyry- and epithermal-style mineralization, and these styles of mineralization are widespread throughout the Stikine Arch.

The Project has a long history of exploration. Copper Fox optioned the project from Teck in 2002 and completed extensive exploration resulting in the preparation of a feasibility study in 2013. In 2013, Teck exercised its “back-in” option and the Schaft Creek JV was formed. The Schaft Creek JV has completed drilling and geophysical surveys, extensive re-logging of historical core, additional metallurgical and geotechnical work, and numerous optimization studies on the Schaft Creek deposit. Between 2016 and 2018, the Schaft Creek JV completed an updated geological and resource model for the Schaft Creek deposit based on the 3,453 m of drilling completed in 2013, 42,888 m of core re-logging, as well as detailed Anaconda-style geological mapping over the deposit between 2013 and 2015. Additional activities included a life of project quality assurance and quality control (QA/QC) review, environmental baseline monitoring, consultation with the Tahltan Nation and optimization studies to right size the project to improve project value. In 2021, an independent Mineral Resource estimate was completed in accordance with National Instrument 43-101 guidelines on behalf of Copper Fox, which is the subject of this Report.

An independent Mineral Resource estimate has been completed by Michael F O’Brien, P.Geo., on behalf of Copper Fox and is the subject of this Report.

The Schaft Creek Project is also subject to various royalty agreements, which are more specifically described in Section 4.0 of this report.

1.3.1 Geology

The Schaft Creek Project is located in the northwestern portion of Stikine Terrane, within the Canadian Cordillera. The Stikine Terrane is comprised of three major lithostratigraphic units: the Paleozoic Stikine Assemblage, the Late Triassic Stuhini Group, and the Early Jurassic Hazelton Group (Logan et al., 2000). These rocks are overlain by younger clastic sediments of the Middle Jurassic to Early Tertiary Bowser Lake and Sustut Groups, and Eocene to Recent volcanic rocks of the Edziza and Spectrum Ranges (Logan et al., 2000).

The rocks of the Stikine Terrane record evidence of several major deformational events ranging in age from Paleozoic to Cenozoic. Evidence for these deformational events is preserved in foliations, folds, faults, and brittle fractures. Several of these deformational events are linked to large-scale tectonic changes and are associated with episodes of orogeny development, exhumation, and erosion that result in stratigraphic unconformities.

The Schaft Creek Project area is predominantly underlain by rocks representing two major lithological domains: the Hickman Batholith and the Stuhini Group volcanic rocks.

1.3.2 Mineralization

The Schaft Creek deposit consists of three mineralized zones that exhibit a variety of mineral assemblages. These mineral assemblages are interpreted to be coprecipitated and to be representative of specific factors including pressure, temperature, pH, fluid composition, and in some instances, wall rock composition. A description of each zone follows:

The **Liard Zone** comprises narrow, porphyritic quartz monzonite to quartz monzodiorite dikes intruding andesitic volcanic and volcaniclastic host rocks of the Stuhini Group. A single, thicker “Central Porphyry” dike occurs within the central portion of the Liard Zone. The porphyritic dikes are spatially

associated with potassic alteration, increased density of quartz-sulphide veins and vein stockworks and a zone of elevated Cu-Au grades. The most intense alteration and highest copper grades commonly occur in the host rock immediately adjacent to the porphyry dikes. Chalcopyrite, bornite, and pyrite also occurs as disseminations in the host rocks and the porphyry dikes. Three styles of vein-hosted mineralization (Cu-Au-Mo) with no preferred trend, occur in the Liard Zone and have associated K-feldspar and epidote alteration assemblages. The boundaries of the Liard Zone are defined by faults in most directions.

The **Paramount Zone** comprises an elongate, multi-phase igneous-hydrothermal, north-northwest trending breccia body emplaced into quartz monzonite and andesitic volcanic host rocks. High-grade mineralization occurs within the breccia body and extends up to 200 m into the quartz monzonite hanging wall and, to a lesser extent, into the footwall andesitic volcanic rocks. Mineralization in the Paramount Zone consists of quartz-sulphide stockwork, outside of the breccia body and three styles of mineralization within the breccia body. Potassic alteration intensity, vein density, and vein thickness all increase towards the breccia zone. A sulphide zonation (from chalcopyrite > pyrite, to chalcopyrite > bornite, to bornite > chalcopyrite) is apparent outside of the breccia body and extends inwards. Molybdenite occurs throughout the Paramount Zone. The mineralization in the Paramount Zone is open at depth and to the south, towards the West Breccia Zone.

The **West Breccia Zone** comprises an elongated, north-northwest trending hydrothermal breccia body that has been emplaced into andesitic volcanic and volcaniclastic rocks. The breccia has a strike length of approximately 500 m and extends at least 200 m below surface. The West Breccia Zone is like the Paramount Zone breccia and comprises different styles of mineralization dominated by low- to medium-temperature breccia mineralogy. The mineralization assemblages in the West Breccia Zone include (1) Cu-Mo-Au, (2) Cu-Mo, and (3) high-grade Cu-Mo-Au. The boundaries of the West Breccia Zone are poorly constrained, and the breccia remains open to the north and south.

1.3.3 Analytical Methods

Since 2013, the following analytical methods have been employed to determine metal and element concentration on samples from the Schaft Creek Project:

1. Ore-grade assays for copper, molybdenum, and silver were determined by 4-acid digest with inductively coupled plasma emission spectrometry (ICP-ES) finish (Acme Group 7TD) including results for major elements (e.g., Fe, K, Al), other commodity elements (e.g., Zn, Pb), and trace elements (e.g., Ni, Bi).

2. Ore grade assays for gold were determined by fire assay with atomic absorption (AA) finish (Acme Code G601).

3. Concentrations of trace elements were determined by aqua regia digest with inductively coupled plasma mass spectrometry (ICP-MS) finish (Acme Group 1DX).

4. Concentrations of carbon and sulphur were determined by LECO analysis (Acme Group 2A12).

5. Whole-rock lithogeochemistry was determined using a multi-part analytical package (Acme Code 4AB1).

The Qualified Person (QP) is satisfied that sample preparation and analysis are appropriate to provide suitable analyses and to maintain data integrity.

1.3.4 Data Verification

The QP compared subsets of drill sampling from historic (pre-2000) and current (since 2000) campaigns to assess the risk of bias. The QP is satisfied that there is no significant bias between the comparable historic and current sampling and assay data within the grade range of practical resource estimation.

The QP compared the high definition topographic surface mesh (Dem_SCK) that was used for geological modelling with public domain data from NASA's Shuttle Radar Topography Mission (SRTM). The two surfaces are in close agreement (average difference 0.038 m) and the QP believes that the uncertainty in topography data does not present a material risk to the Project.

During a site visit on October 30, 2020, the QP reviewed cores and verified the collar of a drill hole.

The QP is satisfied that the sampling and assay data, topographic information, and drill core management for this Project have been comprehensively verified and are suitable to be used for Mineral Resource estimation.

1.3.5 Status of Exploration

The Schaft Creek Project is an advanced exploration project. Formally recorded geological mapping dates from the 1950s by the Government of Canada, predating the discovery of mineralization on the property in 1957. Increasingly more detailed collection of data and geological interpretation was carried out by BIK / Silver Standard / Asarco (1957–1967), Hecla / Paramount (1968–1977), Copper Fox (2007), and the Schaft Creek JV (2014–2018).

The exploration programs conducted on the deposit resulted in completion of several historical resource estimation and feasibility studies. A total of 449 drill holes (about 108,041 m) have been completed in the Project area between the late 1950s up to 2015. No drilling has been completed since 2015. A total of 21 drill holes have no assays, and 40 drill holes within the Project lie outside the resource area.

The Schaft Creek deposit is the largest zone of mineralization currently identified within the Schaft Creek Project. Exploration consisting of ground and airborne geophysical surveys, mapping, and prospecting has identified a 12 km long trend of mineralization along the Hickman/Stuhini contact. Drilling at the Discovery Zone in 2012 and the LaCasse Zone in 2015 to the north of the Schaft Creek deposit intersected significant concentrations of copper-gold-molybdenum-silver over broad intervals. A number of other early stage copper exploration targets have also been identified along the 12 km long mineralized trend.

1.4 Metallurgy

The Schaft Creek deposit is a calc-alkalic polymetallic (copper-molybdenum-gold-silver) porphyry deposit, with a low-sulphidation state, and overlapping mineralized zones.

Between 2004 and 2015, extensive metallurgical test work was completed on samples from the various geometallurgical units and mineralization zones of the Schaft Creek deposit to support several studies. Laboratories that undertook the major test programs include G&T/ALS, PRA (Inspectorate), Hazen Research Inc. (Hazen), Polysius, and Cominco Engineering Services Limited (CESL).

Metallurgical test programs conducted included mineralogy, grindability, flotation, and dewatering tests.

The mineralogical studies showed:

- Chalcopyrite was the dominant copper sulphide mineral together with ancillary bornite and chalcocite.
- The other main sulphide mineral in the mineralization was pyrite. The pyrite contents in the samples used in the test work ranged from 0.04% to 0.15% in the 2010 program to 0.1% to 0.8% pyrite content in the 2012 program. The average pyrite content of the 2012 program was 0.3%.

The test work programs included grindability tests that showed the Ball mill work index (BWi), and Rod mill work index (RWi) to indicate that the mineral samples are high in grinding resistance to ball mill and rod mill grinding. The BWi ranges from 13.7 kWh/t to 25.4 kWh/t, averaging 21.3 kWh/t. The RWi is slightly lower than the BWi, averaging 20.8 kWh/t. The average Bond Abrasion Index (Ai) is 0.25 g, fluctuating from 0.17 g to 0.57 g. The low energy impact work indices (Crushing work index [CWi]) are relatively low, ranging from 6.3 kWh/t to 11.9 kWh/t.

The drop weight and semi-autogenous grinding (SAG) mill comminution (SMC) test results indicate that the mineral samples are moderately hard to very hard for SAG mill milling. The key parameter (A x b) ranges from 27.4 to 44.7.

Studies related to process conditions, included primary grind size, regrinding size of rougher flotation concentrates, reagents regime, and bulk flotation pH, have been developed since the 2004 flotation test work, and locked cycle tests and pilot plant test work have also been completed. The bulk copper-molybdenum flotation locked cycle tests showed that the tested samples responded well to a conventional process, consisting of bulk sulphide flotation followed by regrinding on the bulk concentrate and three stages of cleaner flotation.

The metallurgical performance of the samples used in the 2004 to 2012 test work exhibited a wide range of metal recoveries at various head grades, grind sizes, and reagent regimes. The test results indicate that metal recoveries are related to both sample head grade and mineralogy.

Copper and molybdenum separation tests on bulk concentrates generated from the pilot plant tests, demonstrated that a copper concentrate with significant gold and silver credits and a separate molybdenite concentrate can be produced.

Multi-element assays on the bulk concentrates generated from the locked cycle tests showed that on average the impurities in the concentrates should be below smelting penalty thresholds set forth by

most smelters. According to the metallurgical performance projections conducted in the 2013 study, the metal recoveries for the Schaft Creek deposit are projected to average 86.6% for copper, 73.0% for gold, 58.8% for molybdenum, and 48.3% for silver.

1.5 Mineral Resource Estimate

The Mineral Resource was estimated in January 2021 and constrained within an optimized ultimate pit shell. The estimated Mineral Resources are summarized in Table 1-1.

Table 1-1: 2021 Mineral Resource Statement

		Average Value				Material Content			
	Mass	Cu	Au	Mo	Ag	Cu	Au	Mo	Ag
Category	Mt	%	g/t	%	g/t	million lb	million t. oz	million lb	million t. oz
Measured	176	0.32	0.22	0.018	1.46	1,262	1.28	71	8.26
Indicated	1,169	0.25	0.15	0.017	1.22	6,505	5.69	440	45.99
Total M&I	**1,346**	**0.26**	**0.16**	**0.017**	**1.25**	**7,767**	**6.97**	**511**	**54.25**
Inferred	344	0.17	0.11	0.013	0.84	1,303	1.18	96	9.28

Note: Mineral Resources are reported using the 2014 CIM Definition Standards.
The Qualified Person for the estimate is Mr. Michael F O'Brien, P.Geo., Red Pennant Geoscience. Mineral Resources are tabulated in Table 14-11 and have an effective date of 15 January, 2021.
Mineral Resources are reported within a conceptual constraining pit shell that includes the following input parameters: US$3/lb Cu, US$10/lb Mo, US$1,200/oz Au, US$20/oz Ag, mining cost of CA$1.95/t mined, processing cost of CA$4.94/t processed, and pit slope angles that vary from 40–44º. Metal recoveries; Cu 86.6%, Au 73%, Mo 58.8%, Ag 48.3%. Mineral Resources are reported using a net smelter return cutoff of US$4.31/t, and a Cdn$ to US$ exchange rate of 1.20.
Tonnes are metric tonnes, with copper and molybdenum grades as percentages, and gold and silver grades as gram per tonne units. Copper and molybdenum metal content is reported in pounds and gold and silver content is reported in troy ounces.

1.6 Recommendations

The recommended geotechnical and metallurgical program is set out below and more specifically detailed in Section 26.0 of this report. The program recommends that 7,300 m of drilling ($4.5 million) be completed to collect additional geological and geotechnical data from within the resource area. A metallurgical test work program estimated to cost $460,000 is also proposed to further investigate metallurgical performance and comminution characteristics of the mineralization.

2.0 INTRODUCTION

In 2020, Copper Fox commissioned a team of consultants to complete this Mineral Resource Estimate Report, in accordance with NI 43-101 Standards of Disclosure for Mineral Projects. The project team included:

- Tetra Tech Canada Inc.: overall project management and metallurgical testing
- Red Pennant Geoscience: project description and location, accessibility, history, geological setting, deposit types, exploration, drilling, adjacent properties, and Mineral Resource estimate.

2.1 Terms of Reference

The Resource Estimate was prepared by Tetra Tech Canada Inc. ("Tetra Tech") and Red Pennant Geoscience ("Red Pennant") in accordance with NI 43-101 standards (May 9, 2016), CIM Definition Standards (May 19, 2014) with guidance from CIM Best Practice Guidelines (November 29, 2019). Mineral Resources are presented on a 100% basis. As of January 15, 2021, the effective date for the Mineral Resources, Teck had a 75% interest, with Copper Fox holding a 25% interest.

Mineral Resources can be considered as forward-looking information and actual results may vary. The assumptions used in the Mineral Resource estimate are summarized in the footnotes of the Mineral Resource table, and outlined in Section 14.0 of the Report.

Currency is expressed in Canadian dollars (C$) unless stated otherwise. Units presented are typically metric units, such as metric tonnes, unless otherwise noted. The Report uses Canadian English.

2.2 Site Visit

The following QPs conducted site visits of the Property:

- Mr. Michael F. O'Brien, P.Geo., Red Pennant, visited the property on October 30, 2020 and reviewed drill cores and the general layout of the camp and topography.
- Mr. Hassan Ghaffari, M.A.Sc., P.Eng., Tetra Tech, visited the site on September 22, 2010 and inspected the overall project site, including site access roads.
- Mr. John Huang, Ph.D., P.Eng., Tetra Tech, visited the site on August 9, 2010 and reviewed drill cores and the overall project site, including the potential processing plant site.

A summary of the Qualified Persons (QPs) responsible for this Report is detailed in Table 2-1.

Table 2-1: Summary of Report Sections and Consultants

Report Section		Company	QP
1.0	Summary	All	Sign-off by Section
2.0	Introduction	Tetra Tech	Hassan Ghaffari, M.A.Sc., P.Eng.
3.0	Reliance on Other Experts	Red Pennant	Michael F. O'Brien, P.Geo.
4.0	Property Description and Location	Red Pennant	Michael F. O'Brien, P.Geo.
5.0	Accessibility, Climate, Local Resources, Infrastructure, and Physiography	Red Pennant	Michael F. O'Brien, P.Geo.
6.0	History	Red Pennant	Michael F. O'Brien, P.Geo.
7.0	Geological Setting and Mineralization	Red Pennant	Michael F. O'Brien, P.Geo.
8.0	Deposit Types	Red Pennant	Michael F. O'Brien, P.Geo.
9.0	Exploration	Red Pennant	Michael F. O'Brien, P.Geo.
10.0	Drilling	Red Pennant	Michael F. O'Brien, P.Geo.
11.0	Sample Preparation, Analyses, and Security	Red Pennant	Michael F. O'Brien, P.Geo.
12.0	Data Verification	Red Pennant	Michael F. O'Brien, P.Geo.
13.0	Mineral Processing and Metallurgical Testing	Tetra Tech	John Huang, Ph.D., P.Eng.
14.0	Mineral Resource Estimates	Red Pennant	Michael F. O'Brien, P.Geo.
15.0	Mineral Reserve Estimates	Tetra Tech	Hassan Ghaffari, M.A.Sc., P.Eng.
16.0	Mining Methods	Tetra Tech	Hassan Ghaffari, M.A.Sc., P.Eng.
17.0	Recovery Methods	Tetra Tech	Hassan Ghaffari, M.A.Sc., P.Eng.
18.0	Project Infrastructure	Tetra Tech	Hassan Ghaffari, M.A.Sc., P.Eng.
19.0	Market Studies and Contracts	Tetra Tech	Hassan Ghaffari, M.A.Sc., P.Eng.
20.0	Environmental Studies, Permitting and Social or Community Impact	Tetra Tech	Hassan Ghaffari, M.A.Sc., P.Eng.
21.0	Capital and Operating Costs	Tetra Tech	Hassan Ghaffari, M.A.Sc., P.Eng.
22.0	Economic Analysis	Tetra Tech	Hassan Ghaffari, M.A.Sc, P.Eng.
23.0	Adjacent Properties	Red Pennant	Michael F. O'Brien, P.Geo.
24.0	Other Relevant Data and Information	Tetra Tech	Hassan Ghaffari, M.A.Sc, P.Eng.
25.0	Interpretation and Conclusions	All	Sign-off by Section
26.0	Recommendations	All	Sign-off by Section
27.0	References	All	Sign-off by Section

2.3 Effective Date

The overall effective date of the Report is taken to be the date of the Mineral Resource estimate, which is January 15, 2021.

2.4 Information Sources and References

The reports and documents listed in Sections 2.5 and 27.0 of this Report were also used to support the preparation of the Report. Additional information was obtained from the Schaft Creek JV where required.

2.5 Previous Technical Reports

Copper Fox has filed the following technical reports related to the Schaft Creek Project. The information conferred in these reports are incorporated by reference.

- Ewanchuk, S., Finch, P., and Hanych, W., 2007: 2006 Diamond Drill Report, Schaft Creek Property, Northwestern British Columbia: report prepared for Copper Fox, effective date 19 March, 2007.
- McCandlish, K., 2007: Updated Resource Estimate for the Schaft Creek Deposit, Northwest British Columbia, Canada: report prepared by Associated Geosciences Ltd. for Copper Fox, effective date 22 June, 2007.
- Bender, M.R., McCandlish, K., Gray, J., and Hyyppa, R., 2007: Preliminary Economic Assessment on the Development of the Schaft Creek Project Located in Northwest British Columbia, Canada: report prepared by Samuel Engineering, Inc. for Copper Fox, effective date 7 December, 2007.
- Bender, M., McCandlish, K., Gray, J., Brouwer, K., Holm, K., Uren, S., Hanych, W., Beauchamp, D., Suhbatar, V., Pow, D., and Hyyppa, R., 2008: Preliminary Feasibility Study on the Development of the Schaft Creek Project Located in Northwest British Columbia, Canada: report prepared by Samuel Engineering, Inc. for Copper Fox, effective date 15 September, 2008.
- Bender, M., McCandlish, K., Gray, J., Brouwer, K., Holm, K., Uren, S., Hanych, W., Beauchamp, D., and Hyyppa, R., 2008: Preliminary Feasibility Study on the Development of the Schaft Creek Project Located in Northwest British Columbia, Canada: amended and restated report prepared by Samuel Engineering, Inc. for Copper Fox, effective date 15 September, 2008.
- Kulla, G., Thomas, D., Lipiec, T., 2011. Copper Fox Metals Inc., Schaft Creek Polymetallic Project, British Columbia, Canada, NI 34-101 Technical Report on Updated Mineral Resource Estimate; report prepared by AMEC Americas Limited for Copper Fox, effective date 26 July, 2011.
- Morrison, R., and Karrei, L., 2012: Technical Report and Resource Estimate on the Schaft Creek Cu-Au-Mo-Ag Project, BC, Canada; report prepared by Tetra Tech Wardrop report for Copper Fox, effective date 23 May, 2012.
- Farah, A., Friedman, D., Yang, D.Y., Pow, D.J., Trout, G., Ghaffari, H., Stoyko, H.W., Huang, J., Karrei, L.I., Danon-Schaffer, M., Morrison, R.S., da Palma Adanjo, R., and Hafez, S.A., 2013: Feasibility Study on the Schaft Creek Project, BC, Canada: report prepared by Tetra Tech report for Copper Fox, effective date 23 January, 2013.

3.0 RELIANCE ON OTHER EXPERTS

Michael F. O'Brien relied on the Schaft Creek JV for matters relating to mineral tenure and mining rights permits, surface rights, royalties, agreements, and encumbrances relevant to this Report.

4.0 PROPERTY DESCRIPTION AND LOCATION

The Schaft Creek Project is located on the eastern side of the Coast Mountains in northwestern British Columbia, within the Cassiar/Liard Mining Division. The Property is approximately 120 km southwest of Dease Lake, and 375 km northwest of Smithers (Figure 4-1). The closest population center is Telegraph Creek, located approximately 61 km to the north. Highway 37 is 45 km east of the Property. The deposit is centred at approximately 379850mE, 6360080mN (UTM NAD83, zone 9). An exploration camp is located 1 km to the southwest of the deposit, at 378715mE, 6358605mN. Drill core is stored on site at the core logging facility next to the camp.

The Schaft Creek tenure consists of 182 mineral claims. The tenure is comprised of a north block and a south block, with three isolated claims to the northeast; in total, the Property encompasses 56,124.73 ha (Figure 4-2). The Schaft Creek tenements are presented in Table 4-1.

Figure 4-1: Location of the Schaft Creek Project

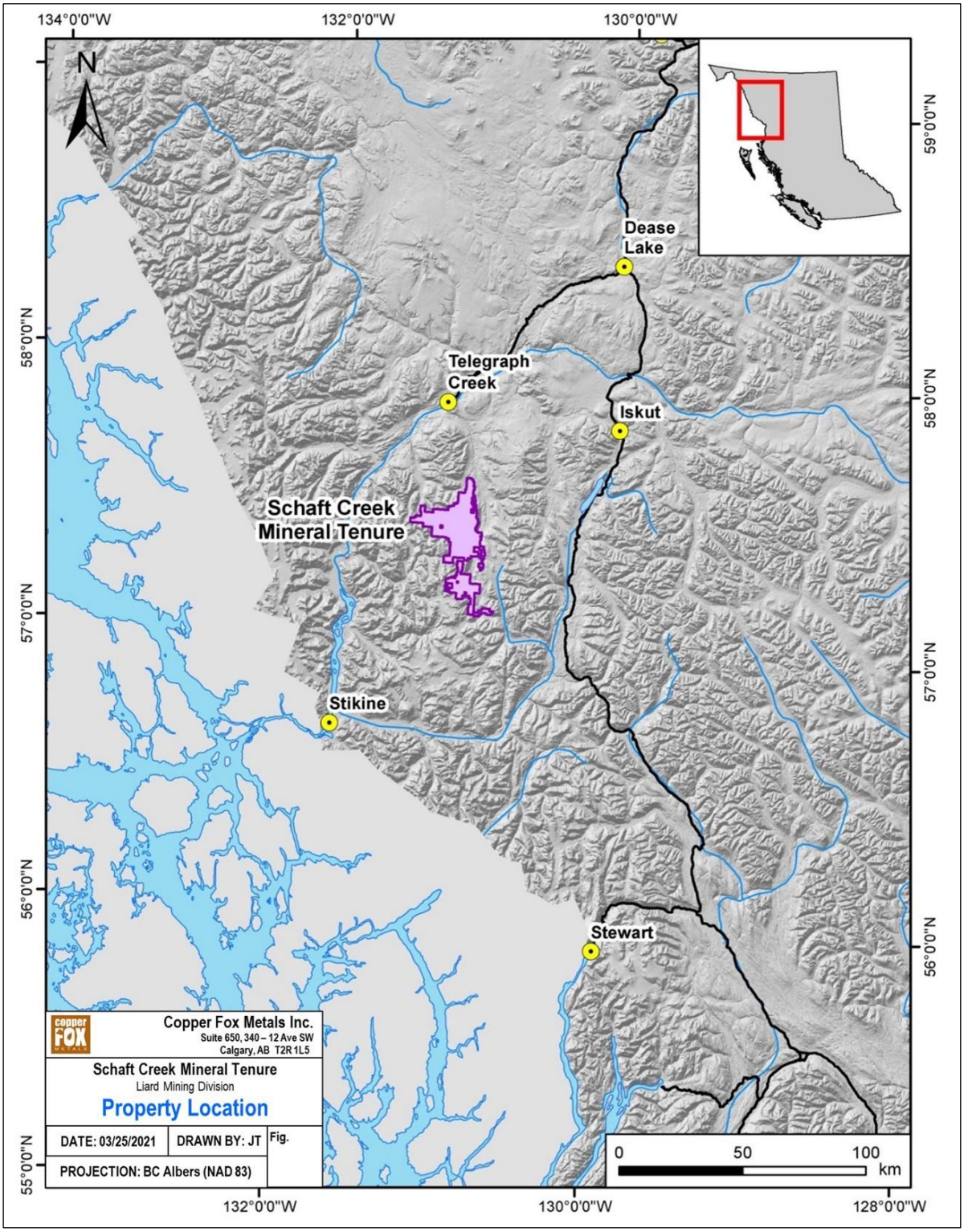

Figure 4-2: Schaft Creek Property Mineral Tenure

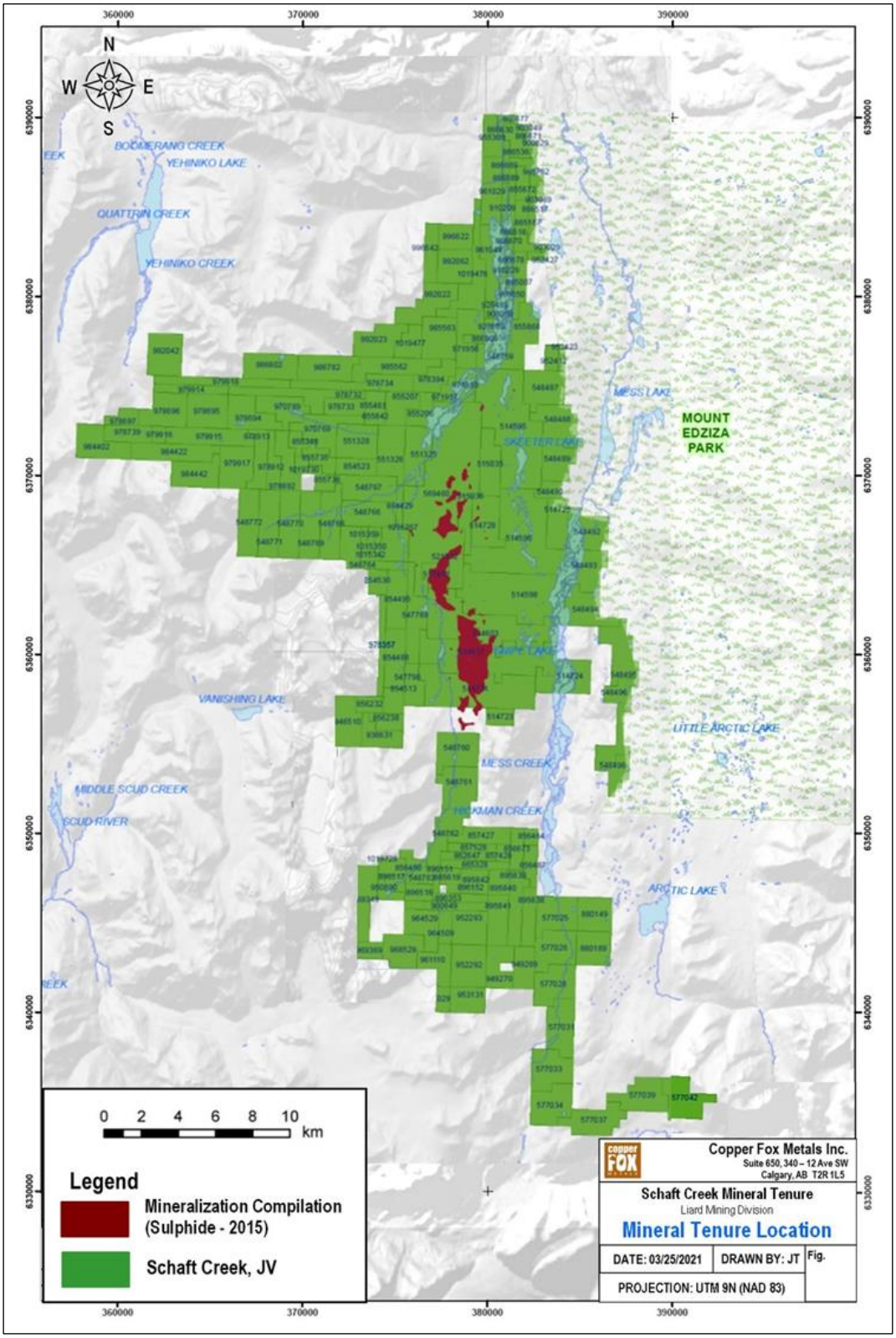

4.1 Project Ownership

4.1.1 Ownership History

The initial claims were staked in 1957 by the BIK Syndicate, a consortium of companies that incorporated as Liard Copper Mines Ltd (Liard) in 1966. These initial claims, and subsequent additions, were staked over the Liard Zone (the Liard Property). In 1968, Liard Copper entered into an option agreement with Hecla Operating Company (Hecla), under which Hecla earned a 70% interest in the Liard Property. Liard Copper retained a 30% carried net proceeds interest (NPI) in the Liard Property. Subsequently, Teck acquired a 78% interest in Liard Copper, which represented a 23.4% interest in the Liard Property.

Paramount Mining Ltd (Paramount) staked claims north of the Liard Property (the Paramount Claims). In 1969, Paramount entered into an option agreement with Hecla for the Paramount Claims. Hecla later terminated their option on the Paramount Claims, and these claims were allowed to lapse. Subsequently, Teck acquired tenure over the area that comprised the Paramount Claims.

In 1978, Hecla assigned its 70% ownership in the Liard Property to Teck, reserving a 5% NPI from this 70% ownership. This yielded for Hecla an effective 3.5% NPI on the property, payable only after Teck has recovered certain expenditures. In February 2005, Hecla assigned this 3.5% NPI to International Royalty Corporation. In 2010, International Royalty Corporation was acquired by Royal Gold Inc, at which time the 3.5% NPI was transferred to Royal Gold Inc.

In January 2002, Teck signed an option agreement with Guillermo Salazar (Salazar). The agreement allowed Salazar to earn Teck's 70% direct participating interest in the Liard Property by incurring certain exploration expenditures, as well as Teck's 23.4% indirect carried interest in the Liard Property (through its 78% shareholding of Liard) by completing a positive bankable feasibility study. In addition to the Liard Property, the option agreement also included the Paramount Claims. Teck retained a back-in right, whereby it could acquire an interest of up to 75%.

In February 2003, Salazar assigned the option agreement to 955528 Alberta Ltd, which amalgamated with Copper Fox in 2004. From 2005 to 2012 Copper Fox conducted work on the Project, filing a feasibility study in 2013.

In July 2013, Teck and Copper Fox entered into an agreement for the formation of the Schaft Creek JV whereby Teck holds a 75% interest and Copper Fox holds a 25% interest in the Schaft Creek property. Teck's 78% interest in Liard was included in the formation of the Schaft Creek JV (see Section 4.5).

In December 2015, the Schaft Creek JV entered into an agreement to acquire an additional 7.4% of the issued and outstanding shares of Liard Copper. As a result, the Schaft Creek JV has a total ownership of approximately 85.5% of the issued and outstanding shares of Liard.

4.1.2 Current Ownership

The Schaft Creek Project is managed through the Schaft Creek JV. Teck is the operator and holds a 75% interest. Copper Fox holds the remaining 25% interest. The mineral claims listed in Table 4-1 are held by Teck on behalf of the Schaft Creek JV.

4.1.3 Mineral Tenure

The Schaft Creek JV consists of 182 mineral claims (56,124.73 ha). The tenure consists of a north block and a south block, with three isolated claims to the northeast (Figure 4-3). A listing of the mineral claims and royalty agreement applicable to the claims is provided in Table 4-1.

Figure 4-3: Mineral Tenure Summary Plan

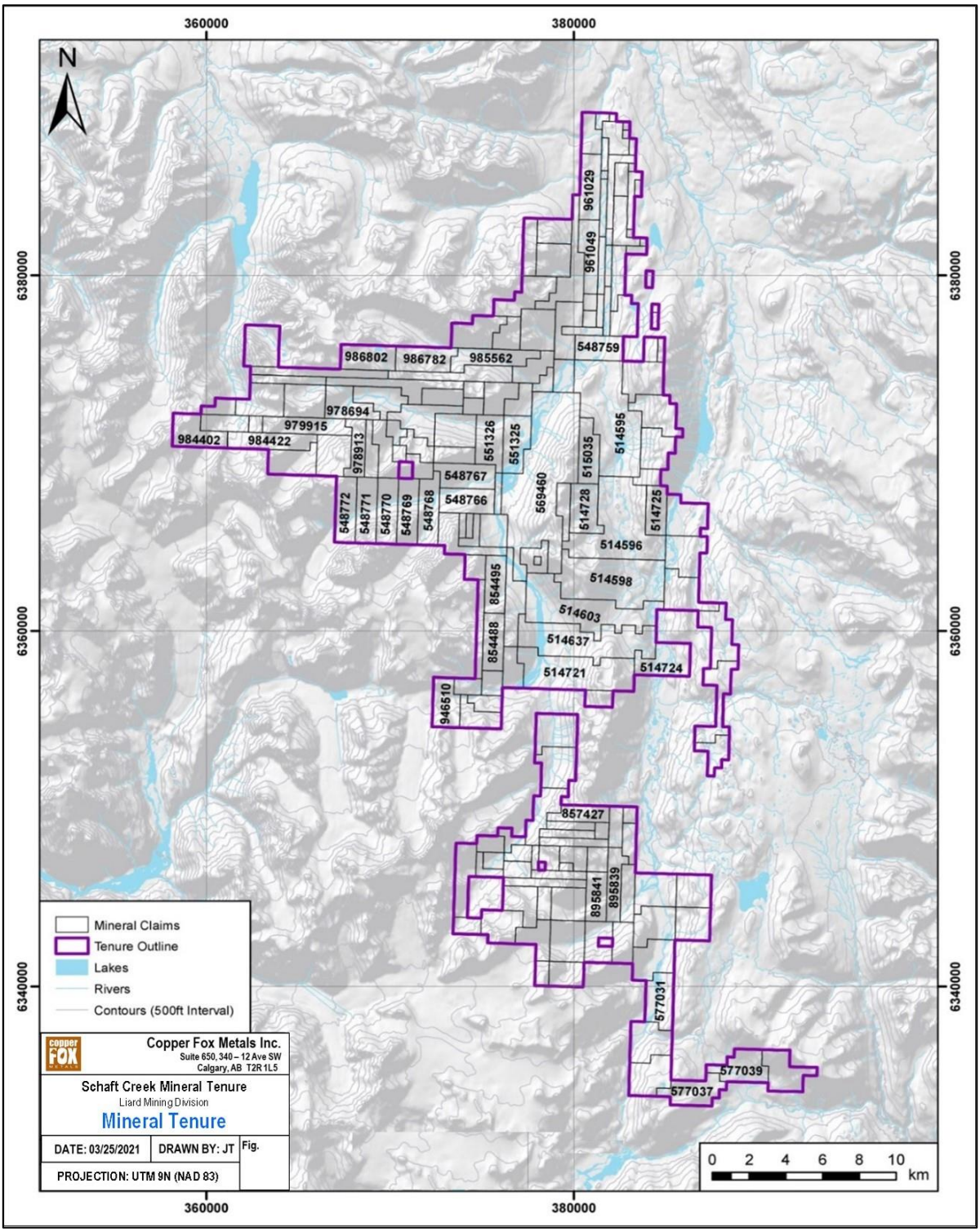

Table 4-1: Schaft Creek JV Mineral Claims Table

ID	Name	Parties	Type	Status	Grant Date	Expiry Date	Official Area (ha)	Royalty
514595	CL 514595	Teck Resources Limited (100%)	Mineral Claim (BC)	Active	6/16/2005	2/13/2026	1,653.04	
514596	CL 514596	Teck Resources Limited (100%)	Mineral Claim (BC)	Active	6/16/2005	2/13/2026	1,550.96	
514598	CL 514598	Teck Resources Limited (100%)	Mineral Claim (BC)	Active	6/16/2005	2/13/2026	1,412.62	
514603	CL 514603	Teck Resources Limited (100%)	Mineral Claim (BC)	Active	6/16/2005	2/13/2026	1,291.06	
514637	CL 514637	Teck Resources Limited (100%)	Mineral Claim (BC)	Active	6/16/2005	2/13/2026	1,256.71	
514721	CL 514721	Teck Resources Limited (100%)	Mineral Claim (BC)	Active	6/16/2005	2/13/2026	1,169.95	
514723	CL 514723	Teck Resources Limited (100%)	Mineral Claim (BC)	Active	6/16/2005	2/13/2026	139.745	
514724	CL 514724	Teck Resources Limited (100%)	Mineral Claim (BC)	Active	6/16/2005	2/13/2026	471.387	
514725	CL 514725	Teck Resources Limited (100%)	Mineral Claim (BC)	Active	6/16/2005	2/13/2026	313.607	
514728	CL 514728	Teck Resources Limited (100%)	Mineral Claim (BC)	Active	6/16/2005	2/13/2026	465.589	
515035	CL 515035	Teck Resources Limited (100%)	Mineral Claim (BC)	Active	6/16/2005	2/13/2026	383.005	
515036	CL 515036	Teck Resources Limited (100%)	Mineral Claim (BC)	Active	6/16/2005	2/13/2026	191.645	
517462	CL 517462	Teck Resources Limited (100%)	Mineral Claim (BC)	Active	7/12/2005	2/13/2026	17.436	Kreft/Greig
521312	Schaft 1	Teck Resources Limited (100%)	Mineral Claim (BC)	Active	10/18/2005	2/13/2026	191.784	Pembrook
547789	CL 547789	Teck Resources Limited (100%)	Mineral Claim (BC)	Active	12/21/2006	2/13/2026	418.7	
547798	CL 547798	Teck Resources Limited (100%)	Mineral Claim (BC)	Active	12/21/2006	2/13/2026	227	
548487	Block B1	Teck Resources Limited (100%)	Mineral Claim (BC)	Active	1/2/2007	2/13/2026	434.782	
548488	Block B2	Teck Resources Limited (100%)	Mineral Claim (BC)	Active	1/2/2007	2/13/2026	434.989	

table continues…

ID	Name	Parties	Type	Status	Grant Date	Expiry Date	Official Area (ha)	Royalty
548489	Block B3	Teck Resources Limited (100%)	Mineral Claim (BC)	Active	1/2/2007	2/13/2026	365.568	
548490	Block B4	Teck Resources Limited (100%)	Mineral Claim (BC)	Active	1/2/2007	2/13/2026	121.904	
548492	Block C1	Teck Resources Limited (100%)	Mineral Claim (BC)	Active	1/2/2007	2/13/2026	435.989	
548493	Block C2	Teck Resources Limited (100%)	Mineral Claim (BC)	Active	1/2/2007	2/13/2026	435.829	
548494	Block C3	Teck Resources Limited (100%)	Mineral Claim (BC)	Active	1/2/2007	2/13/2026	436.064	
548495	Block C4	Teck Resources Limited (100%)	Mineral Claim (BC)	Active	1/2/2007	2/13/2026	436.309	
548496	Block C5	Teck Resources Limited (100%)	Mineral Claim (BC)	Active	1/2/2007	2/13/2026	436.695	
548498	Block C6	Teck Resources Limited (100%)	Mineral Claim (BC)	Active	1/2/2007	2/13/2026	227.243	
548759	Area A	Teck Resources Limited (100%)	Mineral Claim (BC)	Active	1/2/2007	2/13/2026	365.065	
548760	Area C1	Teck Resources Limited (100%)	Mineral Claim (BC)	Active	1/2/2007	2/13/2026	436.903	
548761	Area C2	Teck Resources Limited (100%)	Mineral Claim (BC)	Active	1/2/2007	2/13/2026	437.115	
548762	Area C3	Teck Resources Limited (100%)	Mineral Claim (BC)	Active	1/2/2007	2/13/2026	367.411	
548763	Area C4	Teck Resources Limited (100%)	Mineral Claim (BC)	Active	1/2/2007	2/13/2026	122.542	
548764	Area B1	Teck Resources Limited (100%)	Mineral Claim (BC)	Active	1/5/2007	2/13/2026	366.043	
548766	Area B2	Teck Resources Limited (100%)	Mineral Claim (BC)	Active	1/5/2007	2/13/2026	418.11	
548767	Area B3	Teck Resources Limited (100%)	Mineral Claim (BC)	Active	1/5/2007	2/13/2026	435.38	
548768	Area B4	Teck Resources Limited (100%)	Mineral Claim (BC)	Active	1/5/2007	2/13/2026	435.6	
548769	Area B5	Teck Resources Limited (100%)	Mineral Claim (BC)	Active	1/5/2007	2/13/2026	418.19	
548770	Area B6	Teck Resources Limited (100%)	Mineral Claim (BC)	Active	1/5/2007	2/13/2026	418.19	

table continues…

ID	Name	Parties	Type	Status	Grant Date	Expiry Date	Official Area (ha)	Royalty
548771	Area B7	Teck Resources Limited (100%)	Mineral Claim (BC)	Active	1/5/2007	2/13/2026	418.19	
548772	Area B8	Teck Resources Limited (100%)	Mineral Claim (BC)	Active	1/5/2007	2/13/2026	418.19	
551325	Area D1	Teck Resources Limited (100%)	Mineral Claim (BC)	Active	2/6/2006	2/13/2026	435.18	
551326	Area D2	Teck Resources Limited (100%)	Mineral Claim (BC)	Active	2/6/2006	2/13/2026	435.17	
551328	Area D3	Teck Resources Limited (100%)	Mineral Claim (BC)	Active	2/6/2006	2/13/2026	417.71	
569460	Greater Kopper	Teck Resources Limited (100%)	Mineral Claim (BC)	Active	11/5/2007	2/13/2026	2,769.10	Kreft/Greig
577025	SC South 1	Teck Resources Limited (100%)	Mineral Claim (BC)	Active	2/23/2008	2/13/2026	437.8319	
577026	SC South 2	Teck Resources Limited (100%)	Mineral Claim (BC)	Active	2/23/2008	2/13/2026	438.0366	
577028	SC South 3	Teck Resources Limited (100%)	Mineral Claim (BC)	Active	2/23/2008	2/13/2026	438.2416	
577031	SC South 4	Teck Resources Limited (100%)	Mineral Claim (BC)	Active	2/23/2008	2/13/2026	438.4862	
577033	SC South 5	Teck Resources Limited (100%)	Mineral Claim (BC)	Active	2/23/2008	2/13/2026	438.7322	
577034	SC South 6	Teck Resources Limited (100%)	Mineral Claim (BC)	Active	2/23/2008	2/13/2026	438.9363	
577037	SC South 7	Teck Resources Limited (100%)	Mineral Claim (BC)	Active	2/23/2008	2/13/2026	439.0198	
577039	SC South 8	Teck Resources Limited (100%)	Mineral Claim (BC)	Active	2/23/2008	2/13/2026	438.876	
577042	SC South 9	Teck Resources Limited (100%)	Mineral Claim (BC)	Active	2/23/2008	2/13/2026	438.8966	
854488	Silver Fox 86	Teck Resources Limited (100%)	Mineral Claim (BC)	Active	5/13/2011	2/13/2026	366.5575	Marko/Mott
854495	Silver Fox 87	Teck Resources Limited (100%)	Mineral Claim (BC)	Active	5/13/2011	2/13/2026	366.2694	Marko/Mott
854513	Silver Fox 89	Teck Resources Limited (100%)	Mineral Claim (BC)	Active	5/14/2011	2/13/2026	157.1843	Marko/Mott
854523	White Rabbit 90	Teck Resources Limited (100%)	Mineral Claim (BC)	Active	5/14/2011	2/13/2026	208.9252	Marko/Mott

table continues…

ID	Name	Parties	Type	Status	Grant Date	Expiry Date	Official Area (ha)	Royalty
854536	Silver Fox 91	Teck Resources Limited (100%)	Mineral Claim (BC)	Active	5/14/2011	2/13/2026	156.9374	Marko/Mott
855206	Ptarmigan 93	Teck Resources Limited (100%)	Mineral Claim (BC)	Active	5/18/2011	2/13/2026	208.7684	Marko/Mott
855207	Ptarmigan 95	Teck Resources Limited (100%)	Mineral Claim (BC)	Active	5/18/2011	2/13/2026	278.339	Marko/Mott
855348	White Rabbit 92	Teck Resources Limited (100%)	Mineral Claim (BC)	Active	5/21/2011	2/13/2026	104.4313	Marko/Mott
855461	Ptarmigan 97	Teck Resources Limited (100%)	Mineral Claim (BC)	Active	5/24/2011	2/13/2026	104.3678	Marko/Mott
855735	White Rabbit 101	Teck Resources Limited (100%)	Mineral Claim (BC)	Active	5/26/2011	2/13/2026	191.496	Marko/Mott
855736	White Rabbit 102	Teck Resources Limited (100%)	Mineral Claim (BC)	Active	5/26/2011	2/13/2026	139.3092	Marko/Mott
855842	Ptarmigan 103	Teck Resources Limited (100%)	Mineral Claim (BC)	Active	5/27/2011	2/13/2026	104.3915	Marko/Mott
855868	Tern 120	Teck Resources Limited (100%)	Mineral Claim (BC)	Active	5/30/2013	2/13/2026	295.4047	Marko/Mott
855872	Tern 103	Teck Resources Limited (100%)	Mineral Claim (BC)	Active	5/30/2013	2/13/2026	138.7507	Marko/Mott
856232	Silver Fox 118	Teck Resources Limited (100%)	Mineral Claim (BC)	Active	6/3/2011	2/13/2026	139.7259	Marko/Mott
856238	Silver Fox 119	Teck Resources Limited (100%)	Mineral Claim (BC)	Active	6/3/2011	2/13/2026	157.23	Marko/Mott
856450	Elk 151	Teck Resources Limited (100%)	Mineral Claim (BC)	Active	6/8/2011	2/13/2026	105.0158	Marko/Mott
856464	Elk 152	Teck Resources Limited (100%)	Mineral Claim (BC)	Active	6/8/2011	2/13/2026	69.983	Marko/Mott
856487	Elk152	Teck Resources Limited (100%)	Mineral Claim (BC)	Active	6/9/2011	2/13/2026	157.52	Marko/Mott
856673	Elk 153	Teck Resources Limited (100%)	Mineral Claim (BC)	Active	6/10/2011	2/13/2026	174.9874	Marko/Mott
857427	Elk 154	Teck Resources Limited (100%)	Mineral Claim (BC)	Active	6/21/2011	2/13/2026	279.9349	Marko/Mott
857428	Elk 155	Teck Resources Limited (100%)	Mineral Claim (BC)	Active	6/21/2011	2/13/2026	69.9989	Marko/Mott
857528	Elk 156	Teck Resources Limited (100%)	Mineral Claim (BC)	Active	6/22/2011	2/13/2026	122.4914	Marko/Mott

table continues…

ID	Name	Parties	Type	Status	Grant Date	Expiry Date	Official Area (ha)	Royalty
862647	Elk 158	Teck Resources Limited (100%)	Mineral Claim (BC)	Active	7/4/2011	2/13/2026	140.0061	Marko/Mott
865007	Tern 125	Teck Resources Limited (100%)	Mineral Claim (BC)	Active	7/7/2011	2/13/2026	243.131	Marko/Mott
865167	Tern 127	Teck Resources Limited (100%)	Mineral Claim (BC)	Active	7/8/2011	2/13/2026	242.9604	Marko/Mott
865328	Elk 166	Teck Resources Limited (100%)	Mineral Claim (BC)	Active	7/9/2011	2/13/2026	175.0273	Marko/Mott
865619	Elk 167	Teck Resources Limited (100%)	Mineral Claim (BC)	Active	7/11/2011	2/13/2026	140.0507	Marko/Mott
866050	Tern 128	Teck Resources Limited (100%)	Mineral Claim (BC)	Active	7/13/2011	2/13/2026	104.2511	Marko/Mott
866517	Tern 130	Teck Resources Limited (100%)	Mineral Claim (BC)	Active	7/18/2011	2/13/2026	138.7842	Marko/Mott
866518	Tern 131	Teck Resources Limited (100%)	Mineral Claim (BC)	Active	7/18/2011	2/13/2026	208.137	Marko/Mott
866536	Tern 132	Teck Resources Limited (100%)	Mineral Claim (BC)	Active	7/18/2011	2/13/2026	208.0058	Marko/Mott
866630	Tern 131	Teck Resources Limited (100%)	Mineral Claim (BC)	Active	7/19/2011	2/13/2026	51.9883	Marko/Mott
866669	Tern 133	Teck Resources Limited (100%)	Mineral Claim (BC)	Active	7/20/2011	2/13/2026	69.3512	Marko/Mott
866670	Tern 134	Teck Resources Limited (100%)	Mineral Claim (BC)	Active	7/20/2011	2/13/2026	34.715	Marko/Mott
866671	Tern 135	Teck Resources Limited (100%)	Mineral Claim (BC)	Active	7/20/2011	2/13/2026	17.3328	Marko/Mott
866677	Tern 135	Teck Resources Limited (100%)	Mineral Claim (BC)	Active	7/20/2011	2/13/2026	17.3287	Marko/Mott
866678	Tern 136	Teck Resources Limited (100%)	Mineral Claim (BC)	Active	7/20/2011	2/13/2026	86.822	Marko/Mott
866889	Tern 137	Teck Resources Limited (100%)	Mineral Claim (BC)	Active	7/20/2011	2/13/2026	17.3428	Marko/Mott
866909	Juskatla Resources 2	Teck Resources Limited (100%)	Mineral Claim (BC)	Active	7/20/2011	2/13/2026	104.2799	
880149	Bonanza	Teck Resources Limited (100%)	Mineral Claim (BC)	Active	8/3/2011	2/13/2026	350.2622	

table continues…

ID	Name	Parties	Type	Status	Grant Date	Expiry Date	Official Area (ha)	Royalty
880189	Bonanza1	Teck Resources Limited (100%)	Mineral Claim (BC)	Active	8/3/2011	2/13/2026	350.4197	
884429	Gold Bear	Teck Resources Limited (100%)	Mineral Claim (BC)	Active	8/7/2011	2/13/2026	87.0967	Marko/Mott
895838	Eagle 800	Teck Resources Limited (100%)	Mineral Claim (BC)	Active	9/1/2011	2/13/2026	245.1966	
895839	Eagle 801	Teck Resources Limited (100%)	Mineral Claim (BC)	Active	9/1/2011	2/13/2026	332.7258	
895840	Eagle 802	Teck Resources Limited (100%)	Mineral Claim (BC)	Active	9/1/2011	2/13/2026	157.5583	
895841	Eagle 803	Teck Resources Limited (100%)	Mineral Claim (BC)	Active	9/1/2011	2/13/2026	315.2703	
895842	Eagle 804	Teck Resources Limited (100%)	Mineral Claim (BC)	Active	9/1/2011	2/13/2026	175.0619	
896151	Eagle 805	Teck Resources Limited (100%)	Mineral Claim (BC)	Active	9/6/2011	2/13/2026	52.5198	
896152	Eagle 806	Teck Resources Limited (100%)	Mineral Claim (BC)	Active	9/6/2011	2/13/2026	35.0163	
896353	Eagle 807	Teck Resources Limited (100%)	Mineral Claim (BC)	Active	9/9/2011	2/13/2026	140.0808	
896516	Eagle 808	Teck Resources Limited (100%)	Mineral Claim (BC)	Active	9/11/2011	2/13/2026	140.0725	
896517	Eagle 809	Teck Resources Limited (100%)	Mineral Claim (BC)	Active	9/11/2011	2/13/2026	105.0451	
900609	Juskatla Resources 3	Teck Resources Limited (100%)	Mineral Claim (BC)	Active	9/25/2011	2/13/2026	17.3566	
900629	Juskatla Resource 4	Teck Resources Limited (100%)	Mineral Claim (BC)	Active	9/25/2011	2/13/2026	34.6717	
900649	Eagle 810	Teck Resources Limited (100%)	Mineral Claim (BC)	Active	9/25/2011	2/13/2026	210.1447	
903029	Juskatla Resources 5	Teck Resources Limited (100%)	Mineral Claim (BC)	Active	9/28/2011	2/13/2026	17.3584	
903049	Juskatla Resources 6	Teck Resources Limited (100%)	Mineral Claim (BC)	Active	9/28/2011	2/13/2026	17.3308	

table continues…

ID	Name	Parties	Type	Status	Grant Date	Expiry Date	Official Area (ha)	Royalty
903069	Juskatla Resources 7	Teck Resources Limited (100%)	Mineral Claim (BC)	Active	9/28/2011	2/13/2026	34.6917	
908069	Tern Around	Teck Resources Limited (100%)	Mineral Claim (BC)	Active	10/8/2011	2/13/2026	69.5009	
910209	Tern Around	Teck Resources Limited (100%)	Mineral Claim (BC)	Active	10/12/2011	2/13/2026	121.455	
910229	Tern Around	Teck Resources Limited (100%)	Mineral Claim (BC)	Active	10/12/2011	2/13/2026	121.5508	
927669	Tern Left	Teck Resources Limited (100%)	Mineral Claim (BC)	Active	11/1/2011	2/13/2026	69.5086	
928489	Tern West	Teck Resources Limited (100%)	Mineral Claim (BC)	Active	11/8/2011	2/13/2026	69.493	
936631	Eagle 815	Teck Resources Limited (100%)	Mineral Claim (BC)	Active	12/7/2011	2/13/2026	262.1002	
946510	Eagle 816	Teck Resources Limited (100%)	Mineral Claim (BC)	Active	2/6/2012	2/13/2026	384.3474	
949269	Eagle 812	Teck Resources Limited (100%)	Mineral Claim (BC)	Active	2/13/2012	2/13/2026	262.8877	
949270	Eagle 811	Teck Resources Limited (100%)	Mineral Claim (BC)	Active	2/13/2012	2/13/2026	315.4651	
950890	Eagle 814	Teck Resources Limited (100%)	Mineral Claim (BC)	Active	2/20/2012	2/13/2026	105.0552	
952292	Eagle 813	Teck Resources Limited (100%)	Mineral Claim (BC)	Active	2/23/2012	2/13/2026	438.1459	
952293	Eagle 817	Teck Resources Limited (100%)	Mineral Claim (BC)	Active	2/23/2012	2/13/2026	350.3396	
952412	Retern100	Teck Resources Limited (100%)	Mineral Claim (BC)	Active	2/24/2012	2/13/2026	104.304	
952423	Retern101	Teck Resources Limited (100%)	Mineral Claim (BC)	Active	2/24/2012	2/13/2026	52.1522	
952427	Retern 102	Teck Resources Limited (100%)	Mineral Claim (BC)	Active	2/24/2012	2/13/2026	52.0814	
953131	Eagle 818	Teck Resources Limited (100%)	Mineral Claim (BC)	Active	2/27/2012	2/13/2026	263.0055	
955309	Tern North	Teck Resources Limited (100%)	Mineral Claim (BC)	Active	3/4/2012	2/13/2026	225.3319	

table continues…

ID	Name	Parties	Type	Status	Grant Date	Expiry Date	Official Area (ha)	Royalty
961029	North Tern 2	Teck Resources Limited (100%)	Mineral Claim (BC)	Active	3/13/2012	2/13/2026	416.2977	
961049	North Tern 3	Teck Resources Limited (100%)	Mineral Claim (BC)	Active	3/13/2012	2/13/2026	381.9542	
961110	Silver Eagle 900	Teck Resources Limited (100%)	Mineral Claim (BC)	Active	3/13/2012	2/13/2026	280.4076	
964509	Silver Eagle 902	Teck Resources Limited (100%)	Mineral Claim (BC)	Active	3/16/2012	2/13/2026	140.1358	
964529	Silver Eagle 903	Teck Resources Limited (100%)	Mineral Claim (BC)	Active	3/16/2012	2/13/2026	332.823	
965029	Silver Eagle 901	Teck Resources Limited (100%)	Mineral Claim (BC)	Active	3/17/2012	2/13/2026	105.2024	
968529	Silver Eagle 904	Teck Resources Limited (100%)	Mineral Claim (BC)	Active	3/21/2012	2/13/2026	367.9731	
969349	Silver Eagle 905	Teck Resources Limited (100%)	Mineral Claim (BC)	Active	3/21/2012	2/13/2026	385.2511	
969369	Silver Eagle 906	Teck Resources Limited (100%)	Mineral Claim (BC)	Active	3/21/2012	2/13/2026	140.183	
970769	Silver Rabbit	Teck Resources Limited (100%)	Mineral Claim (BC)	Active	3/24/2012	2/13/2026	435.0489	
970789	Silver Rabbit 2	Teck Resources Limited (100%)	Mineral Claim (BC)	Active	3/24/2012	2/13/2026	347.9524	
971953	Tern South	Teck Resources Limited (100%)	Mineral Claim (BC)	Active	3/26/2012	2/13/2026	208.6899	
971956	Tern South 2	Teck Resources Limited (100%)	Mineral Claim (BC)	Active	3/26/2012	2/13/2026	382.3436	
971957	Tern South 3	Teck Resources Limited (100%)	Mineral Claim (BC)	Active	3/26/2012	2/13/2026	104.355	
976357	Huron 047	Teck Resources Limited (100%)	Mineral Claim (BC)	Active	4/2/2012	2/13/2026	209.4256	
978394	South Tern 4	Teck Resources Limited (100%)	Mineral Claim (BC)	Active	4/6/2012	2/13/2026	260.8388	
978694	Crown 500	Teck Resources Limited (100%)	Mineral Claim (BC)	Active	4/9/2012	2/13/2026	400.1872	
978695	Crown 501	Teck Resources Limited (100%)	Mineral Claim (BC)	Active	4/9/2012	2/13/2026	417.5738	
978696	Crown 502	Teck Resources Limited (100%)	Mineral Claim (BC)	Active	4/9/2012	2/13/2026	417.5846	

table continues…

ID	Name	Parties	Type	Status	Grant Date	Expiry Date	Official Area (ha)	Royalty
978697	Crown 503	Teck Resources Limited (100%)	Mineral Claim (BC)	Active	4/9/2012	2/13/2026	139.2108	
978732	Crown 504	Teck Resources Limited (100%)	Mineral Claim (BC)	Active	4/10/2012	2/13/2026	434.8568	
978733	Crown 505	Teck Resources Limited (100%)	Mineral Claim (BC)	Active	4/10/2012	2/13/2026	208.7595	
978734	Crown 506	Teck Resources Limited (100%)	Mineral Claim (BC)	Active	4/10/2012	2/13/2026	434.779	
978739	Crown 507	Teck Resources Limited (100%)	Mineral Claim (BC)	Active	4/10/2012	2/13/2026	243.6704	
978892	Crown 507	Teck Resources Limited (100%)	Mineral Claim (BC)	Active	4/10/2012	2/13/2026	295.9702	
978912	Crown 508	Teck Resources Limited (100%)	Mineral Claim (BC)	Active	4/10/2012	2/13/2026	191.5177	
978913	Crown 509	Teck Resources Limited (100%)	Mineral Claim (BC)	Active	4/10/2012	2/13/2026	278.5544	
979914	Crown 510	Teck Resources Limited (100%)	Mineral Claim (BC)	Active	4/12/2012	2/13/2026	191.3341	
979915	Crown 511	Teck Resources Limited (100%)	Mineral Claim (BC)	Active	4/12/2012	2/13/2026	435.1219	
979916	Crown 512	Teck Resources Limited (100%)	Mineral Claim (BC)	Active	4/12/2012	2/13/2026	69.6198	
979917	Crown 513	Teck Resources Limited (100%)	Mineral Claim (BC)	Active	4/12/2012	2/13/2026	417.8764	
979918	Crown 514	Teck Resources Limited (100%)	Mineral Claim (BC)	Active	4/12/2012	2/13/2026	347.8393	
984402	Crown 515	Teck Resources Limited (100%)	Mineral Claim (BC)	Active	5/8/2012	2/13/2026	417.7842	
984422	Crown 516	Teck Resources Limited (100%)	Mineral Claim (BC)	Active	5/8/2012	2/13/2026	435.2212	
984442	Crown 517	Teck Resources Limited (100%)	Mineral Claim (BC)	Active	5/8/2012	2/13/2026	383.0989	
985562	Crown 519	Teck Resources Limited (100%)	Mineral Claim (BC)	Active	5/10/2012	2/13/2026	434.6695	
985563	Crown 520	Teck Resources Limited (100%)	Mineral Claim (BC)	Active	5/10/2012	2/13/2026	434.4922	
986762	Retern 105	Teck Resources Limited (100%)	Mineral Claim (BC)	Active	5/16/2012	2/13/2026	17.3408	

table continues…

ID	Name	Parties	Type	Status	Grant Date	Expiry Date	Official Area (ha)	Royalty
986782	Crown 521	Teck Resources Limited (100%)	Mineral Claim (BC)	Active	5/16/2012	2/13/2026	434.6827	
986802	Crown 522	Teck Resources Limited (100%)	Mineral Claim (BC)	Active	5/16/2012	2/13/2026	417.2993	
992022	Panda 1	Teck Resources Limited (100%)	Mineral Claim (BC)	Active	5/31/2012	2/13/2026	434.2899	
992023	Panda 2	Teck Resources Limited (100%)	Mineral Claim (BC)	Active	5/31/2012	2/13/2026	417.1348	
992042	Panda 3	Teck Resources Limited (100%)	Mineral Claim (BC)	Active	5/31/2012	2/13/2026	434.6455	
992062	Panda 4	Teck Resources Limited (100%)	Mineral Claim (BC)	Active	5/31/2012	2/13/2026	347.2546	
996622	Panda 5	Teck Resources Limited (100%)	Mineral Claim (BC)	Active	6/12/2012	2/13/2026	260.3358	
996642	Panda 6	Teck Resources Limited (100%)	Mineral Claim (BC)	Active	6/12/2012	2/13/2026	243.0354	
1015257	CL 1015257	Teck Resources Limited (100%)	Mineral Claim (BC)	Active	12/12/2012	2/13/2026	278.8546	
1015342	CL 1015342	Teck Resources Limited (100%)	Mineral Claim (BC)	Active	12/17/2012	2/13/2026	104.5769	
1015350	CL 1015350	Teck Resources Limited (100%)	Mineral Claim (BC)	Active	12/17/2012	2/13/2026	52.2821	
1015359	CL 1015359	Teck Resources Limited (100%)	Mineral Claim (BC)	Active	12/17/2012	2/13/2026	52.2821	
1019476	Tern 2 U	Teck Resources Limited (100%)	Mineral Claim (BC)	Active	5/13/2013	2/13/2026	503.5922	
1019477	Tern 2 U	Teck Resources Limited (100%)	Mineral Claim (BC)	Active	5/13/2013	2/13/2026	225.9553	
1019728	CL-1019728	Teck Resources Limited (100%)	Mineral Claim (BC)	Active	5/23/2013	2/13/2026	140.0324	
1019730	CL-1019730	Teck Resources Limited (100%)	Mineral Claim (BC)	Active	5/23/2013	2/13/2026	69.642	

The Schaft Creek copper–gold–molybdenum–silver deposit is located within the southern boundary of claim 514603 and the northern boundary of claim 514637.

Pertinent terms and conditions of the Schaft Creek JV are discussed in Section **Error! Reference source not found.**

4.2 Surface Rights

The surface is Crown land. Overlapping surface interests currently known include:

- Trapline TR062IT006.
- Licence of Occupation #6406985 for commercial recreation.
- Outfitting area held by Heidi Gutfruch.

The Property is within the Tahltan Nation territory.

Mining will require the exclusive use of the surface; an Industrial Surface Lease would be required to overlap the claims and provide exclusivity outside any Mines Act Permit boundary. Powerlines, upgraded road access, and other ancillary land use will require appropriate Land Act dispositions (Licences of Occupation, Statutory Rights of Way, etc.). Standing timber outside the existing cut blocks will require an Occupant Licence to Cut if removal becomes necessary.

4.3 Water Rights

The water rights belong to the Crown; the use of water for mining will require the issuance of a Section 10 *Mines Act* Permit to exempt the operator from the *Water Sustainability Act* requirements.

Water use outside of exploration drilling will require a *Water Sustainability Act* approval until a Section 10 permit is issued.

4.4 Royalties and Encumbrances

4.4.1 Schaft Creek Joint Venture

4.4.1.1 Royal Gold and Conversion Royalties

Pursuant to the 2002 Option Agreement with Teck, Copper Fox acquired a 100% working interest in the Schaft Creek Project subject to a 3.5% net profits interest held by Royal Gold Inc., a 30% carried interest held by Liard, and an earn-back option held by Teck.

Teck exercised the earn-back option on July 15, 2013, and has an unconditional 75% direct interest in the Project. Copper Fox retains a 25% interest. Teck is operator of the Schaft Creek JV, formed on 15 July 2013. The Schaft Creek JV agreement includes a provision that if any party's Project interest

falls below 20%, that interest will become a “Conversion Royalty” of 15% net profits interest, and the party will retain no other interest in the Project.

4.4.1.2 Areas of Interest

There are two areas of interest in the Schaft Creek JV, as indicated in Figure 4-4.

The Teck / Copper Fox area of interest is a 2 km zone around the original 2002 tenure holding. Any ground acquired by either party within this zone is added to the JV, unless the ground was previously held and relinquished by either party.

Pursuant to the Liard Agreement, the Project is subject to a 5 mile Area of Interest clause as indicated in Figure 4-4.

4.4.1.3 Pembrook Royalty

Under the terms of an agreement signed on March 22, 2011, between Copper Fox and Pembrook Mining Corp. (Pembrook), a 2% net smelter returns (NSR) royalty is payable to Pembrook on any production from claim 521312. The Schaft Creek JV can purchase half of this royalty for $1.5 M at any time, leaving a 1% NSR on the claim.

4.4.1.4 Kreft/Greig Royalty

A purchase agreement signed on March 18, 2011, between Copper Fox and two private vendors, Kreft and Greig, includes a 2% NSR payable on claims 517462 and 569460. The Schaft Creek JV can purchase half of this royalty for $1.5 M at any time, leaving a 1% NSR on the claims.

4.4.1.5 Marko/Mott Royalty

Copper Fox purchased the claims listed in Table 4-1 that are subject to the Marko/Mott royalty from two private vendors, Marko and Mott, on September 14, 2011. Under the purchase agreement, the claims are subject to a 2% NSR. The Schaft Creek JV can purchase half of this royalty for $1 M at any time, leaving a 1% NSR on the claims.

The mineral claims subject to the Pembrook, Kreft/Grieg, and Marko/Mott royalties are located outside the resource area of the Schaft Creek Project.

4.5 Property Agreements

The Schaft Creek JV has the following key terms:

- Teck will pay a total of $60 million in three direct cash payments to Copper Fox: $20 million upon signing the JV agreement, $20 million upon a production decision, and $20 million upon the completion of the mine facility.
- Teck will fund 100% of costs incurred prior to a production decision, up to $60 million; Copper Fox’s pro rata share of any pre-production costs in excess of $60 million will be funded by Teck and the two remaining direct cash payments payable to Copper Fox will be reduced by an amount

equal to Copper Fox's pro rata share of any pre-production costs in excess of the initial $60 million, to a maximum of total pre-production costs of $220 million.

- Teck will fund any additional costs (in excess of $220 million) incurred prior to a production decision, if required, by way of loan (at an interest rate of prime +2%) to Copper Fox to the extent of its pro rata share, without dilution to Copper Fox's 25% JV interest.
- Management of the Schaft Creek JV will be made up of two representatives from Teck and Copper Fox with voting proportional to equity interests.
- Teck agreed to use all reasonable commercial efforts to arrange project debt financing for not less than 60% of project capital costs of constructing a mining operation. If a production decision is made, Teck will fund Copper Fox's pro rata share of project capital costs by way of loans (at prime + 2%), if requested by Copper Fox, without dilution to Copper Fox's 25% JV interest.

Figure 4-4: Areas of Interest

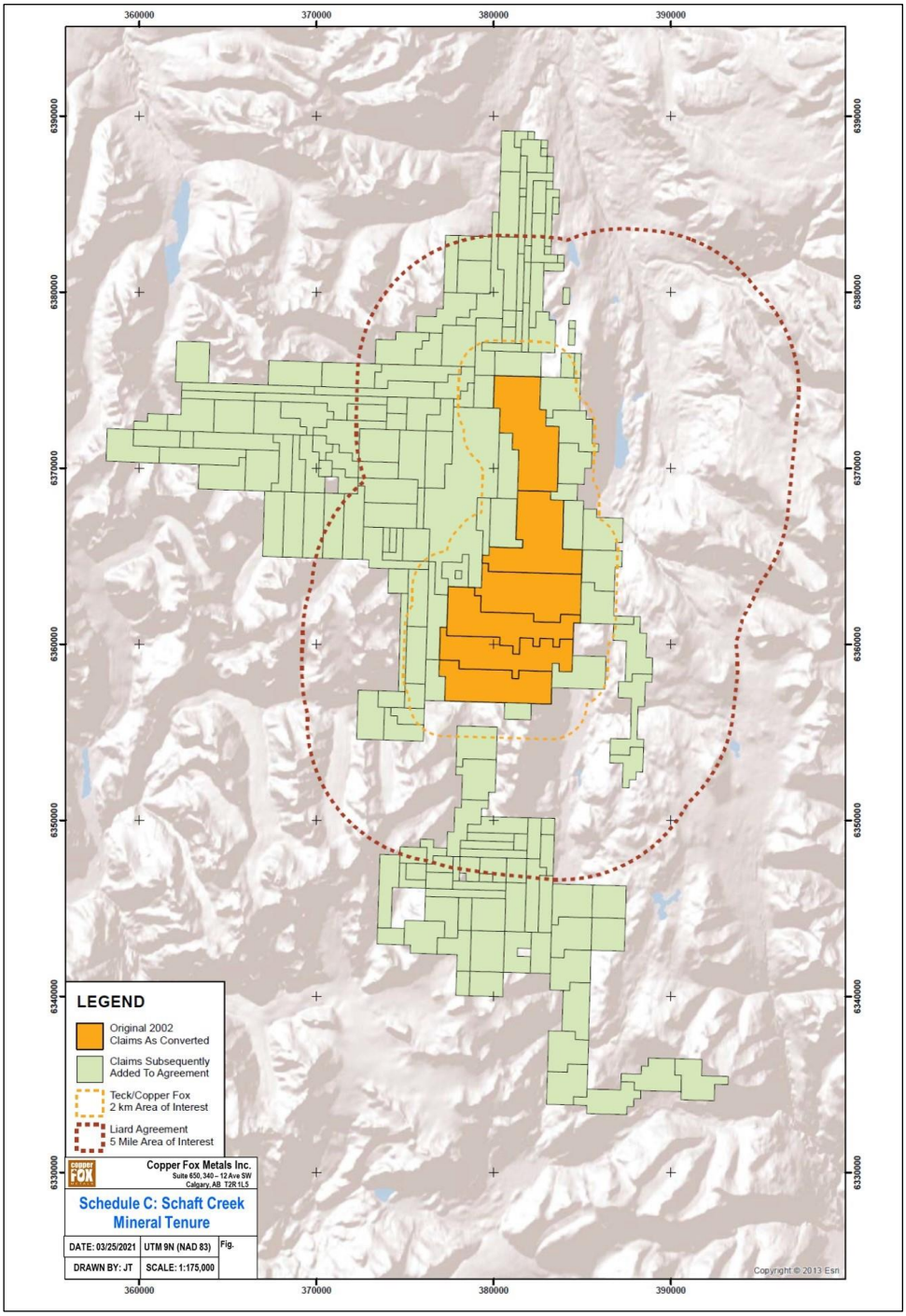

4.6 Permitting Considerations

4.6.1 Environmental Assessment

Permission to develop and operate major mines in British Columbia is granted after the completion of an environmental assessment (EA) and permitting reviews by both the Provincial and Federal governments. The first review phase is conducted by the Provincial British Columbia Environmental Assessment Act (BCEAA) and the Federal Canadian Environmental Assessment Act (CEAA). These reviews involve approval of the mine concept and lead to issuance of an EA certificate under the BCEAA process, and approval from the Federal Minister of the Environment under the Federal CEAA process. Projects in British Columbia that are subject to both Provincial and Federal EA processes undergo a harmonized EA review. The subsequent provincial and federal permitting review phase, which can only be concluded after completing the EA reviews, involves a more detailed review of specific aspects of the mine, and results in issuance of a number of Provincial and Federal permits.

In 2013, Copper Fox had entered into the first stage of the EA process; however, in 2016, subsequent to significant changes in the permitting process, the Schaft Creek JV voluntarily withdrew from the EA process.

4.6.2 Current Permits

The Schaft Creek JV secured a multi-year area-based (MYAB) permit, MX-I-647 in 2018 from the Ministry of Energy, Mine and Petroleum Resources, which included a approval for a maximum of 50 core drill holes, 5 km of new drill road, and 20 km of line cutting.

4.6.3 Future Permits

The majority of the major permits, licences, and authorizations required to support construction activities are under Provincial jurisdiction; however, some are under Federal authority. The key permits would include:

- Provincial: mining lease, discharge permit, water licence, authority to make a change in and about a stream, occupant licence to cut, special use permit, licence of occupation, surface lease, waste management permit, special waste generator permit (waste oil), sewage registration, camp operation permits, waterworks permit, fuel storage approval, food service permits, and highway access permit.
- Federal: CEAA approval; metal mining effluent regulations, fish habitat compensation agreement, Section 35(2) authorization for harmful alteration or disruption, or the destruction of fish habitat, navigable water stream crossings authorization, international river improvement permit, explosives factory licence, explosives magazine licence, ammonium nitrate storage facilities and radio licences.

A number of minor approvals from local governments (regional districts and municipalities) and Crown corporations would also be required, although these approvals are not required to commence construction.

4.7 Environmental Considerations

4.7.1 Copper Fox

Copper Fox initiated baseline environmental studies in the period 2006–2012. These included:

- Terrain.
- Climate.
- Air quality.
- Noise.
- Groundwater quality and quantity.
- Surface hydrology.
- Water quality.
- Aquatic resources: streams, lakes and wetlands, sediment quality, periphyton, phytoplankton, zooplankton, benthic invertebrates.
- Fisheries, fish and fish habitat.
- Vegetation and plant communities.
- Soils.
- Wildlife and wildlife habitat.
- Visual and aesthetic resources.
- Economic.
- Social, including traditional knowledge and traditional land use, non-traditional land use.
- Heritage and archaeology.
- Health, including drinking water and country foods.

These studies remain relevant as baseline information for any future project development.

4.7.2 Schaft Creek JV

Since formation of the Schaft Creek JV, ongoing work has included environmental monitoring and collection of field data including humidity cell tests and other environmental baseline data.

4.8 Social and Community

4.8.1 Copper Fox

During 2006–2012, Copper Fox engaged with various members and institutions of the Tahltan Nation by way of informal meetings, working groups, and open house discussions. These consultations included members of the Tahltan Central Government and the Tahltan Heritage Resources Environmental Assessment Team.

During the consultation process, Tahltan Nation leadership and members raised a range of discussion points under several different categories. These included effects on areas of high archaeological potential, cumulative effects of Schaft Creek worker and family wellbeing, ability to practice Tahltan Nation traditional activities, access to remote areas, interference with past and present Tahltan Nation uses of the Mess Creek Valley, Tahltan Nation food availability and safety, and wildlife habitat and migration corridors.

4.8.2 Schaft Creek JV

Since formation of the Schaft Creek JV, the Schaft Creek JV has continued ongoing consultation with the Tahltan Nation on social and cultural matters. A Communications and Engagement Agreement was signed between the Tahltan Central Government and Teck on behalf of the Schaft Creek JV on May 22, 2020.

4.9 Comments on Section 4.0

In the opinion of the QP:

- Information provided by Copper Fox supports that the Schaft Creek JV has valid title that is sufficient to support declaration of Mineral Resources.
- Surface rights are held by the Crown. Overlapping surface rights include a trapline, a licence of occupation for recreational purposes, and an outfitting area. The Schaft Creek JV would need to conduct appropriate negotiations for use of the surface, and obtain permits such as an Industrial Surface Lease, Licence of Occupation, easements, and rights-of-way to support future operations.
- No water rights are currently held. The Schaft Creek JV would need to obtain a Section 10 *Mines Act* Permit in support of operations.
- The royalty agreements related to various mineral tenures are in accordance with acceptable industry practice at the time these agreements were executed and have not been amended.
- As the Project is at the resource estimation stage, no major permits are in hand, or under application. In 2018, The Schaft Creek JV received a MYAB permit, which included approval for a maximum of 50 core drill holes, 5 km of new drill road, and 20 km of line cutting.
- Environmental liabilities include the reclamation bond posted by the Schaft Creek JV in the amount of $695,000 to cover the cost of reclaiming the camp, airstrip, storage, and core facilities.

To the extent known, there are no other significant factors and risks known to Copper Fox that may affect access, title, or the right or ability to perform work on the Project that are not discussed in this Report.

5.0 ACCESSIBILITY, CLIMATE, LOCAL RESOURCES, INFRASTRUCTURE AND PHYSIOGRAPHY

5.1 Accessibility

The Property is accessible via rotary- or fixed-wing aircraft. The two gravel airstrips adjacent to the Schaft Creek camp are approximately 700 m long and support fixed-wing and helicopter access. Dease Lake and the Ch'iyone camp on the Galore Creek road were used for various staging purposes during the 2015 and 2019 field seasons. In previous years, Telegraph Creek, Bob Quinn, and the Burrage airstrip have been used as staging areas. During the summer months in previous years, scheduled commercial flights have been available from Terrace or Smithers to the Dease Lake airstrip.

5.2 Local Resources and Infrastructure

The main road access route through the region is Highway 37, which runs north from the Terrace and Smithers area to the Yukon. Highway 37 passes by the Bob Quinn airstrip and Dease Lake en route to the Yukon. Telegraph Creek is accessed from Dease Lake via a 110 km drive on gravel roads to the southwest.

Terrace and Smithers have moderate-sized airports with commercial flights that connect to Vancouver. Amenities include a variety of stores, gas stations, rental car providers, hotel accommodations, RCMP detachments, hospitals, government offices, and offices for various exploration services contractors and drilling companies.

Dease Lake has a small airport with a paved runway. Amenities in Dease Lake include a grocery store, a gas station, hotel accommodations, a hardware store, an RCMP detachment, a medical centre, and the Tahltan Central Government office.

Basic services are available in Telegraph Creek, including a general store, an RCMP detachment, a nursing station, and the Tahltan Band Council office. Accommodation can be arranged, and fuel is available for purchase. A small gravel airstrip just outside of Telegraph Creek can be used as a staging area.

The BC Hydro NTL was completed in mid-2014. The NTL is a 287 kV transmission line that connects Bob Quinn to the Skeena Substation, located near the City of Terrace. An extension of the NTL has also been completed from Bob Quinn to Tatogga Lake and from Tatogga Lake to the Red Chris Mine.

5.3 Climate and Physiography

The Property is situated in mountainous terrain on the eastern side of the Coast Mountains of northwestern British Columbia. To the west of the Property is the rugged and glaciated terrain of the Coast Mountains. To the east of the Property is the Edziza Plateau. Elevations in the immediate area range from 850 m at valley bottom to mountain peaks over 2,000 m above mean sea level. The deposit is located west of a low saddle between the Schaft Creek and Mess Creek valleys at the south end of Mount LaCasse. The exploration camp is located at the base of this slope, in the broad valley of the north-flowing Schaft Creek, a braided stream with thick glacial-fluvial and fluvial deposits.

Treeline on the Property is located at approximately 1,400 m elevation. Below treeline, forests are composed primarily of balsam fir, sitka spruce, alder, willow, and cedar. Above this elevation, vegetation consists of scrub bushes, stunted 'krummholz' trees, and alpine grass, moss, and lichen. Above 1,800 m, vegetation is sparse. Much of the area immediately overlying the Schaft Creek deposit was burned during a fire in 1980. Another wildfire occurred in 2013 northeast of Mount LaCasse along the Mess Creek valley near Skeeter Lake.

The Property location on the eastern side of the Coast Mountains corresponds to a transitional zone between the warmer, moist maritime climate of the Coast Mountains to the west and the cooler, drier continental climate of the Interior Ranges to the east (Jones and Volp, 2013). In nearby Dease Lake, high temperature mean values during summer months range from 17°C to 20°C, with low temperature mean values between 3°C and 6°C. In winter months, high temperature mean values range from -5°C to -13°C, with low temperature mean values of -18°C to -22°C (www.climate-charts.com).

In the Project area, annual precipitation ranges between 70 cm and 100 cm at 1,000 m elevation. Snowfall is possible any month of the year, but commonly begins to accumulate at higher elevations in late September or early October. By late October, snow typically begins to accumulate in the valley bottom near the exploration camp (860 m elevation), reaching a typical depth of 1 m to 2 m before melting in May or early June. At 1,200 m elevation, the snowpack typically ranges from 2 m to 3 m, with considerably more snowfall expected in higher elevation alpine areas (Jones and Volp, 2013).

Field work can normally commence at lower elevations in early June and at upper elevations by July. Cold weather, high wind, and snow make field work difficult beyond mid-October.

5.4 Protected Areas

The Project is located within the boundaries of the Cassiar Iskut–Stikine Land and Resource Management Plan (LRMP), which encompasses approximately 52,000 km^2 of northwestern British Columbia. The LRMP supports exploration and development in the area (excluding protected areas), including the development of access roads. Any activities are subject to any applicable environmental review processes. The LRMP identifies 15 resource management zones (RMZs) for area-specific management direction. The Middle Iskut RMZ boundary is approximately 25 km from the proposed Schaft Creek mine site and/or access road. The Schaft Creek project is located adjacent to the Mount Edziza Provincial Park and Tahltan Highlands to the east.

5.5 Seismicity

Information on the Project seismic setting is summarized from Farah et al. (2013).

The coastal northwest region of British Columbia and southwest Yukon is one of the most seismically active areas in Canada. The seismic hazard in the region is also influenced by the seismically active region of southeast Alaska.

A probabilistic seismic hazard analysis was carried out by Knight Piésold using the NRCan database to provide seismic ground motion parameters. The corresponding maximum acceleration is 0.06*g* for a return period of 475 years, indicating a low seismic hazard for the site.

5.6 Comments on Section 5.0

In the opinion of the QP:

- The existing local infrastructure, availability of staff, methods whereby goods could be transported to the Project area are well-established and well understood by Copper Fox, and can support the declaration of Mineral Resources;
- Within the tenure holdings, there is sufficient area to allow construction of infrastructure to support future mining operations.

6.0 HISTORY

6.1 Regional Government Geological Surveys and Academic Research

The area surrounding the Schaft Creek deposit has been mapped by several generations of geologists. The first geological study in the Stikine River area is thought to have been made by a group of Russian geologists who assessed the mineral potential of the district in 1863. Dawson and McConnell were the first Canadian geologists to explore the area in 1887, but the first geological mapping in the region was completed by Forrest Kerr from 1924 to 1929, published in 1948. Kerr's mapping along the Stikine and Iskut Rivers defined the Late Triassic Stuhini Group (Brown et al., 1996).

The Geological Survey of Canada's helicopter-supported 'Operation Stikine'[1] mapped the geology of the 104G Telegraph Creek map sheet in 1956 (Geological Survey of Canada, 1957). Jack Souther directed Operation Stikine and published a series of 1:250,000 scale geologic maps of several National Topographic System (NTS) map sheets, including 104G that contains the Schaft Creek Project (Souther, 1972). James Monger's regional synthesis subdivided the Late Paleozoic rocks and informally named them the Stikine Assemblage (Monger, 1977).

In 1988, Peter Holbek completed a master's thesis study on the BJ prospect, located 24 km south of Schaft Creek. This thesis included a detailed study of the BJ prospect and the host Stikine assemblage, as well as the intrusive and structural history of the region, including the Schaft Creek deposit area. Holbek's study included the Hickman, Yehiniko, and Nightout Plutons, which were grouped and named as the Hickman Batholith.

Logan et al.'s work on the Geology of the Forrest Kerr – Mess Creek Area resulted in the publication of Geoscience Map 1997-3 (Logan et al., 1997), which provides the most recent regional scale mapping available for the deposit area, and the publication of Bulletin 104 (Logan et al., 2000), which provides a detailed description of the regional geology. Brown et al.'s 1996 British Columbia Geological Survey Bulletin 95, detailing the 'Stikine Project' mapping of the Geology of Western Telegraph Creek Map Area in Geoscience Maps 1993-3 to 1993-6, provides the most recent regional scale mapping available for the area west and northwest of the deposit.

Geological descriptions of the Schaft Creek deposit were published following the conclusion of Teck's exploration campaigns during the 1970s and 1980s (Fox et al., 1976; Spilsbury et al., 1995). James Scott's 2007 master's thesis and CIM publication (Scott, 2007; Scott et al., 2008) comprises a more recent, detailed study of the geology and genesis of the deposit.

Recently, both the British Columbia Geological Survey and the Geological Survey of Canada have been active in northwestern British Columbia, and this recent work is relevant to the Schaft Creek Project. Recent investigations of the KSM-Brucejack district (Nelson and Kyba, 2013), and the Khyber-Sericite-Pins mineralized trend (Kyba and Nelson, 2014) have improved the knowledge of regional

[1] Systematic regional mapping of four 1:250,000 map areas of the Stikine Region of northwest BC by the Geological Survey of Canada in 1956.

stratigraphy during the Late Triassic and Early Jurassic and improved the understanding of mineralization in these areas. Recent investigations of Triassic mafic and ultramafic rocks within the Stikine Terrane have identified primitive, magnesium-rich, olivine-bearing rocks that are interpreted to represent a slab-metasomatized mantle environment from which magmatism was sourced during the Late Triassic (Milidragovic et al., 2016).

6.2 Exploration History

The Stikine River was used as an access route to the gold fields of the Klondike, and placer gold was discovered along the river in the early 1920s.

Copper mineralization was first discovered in the Schaft Creek area in 1957 by prospector Nick Bird, employed by the BIK Syndicate. He staked the first four claims in August of 1957 for BIK, a consortium of Silver Standard Mines, Ltd. (Silver Standard), McIntyre Porcupine Mines Ltd., Kerr Addison Mines Ltd., and Dalhousie Oil Ltd. (Linder, 1975). This was a year after the Geological Survey of Canada's Operation Stikine began mapping the regional geology of the area. Only two years earlier, in 1955, copper mineralization had been discovered at Galore Creek. Helicopter access to this remote region played a significant role in these 1950s discoveries. In 1959, while the Project was under option to Kennco Explorations (Western) Limited, an additional 42 claims were staked, and geological, geophysical and geochemical surveys were carried out before the option was dropped (Department of Energy, Mines, and Resources, 1986).

Silver Standard, acting as the operator for the BIK Syndicate, completed geochemical and geophysical surveys, and staked more ground. The first drill holes were completed in 1965, when Silver Standard completed three BQWL-sized drill holes totaling 629 m (Figure 6-1 summarizes the drilling completed on the Schaft Creek Project). Liard Copper Mines Ltd. (Liard), a private company, was incorporated in 1966 by the participants of the BIK Syndicate to hold the Project, with Silver Standard holding a 65.6% interest (Department of Energy, Mines, and Resources, 1986).

Liard optioned the ground to the American Smelting and Refining Company (Asarco) in 1966. Before dropping the option in 1968 Asarco built a camp and an airstrip, and completed an exploration program, including geological mapping and prospecting, induced polarization (IP) surveys, and 3,334 m of drilling in 24 holes (Kulla, 2011).

In 1966, the adjacent tenure to the north was acquired by Paramount Mining Ltd. (Paramount). Paramount completed ground geochemical and geophysical surveys, 450 m of trenching, and one AX-sized drill hole to 150 m depth (Department of Energy, Mines, and Resources, 1986).

In 1968, Liard optioned the Project to Hecla Mining Company (Hecla). Hecla optioned the Paramount ground in 1969, and completed extensive exploration on both the Liard tenure and Paramount tenure from 1968 to 1972. Hecla's work included percussion and diamond drilling totaling 29,616 m in 83 drill holes, in addition to geophysical surveys and geological mapping, as well as a pre-feasibility study (Kulla, 2011). Hecla's interest in the Project waned in 1973, with the company citing provincial and federal government policy changes as the cause of their curtailed work. Hecla dropped the option on Paramount in 1973, stating that future commitments under the option agreement could not be logically fulfilled by due dates, but continued minor work on the Liard tenure, drilling one hole in 1974 and another in 1977 totaling 1,178 m (Department of Energy, Mines, and Resources, 1986).

In 1978, Teck acquired Hecla's option to earn a 70% interest in the Liard Project (Department of Energy, Mines and Resources 1986). The Paramount tenure lapsed, and Teck re-staked this ground (Spilsbury, 1995). In 1980 and 1981, Teck completed 25,642 m of drilling to confirm and expand on Hecla's work. Work included geophysical surveys, condemnation drilling, resource estimation, and engineering studies (Kulla, 2011). Exploration in the area slowed in the early 1980s, with low metal prices curtailing exploration funding.

Copper Fox acquired an option on the Project through an assignment of an agreement made between Teck and Guillermo Salazar dated January 1, 2002. In February 2003, Salazar assigned the option to 955528 Alberta Ltd, which amalgamated with a newly incorporated Copper Fox in 2004. Between 2005 and 2012, Copper Fox carried out extensive exploration work on the Project, including 41,345 m of drilling. In 2004, Copper Fox had an initial Mineral Resource estimate prepared; this resource estimate was updated in 2007 for a preliminary economic assessment. It was again updated, and mineral reserves were declared for a 2008 Pre-feasibility Study. The Mineral Resource was updated in 2011 and again in 2012. The Mineral Resource completed in 2012 is no longer current but is set out below for information.

The 2012 project mineral resource was prepared by Tetra Tech, with an effective date of May 23, 2012 (Table 6-1, see news release dated May 31, 2012).

Table 6-1: Historic 2012 Mineral Resource

Mineral Resource Estimate – Schaft Creek Deposit										
Robert Morrison - Ph.D., MAusIMM (CP), P.Geo., Effective Date: May 23rd, 2012										
Resource Category	Cut-off CuEq (%)	Tonnes	Copper (%)	Molybdenum (%)	Gold (gpt)	Silver (gpt)	Contained Metal			
							Cu (Lbs)	Mo (Lbs)	Au (oz.)	Ag (oz.)
Measured	0.15	146,615,300	0.31	0.017	0.24	1.78	1,001,824,600	55,624,000	1,149,100	8,402,700
Indicated	0.15	1,081,939,500	0.26	0.017	0.18	1.68	6,104,400,000	399,718,500	6,218,000	58,335,500
Measured & Indicated	0.15	1,228,554,800	0.26	0.017	0.19	1.69	7,106,224,600	455,342,500	7,368,000	66,738,200
Inferred	0.15	597,191,300	0.22	0.016	0.17	1.65	2,872,034,300	206,252,100	3,359,600	31,601,400

Notes: These Mineral Resources are not current and the following notes were made at the time 2012 Mineral Resource estimate and do not apply to the current Mineral Resource Estimate.

Mineral Resources are inclusive of Mineral Reserves;

While the terms "Measured (Mineral) Resource", "Indicated (Mineral) Resource" and "Inferred (Mineral) Resource" are recognized and required by National Instrument 43-101 – *Standards of Disclosure for Mineral Projects*, investors are cautioned that except for that portion of Mineral Resources classified as Mineral Reserves, Mineral Resources do not have demonstrated economic viability. Investors are cautioned not to assume that all or any part of measured or indicated Mineral Resources will ever be upgraded into Mineral Reserves. Additionally, investors are cautioned that inferred Mineral Resources have a high degree of uncertainty as to their existence, as to whether they can be economically or legally mined, or will ever be upgraded to a higher category;

A 0.15% CuEq cut-off was selected for the base case resource estimate. A 0.15% CuEq cut-off was the minimum grade of CuEq estimated by Tetra Tech required (using the estimated copper recovery rate, the milling and sales cost) to break-even on an operating cost per tonne basis;

CuEq grade cut-offs were used to report the Mineral Resource estimation as a function of copper, molybdenum, gold, and silver. The CuEq is based on Tetra Tech's long-range metal prices of US $2.97/lb for copper, US $16.80/lb molybdenum, US $1,256.00/oz gold and US $20.38/oz for silver and metal recoveries of 60.90% for molybdenum, 70.6% for gold, and 43.4% for silver. No copper recoveries were applied to the copper equivalent grade;

Rounding as required by reporting guidelines may result in apparent summations differences between tonnes, grade and contained metal content; and

Tonnage and grade measurements are in metric units. Contained copper and molybdenum are reported as pounds and contained gold and silver are reported as troy ounces.

On January 23, 2013, Copper Fox filed a NI 43-101 technical report entitled “Feasibility Study on the Schaft Creek Project, BC Canada” prepared by Tetra Tech with A. Farah, P.Eng. et al. as Qualified Persons. The Mineral Reserve estimate used in the 2013 Feasibility Study are not current and are provided here for information purposes. The Proven and Probable Reserves used in the 2013 Feasibility Study are summarized in Table 6-2.

Table 6-2: Historic 2013 Mineral Reserves

Mineral Reserve					
Reserve Category	**Run of Mine (Mt)**	**Copper %**	**Molybdenum %**	**Gold gpt**	**Silver gpt**
Proven	135.4	0.31	0.0175	0.25	1.81
Probable	805.4	0.26	0.0176	0.18	1.70
Proven & Probable	940.8	0.27	0.0176	0.19	1.72

Notes: These Mineral Reserves are not current and the following notes were made at the time of the 2013 Mineral Reserve estimate. There are no current Mineral Reserves on the Schaft Creek Project.

Mineral Reserves are contained within Measured and Indicated pit designs.

Appropriate mining costs, processing costs metal recoveries, and inter ramp pit slope angles varying from 27 degrees in overburden to 45 degrees in bedrock were utilized to generate the pit phase design;

Mineral Reserves have been calculated using a Net Smelter Return (‘NSR’) cut-off. The NSR was calculated as follows: NSR = Recoverable Revenue – TCRC (on per tonne basis), where NSR = Net Smelter Return; TCRC = Transportation and Refining Costs; Recoverable Revenue = Revenue in Canadian dollars for recoverable copper, molybdenum, gold and silver, respectively, using metal prices of US $3.52/lb, US $15.30/lb, US $1,366.00/oz and US $25.96/oz for copper, molybdenum, gold and silver, respectively; at an exchange rate of CDN $0.96 to US $1.00; metal recoveries used are based on recovery curves if critical average recoveries could be calculated;

The LOM average strip ratio (waste to ore) is 2:1, excluding rehandle;

Rounded significant digits on Run of Mine to one decimal point;

Rounding as required by reporting guidelines may result in apparent summations differences between tonnes, grade and contained metal content, and

Tonnage and grade measurements are in metric units. Contained copper and molybdenum are reported as pounds and contained gold and silver are reported as troy ounces.

The proven and probable Mineral Reserves are included within the Measured and Indicated Mineral Resources as estimated by Tetra Tech on May 23, 2012.

In February of 2013, Copper Fox filed an NI 43-101 technical report to support the 2013 Feasibility Study.

In July 2013, Teck and Copper Fox formed the Schaft Creek JV, with Teck resuming as the project operator. Subsequent to the formation of this JV, the Schaft Creek JV completed a program of nine drill holes totalling 3,454 m in 2013. During 2013 and 2014, the Schaft Creek JV completed geological mapping, relogging of historical core, geological modeling, and an airborne geophysical survey. Table 6-3 outlines the work performed on the Project.

Table 6-3: Exploration History Summary

Year	Company	Comments
1957	BIK Syndicate	Mineral claims first staked in the region by prospector Nick Bird for the BIK Syndicate (consortium of Silver Standard Mines Ltd. (Silver Standard), McIntyre Porcupine Mines Limited, Kerr Addison Mines Ltd., and Dalhousie Oil Ltd.) 914.4 m hand trenching, rock chip sampling.
1965–1966	Silver Standard	Prospecting syndicate was re-organized into Liard Copper in order to recognize the respective interests of its members and to consolidate the holdings in the area. Silver Standard, with a 66% interest, was the operator of the Project. Geological mapping (eight traverses), hand-trenching (3,000 ft), induced polarization (IP) survey, three core drill holes (629 m).
1966	Paramount	450 soil samples, IP and magnetic geophysical surveys, claim 517462 staked
1966	Liard Copper Mines	Consolidated mineral tenures in area, optioned ground to American Smelting and Refining Company (Asarco).
1966–1967	Asarco	Two airstrips constructed, camp built; 24 core drill holes (3,334 m), IP survey.
1968–1977	Hecla	Asarco options property to Hecla, airstrip extended, 29,616 m core drilling and 6,500 m percussion drilling, IP and resistivity surveys, geological mapping (covered area of 10 by 6 miles at a scale of 1:400), aerial photography, tonnage and grade estimates, metallurgical testwork, engineering studies, local grid established.
1969–1972	Paramount	10 drill holes (2,924 m).
1971	Geological Survey of Canada	Regional geology mapped at a scale of 1:250,000.
1972	Phelps Dodge Corporation of Canada Ltd.	Soil and silt geochemical survey, cobra drill and bulldozer trenching, IP and magnetometer geophysical surveys.
1974	Hecla	Established grid of cut lines, low level air photography, IP surveys.
1978	Hecla/Teck	Hecla sold interest to Teck.
1978 – 2002	Teck	1980: 45 diamond drill holes (14,490 m); rock chip samples 1981: 81 diamond drill holes (11,154 m), IP survey, tonnage and grade estimate; metallurgical test work; internal evaluation studies.
2002	Teck / Copper Fox	Teck options property to Salazar / Copper Fox.
2002	Copper Fox	Copper Fox completes assessment of project and geologic model

table continues…

Year	Company	Comments
2005–2006	Pembrook	Limited reconnaissance mapping program, collected five rock samples in 2005; 2006 follow-up work to 2005 program, 24 rock samples on Pembrook claims, identified two gold and copper anomalous zones.
2005–2013	Copper Fox	2005: 15 diamond drill holes (3,160 m); metallurgical bulk sample collected, metallurgical test work. 2006: 42 diamond drill holes (9,007 m); additional metallurgical sample collected; metallurgical test work. Environmental studies including hydrology baseline report, moose baseline report, bird study, meteorology baseline report, fisheries baseline report, aquatics baseline report. 2007: 42 diamond drill holes (6,275 m), Mineral Resource estimate, IP survey. Environmental studies including aquatic resources baseline report, archeological baseline study technical summary, meteorology baseline report, bat inventory, preliminary groundwater baseline report, noise baseline report, soils baseline report, vegetation baseline report, western toad baseline, hydrology baseline, fisheries baseline, Tahltan (country) foods baseline assessment, access road assessment, wetlands baseline report, metal leaching/acid rock drainage (ML-ARD) phase 1 report. 2008: 47 diamond drill holes (6,821 m), preliminary economic assessment (PEA), pre-feasibility study. Environmental studies including environmental and social work plans, alternatives assessment report, geohazard tailings options, tailings assessment engineering, access road assessment Tahltan highland, tailings water management assessment, hydrology baseline, fisheries baseline report, fisheries addendum, bird studies addendum, aquatics baseline report, vegetation and ecosystem mapping baseline, navigable waters assessment, ML-ARD phase 2 report, ML-ARD assessment of surficial samples from the proposed access road, access route geohazards, mountain ungulate baseline. 2009: Metallurgical test work. Environmental studies including meteorology and air quality baseline, country foods baseline update, baseline hydrogeology study. 2010: 14 diamond drill holes (4,010 m). Mineral Resource estimate, metallurgical test work. Titan-24 geophysical survey comprising direct current induced polarization and magneto-telluric surveys. Environmental studies including wildlife habitat suitability baseline, moose literature review, engineering hydrometeorology report, ML-ARD geochemical shake-flask testing of overburden in the proposed pit area, ML-ARD report on 3D modelling of acid-base accounting data, ML-ARD report on acid-base accounting and total solid-phase elements for rock, socio-economic baseline, land use baseline, soils baseline, archaeology baseline study, geomorphic channel assessment and channel migration hazard mapping of Upper Mess Creek.

table continues…

Year	Company	Comments
		2011: 22 diamond drill holes (9,649 m), High-resolution aeromagnetic survey. Titan-24 geophysical survey. Completion of Schaft Creek Mine Project Application Information Requirements/Impact Statement Guidelines. Schaft Creek Project prediction of mine-site-drainage chemistry, ML-ARD through 2011 report. 2012: Mineral Resource estimate, metallurgical test work. Five diamond drill holes (2,266 m) in Discovery and Mike Zones. Additional high-resolution aeromagnetic survey. Winter moose population and distribution survey. 2013: Feasibility study. Z-Axis tipper electromagnetic geophysical survey. Schaft Creek 2011 baseline hydrogeology study.
2008	Claims held by Charles J. Greig, and John Bernard Kreft	Reconnaissance sampling spaced 25 m apart, 183 soil samples, 17 grab and chip samples.
2013–Date	Schaft Creek JV	2013: Five diamond drill exploration and four geotechnical holes (3,453 m). Metallurgical, pit slope design, mapping, core re-logging, geological modelling and environmental studies. Copper-gold-molybdenum-silver mineralization intersected east of the resource block model indicating that the mineralization in the Schaft Creek deposit is open to the east. 2014: Metallurgical, pit slope design, geological modelling and environmental studies; core re-logging, geometallurgical modelling, and collection of additional metallurgical samples for variability testing. Identified LaCasse Zone. 2015: Five diamond drill holes (2,634 m) in LaCasse Zone, optimization studies, core re-logging for geometallurgical, lithogeochemistry, and acid rock drainage investigations, structural modelling, evaluation of soils in areas that could potentially be locations for tailings storage, geophysical survey over the south extension of the Liard zone of the Schaft Creek deposit. A total of 100 representative samples of the lithologies and alteration across the Schaft Creek deposit were collected for geometallurgical test work. Results of the geotechnical, comminution and electrical portions of optimization studies indicated similar findings to those of the 2013 feasibility study. 2016: Core re-logging, environmental monitoring, and collection of field data including humidity cell tests and other environmental baseline data and ongoing consultation with the Tahltan First Nations on social and cultural matters. Voluntary withdrawal from the EA process and the queue for the Northern Transmission Line for the Schaft Creek Project. 2017: Geological and Resource modelling, desktop engineering and trade-off studies, continuation of collection of environmental baseline data and ongoing social activities. Application for a Multi-Year Area-Based permit.

table continues…

Year	Company	Comments
		2018–2019: Updated Resource modelling, ongoing environmental studies, desktop studies to further investigate the geotechnical characteristics of areas that could host tailings facilities, internal sizing and infrastructure alternatives study, internal conceptual study to confirm scenarios that could potentially lower costs, infrastructure and further define access options, and ongoing permitting and community relations activities. A berm reinforcement program was completed with the installation of an extensive gabion wire mesh retaining wall system to protect the camp, drill core, and fuel storage areas from the effects of a 100-year flood event. 2020: Despite the COVID-19 pandemic, a baseline monitoring program was safely completed which consisted of annual servicing of the Schaft Creek Camp and Mount LaCasse climate stations and inspection and downloading of the information from the Skeeter Creek hydrology station located at the northern end of the TMF. A Communications and Engagement Agreement with the Tahltan Central Government was successfully negotiated and signed.

Figure 6-1: Map of Historic Drilling on the Schaft Creek Project

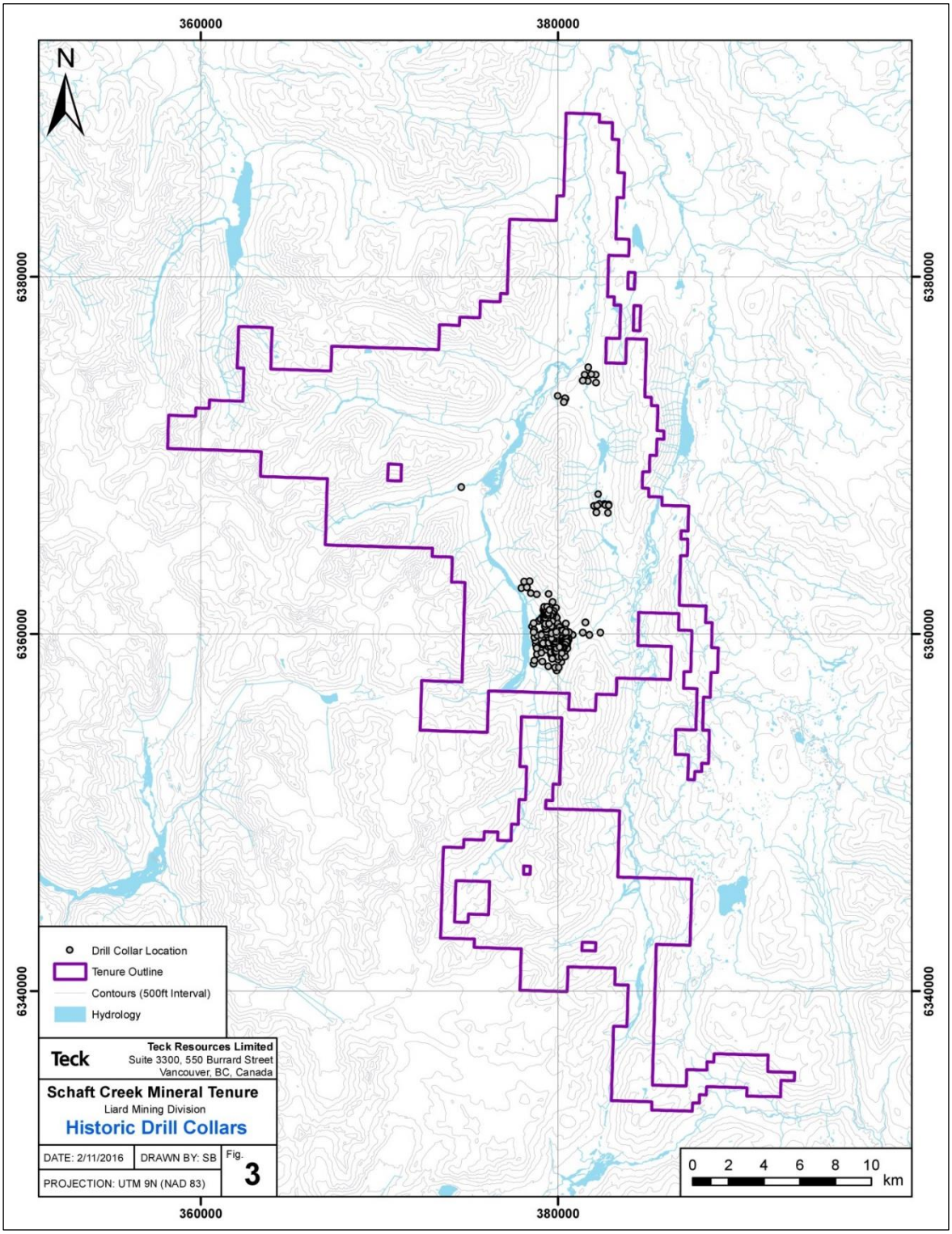

Source: Schaft Creek JV 2016

6.2.1 Schaft Creek JV 2015 Program

The 2015 field campaign completed by the Schaft Creek JV consisted of drilling, IP and magnetometer surveys, rock sampling, soil sampling, geological mapping, surficial geological mapping, geometallurgical sampling, relogging of historical drill core, and updating the 3D geological model.

The 2015 drill program tested the LaCasse Zone, located approximately 4 km north of the deposit area. Drilling at LaCasse consisted of a five-hole, 2,634 m program using a helicopter-portable diamond drill. All five drill holes intersected porphyry-style alteration and veins, as well as associated copper mineralization. The most significant assay results from this program were returned by drill hole SCK-15-444; this hole intersected 182.5 m of 0.20% Cu, including a subinterval of 30 m of 0.40% Cu. Interpretation of drill core and geological mapping suggests that mineralization at LaCasse may be contiguous with the Discovery Zone to the south. In addition, the mineralization style at LaCasse is interpreted to have similarities with the Paramount Zone. Mineralization at LaCasse remains open in several directions, and there is potential in this area to discover high-grade breccia mineralization of the style that occurs at the Paramount Zone.

The 2015 field program explored the Wolverine Creek area, located immediately south of the Liard Zone. The limits of the Liard Zone are not well constrained to the south, and this area has poor outcrop exposure and limited, shallow historical drilling. Exploration activities included geological mapping, relogging of historical drill core, rock sampling, B-horizon soil sampling, and an IP and ground magnetometer survey. As a result of this work, a drill target concept emerged in this area based on coincident chargeability and soil geochemistry anomalies, and structural interpretation. This work better defined the southern limits of the Liard Zone and highlighted potential for resource expansion south of the Basal Fault.

Regional geologic mapping was conducted along the margin of the Hickman Batholith and included two areas of focus: (1) the northern portion of Mount LaCasse; and (2) a mountain located south of the Schaft Creek deposit, colloquially named Mount Hicks. In total, 18 km^2 was mapped at 1:5,000 scale. The mapping completed north of Mount LaCasse included field checking of several historically known mineralized showings, including the Grizzly and Greater Kopper areas.

The 2015 geometallurgical sampling program focused on comminution testing. The test results were used for throughput simulation modelling; the results of this modelling are comparable to the throughput range calculated in the previous feasibility study (Morrison and Karrei, 2012).

Surficial geological mapping was completed in the Skeeter Lake area, which is the location of the proposed tailings storage facility. Colluvial, bedrock, morainal, and fluvial units are the most widespread surficial units within this area. Geological hazards are widespread in the area and mainly include numerous debris flow paths, rock fall and snow avalanche hazards, debris slides, and rock slides. Previous interpretations of a large slope sag structure in the mountains to the east of Skeeter Lake (Holm, 2011) were not supported by the 2015 surficial mapping.

7.0 GEOLOGICAL SETTING AND MINERALIZATION

7.1 Regional Geology

7.1.1 Tectonic Setting

The Schaft Creek Project is located in the northwestern portion of Stikine Terrane, within the Canadian Cordillera. The Stikine Terrane is a tectonostratigraphic domain comprised of Paleozoic to Mesozoic sedimentary rocks as well as volcanic and comagmatic plutonic rocks of island-arc affinity (Monger et al., 1982; Logan et al., 2000). Figure 7-1 shows the position of the Stikine Terrane in northwestern British Columbia. The geological, palaeontological, and paleomagnetic signatures of this island arc indicate that it is allocthonous (Gabrielse et al., 1991), and the terrane is interpreted to have accreted onto the margin of North America by the Middle Jurassic (Nelson and Colpron, 2007). Mineralization at the Schaft Creek deposit, along with the vast majority of other Cu-Au deposits and occurrences in northwestern British Columbia, occurred while the Stikine Terrane was located outboard from North America. During this time, the characteristics of the Stikine island arc were probably analogous to modern island arcs in the southeast Pacific Ocean, such as the Philippine Islands. Following mineralization, the Stikine Terrane accreted onto the margin of North America during the Middle Jurassic and was subsequently impinged upon by accretion of the Insular Terranes and other outboard terranes during the Late Jurassic (Nelson and Colpron, 2007; Nelson et al., 2013).

7.1.2 Regional Stratigraphy

The Stikine Terrane includes three major lithostratigraphic units: the Paleozoic Stikine Assemblage, the Late Triassic Stuhini Group, and the Early Jurassic Hazelton Group (Logan et al., 2000). These rocks are overlain by younger clastic sediments of the Middle Jurassic to Early Tertiary Bowser Lake and Sustut Groups, and Eocene to Recent volcanic rocks of the Edziza and Spectrum Ranges (Logan et al., 2000). The three major units of the Stikine Terrane are described below. Figure 7-2 presents the regional geology of the Schaft Creek area.

The Stikine Assemblage is the structurally and stratigraphically lowest package observed in the Schaft Creek Project area (Figure 7-3). The assemblage consists of a Devonian, Carboniferous, Permian, and Early to Middle Triassic-aged submarine succession of volcanic and sedimentary rocks (Logan et al., 2000). The dominant rock types are tholeiitic to calc-alkaline, mafic and bimodal flows, and volcaniclastic rocks, with interbedded carbonate, shale, and chert. Thick sequences of Permian limestone and mafic volcanic rocks are among the most distinctive rock types of the Stikine Assemblage within the Project area. These rocks occur east of the deposit in the Skeeter Lake Valley and Mess Creek Valley and to the west, south, and southeast of the Hickman Batholith. The Stikine Assemblage is unconformably overlain by the Stuhini Group. This unconformity is locally masked by a steep normal fault or thrust fault.

Figure 7-1: Stikine Arch Map

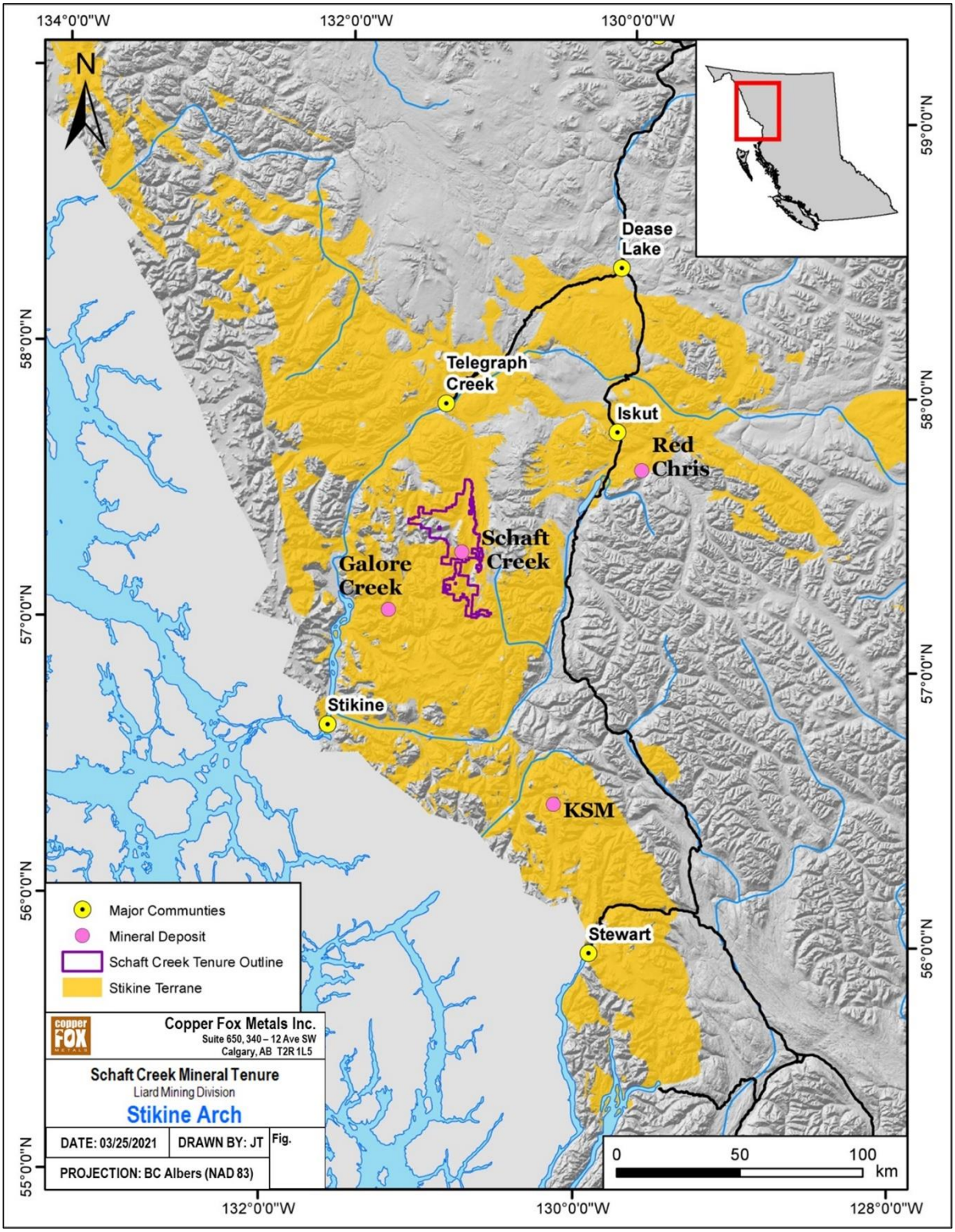

Figure 7-2: Regional Geology Map

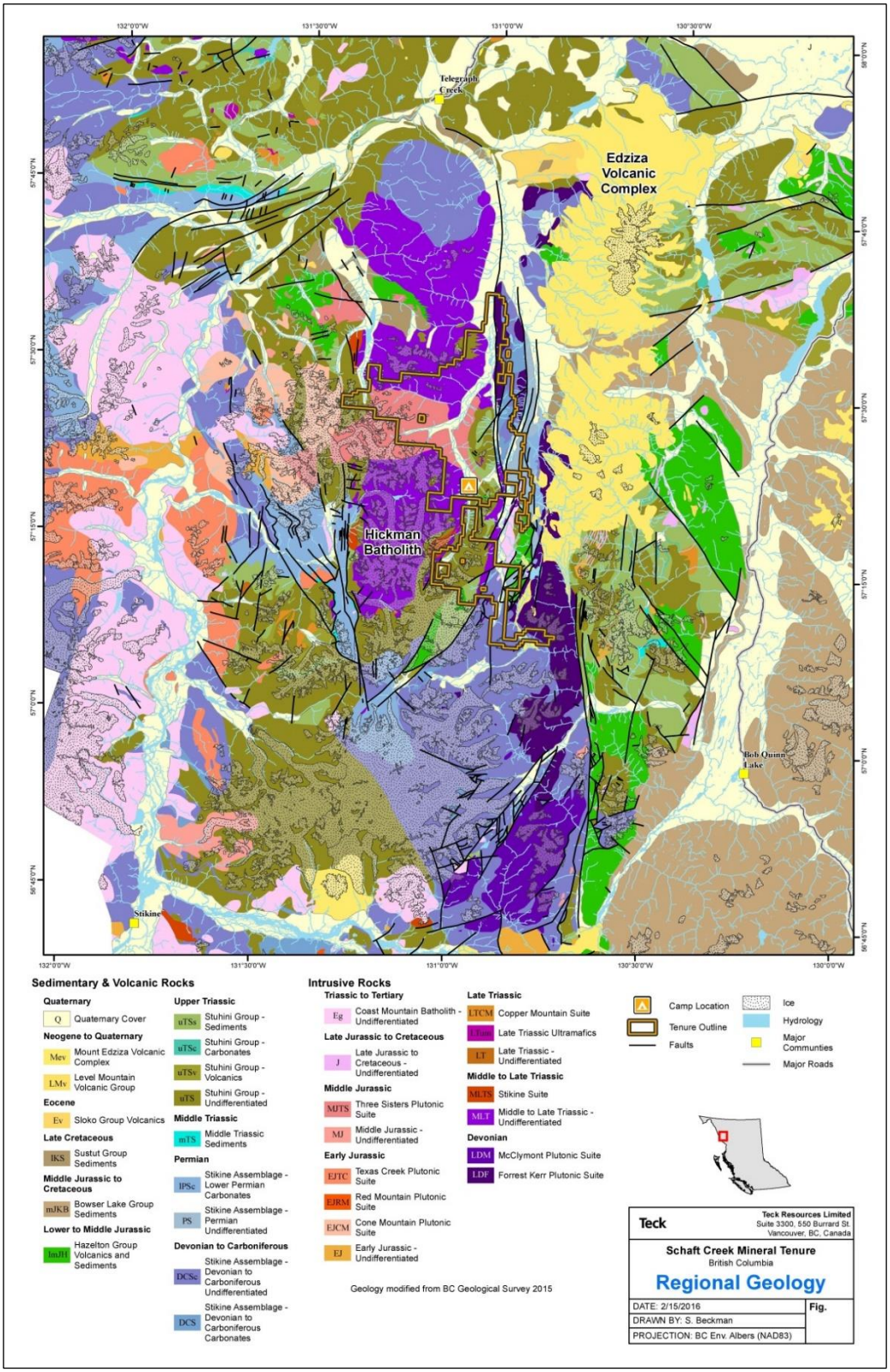

Figure 7-3: Regional Stratigraphic Column

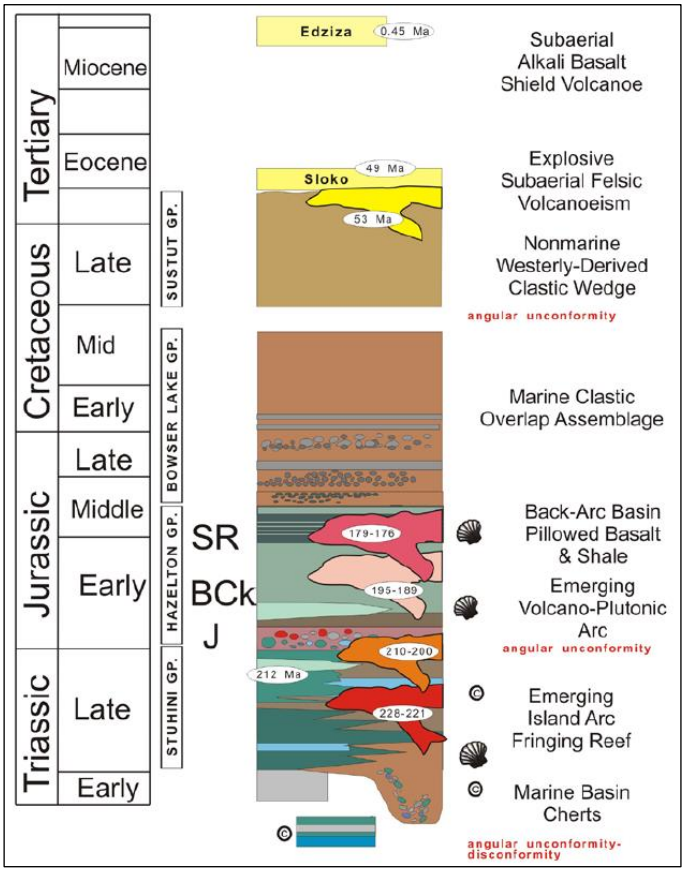

Source: Logan et al., 2000

The Stuhini Group consists of Late Triassic pyroxene and/or plagioclase porphyritic andesitic to basaltic volcanic flows, coarse volcaniclastic breccias, lapilli tuffs, crystal tuffs, and rare epiclastic sandstone and siltstone. Subvolcanic pyroxene and/or plagioclase phyric rocks also occur within the volcanic pile and are considered to be part of the volcanic feeder system (Logan et al., 2000). In the Schaft Creek Project area, the Stuhini Group has been divided by previous workers into five map units. From oldest to youngest, these are (1) a lowermost succession of dun-weathering, recessive, mafic to ultramafic lapilli tuff and minor flows (uTSmt); (2) dark grey, massive plagioclase-phyric basalt and subvolcanic intrusive rock (uTSvb); (3) grey to mauve, massive to weakly stratified, polylithic lapilli tuff and crystal tuff with augite and plagioclase crystal fragments (uTSvt); (4) green to maroon, interbedded, augite-phyric, plagioclase-phyric, augite and plagioclase-phyric, aphyric basaltic andesite flows, and subvolcanic intrusive rocks (uTSpp); and (5) green, well-bedded, fine grained volcaniclastic tuff, tuffaceous siltstone and sandstone, and wacke (uTSs) (Logan et al., 2000). The Schaft Creek deposit and other related mineralization occurs within the Stuhini Group, predominantly within the uTSvt and UTSpp map units. The uppermost Stuhini Group unit (uTSs) has been described to be locally conformable with the overlying basal conglomerate unit of the Hazelton Group (lJHcg) (Logan and Drobe, 1992); however, more commonly, the contact between the Stuhini Group and the overlying Hazelton Group is marked by an angular unconformity or a fault.

The Hazelton Group consists predominantly of volcanic rocks, including basalt, andesite, dacite, rhyolite, and coeval subvolcanic stocks and plugs, as well as lesser sedimentary and volcaniclastic rocks, such as tuff, volcaniclastic wacke, and shale (Logan et al., 2000). The majority of these rocks are subaerial, which is in contrast to the predominantly submarine depositional environment of the Stuhini Group. The lowermost unit of the Hazelton Group is a distinctive polylithic conglomerate that contains a variety of clast types, including volcanic, volcaniclastic, granodioritic, quartz, and limestone clasts (lJHcg). This basal conglomerate unit of the Hazelton Group crops out on top of a mountain colloquially named Mount Hicks, located approximately 3 km south of the Schaft Creek deposit.

7.1.3 Regional Plutonic Suites

The northwestern portion of the Stikine Terrane is intruded by plutonic rocks that represent at least seven magmatic episodes: Late Devonian, Early Mississippian, Late Triassic, Late Triassic to Early Jurassic, Early Jurassic, Middle Jurassic, and Eocene (Logan et al., 2000). Within the Schaft Creek Project area, the majority of plutonic rocks occur in two main north-south trending intrusive belts: (1) the Late Devonian to Early Mississippian belt comprised of the Forest Kerr and More Creek Plutons; and (2) the Late Triassic to Middle Jurassic belt comprised of the Hickman, Yehiniko, and Nighout Plutons and the Loon Lake Stock. To the northeast, the Eocene to Recent rocks of the Edziza and Spectrum Ranges comprise a third major north-south trending volcanic and intrusive belt. Other small plutons occur scattered throughout the region, most notably the volumetrically minor alkalic intrusive rocks of the Late Triassic to Early Jurassic Copper Mountain Suite. The two major intrusive belts in the Schaft Creek Project area are described in more detail below.

The Late Devonian to Early Mississippian intrusive belt occurs to the south and southeast of the Schaft Creek deposit, and is approximately 60 km in length and up to 10 km wide. The two main plutons that comprise the belt, the Forrest Kerr and the Mess Creek Plutons, are separated by the northeast-trending Newmont Lake Graben (Logan et al., 2000). The composition and mineralogy of these two plutons are similar, and each contains several intrusive phases, including hornblende monzodiorite, diorite, tonalite, leucocratic granodiorite, and biotite trondhjemite. In general, the mafic phases occur as inclusions within and are brecciated or crosscut by the felsic phases (Logan et al., 2000). U-Pb zircon dating of the felsic phases of the Forrest Kerr Pluton yielded ages of 369.4 ± 5.1 and 370.7 ± 6.7 Ma, whereas the felsic phase of the More Creek Pluton yielded an age of 356.9 +4.3/-3.8 Ma (Logan et al., 2000).

The Late Triassic to Middle Jurassic intrusive belt occurs immediately west of the Schaft Creek deposit and extends to the north and south along a strike length of approximately 70 km, with a width up to 20 km. The Hickman, Yehiniko, and Nighout Plutons are contiguous in this belt and occur within a distinct physiographical domain of high mountains and large valley glaciers; this geological and physiographical domain has been named the Hickman Batholith (Holbek, 1988). The Loon Lake Stock occurs as a separate intrusion located on the east side of the Mess Creek Valley. These intrusive units are compositionally distinct, and each is described separately below.

The Hickman Pluton is comprised of several distinct phases, including clinopyroxenite, hornblendite, hornblende biotite granodiorite, plagioclase porphyritic diorite, quartz monzonite, and quartz monzodiorite. Ultramafic and mafic phases are crosscut or brecciated by the more felsic phases, which are interpreted to be younger. Locally, mafic and felsic phases of the pluton display magmatic foliation, flow banding, and magma mixing textures. U-Pb zircon dating of samples collected by the Schaft Creek

JV in 2013 and 2014 from the Hickman Pluton yielded ages including 222.32 ± 0.6 Ma for the plagioclase porphyritic diorite in the western part of the pluton; 221.52 ± 0.06 and 221.69 ± 0.07 Ma for granodiorite and monzonite phases in the central part of the pluton; 220.92 ± 0.06, 220.93 ± 0.13, 220.91 ± 0.21, and 220.32 ± 0.15 Ma for granodiorite and quartz monzodiorite phases in the eastern part of the pluton near the Schaft Creek deposit; and 219.27 ± 0.26 and 219.43 ± 0.18 Ma for porphyritic quartz monzodiorite dikes that are spatially associated with mineralization in the Liard Zone within the deposit (unpublished U-Pb dating by Richard Friedman, University of British Columbia; unpublished U-Pb dating by Jim Crowley, Boise State University). Previous U-Pb zircon dating of a porphyritic quartz monzonite dike from the Liard Zone yielded an age of 216.6 ± 2 Ma (Logan et al., 2000).

The Yehiniko Pluton consists of several phases, including coarse grained biotite granite, fine grained monzonite, and syenite. East of the pluton, near Mount LaCasse, a swarm of flow-banded syenite to rhyolite dikes and sills crosscut mineralized veins and breccias that are hosted within the Hickman Pluton. U-Pb zircon dating of samples collected by the Schaft Creek JV in 2013 and 2014 from the Yehiniko Pluton yielded ages including 176.23 ± 0.13 Ma for fine grained syenite in the eastern part of the pluton, 178.87 ± 0.09 and 177.20 ± 0.05 Ma for flow-banded rhyolite and syenite dikes near Mount LaCasse, and 178.20 ± 0.40 Ma for a plagioclase porphyritic felsic dike that crosscuts mineralization in the Paramount Zone within the deposit (unpublished U-Pb dating by Richard Friedman, University of British Columbia; unpublished U-Pb dating by Jim Crowley, Boise State University). The contacts of the Yehiniko Pluton with the Hickman Pluton to the south, and the Nighout Pluton to the north, are obscured by colluvium and alluvium.

The Nightout Pluton consists of hornblende biotite granodiorite, quartz diorite, and quartz monzodiorite and is compositionally similar to the outer phase of the Hickman Pluton (Holbek, 1988). Magmatic foliation and coarse grained poikilitic K-feldspar grains are common throughout much of the pluton (Brown et al., 1995). K-Ar and dating of samples from the pluton yielded ages including 236 ± 9 Ma for biotite and 228 ± 8 for hornblende, whereas Rb-Sr dating of biotite yielded an age of 232 ± 5 Ma (Holbek, 1988).

The Loon Lake Stock occurs to the southeast of the Hickman Batholith, on the east side of Mess Creek Valley, and is approximately 15 km long and 2 km to 3 km wide. The composition of the stock ranges from plagioclase-hornblende porphyritic monzonite to plagioclase porphyritic diorite and fine grained diorite. To the west, the Loon Lake Stock is in contact with a plagioclase diorite unit; this diorite may be a border phase of the Stock, although in part the contact appears faulted and the diorite could also be related to the Hickman Pluton (Logan and Drobe, 1992; Logan et al., 2000). No geochronological data is available for the Loon Lake Stock.

7.1.4 Regional Structural and Deformational History

Evidence of several major deformational events ranging in age from Paleozoic to Cenozoic is present in the rocks of the Stikine Terrane and preserved in foliations, folds, faults, and brittle fractures. Several of these deformational events are linked to large-scale tectonic changes and are associated with episodes of orogeny development, exhumation, and erosion that result in stratigraphic unconformities. The structural history of the Mess Creek area, which is approximately coincident with the Schaft Creek Project area, is described by Logan et al. (2000), and is summarized below.

Evidence of early deformational events (D1 and D2) is preserved in the Paleozoic rocks of the Stikine Assemblage. The earliest event (D1) is characterized by a northeast-striking, moderately northwest-dipping penetrative foliation (S1) that parallel compositional layering within Early to Middle Devonian volcanic and sedimentary rocks. This S1 foliation fabric is axial-planar to mesoscopic, northeast-verging recumbent isoclinal folds (F1). A later event (D2) deforms and transposes the S1 foliation in Devonian rocks and also appears prominently as a foliation fabric (S2) in Carboniferous to Early Permian rocks. The D2 event is associated with southeast plunging, tight to isoclinal, inclined to recumbent folds (F2).

Numerous shear zones and thrust faults developed during D1 and/or D2, within Paleozoic strata that are parallel to compositional layering or that are subparallel to layering and west-dipping. The direction of this faulting and shearing was top plate to the east (Logan et al., 2000; Holbek, 1988). Low-angle faults within the Schaft Creek deposit area, such as the Saddle Fault and the Basal Fault, may represent reactivations of these Paleozoic faults that have projected upwards into the overlying Mesozoic rocks. Elsewhere in the region, similar shallowly west-dipping thrust faults are observed that do not crosscut the Cretaceous Sustut Group, and so this faulting is interpreted to predate the Cretaceous (Logan et al., 2000).

The D1 and D2 deformational events record the Paleozoic development of the Stikine Assemblage. Both events are associated with compressional deformation evidenced by tight to isoclinal folding and thrust faulting, and both events are also associated with greenschist-grade metamorphism. The timing of these two deformational events bounds the emplacement of the Late Devonian Forrest Kerr and More Creek Plutons. Cooling ages obtained from the More Creek Pluton of approximately 330 Ma are interpreted to represent the timing of uplift and unroofing of this pluton, prior to the nonconformable deposition of Mid-Carboniferous to Early Permian carbonates that overlie the pluton. Thus, the Devonian rocks of the Stikine Assemblage were exhumed and subsequently reburied during the Late Paleozoic. The uppermost member of the Stikine Assemblage is an Early Permian carbonate comprised of medium to thickly bedded micritic limestone with local patch reefs that preserve corals in growth positions, indicating a relatively shallow water depositional environment during the Early Permian (Logan et al., 2000).

Following this Paleozoic development of the Stikine Assemblage, the Late Permian to Middle Triassic is marked by a period of non-deposition, or non-preservation of strata, throughout much of Stikine Terrane. However in some areas, such as in the vicinity of the Copper Canyon deposit east of Galore Creek, restricted bands of Middle Triassic thinly bedded chert and siliciclastic rocks are preserved. Elsewhere, such as the Tulsequah and Telegraph Creek areas, this Permian to Triassic period is associated with metamorphism, deformation, and uplift. These features have been linked together as part of an orogenic event that has been named the Tahltanian Orogeny. (Souther, 1972; Brown et al., 1996; Logan et al., 2000). Within the Schaft Creek Project area, the Tahltanian Orogeny is marked by a disconformity or unconformity between the Permian rocks of the Stikine Assemblage and the overlying Late Triassic Rocks of the Stuhini Group. Based upon foliation fabrics and folds preserved in Paleozoic and Triassic rocks, the timing of the Tahltanian Orogeny is constrained to after the D2 deformation event and prior to the D3 deformation event (Logan et al., 2000).

Evidence of a third deformational event (D3) is preserved in the Paleozoic and Late Triassic rocks surrounding the Project area. Within Paleozoic rocks, this event is characterized by a crenulation cleavage (S3) and open to tight crenulation folds (F3). Within Late Triassic Stuhini Group, this event is associated with northwest-trending open folds (F3) that are upright or sometimes overturned. These

folds in the Stuhini Group range in size from outcrop scale to several kilometres in amplitude, with bedding angles typically dipping steeply to the northeast and southwest (Logan et al., 2000). The timing of this deformational event is not well constrained, but the folding that occurs within the Stuhini Group is not present in the overlying Early Jurassic Hazelton Group. The D3 deformational event is therefore interpreted to have occurred during the end of the Late Triassic to Early Jurassic.

An angular unconformity, or in places a non-depositional disconformity, occurs between the Stuhini Group and the overlying Hazelton Group. This unconformity is apparent within the Schaft Creek Project area near the top of Mount Hicks (described below) and is also observed in the surrounding region. Other localities displaying this unconformity include the Kerr-Sulpherets-Mitchell District to the south (Nelson and Kyba, 2013), near Yehinko Lake to the northeast (Brown and Greig, 1990; Brown et al., 1996), and near the GJ deposit to the northwest (Ash et al., 1997; mapping by Teck, 2011–2013). In all of these areas, as well as at other locations in northwestern British Columbia, this unconformity is spatially related to Late Triassic to Early Jurassic mineral deposits and occurrences. The presence of this unconformity has been suggested to be evidence of reactivation of faults, uplift, and erosion occurring broadly coeval with the timing of mineralization in these areas (Nelson and Kyba, 2014).

Evidence for a fourth deformational event (D4) is apparent in Late Triassic and Early Jurassic rocks surrounding the Project area. This deformational event is characteristically associated with northwest-striking, northeast-verging folds (F4) that are upright to overturned. These folds range in amplitude from outcrop-size to several kilometres. Some north-trending faults within the Project area may also be associated with this deformational event. Folds related to this deformational event occur in both the Stuhini group and the Hazelton Group, and as a result, the age of this event is constrained to be Middle Jurassic or younger. This deformation is interpreted to be associated with the accretion of the Stikine Terrane onto the margin of North America during the Middle to Late Jurassic.

Evidence for a fifth deformational event (D5) is widely apparent in the Project area within the Stuhini and Hazelton Groups, as well as to the east within the Bowser Lake Group. This event is characterized by north-trending, moderate to open upright folds with wavelengths ranging from outcrop scale to several kilometres. This phase of folding accommodates most of the shortening observed in Mesozoic rocks, particularly in the Bowser Basin. This deformational event is correlative with the Cretaceous-aged Skeena Fold Belt (Logan et al., 2000). The Skeena Fold Belt is a thin- and thick-skinned fold and thrust belt that is present throughout much of British Columbia. The Skeena Fold Belt accommodates northeastward shortening and is associated with dextral strike-slip faulting. Within the Schaft Creek Project area, there are numerous southwest-striking, northwest-dipping dextral faults that are associated with prominent linear creeks and gullies. These dextral faults are interpreted to have formed during the D5 deformational event. Some of these southwest-trending structures were subsequently reactivated during the Tertiary to accommodate extensional normal faulting and additional dextral translation (Logan et al., 2000).

Large-scale, north-trending fault zones, such as the Mess Creek Fault and Forrest Kerr Fault, are another important structural feature within the region. These fault zones are commonly several hundred metres wide and contain numerous smaller faults within this width. These smaller faults commonly have contradictory offsets, indicating a history of repeated movement along these zones, with different faults active at different times. Other north-south trending valleys, such as the Skeeter Lake valley and the Schaft Creek valley, are interpreted to contain subsidiary structures that are related to the Mess Creek Fault. The Schaft Creek valley has a similar north-trending orientation and is interpreted to be a subsidiary fault structure. Within the Schaft Creek deposit, breccia bodies,

porphyritic dikes, and sheeted quartz-sulphide veins all share a similar north-striking, steeply east-dipping orientation.

The age of these north-trending faults is poorly constrained. Some workers have interpreted these to be ancient faults that originated during the Paleozoic, and which subsequently shaped the tectonic evolution of the region (J. Nelson, personal communication). More recent movement on these faults is apparent at several locations within the surrounding region: To the west of the Hickman Batholith, the north-trending Scud Glacier Fault juxtaposes Permian rocks of the Stikine Assemblage against rocks of the Stuhini Group, implying more than 1,200 m of east-side down displacement that postdates the Late Triassic (Brown et al., 1996). To the south, the Forrest Kerr Fault juxtaposes 2,000 m of Middle Jurassic pillow basalts against rocks representing the Stikine Assemblage and the Stuhini Group, implying more than 2,000 m of east-side down displacement that postdates the Middle Jurassic (Logan et al., 2000). East of the Project area, the Mess Creek fault juxtaposes Late Tertiary to Quaternary rocks of the Mount Edziza volcanic complex against rocks representing the Stuhini Group, indicating east-side down displacement that occurred as recently as 1,340 years ago (Souther 1970; Logan et al., 2000).

7.1.5 Regional Metallogeny

The Schaft Creek deposit is located within a geological and metallogenic domain called the Stikine Arch. The Stikine Arch is located on the north to northwest margin of the Bowser Basin. Within this region, the Stikine Terrane is intruded by numerous Late Triassic to Jurassic plutons, which comprise several major magmatic suites. Several of these magmatic suites are associated with Cu-Au ± Mo ± Ag porphyry- and epithermal-style mineralization, and these styles of mineralization are widespread throughout the Stikine Arch.

The Stikine Arch contains several major undeveloped Cu-Au ± Mo ± Ag mineral deposits (Schaft Creek / Galore Creek) and numerous mineral occurrences. The region hosts an operating mine, Red Chris, a joint venture of Newcrest and Imperial Metals, and several historical mines, including Eskay Creek, Granduc, Premier, Golden Bear, and other smaller producers. Numerous smaller porphyry and epithermal occurrences have been explored by mining companies and junior explorers in recent years.

7.2 Local Geology

7.2.1 Lithology

The Schaft Creek Project area is predominantly underlain by rocks representing two major lithological domains: the Hickman Batholith and the Stuhini Group volcanic rocks (Figure 7-4). The boundary between these two lithological domains is generally obscured by alluvial and colluvial cover in the Schaft Creek valley. West and northwest of Mount LaCasse, the boundary between the batholith and the adjacent volcanic rocks manifests as a steeply east-dipping intrusive contact that is faulted in some places. Within the deposit area, the mineralization straddles the boundary between the batholith and the volcanic rocks, but the orientation of this boundary at depth is not well constrained.

Rock types of the Hickman Batholith that occur within the Project area include, from oldest to youngest, ultramafic dunite and clinopyroxenite, hornblendite, equigranular to weakly porphyritic granodiorite to

granite, porphyritic quartz monzonite to monzodiorite, and various feldspar-quartz porphyritic monzodiorite dikes. Crosscutting relationships between all of these intrusive phases have been observed either in drill core or in outcrops. North of the deposit, on the slopes of Mount LaCasse, syenite to rhyolite dikes and sills occur that are correlative with the Yehiniko pluton. The Yehiniko pluton is comprised of buff to salmon-colored monzonite to syenite.

Rock types of the Stuhini Group that occur within the Project area include basaltic to andesitic volcaniclastic tuffs and breccias, augite and plagioclase phyric coherent volcanic flows, and augite-phyric subvolcanic dikes and gabbroic sills. These Stuhini Group rocks are correlative with regional lithological units uTSvt, uTSv, and uTSvp (Logan and Drobe, 1993; Logan et al., 2000). The strike and dip of these units are not readily apparent within the deposit area due to intense alteration and a lack of marker horizons. Regionally, these rocks generally dip either to the northeast or to the southwest. This contrast in dipping orientations is due to either large-scale folding, fault block rotation, or a combination of both.

A rock type of unknown affinity crops out to the southeast of the summit of Mount LaCasse. In this area, coarse-grained hornblende ± plagioclase phyric volcanic flows (or subvolcanic sills) occur as subcrop and talus over an area of several hundred square metres. Near the periphery of the outcropping area, this unit appears to be conformable with underlying augite-phyric volcanic rocks of the Stuhini Group. The location of this rock type correlates with units “pl” and “h” mapped by Logan and Drobe (1993). The stratigraphic correlation of this unit is uncertain, but the unit may be either a stratigraphically higher part of the Stuhini Group or an isolated volcanic unit of the Hazelton Group.

Major mappable units within the deposit area are described below. The rock types are listed in order from interpreted oldest to youngest, although relative and absolute ages are not well constrained for some of these rock types.

Figure 7-4: Property Geology Map

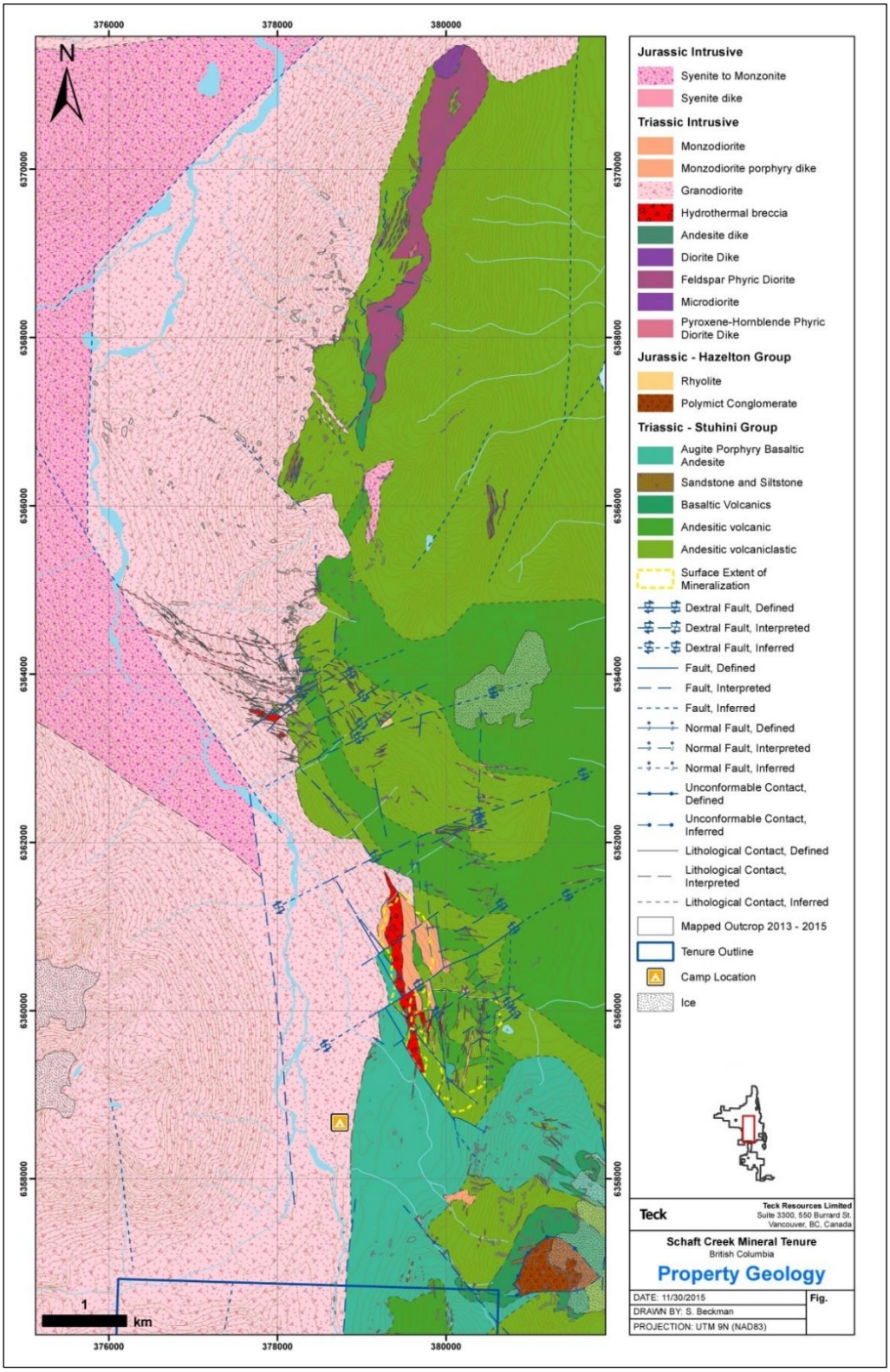

7.2.1.1 Late Triassic Volcanic and Subvolcanic Rock Types

Coherent Andesite (Unit AN): Green to brown to grey, coherent andesite to basaltic andesite flows, and possibly subvolcanic sills. This unit includes variants that are augite-phyric, plagioclase-phryic, and augite-plagioclase-phyric. Augite and plagioclase phenocrysts are 1 mm to 5 mm in diameter, and phenocryst density ranges from sparse to crowded. This rock type is typically weakly magnetic, and locally contains calcite- or chlorite-filled amygdules. This unit is interpreted as the oldest rock exposed in the deposit area and is correlative with the unit uTSv of Logan and Drobe (1993). Locally, this unit is difficult to distinguish from the andesitic volcaniclastic (Unit vAN) described below.

Andesitic Volcaniclastic Rocks (Unit vAN): Green to grey-brown to purple crystal tuff, lapilli tuff, and breccia. These rock types are interpreted as reworked pyroclastic deposits, deposited in a submarine setting. Crystal tuff, lapilli tuff, and breccia facies are commonly interbedded, without obvious marker horizons or consistently mappable grain-size variations. This unit is commonly monolithic, but locally contains clasts of crystalline andesite that are interpreted to be part of Unit AN described above. Crystal tuff and lapilli tuff facies both contain broken crystals of augite and plagioclase 1 mm to 2 mm in diameter, along with glassy lapilli fragments up to 1 cm in diameter. Angular to sub-angular breccia fragments occur in some areas, with diameters up to 10 cm observed in drill core. These breccia fragments commonly contain intense epidote alteration that does not occur in the surrounding matrix. Locally, this unit is interbedded with lenses of brown to grey epiclastic volcanic siltstone, sandstone, and conglomerate, similar to Unit SST described below. This unit appears to be interlayered with Unit AN, although some of this interlayering is suspected to reflect structural imbrication and stratigraphic repetition. This unit is correlative with the unit uTSvt of Logan and Drobe (1993).

This volcaniclastic unit can be difficult to distinguish from coherent andesite flows. Typically, sedimentary textures are used to distinguish volcaniclastic andesite (Unit vAN) from coherent andesite (Unit AN). Specifically, bedding, lamination, normal and reverse graded beds, and lapilli or breccia, or a distinctive ‘grainy’ weathering surface are often used to distinguish Unit vAN from Unit AN. In some cases, it is extremely difficult to differentiate these units during outcrop mapping, and better classification can sometimes be made from drill core or hand samples that have been cut and polished.

Augite-Phyric Basaltic Andesite (bAN): Grey to green, plagioclase-augite ± olivine-phyric basaltic andesite. Augite and plagioclase phenocrysts are 1 mm to 3 mm in diameter and vary from moderately crowded to extremely crowded, with a cumulate texture in some areas. The groundmass for this unit is a glassy, dark green, fine-grained to aphanitic. The genesis of this unit is ambiguous: Near the Schaft Creek deposit, this unit is inferred from drill core intersections to be a subvolcanic sill, although contact relationships with Unit AN and vAN are rarely intact due to hydrothermal alteration and fault deformation. Near Mount Hicks, this unit is interpreted from mapping to be a volcanic unit with local evidence for flow-top brecciation, pillow textures, and conformable stratigraphic relationships with Units BAS and SST. Additionally, this unit has an extremely distinct geochemical signature with high Mg, Ni, and Cr relative to other nearby rock types. Overall, we have thus far been unable to differentiate a subvolcanic component from a volcanic component, and the main identifying characteristic of this unit is the crowded augite-phyric texture and the unusual geochemistry. Historically, this unit was mapped as ‘augite porphyry’ by Salazar (1978), and Logan and Drobe (1993) and included this rock type within unit uTSv.

Olivine-Phyric Basalt (Unit BAS): Grey to green, aphanitic to plagioclase-olivine-phyric basalt. This unit is locally scoriaceous and vesicular, and flow-top breccia textures are apparent in some areas. Vesicles, typically 1 mm to 5 mm in diameter, are filled with either calcite or zeolite. Pillow textures indicative of submarine volcanic deposition occur in several areas near Mount Hicks and Mount LaCasse. The pillows are 0.6 m to 1.5 m in length and with dark halos 1 cm to 2 cm thick. These pillows are commonly altered to epidote or hematite, with local disseminated pyrite. Mapping at several locations during 2015 indicates that the pillows are oriented right-way up. This unit is included within unit uTSv of Logan and Drobe (1993). Near Mount Hicks, the transition between this unit and Unit bAN appears to be gradational, and the rocks near the transition are fine-grained and difficult to categorize.

Plagioclase-Phyric Andesite to Diorite (pAN): Green to grey, plagioclase-phyric andesite to diorite. Plagioclase phenocrysts vary in both abundance and size (commonly 3 mm to 4 mm in length) and are hosted in an aphanitic green groundmass. The composition of this rock type is more dioritic adjacent to the contact with Unit vAN, but away from this contact, this rock type appears to be more andesitic. The dioritic variation is crowded with plagioclase and hornblende crystals. Previous mapping by Logan and Drobe (1993) incorporated this rock type into unit uTSv in some locations, whereas in other locations, it was mapped as plagioclase porphyry. We interpret this andesitic to dioritic unit to be a subvolcanic sill or dike complex, possibly coeval with Unit dDIO described below.

Volcanic Sandstone / Siltstone / Conglomerate (Unit SST): Brown to grey, epiclastic volcanic siltstone, very fine- to coarse-grained sandstone, and conglomerate. Siltstone and sandstone facies are laminated to bedded with beds ranging from 5 cm to over 10 cm thick. Conglomerate clasts are 5 cm to 20 cm in diameter, moderately sorted, and sub-angular. Other sedimentary structures observed locally, include ripple cross-lamination in sandstone and rip-ups of sandstone at the base of the conglomerate units. This rock type occurs interbedded with Unit vAN; this interbedding is particularly apparent on the northeastern and eastern ridges of Mount LaCasse. This unit is included in Logan and Brown's (1997) uTSvt unit as "minor bedded epiclastics".

Diorite Dike (Unit dDIO): Grey to green, plagioclase- and pyroxene-phyric diorite dike. Plagioclase phenocrysts are up to 5 mm long. The width of this unit is typically 1 m to 5 m. Trachytic textures are locally apparent. North of Mount LaCasse, this rock type is observed to occur as a dike that crosscuts interbedded sandstone and volcaniclastic rocks (SST and vAN). Nearby, this unit is observed to transition from a crosscutting dike into a bedding parallel sill within this interbedded sequence. This unit is interpreted to be coeval with Unit pAN described above.

Microdiorite (Unit mDIO): Grey, equigranular, fine-grained, plagioclase- and pyroxene-phyric diorite with fine-grained to aphanitic groundmass. This rock type occurs on the northwestern side of Mount LaCasse, near the limit of the recent mapping by the Schaft Creek JV. This unit may be correlative with unit uTpd mapped by Logan and Drobe (1993). The age of this intrusive unit is not known.

Hornblende- and Pyroxene-phyric Diorite Dike (Unit dhpDIO): Grey to light grey, hornblende-phyric ± pyroxene-phyric diorite. Hornblende phenocrysts are up to 2 cm long, and 4 cm to 5 cm wide. Pyroxene phenocrysts range from 5 mm to 25 mm in length. Locally, phenocryst size decreases with proximity to intrusive contacts. This unit intrudes Units AN and vAN.

7.2.1.2 Late Triassic Intrusive Rock Types

Granodiorite (Unit GDR): Pink and grey, medium-grained, equigranular, hornblende-biotite granodiorite to granite. Characteristically, this rock type has a crowded, cumulate-like, equigranular texture that distinguishes it from other porphyritic intrusive phases. Locally, this rock type contains xenoliths of andesitic volcanic rocks (Unit AN or vAN). This rock type is the oldest phase of the Hickman Batholith within the deposit area. Zircon grains from this unit have yielded U-Pb ages of ~221.7-220.3 Ma. This rock type is crosscut by Unit QMZ, described below, and is interpreted to be pre-mineral.

Monzonite (Unit MONZ): Grey, feldspar-phyric monzonite. This unit has crowded feldspar phenocrysts 1 mm to 3 mm in length, and smaller hornblende and biotite phenocrysts ~2% in a fine-grained groundmass. This unit is more porphyritic near the intrusive contact and more equigranular away from the margins. In addition, mafic phenocrysts increase (up to 10%) adjacent to the intrusive contact. This unit was not mapped by Logan and Drobe (1993), but may be correlative with either the Late Triassic Hickman Pluton or the Early Jurassic Yehiniko Pluton.

Quartz Monzonite (Unit QMZ): Pale pink and grey, medium-grained, equigranular to slightly porphyritic, feldspar-hornblende-quartz phyric monzodiorite to monzonite. Characteristically, this rock unit contains 1% to 5% rounded quartz phenocrysts. Locally, hornblende and feldspar phenocrysts display a trachytic texture. This unit is observed to crosscut Unit GDR and contains xenoliths of the granodiorite. This rock unit is interpreted to be pre-mineral or early-syn-mineral, as it is commonly proximal to mineralization and crosscut by quartz-sulphide veins, particularly in the Paramount Zone. Zircon grains from this rock unit have yielded U-Pb ages of ~220.9 Ma to 220.3 Ma.

Regionally, the quartz monzonite unit may be difficult to distinguish from Unit GDR, particularly in areas with weathered outcrop or limited exposure. More confident identification can sometimes be made from drill core or hand samples that have been cut and polished. Staining using hydrofluoric acid and sodium cobaltinitrate is also useful for determining the amount of K-feldspar and hematite in these rock types.

Quartz Monzodiorite Dikes (Unit sPOR): Pink to buff-grey, fine- to medium-grained, porphyritic, feldspar-hornblende-quartz phyric monzonite to monzodiorite. Characteristically, this rock unit has a crowded porphyritic texture with an aphanitic to fine-grained groundmass. This unit commonly occurs as narrow, 1 m to 30 m thick, porphyritic dikes that vary in thickness along strike and down dip. These dikes are observed to crosscut Units GDR and QMZ. In some locations, these dikes crosscut hydrothermal breccias, but this is not a consistent relationship. This rock type is interpreted to be syn-mineral because it has a close spatial association with sulphide mineralization, potassic alteration, and zones containing quartz-sulphide vein stockworks. Zircon grains from this rock unit have yielded U-Pb ages of ~219.4 Ma to 219.3 Ma, as well as older grains with ages of ~220.5 Ma to 220.1 Ma. These older grains are interpreted to be antecrysts inherited from the Hickman Batholith.

In previous years, efforts were made to differentiate this unit into separate dike variants based upon phenocryst composition. However, these compositional differences could not be consistently mapped between drill holes and between outcrops, and so all variants of syn-mineral monzodioritic dikes have been combined into Unit sPOR.

Intrusive Breccia (Units IBX1 and IBX2): Tan, grey, and pink, polylithic or locally monolithic breccia. Generally this unit is matrix-supported, with a coherent (igneous) matrix of quartz-feldspar ± hornblende ± biotite. Breccia cement typically consists of quartz ± sulphides, but also locally includes calcite and anhydrite. Clasts are typically subround to subangular and 1 cm to 10 cm in diameter. Clast types include Units QMZ and sPOR. In some locations, clasts have been observed to contain quartz-sulphide veins with potassic alteration that pre-dates brecciation. This unit is interpreted to be syn-mineral because it contains sulphide-bearing cement, and because it is closely associated with zones of quartz-sulphide vein stockwork. In some areas, this unit is associated with autobrecciation textures and a gradational contact into Unit sPOR, suggesting that these two units are genetically linked.

Hydrothermal Breccia (Units cHBX1, cHBX2, cHBX3, cHBX4, cHBX5, cHBX6, cHBX7): Tan, green, and pink, polylithic or locally monolithic breccia. Generally clast-supported and lacking a distinct matrix. Several varieties of hydrothermal breccia have been differentiated based upon their cement composition, including the following: quartz-epidote-chlorite-chalcopyrite ± molybdenum ± bornite cement (cHBX1); quartz-biotite-K-feldspar ± magnetite ± chalcopyrite (cHBX2); tourmaline-quartz-carbonate ± chalcopyrite ± bornite ± molybdenum (cHBX3); pyrite-carbonate-chlorite (cHBX4); feldspar-anhydrite ± quartz ± chlorite ± chalcopyrite ± bornite ± pyrite (cHBX5); sericite-quartz-pyrite-chlorite (cHBX6); and chlorite-actinolite-calcite ± tourmaline ± chalcopyrite-pyrite. Clasts in these breccias are generally subrounded to angular, locally with a jigsaw texture, and are 1 cm to 20 cm in diameter. The clasts include a variety of rock types, including Units AN, vAN, QMZ, and sPOR. As with the intrusive breccia unit, in some locations, this unit contains clasts containing truncated quartz-sulphide veins. Locally, there appears to be a gradational contact between hydrothermal breccia and intrusive breccia, and these two units are interpreted to be approximately coeval. Spatial and genetic relationships between the different breccia cement types are not well understood, and more work is required to resolve the distribution of these hydrothermal breccias.

7.2.1.3 Early Jurassic Sedimentary Rock Types

Polymictic Conglomerate and Volcanic Sandstone (Unit CGL): This unit consists of interlayered polymicitic conglomerate and volcanic sandstone. The sandstone is purple-pink with medium-grained quartz and feldspar broken crystals that are interpreted to be reworked tuffaceous material. The sandstone contains sub-angular fragments of basaltic andesite and volcanic sandstone that range from 1 cm to 10 cm in diameter. The polymicitic conglomerate is a conspicuous, purple-colored, pebble to boulder clast-supported to matrix-supported conglomerate with subrounded to subangular clasts. Clasts include rhyolite, basaltic scoria, and plagioclase-phyric andesite. The matrix is comprised of red-colored, fine-grained sand to mud-sized material. Near Mount Hicks, the conglomerate and the sandstone are interlayered, and both form beds that dip to the southeast, unconformably overlying the andesitic volcanic rocks of the Stuhini Group. Upsection, the layers of volcanic sandstone become thicker and more abundant than the layers of conglomerate. This unit was mapped as Unit lJcg by Logan and Drobe (1993).

7.2.1.4 Early Jurassic Intrusive Rock Types

Plagioclase Diorite Dikes (Unit pPOR): Green-grey, fine-grained, sparsely porphyritic, plagioclase-phyric diorite dikes, typically 1 m to 10 m thick. This unit crosscuts all the rock types described above, and also crosscuts quartz-sulphide vein stockworks and potassic alteration. This unit typically contains chlorite-epidote alteration and trace pyrite ± chalcopyrite mineralization. This rock unit is therefore interpreted to be post-mineral with respect to the main porphyry mineralization event at Schaft Creek. Zircon grains from this rock unit have yielded a U-Pb age of ~178.2 Ma, as well as an older U-Pb age of ~221.6 Ma. This older age is interpreted to be caused by antecrysts inherited from the Hickman Batholith.

Basaltic Andesite Dikes (Units dAN and dANp): Green to grey-green, fine-grained, plagioclase- and pyroxene-phyric basaltic andesite dikes, typically 1 m to 10 m thick. This unit has several characteristic features including chilled margins; calcite amygdules; and abundant, fine-grained magnetite. In the field, this unit forms blocky, resistive, rounded outcrops. This unit crosscuts all of the rock types described above and is not typically observed to host any significant sulphide mineralization. An absolute age has not yet been determined for this unit.

Syenite to Rhyolite Dikes (Unit dSY): Pink to buff, fine-grained, syenite to rhyolite dikes, typically 1 m to 10 m thick. Commonly quartz- or plagioclase-phyric and occasionally has an aphanitic texture. Flow banding and chill margins are a common feature of this unit, and in some instances, the banded appearance makes this rock type look similar to a bedded volcanic or sedimentary rock. This rock type crops out commonly on the southwest side of Mount LaCasse, and talus from this unit form rusty red talus fields that can appear similar to a hematite gossan from a distance. This unit also occurs commonly within the LaCasse Zone and crosscuts sulphide mineralization in this area. Zircon grains from a syentic dike yielded a U-Pb age of ~177.2 Ma, whereas grains from a rhyolitic dike yielded two U-Pb ages: a younger age of ~178.8 Ma and an older grain population with an age ranging from 221.3 Ma to 220.6 Ma. These older grains are interpreted to be antecrysts inherited from the Hickman batholith. The 178 Ma to 177 Ma ages are similar to the Unit pPOR described above and also similar to the Yehiniko Pluton, which is located to the west.

7.2.2 Structure

Major structures in the resource area that either truncate or offset mineralization, or are considered potentially significant geotechnical domains, are described below. The structures are described in order from interpreted oldest to youngest.

The **Basal Fault** is interpreted to be one of the oldest faults in the deposit area, based upon crosscutting relationships interpreted from drill core. The fault is an important boundary for mineralization in the Liard Zone and is interpreted to be late-mineral or post-mineral. The fault dips gently to the northwest and consists of a narrow sheared or cataclastic zone, sometimes with several separate anastomosing fault strands. These anastomosing strands commonly enclose slivers of mineralized rock within the fault zone. The anastomosing nature of the fault strands, the low angle of the fault, and other field relationships, suggest that the Basal Fault is most likely a thrust fault, although other interpretations are possible. Currently, it is not apparent if this fault extends under the West Breccia Zone or under the Paramount Zone; drill holes in these areas are generally not deep enough to intersect the modelled position of this fault. The Basal Fault is interpreted to daylight south of the Liard Zone.

Work completed by the Schaft Creek JV during 2015 has highlighted the possibility of mineralization in the footwall of the Basal Fault, and to the south of the Liard Zone. Additionally, interpretation of geophysical data from the Wolverine Creek area suggests that there may be another flat-lying structure further south at depth; this could be an additional, lower, sub-parallel fault to the Basal Fault.

The **Saddle Fault** is interpreted to be a splay off of the Basal Fault and is an important boundary for mineralization on the north side of the Liard Zone. The fault dips moderately to the north and consists of a broken, fractured, or sheared zone. Late movement on this fault is interpreted to have normal offset based upon geological mapping observations, but it is not clear if the fault has an earlier movement history with reverse offset. The Saddle Fault has been modelled to truncate against the Paramount Fault, and it is not clear if the Saddle Fault extends further westward.

The **Breccia Footwall Fault** and the **Silica Fault** are important boundaries for mineralization in the West Breccia Zone. These faults strike to the northwest and dip steeply to the east. The offset of these faults is not known with certainty, but the Silica Fault has been modelled to have an apparent sinistral offset of approximately 300 m. The faults are inferred to be related because of their similar orientation, although their appearance can be different locally. The Breccia Footwall Fault has broken, fractured, gouged, and sheared textures, and is typically 5 m to 10 m wide. In contrast, the Silica Fault has broken, gouged, sheared, or healed textures, but is typically much wider, with a fault damage zone approximately 30 m to 50 m thick that contains several fault strands. The large damage zone of the Silica Fault is potentially an important geotechnical consideration.

The **Paramount Fault** and the **Snipe Fault** do not appear to be major boundaries for mineralization, but both faults have large damage zones that are potentially important geotechnical features. These faults strike approximately north, and dip vertical or steeply to the east. These faults are interpreted to be younger than the four faults described above, although this is an observation from geological mapping that is difficult to confirm in drill core. These faults contain broken, fractured, and gouged textures, with fault damage zones that are 10 m to 20 m thick. To the east of the Paramount Zone, the Paramount Fault has been modelled as a single structure. However, widely spaced drilling in this area has intersected a large amount of faults, and there may be several other faults that are sub-parallel to the Paramount Fault. This area is the location of the highwall for the proposed open pit, and the large damage zones of faults in this area are an important geotechnical consideration.

The **Northeast Fault** and the **Mike Fault** are the youngest faults in the deposit area that have been modelled. These faults are associated with northeast trending gullies that occur on the slopes of Mount LaCasse. There are numerous northeast trending faults throughout the deposit area, although many of these are too small to warrant modelling. These northeast trending faults contain broken and fractured damage zones, and are typically 5 m to 20 m thick and may be important for geotechnical consideration in some areas. These faults dip steeply to the north and have an apparent dextral sense of movement, although a component of normal movement is also inferred. These northeast faults do not appear to be major boundaries for mineralization.

7.2.3 Alteration

Hydrothermal alteration in the Schaft Creek Project area includes a variety of mineral assemblages. These mineral assemblages are interpreted to be coprecipitated and to be representative of specific factors including pressure, temperature, pH, fluid composition, and in some instances, wall rock composition. Many of these hydrothermal alteration assemblages are spatially associated with sulphide mineralization, either as proximal assemblages or distal assemblages. The zonation pattern of these alteration assemblages can be a useful tool for locating areas of sulphide mineralization, although consideration must be given to post-mineral faults that disrupt the alteration zonation. Similar alteration assemblages throughout the property suggest a shared origin for sulphide-mineralized zones at Schaft Creek, Discovery, LaCasse, Grizzly, and other mineralized occurrences throughout the property area. Major alteration assemblages within the Project area are described below.

Early Magnetite Alteration (FEO): This alteration type is characterized by thin, wispy magnetite veinlets that sometimes have K-feldspar selvages as well as minor chalcopyrite and bornite. Mapping and identification of this early magnetite alteration is challenging because much of the magnetite has been subsequently replaced by hematite during a later alteration episode. Nevertheless, there is consistent, sparse evidence of early wispy magnetite/hematite veins throughout the deposit area. There is some evidence to suggest that this early magnetite alteration is best preserved around the fringes of the mineralized zone, but this spatial relationship is equivocal. A rare variant of this alteration assemblage consists of intense magnetite/hematite pseudomorphic alteration of augite phenocrysts within volcanic rocks.

K-Feldspar-Biotite Alteration (Potassic) (kPOT, bPOT, kbPOT): This alteration assemblage is characterized by K-feldspar ± biotite that occurs as a halo around quartz-sulphide veins or, less commonly, as pervasive alteration of a groundmass or matrix. Vein types that have been observed with this halo include quartz-only veins, quartz-molybdenite veins, quartz-chalcopyrite-bornite veins, and quartz-chalcopyrite-pyrite-veins. Rare biotite-only veins with K-feldspar selvages have also been observed locally. Some quartz veins with K-feldspar selvages have irregular to slightly wavy margins that are indicative of vein formation at higher temperatures. Some of these veins can be correlated with the “A vein” and “B vein” terminology that is classically applied at many porphyry deposits. However, other potassic veins at Schaft Creek exhibit sheared textures that do not fit this classic terminology. Within the core of the deposit, veins with K-feldspar alteration halos also commonly have selvages containing green mica. This green mica is inferred to be muscovite, and this mineral appears to be spatially associated with high-grade mineralization. Some other minerals also occur locally as part of the potassic assemblage, including calcite within the veins and epidote within the vein halo. At the LaCasse Zone, epidote is commonly associated with K-feldspar, in an assemblage that has been labeled as Calc-Potassic.

Potassic alteration appears to be the assemblage that is most closely associated with Cu-Au mineralization within the deposit area. Because of this important association, “Weak Potassic” and “Strong Potassic” domains have been differentiated during geological mapping and 3D modeling; the distinction between these domains is based upon intensity of alteration.

Albite-Hematite Alteration (Albitic) (ALB, SOD): This alteration assemblage is characterized by white feldspar (presumed albite) with hematite ± anhydrite ± chlorite. Vein types that have an albitic selvage include quartz ± bornite-chalcopyrite-molybdenite, quartz-albite ± bornite-chalcopyrite-molybdenite, and anhydrite-albite ± bornite-chalcopyrite-molybdenite. Narrow, wispy, anhydrite-only veins also occur in zones of albitic alteration, and these are presumed to be part of the same assemblage. However, there are also other, thicker anhydrite-only veins elsewhere in the deposit area that are interpreted to be paragenetically late. Locally, there is evidence of veins with albite selvages crosscutting veins with potassic selvages; however, this relationship is rarely observed. Overall, the abundance of albite-hematite alteration is difficult to quantify, because this alteration assemblage is difficult to distinguish from K-feldspar alteration or quartz alteration. However, albite alteration is closely associated with some areas of higher-grade Cu-Au mineralization, particularly in some breccia phases within the Paramount Zone.

Quartz Alteration (Silicic) (SI): This alteration assemblage is characterized by fine-grained silicification that is typically fracture-controlled, although selective phenocryst alteration and pervasive alteration also occur locally. Silicic alteration is characteristically associated with tourmaline alteration, which helps to differentiate this assemblage from other feldspar alteration. Vein types that have a silicic selvage include quartz-only, quartz-carbonate ± chlorite, tourmaline ± chlorite, and tourmaline-quartz-carbonate ± chlorite ± bornite ± chalcopyrite ± molybdenite. Silicic alteration and tourmaline-bearing veins are sometimes associated with high Cu-Au grades, particularly in the Paramount and West Breccia Zones, although high grade material in these zones is also associated with other alteration assemblages.

Sericite-Carbonate-Clay Alteration (SER, SCC, PHY): This alteration assemblage is characterized by fine-grained white mica ± trace clay. Vein types that have a phyllic alteration selvage include quartz-only, carbonate ± quartz ± pyrite, pyrite-only, and tourmaline-bearing veins. Some grey sericite-pyrite-quartz veins occur that are broadly analogous to the “D vein” terminology classically used for porphyry deposits; however, veins of this type are rare at Schaft Creek.

Sericite-Albite-Carbonate-Chlorite-Tourmaline (Phyllic) (PHY): This alteration assemblage occurs in patchy zones around the periphery of the Schaft Creek deposit. For example, a “phyllic breccia” with intense sericite-chlorite-pyrite-albite ± tourmaline alteration occurs in the gap between high-grade mineralization at the Paramount Zone and the lower-grade mineralization at the West Breccia Zone. Another large, phyllic alteration zone occurs northeast of the deposit at the Mike target area. This area contains a sericite-pyrite-chlorite assemblage that is coincident with a large IP chargeability high.

Chlorite-Epidote-Carbonate (Sodic Calcic, Propylitic) (CHL, SOC, CAL): This alteration assemblage is characterized by chlorite-epidote ± calcite ± actinolite ± hematite. This alteration is widespread, but the intensity of alteration is generally low. Chlorite alteration of mafic phenocrysts and volcanic groundmass is common throughout the deposit area. Vein types that have a chlorite-epidote halo include quartz-carbonate-chlorite ± chalcopyrite ± pyrite, chlorite-only, and calcite-only. Rare magnetite-quartz-carbonate-chalcopyrite-pyrite veins are observed in chlorite-altered areas within the deposit, and these are interpreted to be related to this assemblage. Chlorite-epidote alteration occurs in all rock types within the deposit area, and commonly overprints earlier alteration assemblages such as potassic and sericitic. An assemblage of chlorite-epidote-pyrite appears to be the most distal part of the deposit footprint; this alteration extends several hundred metres beyond the limits of potassic alteration.

Hematite Alteration (HEM): This alteration assemblage consists of hematite ± chlorite ± calcite. This alteration is characterized by red, brown, or purple coloration, and can occur pervasively or selectively along fractures. This alteration is not typically associated with veins, except where it replaces other vein-hosted minerals (e.g., magnetite). This hematite alteration is interpreted to have a relatively late timing and is inferred to be part of the late propylitic alteration that overprints much of the deposit area. Hematite staining of feldspars is also common throughout the deposit area, although this is interpreted to be related to the albite alteration described above.

Purple-colored volcanic rocks containing abundant hematite occur immediately north of the Liard Zone, above the Saddle Fault. Historically, the rocks in this zone have been differentiated by some workers into a separate lithological unit labeled as “purple volcanics”. This area contains no mineralization, and some workers have argued that these purple volcanic rocks are a post-mineral unit that unconformably overlies the deposit. Based upon mapping and extensive relogging completed in 2013 to 2014, the Schaft Creek JV argues that this historical interpretation is incorrect, and that these rocks are part of the Stuhini Group. This area contains no mineralization because the “purple volcanics” are juxtaposed against the deposit by a major fault (the Saddle Fault).

7.2.4 Mineralization

Mineralization at Schaft Creek (Caron et al. (2012) has been described in terms of three separate zones: the Main (or Liard) Zone, the Paramount Zone, and the West Breccia Zone. Although mineralization in the Main Zone and the West Breccia Zone is found in two generally spatially separate areas in the southern portion of the Schaft Creek deposit, the same cannot be said for mineralization found further to the north. There, most mineralization is hosted within structurally prepared and altered breccias, with a lesser amount of mineralization found in proximal volcanic units. It seems clear that mineralization at Schaft Creek can be readily described in terms of an earlier phase of mineralization in the Main Zone and a later phase of mineralization related to breccias and proximal volcanic rocks found along the west margin of the Main Zone and extending to the north.

More details on the mineralization styles specific to the Liard, Paramount, and West Breccia Zones can be found in Section 8.0 Deposit Types.

8.0 DEPOSIT TYPES

The Schaft Creek deposit has been described by many workers as a calc-alkaline Cu-Mo-Au porphyry deposit (Fox et al., 1995; Spilsbury, 1995; Scott et al., 2009; Morrison and Karrei, 2012). Other workers have considered it a shear-hosted, low-sulphidation Cu-Mo-Au-Ag vein deposit (Le Boutillier, 2013). Early mapping assigned the intrusive host rocks of the Schaft Creek deposit to the Early Jurassic (e.g., Logan and Drobe, 1993), but subsequent geochronology work constrained the age of the host rocks to the Late Triassic (Logan et al., 2000; Scott et al., 2009; unpublished U-Pb dating by Richard Friedman, University of British Columbia; unpublished U-Pb dating by Jim Crowley, Boise State University). Interpretation of the deposit is complicated by a lack of outcrop, complex hydrothermal alteration, post-mineral faults, and sparsity of drilling near the fringes of the hydrothermal system.

The deposit has historically been subdivided into two or three distinct mineralized zones, although the boundaries of this subdivision have changed during the history of the Project. These three mineralized zones are named the Liard, Paramount, and West Breccia Zones. Historically, the West Breccia and Liard Zones have been grouped by some workers into a larger domain called the Main Zone. Other workers have grouped the Paramount and West Breccia Zones into a single domain called the Breccia Zone.

The division between these various zones originated during the earliest years of the Project, when the mineral claims overlying the deposit were divided between Paramount Mining Ltd. (to the north) and Liard Copper Mines Ltd. (to the south). The old property line between these two companies coincides with a change from predominantly breccia-style mineralization in the Paramount Zone to predominantly vein stockwork-style mineralization in the Liard Zone. Recent work has shown that there is considerable spatial overlap between breccia and vein-hosted mineralization styles in both zones and that brecciation in the Paramount Zone extends southwards into the West Breccia Zone.

For this Technical Report, we retain the basic nomenclature of the Liard, Paramount, and West Breccia Zones to describe the Schaft Creek deposit. We caution that the historical boundaries between these zones were commonly based upon geography, and that there is considerable overlap in mineralogy and texture between these geographical boundaries. The characteristics of each of these three zones, along with the faults and other boundaries that constrain them, are described below.

8.1 Liard Zone

The Liard Zone comprises narrow, porphyritic quartz monzonite to quartz monzodiorite dikes that have been emplaced into andesitic volcanic and volcaniclastic host rocks. The dikes are typically 5 m to 50 m thick, strike north-northwest to north-northeast, and dip steeply to the east. Numerous narrow dikes occur within the eastern part of the Liard Zone, and in this area it can be difficult to trace individual dikes with confidence between drill holes or outcrops. In contrast, a single, thicker “Central Porphyry” dike occurs within the central portion of the Liard Zone.

The porphyritic dikes in the Liard Zone are spatially associated with potassic alteration, increased density of quartz-sulphide veins and vein stockworks, and a zone of elevated Cu-Au grade. The most intense alteration and highest copper grades commonly occur in the host rock immediate adjacent to the porphyry dikes, rather than within the dikes themselves. In some areas, chalcopyrite, bornite, and

pyrite all occur disseminated within the host rocks and porphyry dikes, suggesting multiple mineralization episodes that have juxtaposed bornite and pyrite into the same area.

Several types of vein-hosted mineralization are recognized in the Liard Zone. These include (1) Cu-Au-Mo mineralization resulting from quartz-biotite-bornite-chalcopyrite ± hematite veins with associated K-feldspar ± green mica selvages; (2) overprinting Cu-Au mineralization resulting from quartz-chlorite-pyrite-chalcopyrite ± calcite ± epidote ± hematite with associated sericite and chlorite-epidote selvages; and (3) late, Mo mineralization resulting from veins of massive to semi-massive molybdenite with no apparent selvage. No preferred structural trend has been identified for this vein-hosted mineralization in the Liard Zone.

The boundaries of the Liard Zone are defined by faults in most directions. To the north, the mineralization is abruptly truncated by the Saddle Fault, which strikes west and dips moderately to the north. To the south and at depth, the mineralization is abruptly truncated by the Basal Fault, which strikes west and dips shallowly to the north. To the east, mineralization diminishes in proximity to the Snipe Fault, but this fault is not a hard boundary. To the west, mineralization diminishes in the vicinity of the Silica Fault, although the West Breccia Zone occurs to the west of this fault.

8.2 Paramount Zone

The Paramount Zone comprises an elongate, multiphase igneous-hydrothermal breccia body that has been emplaced into quartz monzonite and andesitic volcanic host rocks. The breccia body strikes north-northwest, dips steeply east, is 100 m to 300 m thick, has a strike length of approximately 1,200 m, and extends at least 600 m below surface. High-grade mineralization occurs within the breccia body and also extends 100 m to 200 m into the quartz monzonite hanging wall and, to a lesser extent, into the footwall andesitic volcanic rocks. Mineralization outside of the breccia body is associated with stockwork zones containing quartz-sulphide veins.

Three styles of mineralization occur within the Paramount breccia body, each of which is associated with different breccia cement minerals. These mineralization styles include (1) Cu-Mo mineralization associated with K-feldspar-biotite-quartz-chalcopyrite-molybdenite ± bornite veins and breccias with associated potassic alteration (Unit cHBX2), (2) Cu-Au-Mo mineralization associated with anhydrite-bornite-chalcopyrite ± molybdenite veins with associated albitic alteration (Unit cHBX5), and (3) Cu-Au-Mo mineralization associated with tourmaline-quartz-carbonate-chalcopyrite ± bornite ± molybdenite veins and breccias with associated silicic alteration (Unit cHBX3). All three of these breccia styles include sulphide cement, and the assay grade of sample intervals typically correlate with the amount of sulphide cement present (typically 0.5% to 3%). Locally, there appears to be an association between high-grade mineralization and a dark-colored intrusive breccia phase. The mineralogy of this intrusive breccia appears similar to the syn-mineral sPOR dikes in the Liard Zone, but work is required to confirm the link between these two rock types.

A mineral zonation pattern is apparent around the main breccia body in the Paramount Zone. Potassic alteration intensity, vein density, and vein thickness all increase towards the breccia zone. A clear sulphide zonation (from chalcopyrite > pyrite, to chalcopyrite > bornite, to bornite > chalcopyrite) is apparent outside of the breccia body and extends inwards. No pyrite was observed in bornite-bearing areas, which is in contrast to late pyrite that overprints areas of the Liard Zone. Bornite correlates closely with Au grades, and assay ratios of Cu:Au are an effective vectoring tool towards bornite-rich

zones. Molybdenite occurs throughout the Paramount Zone, and does not appear to be a useful mineralization indicator.

The boundaries of mineralization in the Paramount Zone are related to the extent of the Paramount breccia body, and this body is reasonably well-constrained by the current drill pattern, although the breccia remains open at depth. The limits of the breccia are well defined by drilling to the east and west and to a considerable depth. To the north, the breccia appears to pinch out, although this area has only sparse drilling. To the south, the breccia body continues towards the West Breccia Zone; however, there is an important change in breccia mineralogy in the vicinity of 6360250N. In this area, the dominant mineralogy of the breccia changes from quartz-feldspar-sulphide ± chlorite cement (Units cHBX1, cHBX2, cHBX3, cHBX5), to an assemblage comprised of sericite-tourmaline-chlorite-pyrite ± minor chalcopyrite (Unit cHBX6). This domain has been labeled as a “phyllic breccia”, and mineralization in this area is pyrite-rich and low grade. The changes in cement mineralogy throughout the breccia body are not well understood, and more work is required to understand this mineral zonation pattern.

8.3 West Breccia Zone

The West Breccia Zone comprises an elongated, hydrothermal breccia body that has been emplaced into andesitic volcanic and volcaniclastic rocks. The breccia body strikes north-northwest, dips steeply east, is 80 m to 160 m thick, has a strike length of approximately 500 m, and extends at least 200 m below surface. Mineralization is limited to the breccia body and seldom extends far into the adjacent footwall or hanging wall. There are a few narrow monzodiorite dikes in the vicinity of the breccia that appear similar to the monzodiorite dikes seen in the Liard Zone.

The West Breccia Zone is similar to the Paramount Zone breccia and comprises different styles of mineralization associated with certain breccia cement minerals. However, the West Breccia Zone is dominated by low- to medium-temperature breccia mineralogy and lacks the higher temperature assemblages that are observed within the Paramount Zone. The three prominent styles of breccia mineralogy at the West Breccia Zone include (1) Cu-Mo-Au mineralization associated with tourmaline-carbonate-chalcopyrite-pyrite ± molybdenite veins and breccias with associated silicic alteration (Unit cHBX3), (2) Cu-Mo mineralization associated with chlorite-calcite-pyrite veins and breccias with associated propylitic alteration (Unit cHBX4), and (3) high-grade Cu-Mo-Au mineralization associated with chlorite-actinolite-calcite-tourmaline breccia cement (cHBX7). Interestingly, although the West Breccia Zone lacks bornite, assay grades in this area are sometimes very high because of the abundance of sulphide cement (typically 2% to 10%).

The boundaries of the West Breccia Zone are generally poorly constrained. Historical drilling in this area is sparse and shallow. The breccia body remains open to the north and south, and the recent drilling has only identified the breccia to a depth of 160 m to 200 m. There is no evidence that the breccia body pinches out in any of these directions; however, the grade in historical drill holes is inconsistent and the structural controls on the breccia body are poorly understood. To the east, the Silica Fault is interpreted to offset the West Breccia Zone with a sinistral sense of movement, but more work is required to confirm this. To the west, the Breccia Footwall Fault is interpreted to truncate the West Breccia Zone, but more work is required for confirmation.

8.4 Other Mineralized Zones Outside of the Deposit Area

The Schaft Creek deposit is situated within a 12 km long trend of mineralization that occurs along the margin of the Hickman Batholith (Figure 8-1). This trend straddles the contact between intrusive rocks of the batholith and the adjacent volcanic host rocks. The trend was recognized by previous workers including Adera Mining (Lammle, 1966), Phelps Dodge (Phelps and Gutrath, 1972), and Teck (Betmanis, 1978; Raven, 1979; and Holbeck, 1981), and various workers at the Schaft Creek deposit. The history of work along this trend is comprehensively summarized by Greig (2009).

Mineralization along the trend consists of pyrite, chalcopyrite, and occasionally bornite that occur variably as fracture-controlled, shear zone-controlled, or sparsely disseminated. Sulphide mineralization occurs in an area that is typically 100 m wide along the intrusive contact, but locally expands into wider zones that are 200 m to 500 m wide. This sulphide mineralization appears to be continuous along the margin of the batholith, from Grizzly Canyon in the north to Wolverine Creek in the south.

Alteration along the trend consists predominantly of chlorite-epidote alteration of the volcanic host rocks and pink-colored or buff-grey-colored alteration of the intrusive rocks. Previous workers have recognized that the pink-colored alteration results predominantly from hematite rather than from K-feldspar. At the LaCasse Zone, mineralization and alteration are crosscut by syenite to rhyolite dikes that are associated with the Yehiniko Pluton; however, these dikes also contain disseminated chalcopyrite. More work is required to understand if the Yehiniko Pluton is associated with a second, younger mineralization episode during the Late to Middle Jurassic.

There is potential to discover and delineate additional zones of porphyry mineralization along this trend. Much of the trend has only been examined through piecemeal prospecting, soil and rock sampling, and limited geological mapping. Prior to 2015, the only substantial drill test of this trend was conducted at the Discovery Zone by Copper Fox in 2011 to 2012. This drilling returned encouraging results, including sizeable intervals of Cu-Au mineralization associated with intrusive breccias, quartz-sulphide vein stockwork zones, and high temperature potassic and albitic alteration assemblages. There is opportunity to conduct systematic exploration along this trend and to prioritize key targets for additional work. Some of the more interesting target areas that have been identified along this trend are summarized below.

Figure 8-1: Mineralized Corridor and Target Areas

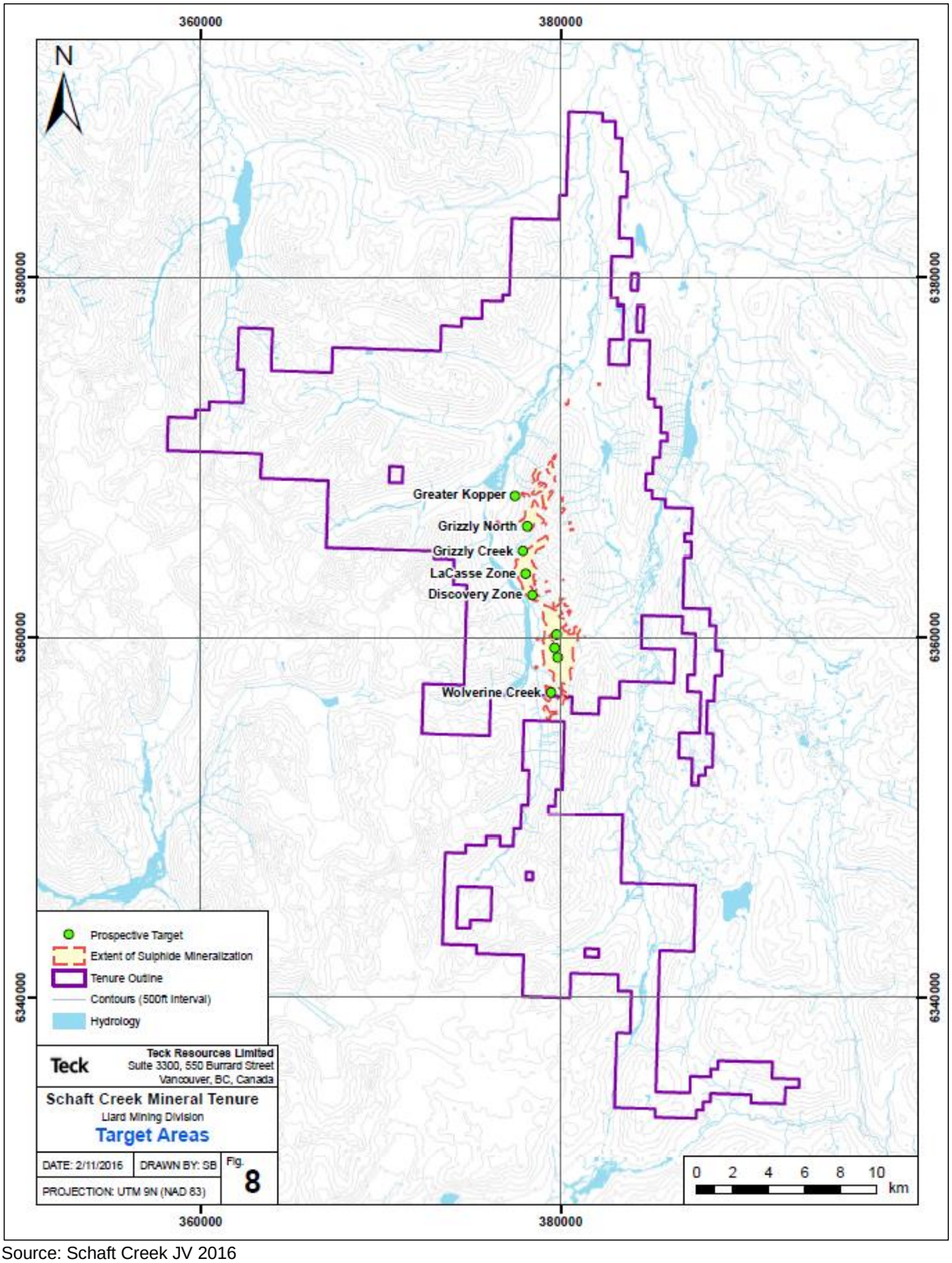

Source: Schaft Creek JV 2016

8.4.1 LaCasse-Discovery Zone

The LaCasse-Discovery Zone is located 3 km to 5 km north of the Schaft Creek deposit, along the margin of the Hickman Batholith. Early workers recognized a trend of mineralization that extended into this area (e.g., Lamelle, 1966). In the 1980s, an area of “consistent copper mineralization” was documented (Betmanis, 1978; Raven, 1979). Rock chip samples from within this zone included numerous samples with grades of 0.5% to 3.15% Cu. Key geological features mapped include disseminated chalcopyrite, bornite, pyrite, quartz veins, and mineralized breccia zones. In particular, the presence of outcropping breccias is considered to be a favorable indicator of prospectivity, because breccias are intimately associated with mineralization at the Paramount Zone and the West Breccia Zone.

Within the LaCasse area there is a timber platform of unknown age located at 378016E, 6363460N (UTM NAD 83 Zone 9N). At this site, narrow diameter drill casing is observed to be sticking out of the ground, but the depth of this drill hole is unknown, and there is no known record of drill core being recovered from this area.

During 2014, the Schaft Creek JV expanded their geological mapping program to encompass the LaCasse area and to collect additional rock chip samples. This mapping largely confirmed the previous mapping, but added an additional level of detail. The predominant rock type in the mineralized zone consists of quartz monzonite to monzodiorite to granodiorite, with crosscutting andesite and syenite dikes. The mineralized area at LaCasse was delineated as a zone of chalcopyrite > pyrite mineralization approximately 1 km by 1.5 km in size. This area contains patchy zones of K-feldspar-biotite-quartz (potassic assemblage) and hematite-albite-epidote-chlorite (sodic-calcic assemblage), as well as widespread chlorite, epidote, and magnetite. Sulphide mineralogy and zonation is similar to the Schaft Creek deposit, although only trace bornite has been observed at LaCasse.

During 2015, the Schaft Creek JV conducted a drill program at the LaCasse area. A key outcome of this program was the recognition that the LaCasse Zone and nearby Discovery Zone have similar mineralization styles. The results obtained from the widely spaced drilling at LaCasse and Discovery are suggestive of a large hydrothermal system with a sizeable mineralized footprint. The geometry of the mineralized system is inferred to be approximately tabular, paralleling the margin of the batholith, striking approximately north, dipping steeply east, and plunging to the south.

8.4.2 Grizzly Area

The Grizzly Area is located approximately 2 km north of the LaCasse Zone, or approximately 5 km north of the Schaft Creek deposit. In this area, pyrite-chalcopyrite mineralization occurs at the boundary between the Hickman Batholith and adjacent volcanic rocks of the Stuhini Group. Mineralization occurs as disseminated sulphides, and also as small sulphide veinlets. The most intense mineralization occurs in the fine-grained volcanic siltstone unit that out crops within the Grizzly area. This mineralization is associated with moderate to intense K-feldspar-epidote-chlorite alteration. Scree and talus slopes around the mineralized outcrops have abundant float with malachite and azurite. This area was previously mapped and sampled by several historical workers (Betmanis, 1978; Raven, 1979; Greig, 2009).

8.4.3 Greater Kopper Area

The Greater Kopper Area is located approximately 2 km north of the Grizzly Area, or approximately 7 km north of the Schaft Creek deposit. In this area, relatively intense chalcopyrite-pyrite mineralization occurs over a small area within intrusive rocks of the Hickman Batholith, near the contact with the volcanic rocks of the Stuhini Group. This copper sulphide mineralization occurs disseminated and within sulphide veins. Mineralization is associated with hematite-albite ± epidote alteration, and possibly with some K-feldspar alteration. This area was previously mapped and sampled by several historical workers (Betmanis, 1978; Raven, 1979; Greig, 2009). Mapping in the vicinity of the showing also identified numerous aplite dikes and barren quartz veins with K-feldspar halos. These features are interpreted as evidence of high temperature hydrothermal alteration in the Greater Kopper Area. Historically, the intrusive rocks hosting the Greater Kopper mineralization have been mapped as part of the Early Jurassic Yehinkio Pluton (Logan and Drobe, 1993). However, based on recent mapping from 2015, the Schaft Creek JV interpreted the host rocks to be Late Triassic granodiorite to quartz monzodiorite and thus similar to the Hickman Pluton further south.

8.4.4 Wolverine Creek Area

The Wolverine Creek Area is located immediately south of the Schaft Creek deposit, within a heavily forested area on the lower northwestern slopes of Mount Hicks. This area contains several separate mineralized showings, believed to be related to a possible southern extension of the Schaft Creek mineralized system. Four of these showings were examined in 2015, and each is described here.

Basal Fault Footwall Breccia: A previously unrecognized hydrothermal breccia was identified by relogging of historical drill core from near the southern limit of the Liard Zone during 2015. This breccia is a monomictic, clast-supported breccia with quartz-calcite-epidote-albite-chalcopyrite ± bornite cement. The clasts are typically subround to subangular andesitic volcaniclastic rocks and augite-phyric basaltic andesite. This breccia appears similar to a volcaniclastic breccia; however, the cement composition is interpreted as evidence of a hydrothermal origin. Currently, this breccia has only been identified over a relatively small area in approximately three historical drill holes; however, drilling in this area is very sparse and the breccia is open in several directions. Other drill holes nearby contain narrow intervals of pyrite-chalcopyrite-bearing monzodiorite dikes that appear similar to the mineralized dikes within the Liard Zone. Recognition of this breccia is potentially significant because it represents the first evidence of mineralization in the footwall of the Basal Fault.

Wolverine Creek Showing: Outcropping sulphide mineralization occurs along the creek bed of Wolverine Creek, approximately 1 km south of the breccia zone described above. In this area, monzodiorite dikes are observed to crosscut augite-phyric basaltic andesite. Pyrite and chalcopyrite mineralization and sericite-chlorite-epidote alteration occurs in the vicinity of these dikes. Historical mapping also identified chalcopyrite, pyrite, and minor bornite in outcrops along the creek bed of Wolverine Creek, as well as nearby along the creek bed of Hickman Creek (Salazar, 1978).

Monzodiorite Bluff Showing: Outcropping sulphide mineralization and intense chlorite-epidote-sericite alteration occurs near a small quartz monzodiorite stock that has been mapped northeast of Wolverine Creek, on the slopes below Mount Hicks. In this heavily forested area, several outcrops were observed that contained disseminated pyrite-chalcopyrite and pyrite-chalcopyrite-calcite veins with chlorite-epidote halos.

Mount Hicks Showing: A narrow zone of structurally controlled, high-grade Cu-Au mineralization occurs southwest of the summit of Mount Hicks. This structurally controlled zone is located at the faulted boundary between the Early Jurassic polymictic conglomerate and the underlying Late Triassic volcanic rocks. In this area, copper oxide mineralization occurs with quartz-chlorite-epidote-chalcopyrite veins that are up to 5 cm thick. These veins host highly anomalous copper and gold grades.

In addition to these four showings, the Wolverine Creek Area has been historically mapped and found to contain numerous other small zones of pyrite-chalcopyrite mineralization and chlorite-epidote ± sericite alteration (Salazar, 1978). The showings within the Wolverine Creek Area cover approximately 3 km^2. Much of this area is covered by colluvium and mature forest. The scattered occurrences of mineralization and alteration in this area are suggestive of a large contiguous zone that is poorly exposed. This zone could either represent the southernmost portion of the Schaft Creek deposit, or it could represent a separate hydrothermal center that is either located at depth or possibly to the south. The Wolverine Creek Area was a focus for soil sampling and an IP survey during 2015.

9.0 EXPLORATION

9.1 Introduction

Copper Fox acquired the Schaft Creek Project in 2002 and performed exploration activities and completed several technical reports on the Project until formation of the Schaft Creek JV with Teck in July 2013. Since formation of the Schaft Creek JV, exploration activities have been completed by the Schaft Creek JV. A summary of the historical work programs by survey type completed on the property to the effective date of this Report are summarized below.

9.2 Historical Mapping Programs

The initial geological investigation of the region was conducted by the Geological Survey of Canada, as part of the Operation Stikine project, with mapping of the 104G 1:250,000 map sheet, on which Schaft Creek is located. The geological investigation was carried out in 1956 and preceded the discovery of mineralization at Schaft Creek in 1957.

In 1964, a trenching and geological mapping program was carried out for Silver Standard and the BIK Syndicate. This program mapped the distribution of the known showings and the contact of the Hickman Batholith and Triassic andesites, noting chalcopyrite-bornite mineralization in closely spaced fractures in outcrop. Asarco's 1967 exploration program at Schaft Creek included geological mapping.

Exploration work carried out by Kennco Explorations (Western) Limited under option from the BIK Syndicate in 1959 included geological surveys. In 1964, a trenching and geological mapping program on eight profiles across the Schaft Creek deposit was carried out on what were then the Bud, Sno, and Bird claims for Silver Standard and the BIK Syndicate. This program assessed the prospectivity of claims, mapped the distribution of the known showings and attempted to understand the relationships between the mineralized zones. The party mapped the contact of the Hickman Batholith and Triassic andesites, noting chalcopyrite-bornite mineralization in closely spaced fractures in felsites at the Bird showing. Asarco's 1967 exploration program at Schaft Creek included geological mapping.

9.2.1 Hecla / Paramount, 1968–1977

In 1969, Hecla optioned the property and continued work on the Project until 1973, conducting extensive exploration work. Hecla's geological map and cross sections of the deposit have stood the test of time, identifying many key features of the deposit, including the Paramount and West Breccias, syn-mineral porphyry dikes, and major structures. The level of detail of the Hecla work is demonstrated in the geological map shown in Figure 9-1, which formed the basis for the modern interpretation (Figure 9-4).

Figure 9-1: Hecla's Historic 1978 Geological Map of the Schaft Creek Deposit

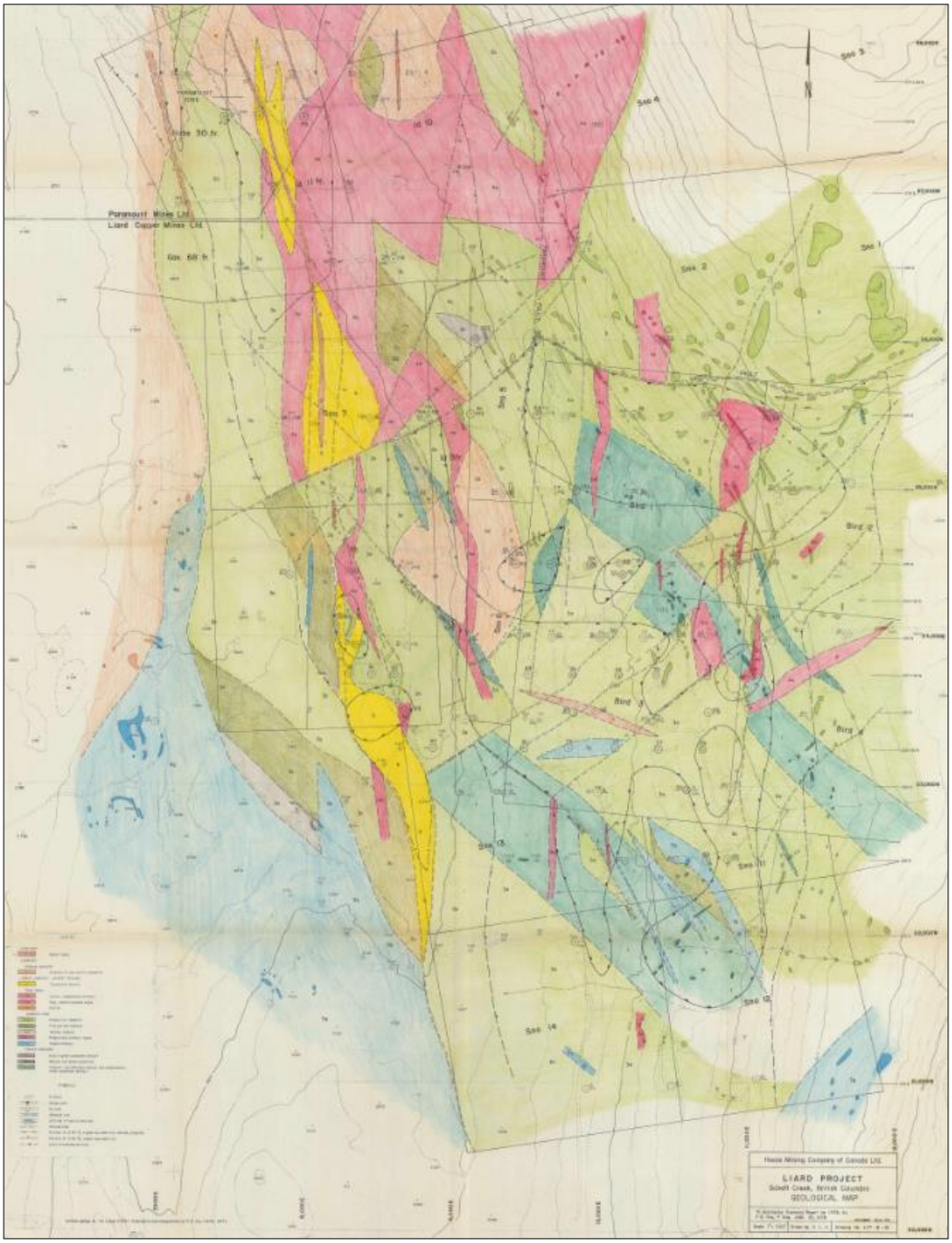

9.3 Grids and Surveys

In 1969, Hecla contracted Underhill and Underhill to set up a local grid. Nine cairns were erected using a helicopter. A survey of the claims separating the Liard and Paramount properties was completed, and a legal boundary was established.

In 1980, Teck contracted McElhanney Associates (McElhanney) to survey all drill hole collars using a laser theodolite located at fixed, previously surveyed points with prisms at drill hole collars. McElhanney also surveyed some of the Hecla drill holes to tie in the survey to the previous Hecla surveys.

Eagle Mapping completed a photogrammetry survey during 2005. Data were provided at 1:2,000 scale and on 5 m contour intervals.

A light detection and ranging (LiDAR) survey was flown over the deposit area in 2011. A helicopter Z-Axis tipper electromagnetic (ZTEM) geophysical survey was conducted in 2013. Both surveys produced digital terrain models (DTMs) and digital elevation models (DEMs). The provincial government's Terrain Resource Information Management provides base topographic data for the Province of British Columbia, and a DEM can be purchased from the government.

The topographic surface used by the Schaft Creek JV in resource estimation was generated from a 1 m DTM. This file has been inherited from previous resource estimation efforts, and the ultimate source of the file has not been resolved, though it was likely originally sourced from the 2011 LiDAR survey. The collar locations were compared to the topographic surface, and due to some differences in elevation, all collar locations were relocated to the topographic surface.

9.4 Geological Mapping

In 1964, the BIK syndicate completed basic mapping of eight traverses crossing the area of the Schaft Creek deposit.

In 1969, Hecla completed regional geological mapping of the area surrounding the Schaft Creek deposit covering an area of 10 miles by 6 miles at a scale of 1″:400′.

In 1971, the Geological Survey of Canada mapped the regional geology at a scale of 1:250,000.

In 2007, Copper Fox completed a mapping program that encompassed an area of 3.6 km by 2.6 km (936 ha) at a scale of 1:5,000 using global positioning system (GPS) control. Targeted outcrops were identified by airphoto interpretation and archival geological maps. Locations were subsequently plotted on a 1:5,000 topographical base map derived from digital orthophoto georeferenced maps produced by Eagle Mapping Ltd.

9.4.1 Schaft Creek JV, 2014

Geological mapping of the Schaft Creek deposit area was conducted during 2014 at two scales: The northeastern portion of the Liard Zone was mapped at a 1:1,000 scale utilizing the excellent exposure provided by a large number of historical drill road cuts, trenches, and drill pads. The remainder of the deposit area was mapped at a 1:5,000 scale. This work primarily focused on the

outcrop above treeline to the northeast of the Main and Paramount Zones, and further north near the Discovery and LaCasse Zones. Geological information outside of this field mapping area was compiled from historical maps by Hecla, Teck, Copper Fox, the British Columbia Geological Survey, and other workers.

The geological mapping was conducted using a modified version of the paper-based Anaconda-style. This method captures outcrop-based information on lithology, structure, veins, alteration, and mineralization, with a focus on alteration minerals and crosscutting relationships. Mapping was conducted on mylar sheets using aerial photographs, topographic maps, and a handheld GPS. Structural measurements were made using a Brunton compass. The geological mapping was supplemented by top-of-hole relogging of drill holes in areas with limited outcrop exposure.

9.4.2 Schaft Creek JV, 2015

The 2015 mapping program focused on two areas: Mount LaCasse to the north and Mount Hicks to the south. Mapping was carried out at a scale of 1:5,000 using a modified Anaconda-style, providing 18 km^2 of coverage. The Mount LaCasse mapping continued on from where the 2014 mapping left off at the LaCasse target, providing coverage northward along the prospective contact of the Hickman batholith and the Stuhini volcanics, including assessment of mineral occurrences along this trend. Mapping to the south in the Mount Hicks area aimed to put the south end of the Liard Zone into context with an improved understanding of the stratigraphy and structure to the south of the deposit, and to assist in the target development work carried out over a covered area immediately south of the resource area.

Geological maps were scanned, georeferenced, digitized into ArcGIS, and merged with 2014 and 2015 mapping to create a seamless geology map (Figure 9-4).

9.5 Geophysics

In 1974, Hecla established a grid for mapping and geophysical surveys, and conducted low level air photography. IP surveys completed by McPhar Geophysics Ltd. revealed the distribution of sulphides, in particular, the pyritic halo.

In 2007, Copper Fox retained Associated Geosciences Ltd. to performed IP, electrical imaging, and magnetic total field surveys to map bedrock topography to support project infrastructure. The IP survey located a 250 to 300 m wide IP-chargeability anomaly immediately east of the Liard Zone.

In 2010 and 2011, Copper Fox completed 70.2 km of direct current induced polarization (DCIP) and 64.0 km of magneto-telluric (MT) surveys over the Schaft Creek deposit. The surveys were completed on 24 east-west oriented lines and 3 north-south oriented tie lines that were surveyed using differential GPS instrumentation. The surveys were completed at 400 m line spacing, with stations at 50 m intervals along lines. The IP survey failed to reconfirm the chargeability anomaly located immediately east of the Liard Zone identified in 2007.

The main results of the 2010 to 2011 surveys are:

a. The chargeability anomaly associated with the Schaft Creek deposit extends over a strike length of 3,200 m.

b. The chargeability anomaly suggested that the majority of the historical drilling was completed on the west flank of the deposit (Liard Zone) and was too shallow to test the eastern deeper part of the chargeability anomaly.

c. New chargeability anomalies were identified over the Mike Zone and the ES and GK Zones (all within a 6 km strike length) located north of the Schaft Creek deposit.

d. A total of 31 potential targets with different priority levels were identified by the 2010 to 2011 survey.

Results of the surveys are shown graphically in Figure 9-2.

Figure 9-2: Results of the Quantec Titan 24 IP and MT Survey, with Chargeability Anomalies Outlined

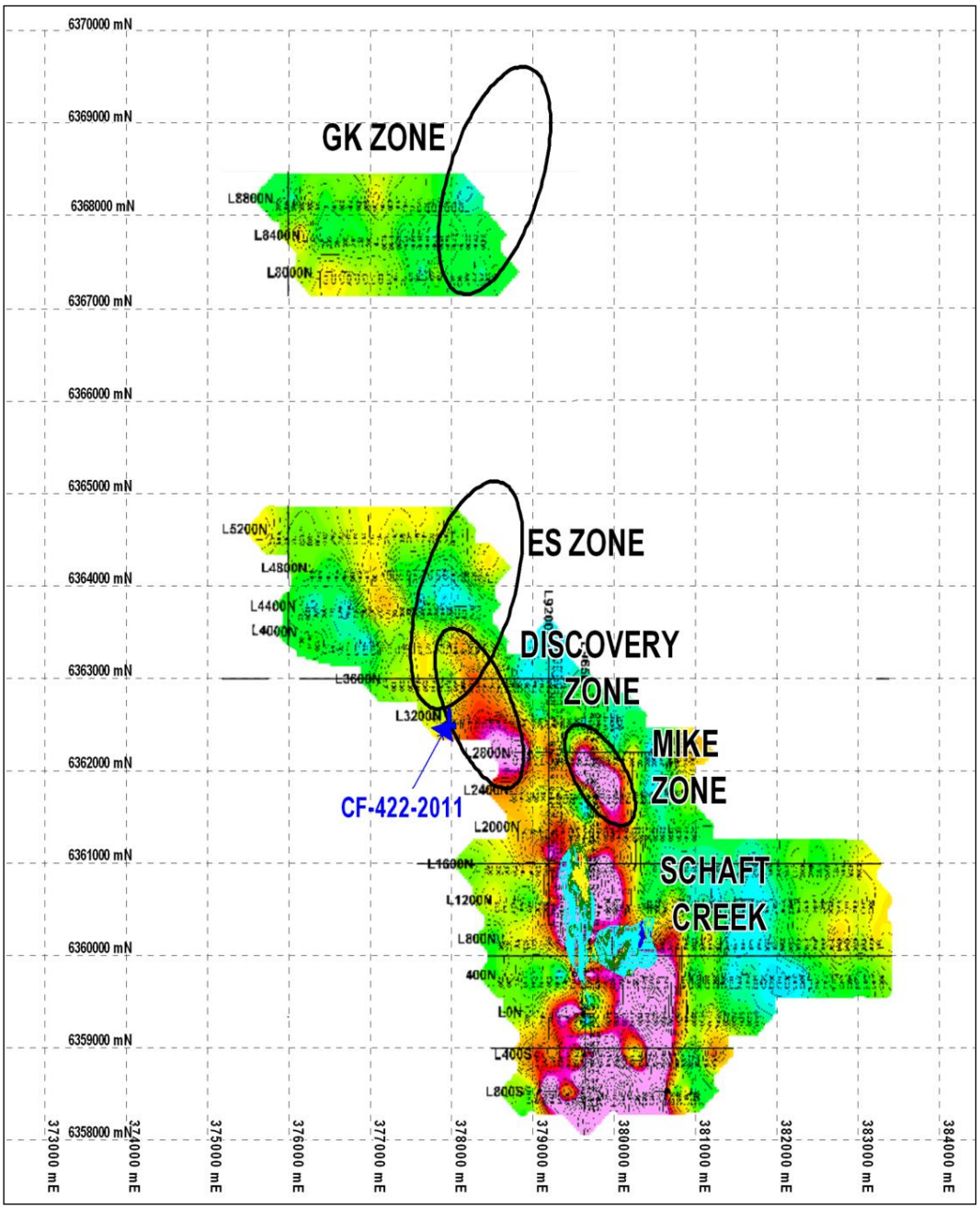

Source: Copper Fox (2021)

In 2011 and 2012, Copper Fox contracted Precision GeoSurveys Inc. from Vancouver, British Columbia.to complete high-resolution aeromagnetic surveys that effectively delineated the extent of the major intrusive rock units located near the deposit, and identified some areas of magnetite alteration that were verified through logging and surface mapping.

The aeromagnetic surveys were flown at 200 m spaced flight lines at an average altitude above ground level of 39 m. Tie lines were flown at 2 km intervals. The magnetic data were collected using a Scintrex cesium vapour CS-3 magnetometer, which is a high sensitivity / low noise magnetometer. The magnetometer and the base station used in the survey have absolute accuracy range of 0.1 nT (gamma) and a sensitivity of 0.1 nT (gamma) at a two-second sampling rate.

The survey covered a 25 km long by 17 km wide area. A total of 2,514 line kilometres (including tie-lines) of survey were completed. The total magnetic intensity map including the locations of the Schaft Creek deposit and the ES and GK zones of copper mineralization are shown in Figure 9-3.

Figure 9-3: Total Magnetic Intensity Map

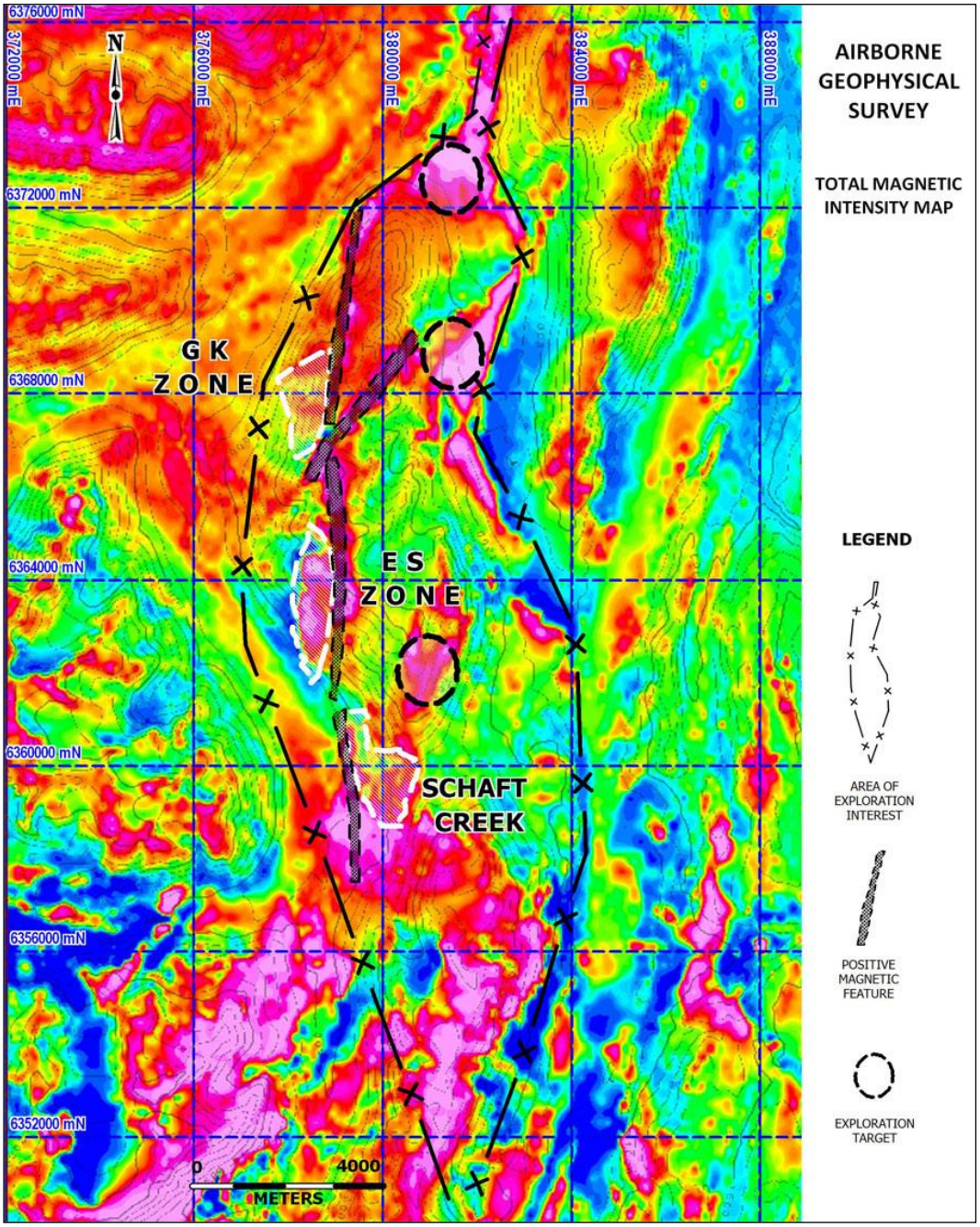

Source: Copper Fox (2021)

During 2013, the SCJV completed a ZTEM survey over the deposit area. The survey was flown at a high and variable sensor height, so the magnetic data acquired is of inferior quality to that obtained from the 2011 survey. The ZTEM data, however, provide an indication of the resistivity throughout the deposit area and these data can show major faults and also low resistivity layers at surface related to landslides or hydrothermal alteration. The resolution of these data is less than that of the DCIP resistivity inversion models produced in 2010 to 2011, but the ZTEM system has superior depth

penetration; therefore, it can show the depth extent of faults and any resistive features underlying the conductive surface material.

In 2015, the Schaft Creek JV completed an IP/ground magnetometer survey (16 line km) consisting of eight east–west-trending lines spaced 300 m apart, with line lengths ranging from 1.5 km to 2.5 km. This survey identified an anomaly in the southern portion of the Liard Zone, consistent with pyrite, chalcopyrite, and molybdenum mineralization. The resistivity data were used to outline structures such as the Breccia Footwall Fault and an interpreted fault along Wolverine Creek.

9.6 Pits and Trenches

Little trenching has been conducted at Schaft Creek due to the presence of thick till and alluvial layers, which prevent surficial excavations from exposing bedrock. Prospector Nick Bird employed by BIK Syndicate in 1957 discovered copper mineralization that became the Schaft Creek Property and explored the occurrences using hand tools to excavate narrow trenches on outcrop in the Saddle area.

In 1972, Phelps Dodge Corporation of Canada Ltd. completed cobra drill trenching and bulldozer trenching. All of the trenches yielded disappointing results. The copper mineralization in the trenches appeared to be best developed in the vicinity of sericitized shears and fractures.

9.7 Petrology, Mineralogy, and Research Studies

Petrography, mineralogical, and paragenetic studies in support of mineralogical and geological interpretations have been completed on the Project.

In 2011, Copper Fox completed a geochemical study to refine the volcanic stratigraphy and investigate the chemical variability within the deposit. The study utilized 185 samples collected specifically for whole rock geochemical analysis and approximately 12,000 assay samples. Samples had been analyzed by lead (Pb)-fire assay, ICP-MS, and ICP-ES methods with an open vessel four-acid digestion. The whole rock geochemical data was used to construct a Pearce diagram.

The Pearce diagram generated 10 geochemical units and indicated the majority of the volcanic units were of sub-alkaline basaltic composition and that the majority of the felsic intrusives were likely derived from an intermediate felsic magma. The inconsistencies between geochemical grouping classifications and the lithologies from field logging were found to be a reflection of the intense alteration (Caron et al., 2012).

In January 2013, Copper Fox completed a petrographic, mineralogical (QEMSCAN) and geochemical study of 147 drill core samples from 41 core holes, plus two samples from the Hickman Batholith (LeBoutillier, 2013). The core holes span a period from 1966 to 2011 and represent drilling campaigns by Hecla, Teck and Copper Fox. The samples cover all the main zones of the Schaft Creek deposit as well as its surrounding margins. The samples were analysed for major oxides and trace elements.

9.8 Geotechnical and Hydrological Studies

Geotechnical studies were performed by Knight Piésold in support of pit slope assumptions for the 2013 feasibility study. Six pit design sectors were identified, and pit inter-ramp slope angles were recommended that ranged from 42° to 50°. The initial pit slope in overburden was recommended at 27°.

McElhanney conducted a preliminary hydrology assessment of the streams in the Project area in support of mining studies. BGC conducted an independent hydrological assessment of the streams along the proposed mine access road.

9.9 Metallurgical Studies

Metallurgical test work is discussed in Section 13.0.

9.10 3D Geological Model, 2011

Copper Fox retained Cambria Geosciences to assist in updating the 3D geological model for the Schaft Creek deposit. Wireframes were constructed in Surpac™ software, and were generated for various geological domains including base of overburden, breccia zones, fragmental zones, alteration zones, intrusive units, and fault zones. The model assisted Copper Fox in identifying future targets for definition drilling.

9.11 NI 43-101 Technical Studies

In 2007, Copper Fox released the results of a preliminary economic assessment of the Schaft Creek deposit. The technical report entitled “Preliminary Economic Assessment on the Development of the Schaft Creek Project located in Northwest British Columbia Canada” was prepared by Samuels Engineering Inc, with an effective date of December 7, 2007, Bender, M.R. et al as QPs.

In 2008, Copper Fox announced the results of a preliminary feasibility study on the Schaft Creek Project. The technical report entitled “Preliminary Feasibility Study on the Development of the Schaft Creek Project located in Northwest British Columbia Canada” was prepared by Samuels Engineering Inc. with an effective date of September 15, 2008, Bender M.R. et al as QPs.

In 2013, Copper Fox announced the results of a feasibility study on the Schaft Creek Project. The technical report entitled “Feasibility Study on the Schaft Creek Project British Columbia Canada” was prepared by Tetra Tech. with an effective date of January 23, 2013, Farah, A. et al as QPs.

Figure 9-4: Consolidated Geology Map of the Schaft Creek Property

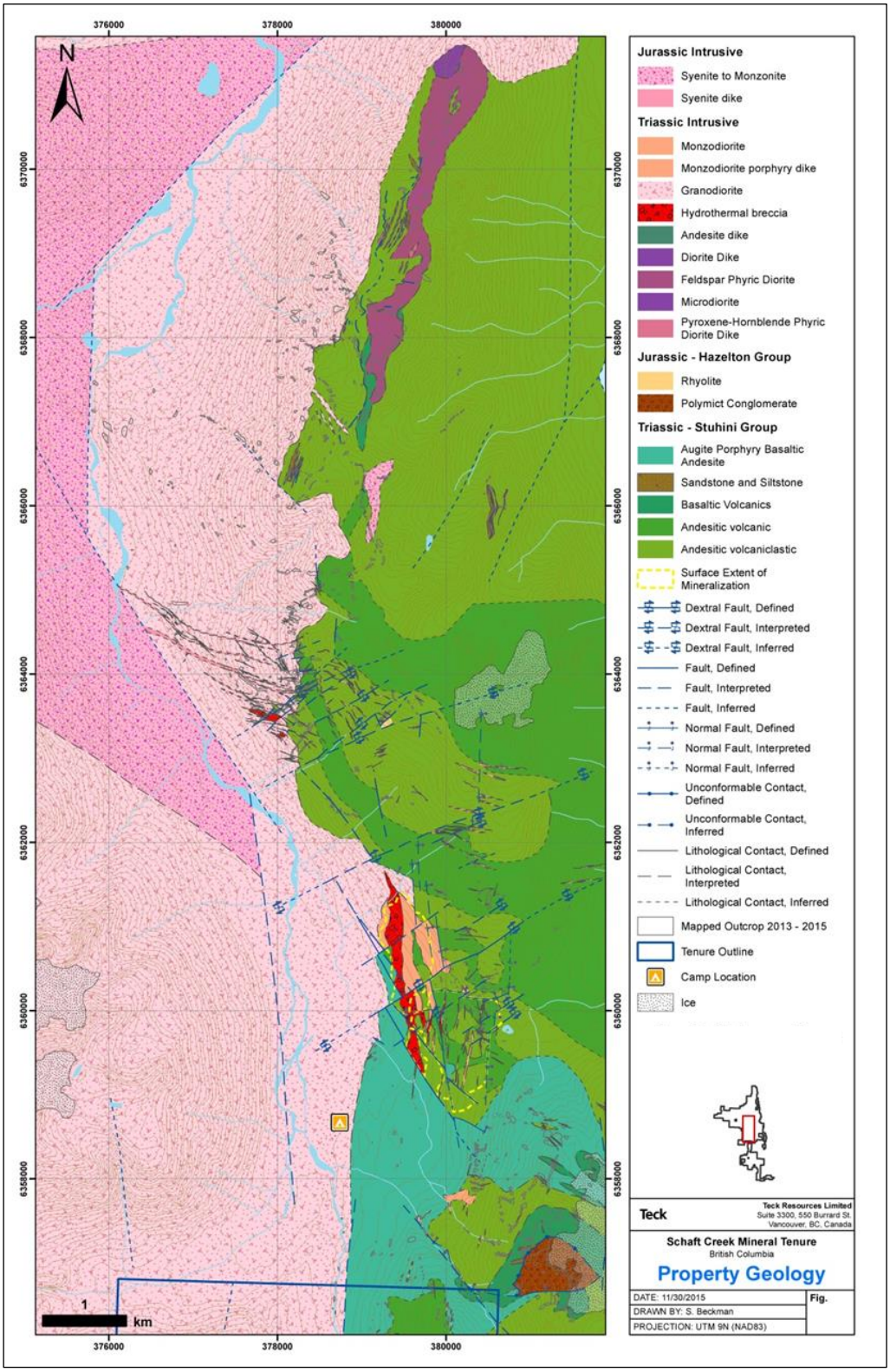

9.12 Drill Core Relogging

9.12.1 Copper Fox, 2011

In 2011, Copper Fox completed re-sampling and re-logging of historical drill core from the Schaft Creek deposit. Select holes and intervals of historic drill core were re-logged to formulate a consistent geological and structural interpretation as inputs for the construction of a 3D model of the deposit and to confirm or revise the descriptions for lithologies, alteration, and structures (Caron et al., 2012). During this program, the rejects of 5,359 historic samples were re-assayed at Acme Analytical Laboratories Ltd. (Acme Labs) in Vancouver, British Columbia.

This work identified a significant amount of sodic feldspathization overprinting in the Schaft Creek deposit, and the gently dipping porphyritic units previously considered to be intrusives were found to be volcanic or sub-volcanic porphyritic feldspar phyric flows with sodic feldspar overprints.

The 2011 work also demonstrated early, strong potassic alteration in the breccias of the Paramount Zone. The structural mapping program identified three faults as the main structural controls on the mineralization as well as the structurally controlled hydrothermal breccia.

9.12.2 Schaft Creek JV, 2013–2015

Relogging of historical drill core was a key component of the three field programs that the Schaft Creek JV completed from 2013 to 2015. This relogging was critical to understand historical work on the Project, as well as advancing the knowledge of the deposit. Relogging of historical drill core was conducted in camp at the core-logging facility. The majority of the historical drill core is stored in wooden storage racks that allow for easy access to individual holes or sections within a hole.

Geological relogging was conducted using a modified version of the paper-based Anaconda-style. This method captures interval-based information on lithology, structure, veins, alteration, and mineralization, with a focus on mineral paragenesis and crosscutting relationships. Select information from these paper logs was subsequently digitized into an Excel format, imported into an acQuire database, and incorporated into a 3D geological model. Geological relogging was conducted by a large team of geologists; efforts were made throughout the programs to maintain consistency between loggers. This was done by having group discussions regarding individual drill holes and by developing a library of reference samples, which is housed in the core-logging facility.

During 2013, approximately 10,850 m of drill core from 30 holes was relogged. This relogging was used as the basis for developing a new lithological classification scheme intended to be more consistent and simpler than the previous lithological naming convention scheme (as described in the geology section). This relogging work also improved understanding of major structures in the deposit and provided a basis for a new alteration assemblage classification scheme (as described in the geology section). The latter clarified the understanding of the distribution of hydrothermal alteration in the deposit.

In 2014, relogging focused predominantly on three cross sections within the Main Zone. The three main goals for this relogging were to understand (1) the controls on mineralization in the Liard Zone; (2) variations in mineralization within the Liard Zone; and (3) the transitions between the Liard, West

Breccia, and Paramount Zones. In addition to these cross sections, additional holes within the deposit were logged to verify faults and examine geological relationships. Top-of-hole data was obtained for a large number of holes to add information to the geological map in areas without surficial outcrop exposure.

A preliminary 3D geological model was completed at the end of 2014. As part of this modeling process, a conversion was created to combine historical logging codes and recent relogging codes used by the Schaft Creek JV (Bailey et al., 2014). The preliminary 3D model completed in 2014 highlighted several regions of uncertainty that require additional work to resolve.

During the 2015 field program, 11,439 m of historical drill core was relogged from the deposit area, bringing the total metres relogged to 42,999 m, approximately 40% of the total drilled metres on the Project. The relogging in 2015 intended to accomplish three goals: (1) improve the 2014 3D geologic model; (2) increase the knowledge of areas within the deposit that have been recognized as opportunities to expand the resource and/or delineate additional higher-grade zones; and (3) collect data on intervals that had been selected for geometallurgical sampling and that had not previously been relogged by the Schaft Creek JV.

Following the completion of the 2015 field program, relogging data from 2013 to 2015 was combined with historical logging information and geological mapping data to create an updated 3D geological model. Further detail on geological modelling is provided in Section 14.0.

9.13 Surveying

Various surveying methods have been used over the life of the Project. The 2012 Technical Report details surveying methods used by Copper Fox between 2005 and 2011. Surveying methods used for the 2013 and 2015 drill programs are described below in Section 9.15.

9.14 Topographic Surface

The topographic surface used is called topo_trim.00t and was generated from a 1 m resolution DTM. The data was sourced from a 2016 DEM named DEM_sck_topo1m_validated_higherRes.dxf. This file has been inherited from previous resource estimation efforts, and the ultimate source of the file has not been resolved. The collar locations were compared to the topographic surface, and due to some differences in elevation, all collar locations were relocated to the topographic surface. The QP compared the 2016 DEM against downloaded NASA Shuttle Radar Topography Mission (SRTM) data (see Section 12.2). The high-resolution 2016 DEM compares well with the low-resolution SRTM with a mean difference of less than 0.04 m.

9.15 Exploration Potential

9.15.1 Overview

Schaft Creek is part of an extensive porphyry complex with copper mineralization occurring over a 12 km strike length along the Stuhini/Hickman contact. Geological mapping and geophysical surveys and limited exploratory diamond drilling located a number of mineralized areas that indicate good potential for additional porphyry copper–gold mineralization within the complex. The 2011 to 2012 geophysical surveys outlined an exploration area of interest that is approximately 4 km wide by 20 km long (Figure 9-3) Exploration activities in 2012–2016 outlined the prospects and zones shown in Figure 9-2. A number of these zones had been identified during legacy exploration activities.

9.15.2 Wolverine Creek / Liard Zone Extension

The limits of the Liard Zone are not well constrained to the south. This extension covers a large area that hosts a positive chargeability anomaly, a limited number of drill holes with chalcopyrite-bornite-molybdenite, and poor outcrop exposure. A previously unrecognized hydrothermal breccia was identified during the re-logging programs during the 2015. Recognition of this breccia is potentially significant because it represents the first evidence of mineralization in the footwall of the Basal Fault.

The Wolverine Creek Area is located immediately south of the Schaft Creek deposit, within a heavily forested area on the lower northwestern slopes of Mount Hicks. This area contains several separate mineralized showings, all of which are believed to be related to a possible southern extension of the Schaft Creek mineralized system.

10.0 DRILLING

A total of 449 drill holes (about 108,041 m) have been completed in the Project area. Of this total, 238 holes (60,432 m) were drilled by Silver Standard, Asarco, Hecla, Paramount, and Teck in the period from 1956 to 1981, 197 holes (41,524 m) were completed by Copper Fox from 2005 to 2012, and 14 holes (6,087 m) were drilled by the Schaft Creek JV from 2013 to 2015. No drilling has been completed on the Project since 2015.

A total of 21 drill holes have no assays and 40 drill holes within the Project lie outside the resource area.

Drilling conducted by Copper Fox and earlier operators to year end 2011 is described in the 2012 technical report (Sections 6.0 and 10.0). Drilling conducted by Copper Fox in 2012 and the Schaft Creek JV in 2013 and 2015 is described below with drill hole collars shown in Figure 10-1.

10.1 Copper Fox, 2012

10.1.1 2012 Diamond Drill Holes

In 2012, Copper Fox drilled six holes targeting chargeability anomalies 700 m to 1,600 m north of the Paramount Zone. These anomalies were identified in the 2011 geophysical surveys and named the Discovery and Mike Zones (Figure 10-1). In 2012, DDH 2011CF422 tested one of the chargeability anomalies and intersected significant porphyry style copper mineralization. Table 10-1 provides details for diamond drill holes completed in 2012.

Table 10-1: Summary 2012 Diamond Drill Holes

Drill Hole	Northing	Easting	Elevation (m)	Depth (m)	Collar Azi	Dip
2012CF426	378264.16	6362615.28	957.45	789.43	91.6	60.2
2012CF427	378113.24	6362930.99	1019.27	769.92	90.1	59.1
2012CF428	378812.97	6362213.35	1116.79	223.11	270.0	74.7
2012CF429	379498.94	6362219.71	1457.05	132.89	90.0	65.0
2012CF429B	379498.94	6362219.71	1457.05	178.61	90.6	73.1
2012CF430	378442.50	6362948.36	1176.59	171.30	265.0	76.6

Of the four holes drilled in the Discovery Zone, DDH 2012CF428 and DDH 2012CF430 were terminated prematurely due to drilling difficulties. In the Mike Zone, DDH 2012CF429 and DDH 2012 CF429B were drilled from the same collar location approximately 700 m east of DDH 2012CF428 on the same section line and drilled due east. DDH 2012CF429B was drilled at a shallower angle than hole 2012CF429. Both holes were terminated prematurely in a major fault zone. Table 10.2 provides a summary of all significant mineralized intervals in the Discovery Zone.

Table 10-2: Significant Mineralized Intervals Discovery Zone

DDH ID	Azi.	Dip	Northing	Easting	From (m)	To (m)	Interval (m)	Cu (%)	Au (g/t)	Mo (%)	Ag (g/t)
2011CF422	90	-50	6362561	377976	83.00	184.35	101.35	0.204	0.09	0.009	1.60
					184.35	318.00	133.65	0.101	0.04	0.011	0.56
CF426-2012	90	-60	6362615	378264	76.55	767.66	691.11	0.16	0.04	0.003	0.81
				including	76.55	123.65	47.10	0.24	0.05	0.001	2.05
				including	476.50	658.40	181.90	0.21	0.05	0.003	0.68
				including	702.66	767.66	65.00	0.24	0.04	0.004	0.94
CF-427-2012	90	-60	6362930	378113	428.12	764.84	336.72	0.24	0.14	0.006	0.57
				including	509.00	556.00	47.00	0.62	0.59	0.006	2.02
				including	511.00	523.00	12.00	1.23	2.12	0.019	6.36
CF428-2012	270	-75	6362213	378812	No Significant Mineralization						
CF430-2012	90	-75	6362948	378442	122.75	132.14	9.39	0.14	0.01	tr.	5.55
				including	130.75	132.15	1.40	0.16	0.03	tr.	414.00
SCK13-436	90	-60	6362264	378492	50.50	68.50	18.00	0.09	0.117	0.00	0.56

Note: SCK-13-436 was drilled by the Schaft Creek JV in the 2013 drill campaign.

Tahltan Drilling Services Corporation provided diamond drilling services using a skid-mounted Zinex A5 drill rig and a helicopter-portable Zinex A5 drill. All drill holes were started with either HQ diameter coring tools (63.5 mm diameter core) or with HQ3 diameter coring tools (61.1 mm diameter core) with HW or HWT surface casing.

10.1.2 Core Logging Procedure

The 2012 core logging procedures included geotechnical core logging and core orientation measurements (where possible) at the drill site, and core interval and magnetic susceptibility measurements at the core logging facility. Observations of the general rock type, rock weathering, veining type, presence/absence of mineralization, and an estimate of the overall rock strength were also recorded. Preliminary analysis of rock and mineral geochemistry was performed using the Niton portable XRF analyzer to help identify unknown minerals. Data gathered from the logging were entered directly into a master database using an acQuire database system.

Thirty samples of full diameter drill core representative of lithology, alteration, or mineralization. were selected at 100 m intervals from drill holes 2012CF426 to 2012CF430 for specific gravity determination. The specific gravity of these samples were measured according to Acme Labs code G813-WAX.

10.2 Diamond Drill Hole Results

Significant results of the drill holes completed in the Discovery Zone in the period 2011 to 2013 are summarized below.

DDH 2011CF422 is located approximately 1,200 m north of the Paramount Zone and intersected copper-molybdenum mineralization at a core interval depth of 83 m and remained in mineralization to the bottom of the hole at 318 m. The mineralization shows a strong correlation to the outer edge of a large (1,800 m by 800 m) chargeability anomaly identified in 2011. The strongest portion of the chargeability anomaly is located east of the drill hole collar location.

DDH CF426-2102 is located approximately 300 m east of DDH 2011CF422 and tested the eastern extension of the chargeability anomaly in the Discovery Zone. The hole intersected variable concentrations of chalcopyrite mineralization occurring as disseminations, and in veins and veinlets in variably altered andesite. Visible molybdenite mineralization occurs sporadically throughout the core in quartz veinlets and in some instances also with chalcopyrite mineralization.

DDH CF427-2012 is located approximately 400 m northwest of DDH 2012CF426 and tested the strike extension of the chargeability anomaly located in 2011. The hole intersected variable concentrations of chalcopyrite and sporadic molybdenite mineralization from a core depth of 250.0 m to the end of the drill hole at 764.8 m. The chalcopyrite ± molybdenite mineralization occurs as disseminations, and in quartz veins and veinlets in a granodiorite intruded by a number of thin mafic dikes. Broad intervals of silicification were noted in this drill hole.

DDH CF430-2012 is located approximately 300 m east of DDH CF-427-2012 and tested the eastern extension of the 2011 chargeability anomaly (the Discovery Zone). This hole was terminated due to drilling difficulties before reaching the chargeability anomaly intersected in DDH-2012CF727. The hole intersected a narrow interval of mineralization. The average silver grade in the mineralized interval is significantly affected by one sample that assayed 414 g/t (13.31 oz/t) silver. In determining the weighted average grade of this interval, the 414 g/t silver assay was arbitrarily cut to 31.1 g/t silver.

DDH SCK-13-436 was drilled by the Schaft Creek JV in 2013 to test the projected extension of the chargeability anomaly that exhibited high magnetism in the Discovery Zone. The hole was abandoned prematurely before reaching the projected top of the chargeability anomaly. The hole intersected volcaniclastic lapilli tuff, andesitic volcanics, and minor volcaniclastic breccia. Intense fracturing occurs to a depth of approximately 90 m accompanied by copper oxide staining of the fracture surfaces. The drill hole intersected predominantly propylitic and sodic-calcic alteration assemblages with minor zones of silicification. Iron oxide alteration consisted of disseminated magnetite and vein-controlled hematite. Sulphide mineralization in the hole is minimal, consisting of vein-hosted and disseminated chalcopyrite and pyrite to a depth of 124 m, below which pyrite was the only sulphide mineral encountered. The overall sulphide content diminishes downhole.

10.2.1 Mike Zone

DDH CF429-2012 and DDH CF429B-2012 were completed to test the 1,000 m long by 500 m wide strong chargeability anomaly identified in 2011 the (Mike Zone). Both drill holes were terminated at core intervals of approximately 140 m due to extremely difficult ground conditions. These holes did not reach the chargeability anomaly.

DDH SCK-13-431 was drilled by the Schaft Creek JV in 2013 and tested a chargeability anomaly (Mike Zone) located northeast of the Paramount Zone of the Schaft Creek deposit. This drill hole intersected a broad interval of disseminated pyrite and trace chalcopyrite hosted in propylitic altered (chlorite-epidote ± hematite ± calcite) andesitic volcanics and volcaniclastic tuff. Very minor K-feldspar alteration occurs in a porphyritic dike intersected over the core interval 593.4 m to 604.2 m. This hole is located further north and at higher elevation compared to all other historical drilling in the Schaft Creek deposit area and contains lithologies that could be representative of the overlying Hazelton Group. Pyrite concentrations of up to 15% occur between 113 m to 269 m and 10% between 560 m to 575 m to ~10%.

10.3 Schaft Creek JV, 2013

The Schaft Creek JV drilled five exploration drill holes and four geotechnical holes in in the Schaft Creek deposit in 2013, for a total of 3,453 m (Figure 10-1, Table 10-3, and Table 10-4). The geotechnical drill holes were designed to collect information on the Paramount Zone and on the slope to the northeast of the Paramount Zone. The exploration drill holes were designed to test for extensions to the Paramount Zone along strike and at depth, and to test targets in the Discovery and Mike Zones. Of the holes drilled in 2013, three exploration drill holes (SCK-13-434, 436, and 438), and one geotechnical drill hole (SCK-13-437) did not reach their target depths due to difficult ground conditions.

Table 10-3: 2013 Drill Hole Collar Information – Exploration Program

Collar ID	Easting NAD83	Northing NAD83	Elevation (m)	Collar Azimuth	Collar Dip	Depth (m)	Zone
SCK-13-431	379712	6361778	1332	090	65	628	Mike
SCK-13-434	379953	6360884	1171	270	80	180	Paramount
SCK-13-435	379822	6360465	996	270	70	797	Paramount
SCK-13-436	378493	6362265	972	090	60	224.5	Discovery
SCK-13-438	380103	6360393	1125	090	60	15	Paramount

Table 10-4: 2013 Drill Hole Collar Information – Geotechnical Program

Collar ID	Easting NAD83	Northing NAD83	Elevation (m)	Collar Azimuth	Collar Dip	Depth (m)	Zone
SCK-13-432	379538	6361178	1059	270	60	538.5	Paramount
SCK-13-433	379745	6360800	1040	090	55	566.5	Paramount
SCK-13-437	379995	6360572	1094	090	55	202.5	Paramount
SCK-13-439	379345	6360500	900	270	60	302.5	Paramount

Figure 10-1: 2012–2015 Exploration and Geotechnical Drill Holes Location Map

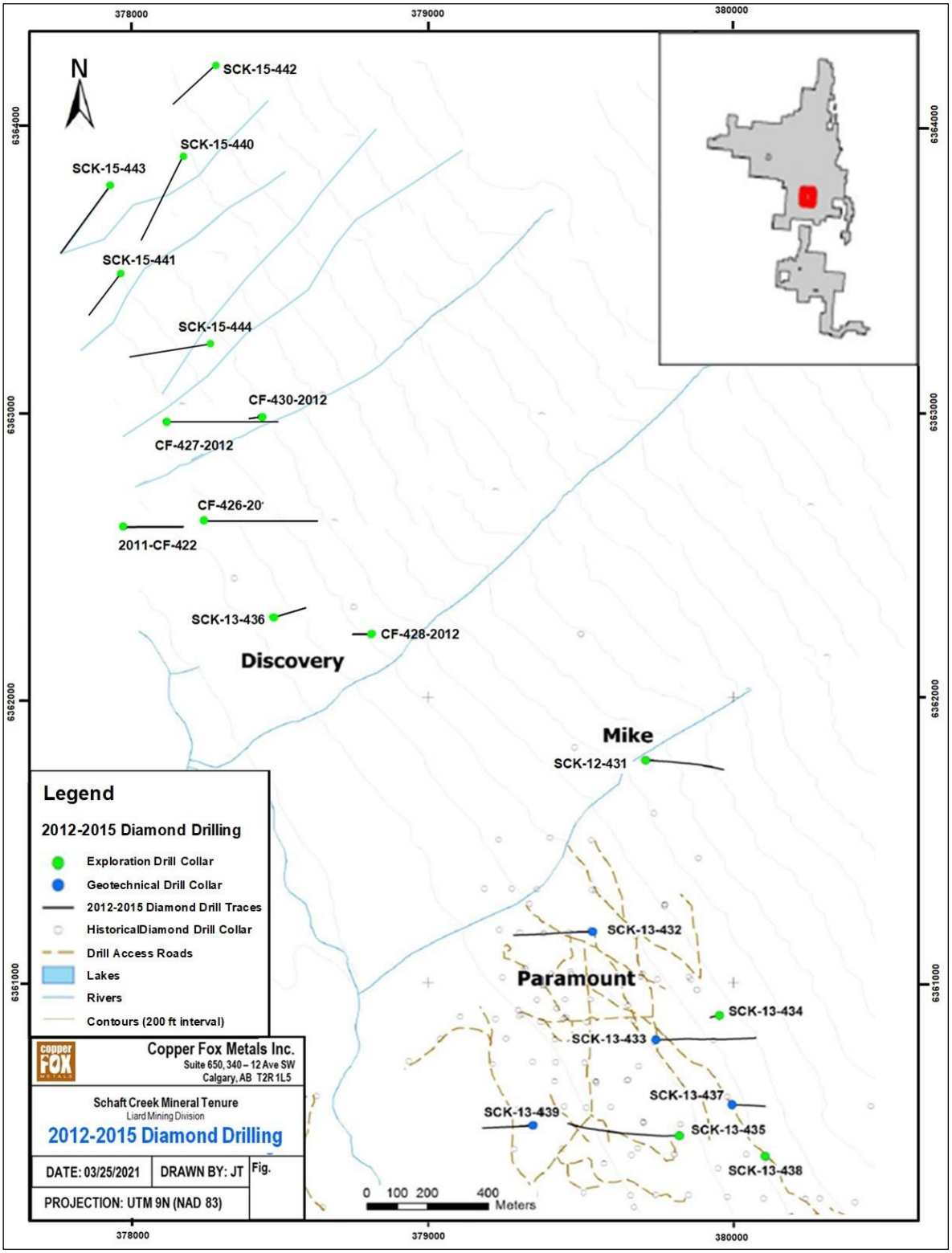

10.3.1 Diamond Drilling Procedures

Two separate drilling contractors conducted the diamond drilling in 2013. Geotechnical drilling was performed by Geotech Drilling Services Ltd. using two skid-mounted drill rigs. Exploration drilling was performed by Tahltan Drilling Services Corp using two helicopter-portable drill rigs. Drills were mobilized to site from the airstrip in Telegraph Creek beginning on August 22nd. Drilling typically commenced using PQ or HQ diameter core, and the core size was typically reduced downhole to accommodate for poor ground conditions. Drill operations were completed in mid-October.

Prior to drilling each hole, collar locations and orientations were surveyed and staked by project geologists using a handheld global positioning system (GPS) and Brunton compass. Timber drill pads were constructed by Sawtooth Range Enterprises Ltd. for the helicopter-supported drill sites. Skid rigs were dragged into position using pre-existing drill roads. All drilling was supported by an AS350B2 helicopter on contract from Pacific Western Helicopters. Drill core was transported to the exploration camp by helicopter for logging. Down-hole survey measurements of drill hole orientation were collected using a Reflex EZ-Shot tool, with measurements typically taken every 50 m. Following completion of drilling, timber drill pads were removed and drill sites were cleared and rehabilitated. Drill hole collar locations were then surveyed using a Trimble differential GPS.

10.3.2 Core Logging Procedures

Core logging was conducted at the core-logging facility located in the exploration camp. Upon arrival at the core-logging facility, core boxes were re-labeled, core recoveries calculated, and rock quality designation (RQD) geotechnical measurements taken. Geological logging was conducted using a modified version of the Anaconda-style to capture interval-based information on lithology, structure, veins, alteration, and mineralization. Select information from these paper logs was subsequently digitized into an Excel format and then imported into an acQuire database.

Photographs of drill core were taken following completion of logging and sample assignment. The core was then subsequently cut and sampled. After sampling, all core boxes were stacked outside on racks within the core storage area. All 2013 drill core is stored in the core storage area beside the core logging facility in the Schaft Creek exploration camp.

More details on the core logging procedures and an example log can be seen in Section 10.4.2 Core Logging Procedures from the 2015 program. The core logging procedures from both the 2013 and 2015 programs were the same.

10.3.3 Diamond Drilling Results

A summary of significant mineralized intercepts from 2013 drilling is presented in Table 10-5.

Four holes (SCK-13-434, 436, 437, and 438) were abandoned prior to reaching their target depths. Of the remaining five holes, two contain significant mineralized intercepts, including Geotechnical hole SCK-13-432 and Exploration hole SCK-13-435. Significant mineralized intercepts from the 2013 program are summarized here briefly.

SCK-13-432 (18 m to 286.1 m, grading 0.237% Cu, 0.238 g/t Au, 0.015% Mo): This hole was drilled at the northern limit of the Paramount Zone. This hole is significant because it extends the strike length of the Paramount Zone to the north, and also because mineralization occurs near-surface. In particular, the interval at 67.3 m to 166.5 m is significant because it demonstrates unusually high grade at fairly shallow depths (99.15 m grading 0.361% Cu, 0.401 g/t Au, 0.031% Mo).

SCK-13-435 (239 m to 665.5 m, grading 0.324% Cu, 0.112 g/t Au, 0.021% Mo): This hole was drilled to test the down-dip extent of the central Paramount Zone at depth, in an area with a high chargeability IP anomaly. No deep drilling had been conducted previously within this particular part of the Paramount Zone. This hole is significant because it demonstrates the continuity of the Paramount Zone at depth, and indicates that there are more opportunities remaining to expand the Paramount Zone resource at depth. This hole also intersected two small intervals of high grade mineralization (i.e., 307 m to 335 m grading 0.817% Cu, 0.324 g/t Au, 0.051% Mo). These high-grade intervals consist of hydrothermal breccias with abundant chalcopyrite-bornite-molybdenite cement. Further drilling and relogging is required to determine if these high-grade breccia intervals represent traceable domains that can be delineated by future drilling.

SCK-13-431 (Mike target area): This hole was designed as an initial drill test of the Mike target area. The Mike target area is defined by a large high-chargeability IP anomaly. This drill hole did not intersect any significant mineralization; however, a large amount of disseminated pyrite was intersected over a wide interval in this hole which explains the large high-chargeability IP anomaly in the Mike target area.

Table 10-5: Summary of 2013 Drilling Results

Zone	Drill Hole ID	From (m)	To (m)	Interval (m)	Cu (%)	Au (g/t)	Mo (%)	Ag (g/t)
Mike	SCK-13-431	*no significant results—exploration hole*						
North Paramount	SCK-13-432	18.0	286.1	268.1	0.237	0.238	0.0155	2.22
	including	67.4	166.5	99.2	0.361	0.401	0.031	4.04
	including	108.0	139.2	31.2	0.561	0.541	0.028	6.52
Paramount	SCK-13-433	400.8	456.0	55.2	0.275	0.040	0.022	1.85
Paramount	SCK-13-434	*no significant results—hole abandoned before target depth*						
Paramount	SCK-13-435	239.0	665.5	426.5	0.324	0.112	0.021	1.13
	including	307.0	335.0	28.0	0.817	0.324	0.051	1.84
	including	550.0	571.0	21.0	0.740	0.094	0.065	2.81
Discovery	SCK-13-436	50.5	68.5	18.0	0.088	0.117	0.001	0.56
Paramount	SCK-13-437	*no significant results—geotechnical hole*						
Paramount	SCK-13-438	*no significant results—hole abandoned before target depth*						
Paramount	SCK-13-439	59.0	71.3	12.3	0.202	0.035	0.001	1.49

10.4 Schaft Creek JV, 2015

The Schaft Creek JV completed five diamond drill holes in the LaCasse target area during the 2015 field season, for a total of 2,634 m drilled (Figure 10.1, Table 10-6).

Table 10-6: Collar Details for Holes Drilled During the 2015 Drill Program

Collar ID	Easting	Northing	Elevation (m)	Collar Azimuth	Collar Dip	Depth (m)
SCK-15-440	378232	6363815	1480	205	60	624
SCK-15-441	378037	6363422	1200	215	65	405
SCK-15-442	378331	6364121	1639	225	70	555
SCK-15-443	378003	6363717	1312	215	60	543
SCK-15-444	378304	6363191	1204	260	60	507

Note: Collar locations (Easting, Northing, and Elevation) were measured using a differential GPS. Azimuth is recorded relative to true north. The coordinate system used is UTM NAD 83 Zone 9N.

Prior to drilling, collar locations were located and staked by project geologists using a handheld GPS and Brunton compass. Archaeological assessment of the proposed collar locations was conducted by Rescan Tahltan Environmental Consultants; no archaeological concerns were identified at any of the proposed collar locations. Timber drill pads and secondary timber platforms were constructed at each collar location by Rugged Edge Holdings Ltd. of Smithers, British Columbia.

10.4.1 Diamond Drilling Procedures

Hy-Tech Drilling Ltd. of Smithers, British Columbia, was responsible for performing the drilling by using a helicopter-portable FlyTech 5000 drill rig. The drill rig was equipped with a rod manipulator to reduce manual handling and a centrifuge system to manage drill cuttings and reduce water consumption. The cuttings management system was only functional when there was water return; this occurred only sporadically throughout the program. All drilling was completed using HQ tooling, with the exception of SCK-15-440, which was reduced to NQ at 393.4 m. Downhole survey measurements of drill hole orientation were collected using a Reflex EZ-Shot tool, with measurements typically collected every 50 m. Downhole depth was measured from the ground, rather than from the top of the drill string on the drill pad, because the pad was typically several metres above the steeply dipping slope. Drilling activities were supported by an AS350D2 helicopter on contract from Lakelse Air Ltd. of Terrace, British Columbia.

Following completion of drilling, the drill casing was broken near the ground and the holes were capped. Each collar location was surveyed using a differential GPS, with the instrument measuring the position where the casing met the ground. The timber drill pads were disassembled and each site was cleared and reclaimed. Drill cuttings captured by the centrifuge system were flown in bags to a historical un-reclaimed drill pad in the Liard Zone, where they were emptied into a sump. Following the completion of the drill program, this sump was backfilled.

Figure 10-2: 2015 Drill Holes Location Map

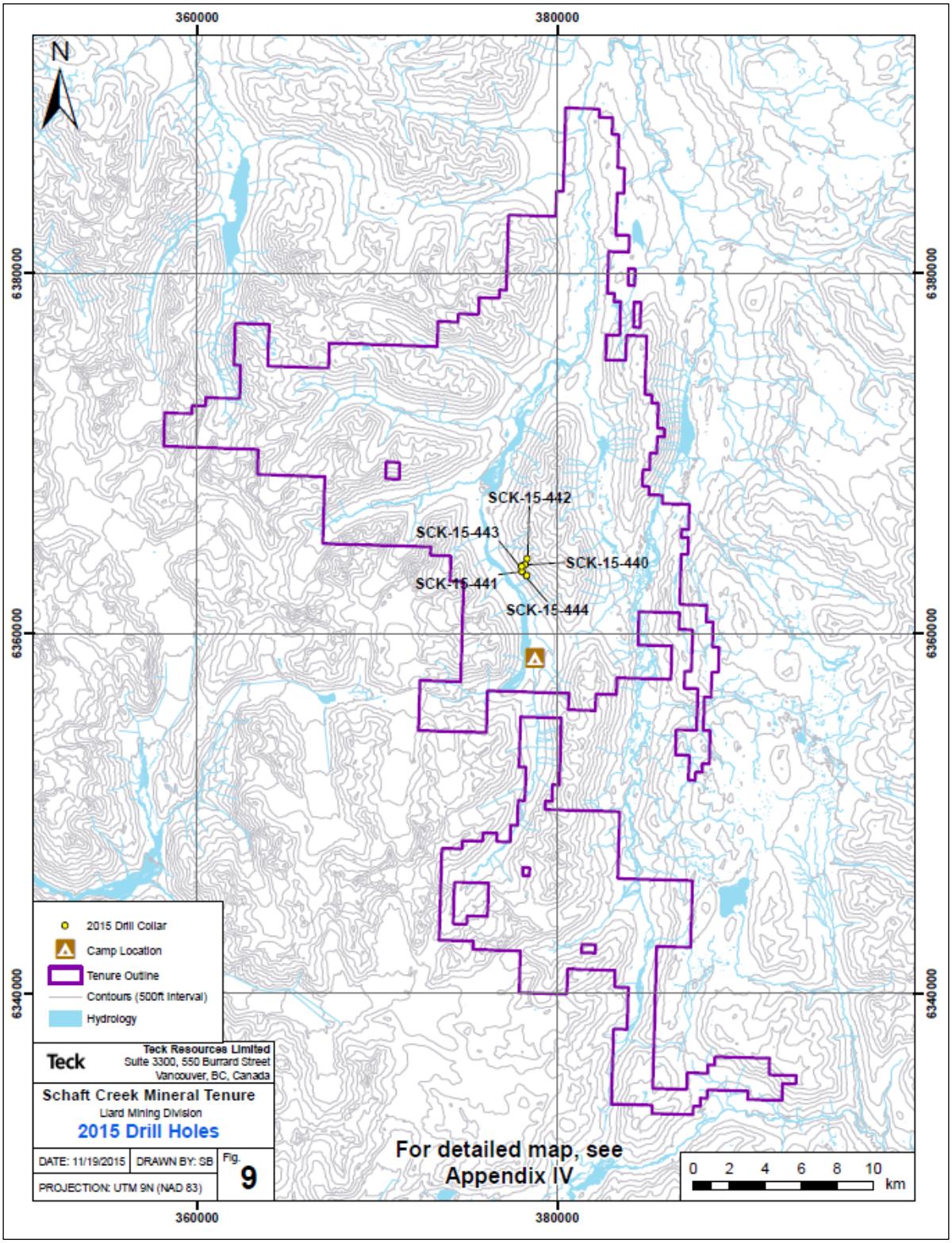

10.4.2 Core Logging Procedures

Drill core was logged in camp at the core-logging facility. Upon arrival, the core boxes were reviewed by the logging geologist to ensure there were no mistakes with run-blocks or box labels. Core boxes were then labeled with hole-id and “from-to” intervals on metal tags on the front of the boxes. The core was cleaned with a brush, and then the boxes were photographed while wet. Additional core photographs at a smaller scale were also collected at the discretion of the logging geologist to capture specific geological details.

Geotechnical measurements of core recovery and RQD were collected using a tape measure. Magnetic susceptibility measurements were collected using KT-9 or KT-10 magnetometers. Geotechnical and magnetic susceptibility measurements were initially recorded using a Trimble Juno T41 handheld computer; however, this was abandoned partway through the field program in favor of paper-based data recording. This data was subsequently entered into Excel and imported into the acQuire database.

Geological logging was conducted using paper logging sheets, following a modified version of the Anaconda-style logging sheet (Figure 10-3). This method captures interval-based information, while incorporating graphical logging of lithology, structure, veins, alteration, and mineralization data, with a focus on mineral paragenesis and textural relationships. Information from these paper logs was digitized into an Excel format, and then checked and validated before being imported into the acQuire database.

Throughout the program, efforts were made to ensure consistency between loggers. This was done through group discussions regarding drill core geology and by developing a library of polished reference samples.

Figure 10-3: Example of Modified Anaconda-Style Drill Log Used at Schaft Creek in 2013

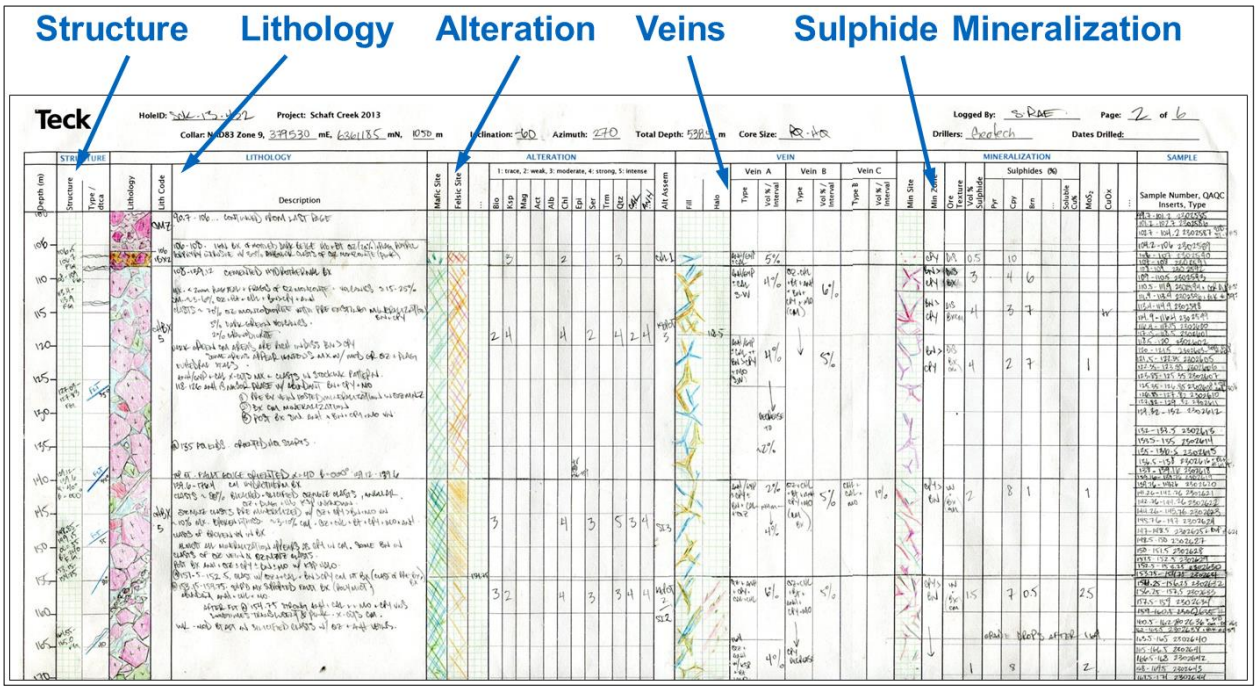

10.4.3 Diamond Drilling Results

The drilling program completed during 2015 focused on testing the LaCasse Zone, located 3 km to the north-northwest of the Schaft Creek deposit area. The LaCasse area contains outcropping chalcopyrite-pyrite mineralization associated with hydrothermal-intrusive breccias and sheeted quartz veins, as well as disseminated sulphide mineralization. Mineralization in this area has been recognized by various historical workers (e.g., Lamelle, 1966; Betmanis, 1978; Raven, 1979; Luckman, 2005; Bradford, 2006; Greig and Kreft, 2009); however, there is no known record of previous drilling in this area.

The 2015 drilling program was designed to test a large area of outcropping sulphide mineralization along a strike length of approximately 1 km. Five holes were completed (2,634 m), with a spacing of 200 m to 300 m of horizontal distance between drill collars. Major rock types intersected by the drilling at LaCasse include fine- to medium-grained, weakly porphyritic granodiorite to quartz monzonite, pyroxene-phyric andesitic volcanic rocks, andesitic dikes, and post-mineral syenite to rhyolite dikes with distinctive flow banding near the intrusive margins. Two of the drill holes intersected hydrothermal-intrusive breccia containing rounded to subangular clasts of granodiorite and pyroxene-phyric andesite, with a pink colored matrix of quartz and K-feldspar. Locally, this breccia matrix appears to contain plagioclase phenocrysts and is interpreted to have an intrusive origin, whereas in other areas, the matrix is aphanitic and is interpreted to be hydrothermal in origin. The cement of the breccia is generally quartz and calcite, although rarely the breccia contains small intervals of chalcopyrite-cement with sulphide content up to 3% to 5% locally. The breccia also contains some clasts comprised of quartz vein fragments, and some clasts containing abundant disseminated chalcopyrite. These clast types suggest that some brecciation postdates the mineralization, and that there may have been multiple brecciation and mineralization episodes.

Major alteration assemblages include a potassic assemblage of K-feldspar-biotite ± hematite that is overprinted or crosscut by a sodic-calcic assemblage of chlorite-epidote-calcite-hematite ± albite. Both assemblages are associated with chalcopyrite-pyrite mineralization, although the potassic alteration is more closely correlated with the sulphide mineralization. Magnetite occurs locally as part of the potassic alteration assemblage within the granodiorite and within the chlorite-altered andesitic volcanic rocks adjacent to the granodiorite. The syenite to rhyolite dikes, which crosscut all other rock types and alteration assemblages, are associated with an alteration assemblage of clay-chlorite-sericite.

Sulphide mineralization includes quartz-chalcopyrite-pyrite-molybdenite veins with potassic halos, chalcopyrite-pyrite mineralization replacing mafic phenocrysts, disseminated and fracture-controlled chalcopyrite-pyrite with minor bornite, and rare well-mineralized breccia clasts containing disseminated chalcopyrite-pyrite with minor bornite. Generally, sulphide mineralization is sparse and low grade (0.3% to 0.5% total sulphide), although locally disseminated sulphide mineralization is more abundant (up to 2% to 3% locally). Quartz-sulphide veins occur throughout all of the drill holes, but are generally sparse (1 to 5 veins per meter) and thin (0.2 cm to 1 cm thick). Locally, quartz-sulphide veins are sheeted and more abundant (5 to 20 veins per meter); however, the overall sulphide content of these sheeted vein zones is still relatively low (0.4% to 0.7% total sulphide). Very fine-grained bornite occurs locally, particularly in SCK-15-444, and is associated with a notable increase in gold grade relative to copper grade, corresponding to an elevated Au:Cu ratio. Sparse, irregular clots of partially oxidized chalcopyrite and minor bornite also occur within the syenite to rhyolite dikes. However, based upon these textures, these sulphides are interpreted to have been “digested” or remobilized into these dikes from other rock types.

The drilling at LaCasse intersected rock types, alteration assemblages, and sulphide mineralization styles that are generally comparable to what had been mapped at surface. In many areas, features such as intrusive contacts, zones of sheeted veins, faults, and post-mineral dikes could be correlated with confidence between drill holes and geological mapping at surface. In some areas, the abundance and thickness of post-mineral dikes were greater than expected. These dikes introduced a significant amount of dilution to some of the mineralized zones (e.g., SCK-15-440).

In some key areas, the drilling did not correlate with previous mapping: in particular, SCK-15-441 failed to intersect any hydrothermal breccia at depth, although the collar location for this hole was positioned near several outcrops that contain breccia textures. The breccia body is therefore interpreted to have an irregular shape and/or to be offset by northeast-trending faults that parallel the prominent gullies in the slope. This fault set was intersected by at least two drill holes, and both encountered large zones of gouge and intensely fractured rock.

A summary of significant mineralized intercepts from the 2015 drilling is presented in Table 10-7. DDH SCK-15-444 intersected an interval or 182.5 m grading 0.20% Cu and is the southern-most hole completed in 2015, and is the closest to the drill holes completed in 2011 and 2012 in the Discovery Zone.

Table 10-7: Summary of Results From the 2015 Drill Program at the LaCasse Target

Drill Hole ID	From (m)	To (m)	Interval (m)	Cu (%)	Mo (%)	Au (g/t)
SCK-15-440	*Mineralization hosted in granodiorite cut by andesite and syenite dikes adjacent to contact with volcanics*					
	120.5	167.6	47.1	0.13	0.004	0.2
including	121.5	134.3	12.8	0.21	0.007	0.69*
including	158.3	165.5	7.3	0.24	0.009	0.06
SCK-15-441	*Planned test of breccia – not intersected* *Chalcopyrite in disseminations and veins in granodiorite*					
	120.5	150.0	29.5	0.1	0.001	0.01
	178.5	205.5	27.0	0.09	0.016	0.06
SCK-15-442	*Test of quartz-chalcopyrite vein target*					
	439.7	454.1	14.4	0.13	0.004	0.01
SCK-15-443	*Mineralization hosted in hydrothermal and intrusive breccia*					
	354.6	369.0	14.4	0.16	0.002	0.02
	404.0	424.0	20.0	0.17	0.011	0.02
	454.0	463.0	9.0	0.08	0.001	0.21

table continues…

Drill Hole ID	From (m)	To (m)	Interval (m)	Cu (%)	Mo (%)	Au (g/t)
SCK-15-444	*Test between Lacasse and Discovery* *Disseminated and vein chalcopyrite in granodiorite*					
	283.5	466.0	182.5	0.2	0.002	0.02
including	283.5	363.0	79.5	0.29	0.002	0.02
including	283.5	313.5	30.0	0.4	0.005	0.05
including	337.8	361.9	24.1	0.34	0.001	0.01

*Au grade is mostly due to two assays: 1.1 g/t and 6.7g/t.

11.0 SAMPLE PREPARATION, ANALYSES AND SECURITY

11.1 Schaft Creek JV, 2013

11.1.1 Sample Transportation and Security

Upon completion of logging and core cutting, cut core samples were collected in plastic sample bags secured with zip ties. For shipping, these plastic sample bags were put into numbered rice sacks and secured with zip ties. Rice sacks containing samples were picked up by a Cessna 208 Caravan operated by Northern Thunderbird Air at the exploration camp airstrip and flown directly to Smithers where Acme Labs personnel received the shipment.

11.1.2 Drill Core Preparation and Analysis

For the 2013 program, all sample preparation was conducted by Acme Labs in Smithers using the preparation method R200-1000. Sample preparation included drying, crushing, riffle splitting, and pulverizing. Drying was accomplished using an oven to dry the samples at 60°C for 24 hours to 48 hours. Prior to crushing, the crusher was cleaned using a charge of quartz sand. An additional blank sample was inserted at the start of each sample batch to limit contamination between sample batches. Samples were crushed to 80% passing 10 mesh using a Terminator crusher. This coarse crush material was riffle split three times for homogenization, and then split down to 1,000 g with the remaining material set aside as a coarse reject. The 1,000 g split was placed in a barcoded envelope and sent to pulverizing. For crusher duplicate samples, an additional split was collected at this stage and analyzed as a separate sample. Crushed samples were then pulverized using a bowl and puck pulverizer to a tolerance of 85% passing 200 mesh.

Following sample preparation, sample assays were completed on pulps using a variety of routine analysis methods. These methods are detailed below:

1. Ore-grade assays for copper, molybdenum, and silver were determined by 4-acid digest with ICP-ES finish (Acme Group 7TD). This assay package also includes results for major elements (e.g., Fe, K, Al), other commodity elements (e.g., Zn, Pb), and trace elements (e.g., Ni, Bi). The analysis method uses a 0.5 g sample split, which is digested in a hot 4-acid solution and then taken to dryness. The sample is then leached with HCl and analyzed using an ICP-ES finish.

2. Ore grade assays for gold were determined by fire assay with atomic absorption (AA) finish (Acme Code G601). This analysis method includes lead-collection fire assay fusion on a 30 g sample split. After fusion, the doré bead is digested in HCl and HNO_3, and then analyzed for gold with an AA finish.

3. Concentrations of trace elements were determined by aqua regia digest with ICP-MS finish (Acme Group 1DX). This analytical method uses a 0.5 g sample split, which is digested in a hot (≈95°C) modified aqua regia solution (HCl, HNO_3, and H_2O). Following digestion the sample is analyzed by ICP-MS.

4. Concentrations of carbon and sulphur were determined by LECO analysis (Acme Group 2A12). This analytical method uses a 0.2 g sample split and LECO analysis.

5. Whole-rock lithogeochemistry was determined using a multi-part analytical package (Acme Code 4AB1). This analytical method includes results for major oxides determined by lithium borate fusion and ICP-ES finish (Code 4A), rare and refractory elements determined by lithium borate decomposition and ICP-MS finish (Code 4B), base and precious metals determined by aqua regia digestion and ICP-MS finish (Group 1DX), low to ultra-low trace element concentrations determined by aqua regia digestion and ICP-MS finish (Code 1F04), and loss on ignition determined by weighing a sample split before and after ignition.

The QP is satisfied that sample preparation and analysis were carried out in an appropriate manner to provide suitable analyses and to maintain data integrity.

11.2 Schaft Creek JV, 2015

11.2.1 Core Sampling Procedures

All drill holes completed during the 2015 field program were sampled from the top of bedrock to the bottom of hole. Sample intervals were determined by the logging geologist. Sample intervals were selected to conform to natural variation in the geology, with breaks at all geologic contacts and major structures, and intervals selected to represent variation in alteration and mineralization as accurately as possible. Sample intervals generally ranged from 1 m to 2 m, with nearly all samples within the range of 0.5 m to 3 m; the shortest sample was 0.4 m and the longest 3.5 m. Sample intervals were marked in the box with metal tags and barcoded laboratory tags corresponding to tags included in submitted sample bags.

QA/QC samples were inserted into the core sample sequence by the core logging geologist. Three different QA/QC sample types were inserted, including standards, field blanks, and field duplicates. One of each of these QA/QC sample types was inserted into each batch of 20 samples, for a total of three QA/QC samples per 20 samples. Standards were matrix-matched and also matched to the estimated Cu-Mo-Au grades of the surrounding samples. Barren granite was used as blank material. Field duplicates consisted of quarter core duplicates, with half the core left remaining in the core box.

Core cutting was conducted on site in the core-cutting facility adjacent to the core logging area. Core cutting was performed by Northern Labour Services, under supervision of the geologists on site. Cutting was done using electrical core saws. Following the completion of cutting and sampling, all core boxes from the 2015 program were placed into newly built racks in the core storage area.

During the logging process, sample intervals were selected for additional lithogeochemical study. Selected sample intervals were flagged on the laboratory requisition form requesting separate 250 g crusher splits be created for these samples for later lithogeochemical analysis. These splits were held by the lab until the end of the program and were run under a separate work order. Intervals selected for lithogeochemistry were selected for best geological consistency throughout the sample interval, with a minimum of veins or other dilution.

Samples from the 2015 drilling were also selected for petrographic thin sections and K-feldspar staining; these were collected after the core cutting was completed. For petrographic thin sections, small billets were cut and labeled to indicate the area to be preserved in the thin section. For K-feldspar staining, wafers or slabs were cut and labeled to indicate the area to be stained. Samples for petrographic thin sections and K-feldspar staining were submitted to Vancouver GeoTech Labs of Vancouver, British Columbia for thin section preparation.

The QP believes that sampling was comprehensive and that the methodology applied is suitable for the deposit and meets industry standards.

11.2.2 Sample Transportation and Security

Samples including drill core, geometallurgical samples, rock samples, and soil samples were all transported in a similar fashion. Drill core, geometallurgical samples, and rock samples were collected in plastic sample bags secured with zip ties. Soil samples were collected in Hubco bags and allowed to air-dry inside a building on site, before being placed inside plastic sample bags. Barcoded sample label tags were placed inside all sample bags, and the corresponding sample number was written on the outside of the bag. For shipping, the samples were then put into numbered rice sacks and secured with zip ties. Rice sacks were batched into groups of 10 to 30 bags, and each batch was transported as a group. Rice sacks were transported by helicopter to a secure staging area at Ch'iyone Camp, located on the Galore Creek access road. From Ch'iyone Camp, sample batches were picked up and transported to the Bureau Veritas (BV) Laboratories preparation lab in Smithers by Bandstra Transportation Systems Ltd. Sample batching, shipping, and shipment pick-up was supervised by geologists on site.

11.2.3 Sample Preparation and Analysis

For the 2015 program, all sample preparation was conducted by BV Mineral Laboratories in Smithers. The preparation methods used are detailed below.

Samples were dried, crushed, split, and pulverised (BV laboratory code PRP80-1000). Drying was accomplished using an oven to dry the samples at 60°C for 24 hours to 48 hours. Prior to crushing, the crusher was cleaned using a charge of quartz sand. An additional blank sample of barren granite was inserted at the start of each sample batch to limit contamination between sample batches (reported as ROCK-SMI in the data certificates). Samples were crushed to 80% passing 10 mesh using a Terminator crusher. This coarse crush material was riffle split three times for homogenization, and then split down to 1,000 g with the remaining material set aside as a coarse reject. The 1,000 g split was pulverized using a bowl and puck pulverizer to a tolerance of 85% passing 200 mesh.

Routine analysis of drill core:

1. Ore-grade assays for copper, molybdenum, and silver were determined by 4-acid digest with ICP-ES finish using a 0.5 g sample split (BV laboratory code MA370). This assay package also includes results for major elements (e.g., Fe, K, Al), other commodity elements (e.g., Zn, Pb), and trace elements (e.g., Ni, Bi).

2. Ore grade assays for gold were determined by fire assay with AA finish using a 30 g sample split (BV laboratory code FA430).

3. Concentrations of trace elements were determined by hot aqua regia digest with ICP-MS finish using a 0.5 g sample split (BV laboratory code AQ200).

4. Concentrations of carbon and sulphur were determined by LECO analysis using a 0.2 g sample split (BV laboratory code TC003).

Lithogeochemical analysis of surface rock samples and select drill core samples:

1. Concentrations of major element oxides were determined by lithium borate fusion with ICP-ES/ICP-MS finish using a 5 g sample split (BV laboratory code LF302).

2. Concentrations of lithophile elements including rare earth elements to low and ultra-low levels were determined by lithium borate fusion with ICP-MS finish using a 5 g sample split (BV laboratory code LF100).

3. Concentrations of trace elements to low and ultra-low levels were determined by hot aqua regia digest with ICP-MS finish using a 30 g sample split (BV laboratory code AQ252-EXT).

4. Concentrations of carbon and sulphur were determined by LECO analysis using a 0.2 g sample split (BV laboratory code TC003).

5. Loss on ignition (LOI) was reported as part of the major element analysis suite.

6. Overlimit analyses were applied. If gold by AQ252 reported > 0.1 pmm then gold by FA430 (30 g fire assay) was applied. Likewise, if copper by AQ250 reported > 1,000 pmm then copper by MA370 (4-acid digest with ICP-ES finish) was applied.

The QP is satisfied that the sample preparation and analytical procedures are appropriate for the deposit and industry standard.

11.3 QA/QC

A life-of-project QA/QC review was requested in advance of and in support of the 2017 Schaft Creek resource estimation, completed by the Schaft Creek JV. Given the history of the project and the large number of methods used through the life of the project, the suite of elements evaluated has been limited to seven: silver, arsenic, gold, copper, molybdenum, rhenium, and sulphur. Even with this suite, 114 individual methods need to be assessed for precision and accuracy.

No spatial limit is applied to the sample locations, and samples from outside the current resource model were included in this QA/QC evaluation.

The suitability of all data is assessed against current and historical best practice recommendations given that some data in previous resource estimates is derived from drilling in the 1960s.

11.3.1 QA/QC Review of Copper Fox and More Recent Data

There are several plots commonly reproduced in the sections below. The control charts (e.g., Figure 11-3) have all the data ordered by drill hole age. The database does not have complete

information on the return dates for all the generations of assay data, so it is not possible to order the data by report date, which would be more common practice given that this dataset contains several reassay campaigns. There are several sets of control lines on these charts. The blue lines are the certificate values, with the solid line as the average. The dashed lines are the average ± 2sd (standard deviation) and the dotted lines are the average ± 3sd. Note that these are missing for some or all of the elements, depending on the extent and availability of certification data. The red lines are these same limits derived from the data itself. Using the recommendations of AMEC summarized in Simon (2014), these limits are used to assess whether the precision of the process is under control. For each certified reference material (CRM) and for each element, the outliers were removed by successive Grubbs tests. Once the null hypothesis that the furthest point from the centre of the population was an outlier cannot be rejected, mean and standard deviations of the coherent dataset were calculated. If a data point is outside of six standard deviations from the mean, then the data point is not plotted and there is a break in the line between points.

The bias plots show the certified (or in some cases recommended) means against the reported data (e.g., Figure 11-4). These plots show a 1:1 line in red and the slope of regression in blue, with the error in regression as a shaded zone around this. Note that this is the regression error, not the prediction error. Below this are statistics for the regression, which assess the significance of the bias. If 1.00 is within error of the slope, then there is no evidence of bias. If there is evidence of bias, Simon (2014) recommends that it should be within 5%, so a slope of between 0.95 and 1.05, in order to be acceptable.

There are two blank plots used (e.g., Figure 11-5). The top plot shows the blank values ordered by drill-hole age. The lower plot shows the blank values plotted against the average of the three previous samples and one subsequent sample. This is not ideal, but there are generations of data where the blanks were inserted only at the beginning of the drill hole and generations where it is more random. Blanks at the beginning of a job offer no measure of the degree of contamination from sample into the blank. The red line is the mean +3sd of a coherent population of blank data, again assessed after the removal of outliers using successive Grubbs tests. This method allows the assessment of blanks independent of the detection limit of the method, which is an inherently contradictory way of defining an acceptable level of contamination. The statistics below the graphs show the number of samples that exceed this blank threshold and the probability that the slope of correlation is not different to 0. If a sample has a < 5% probability that the slope is not different to 0, then there is evidence of systematic carryover from samples into the blank. Simon (2014) recommends that there should be no systematic carryover evident in blanks.

The duplicate plots show the minimum of a sample pair against the maximum of that pair. All data are therefore plotted above the red 1:1 line. For each type of duplicate (sample, crush, pulp) there is a threshold for acceptable repeatability. This uses the hyperbolic method recommended by Simon (2014) and all the parameters for allowable variability defined therein. This method allows for greater variability nearer the detection limit. The variability at high concentrations ranges from tight precision in pulp duplicates and more variability at higher stages of sample reduction. The variability limits for gold are higher than for other elements.

A significant component of this review is to define the way that acQuire exports data where there is more than one data source for an interval, whether that means the interval was resampled or the pulp was reassayed. In order to define this, the QA/QC of each method must be reviewed and ranked. Once this is complete, acQuire can export the most appropriate data for each sample for each element.

Acquire exports these with the suffix “BESTEL” in order to identify it, and through the course of this document, this derived column is referred to as the BESTEL column.

11.3.1.1 Silver

There are 21 silver methods including the historical data, which is attributed as Ag_UNK_UNK_opt. For the purpose of this review, all methods reported in oz/t are converted into ppm; these then carry both the initial and converted units in their column name, for instance Ag_UNK_UNK_opt_gpt. Of the 20 methods that have laboratory, method, and unit attribution, there are a range of detection limits and assumed precisions (geochemical methods vs. assay methods) and with a range of supporting QA/QC data. These are summarized in Table 11-1, which has the method detection limit, the number of samples with a valid result, the number of samples greater than the detection limit, the number of samples greater than three times the detection limit, the number of associated standards and blanks, and the number of duplicates (including laboratory duplicates). Also in this table are the number of occurrences in the previous BESTEL-derived column.

Table 11-1: Summary of the Available Ag Data in the Schaft Creek Database

Method	DL	No. Samples	No. > DL	No. > 3DL	No. in BESTEL	Standards + Blanks	Duplicates*
Ag_1DX1_ACME_ppm	0.1	2444	1528	824	2091	107	208
Ag_1EX_ACME_ppm	0.1	12368	10454	7946	12364	1498	2024
Ag_1F04_ACME_ppb	0.002	111	111	111	111	0	0
Ag_1F06_ACME_ppb	0.002	10	10	10	10	0	3
Ag_7AR2_ACME_gpt	2	37	16	2	10	3	3
Ag_7TD2_ACME_gpt	2	21854	4069	305	6922	1673	2865
Ag_AQ200_ppm	0.1	2110	548	236	57	204	101
Ag_AQ250_ppb	0.002	115	115	115	0	5	5
Ag_AQ252_ppb	0.002	28	28	28	28	0	0
Ag_FA_LOR_gpt	0.1	1089	1061	947	1089	55	27
Ag_G613_ACME_gpt	?	6	0	0	2	0	2
Ag_ICP_IPL_ppm	0.5	7717	2494	1120	2182	363	151
Ag_MA200_ppm	0.1	67	65	57	2	0	0
Ag_MA370_gpt	2	2121	39	1	2115	201	101
Ag_MEICP61_ALS_gpt	0.5	14	6	2	0	3	1
Ag_MEICP61a_ALS_gpt	1	443	234	34	136	58	12
Ag_MEICP61a_ALS_ppm	1	479	227	25	285	9	6
Ag_MEMS61_ALS_ppm	0.02	926	922	829	612	0	0
Ag_MEMS62_ALS_ppm	0.02	642	639	616	0	67	17
Ag_OG62_ALS_gpt	1	278	148	14	0	0	1
Ag_UNK_UNK_opt	0.34286	8791	7870	6047	8795	0	0

Table 11-1 shows that the detection limits range from 0.002 ppm to 2 ppm. To judge whether this is suitable, the distribution of primary samples must be reviewed in a robust, low detection limit method of analysis. The Ag_1EX_ACME_ppm method is a low detection limit geochemical method, providing analysis of a mixed acid digestion and which is shown to provide acceptable quality data. It has some 12,000 samples, and therefore, provides a good estimate of the whole population. This digestion is at times criticized as a method for silver because of the complex interferences from ZrO on an ICP-MS, but these interferences were well understood and were effectively corrected for by ACME at the time these data were collected.

Figure 11-1 shows the population density plot for silver by 1EX. Silver has a median of 0.4 ppm, a 95th percentile of 3 ppm and a 99th percentile of 5.9 ppm. This strongly suggests that the 1 ppm and 2 ppm detection limit methods will significantly limit the number of available valid analyses. The practicality of this is evident in Table 11-1 in the row for the Ag_7TD2_AMCE_gpt. There are nearly 22,000 valid analyses, but only 4,069 have a result of the detection limit or greater, and only 300 samples are greater than three times the detection limit. Figure 11-2 shows a statistically significant correlation between the results where there are comparable data by both methods. On the right is the same data but with only the samples at or below the detection shown. The majority of samples with a 2 ppm reported concentration by the assay method have a comparable low-level analysis. In fact, more than 90% of samples with a 2 ppm assay concentration have > 1 ppm reported by the low-level method and more than 80% have > 1.5 ppm reported. Therefore, very few samples with an above detection limit assay will result in an overestimation of silver concentration. It is therefore recommended that samples with a result of the detection limit or greater for these methods be included in the _BESTEL calculation. Samples with a result reported < 2 ppm should have an inputted value based on the regression models for silver.

Because the 1EX samples seem to have been selected with a strong bias towards providing good low-level analysis on low concentration samples, the removal of < 2 ppm 7TD Ag data affects only ~20 primary samples. All other samples either have a 1EX_ACME, ICP_IPL, or FA_LOR low-level analysis.

The MA370_ACME data and OG62_ALS data appear biased high, but all samples have an accompanying low-level method that provides more precise data, so the data can be excluded from the _BESTEL calculation with no consequence.

Figure 11-1: Population Density Plot for Ag_1EX_ACME_ppm, Presumed to be Representative of the Entire Population

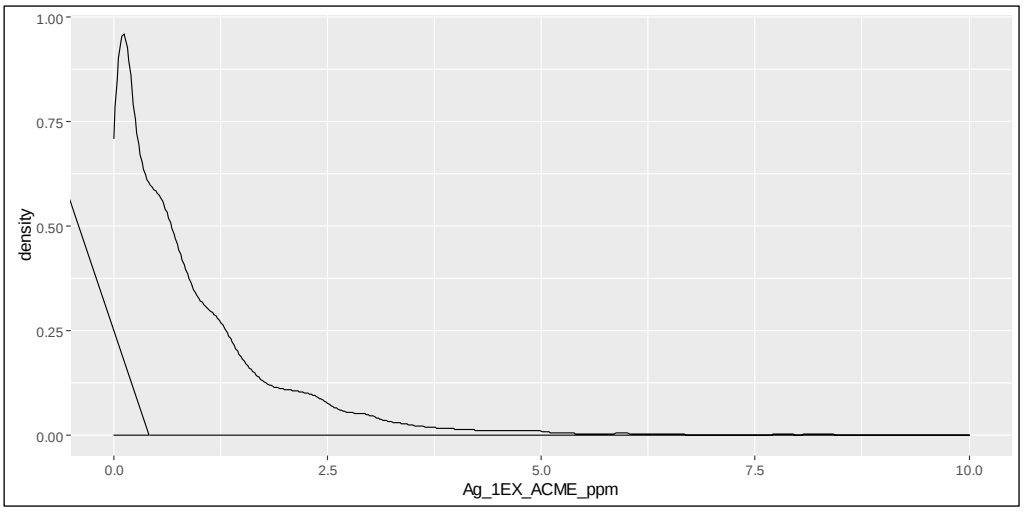

The left graph in Figure 11-2 shows the full range of data, and the right graph shows the data at below detection (shown as 1 ppm by the assay method) and at detection (shown as 2 ppm by the assay method). The red line is a 1:1 line and the blue line is the standard major axis (SMA). The grey cloud is essentially a population density representation at the particular assay concentration.

Figure 11-2: Scatter Plots of Silver by a Geochemical Method and an Assay Method

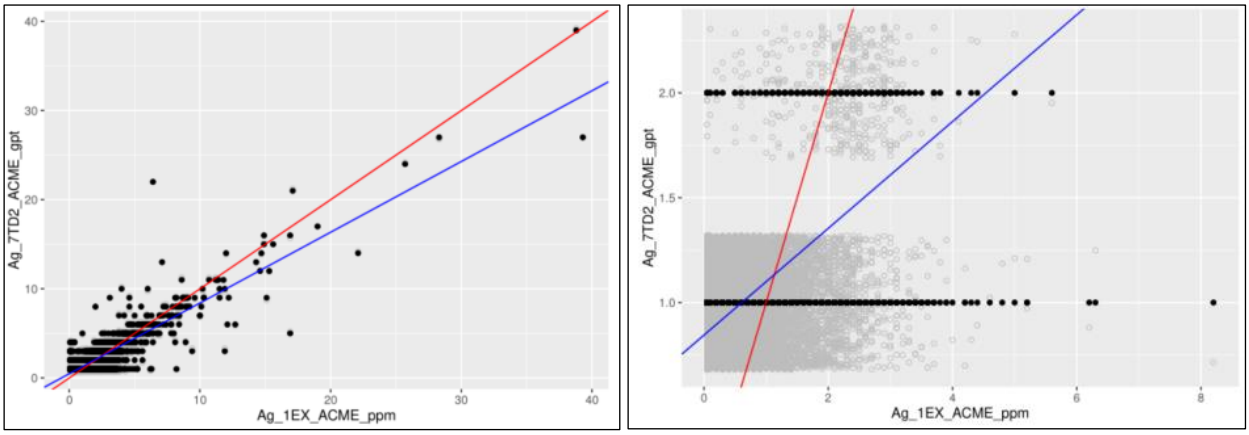

The remaining methods for silver can be grouped as ACME/BV (BV acquired ACME in 2014) aqua regia geochemical methods and mixed acid digestion methods, ALS mixed acid digestion methods, Loring assay data, and Independent Plasma Labs data.

The ACME/BV data is primarily 1DX (aqua regia) and 1EX (4-acid digestion) data, with minor additional 1F## and AQ2## (aqua regia) data and is shown in Figure 11-3. There are limitations to the completeness of QA/QC assessment that can be completed for silver as the majority of CRMs do not have a certified value for silver. The CRMs for both the 1EX and 1DX methods have an acceptable CV% given the proximity to the method detection limits. There is also an acceptably low failure rate for these data in all cases.

Figure 11-3: Example Control Charts for the 1DX and 1EX Silver Data

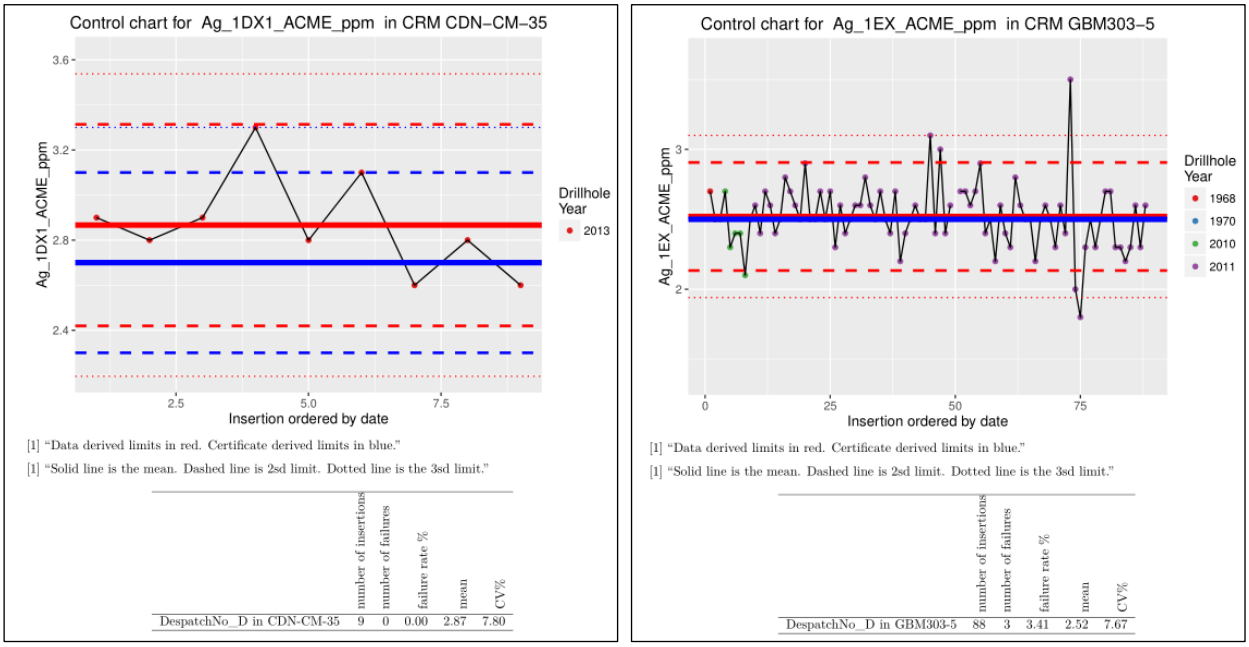

There is an acceptable bias in the 1DX data and the 1EX data (see Figure 11-4) from the samples with a CRM value for silver. The slope of regression is not significantly different to 1.00 if the low concentration CRM at 0.88 ppm is excluded (this is just a recommended value rather than a certified value). It is clear looking at the 1EX data that there are a number of outliers in these datasets and at least some of these are instances where the wrong CRM has been inserted.

Figure 11-4: Bias Plots for 1DX and 1EX Ag Data

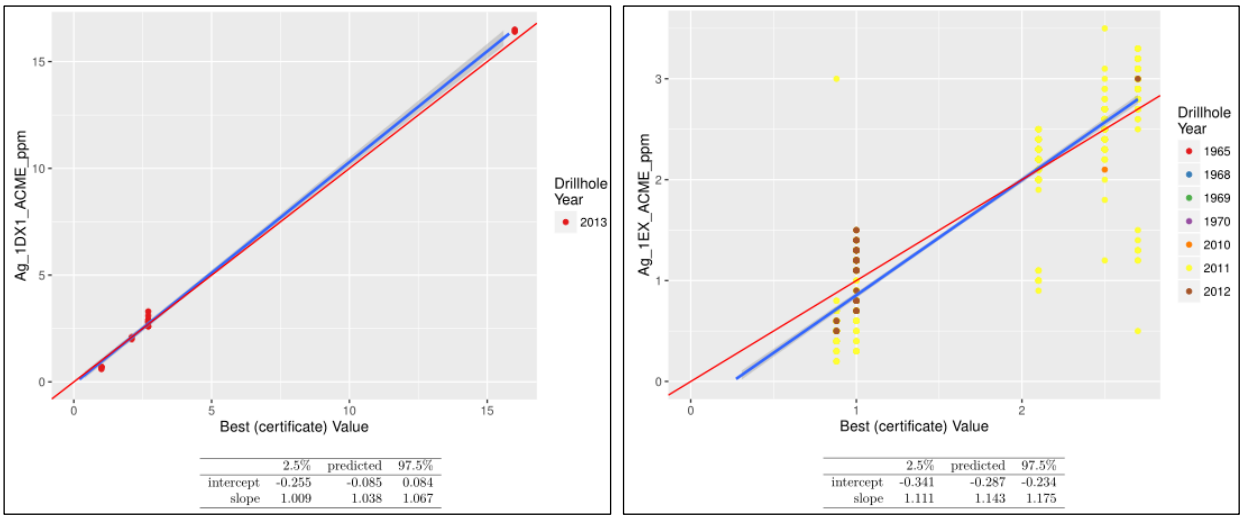

The blanks, summarized in Figure 11-5, show an acceptable failure rate and no evidence of systematic contamination.

Figure 11-5: Blank Plots for Ag by 1DX

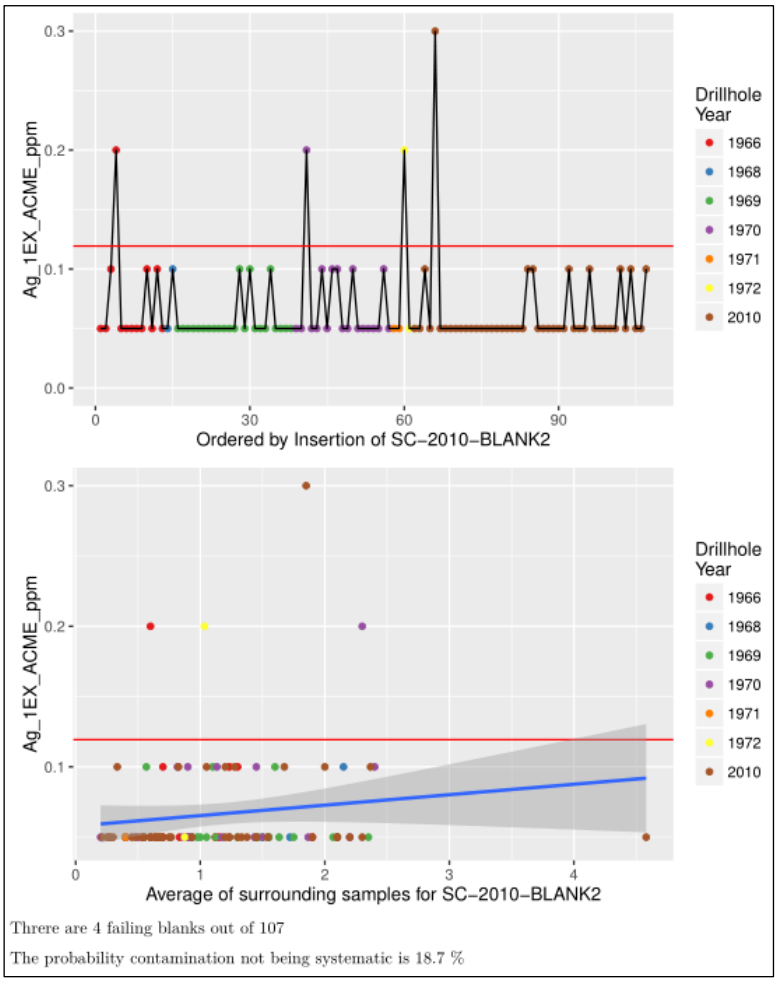

The sample duplicate plots for the 1DX method all show overall acceptable data. The 1EX data (see Figure 11-6) shows good repeatability of the overall sampling technique, but the pulp duplicates have a failure rate exceeding 10% (Figure 11-6). This suggests the analytical imprecision is a significant source of the overall variance, which is acceptable as a whole. If these data were being received on a live program, it would be recommended to consider changing to a higher precision method so that the analytical variance was minimised, but this does not make the overall sampling variance problematical.

Figure 11-6: Samples and Pulp Duplicate Pair Plots for Ag by 1EX

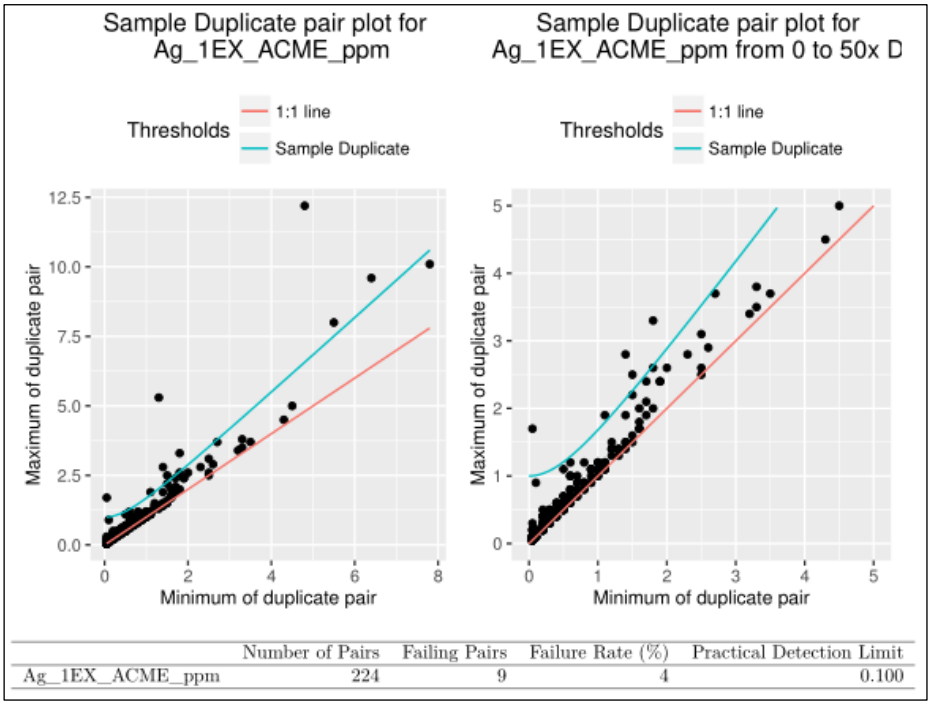

	Number of Pairs	Failing Pairs	Failure Rate (%)	Practical Detection Limit
Ag_1EX_ACME_ppm	224	9	4	0.100

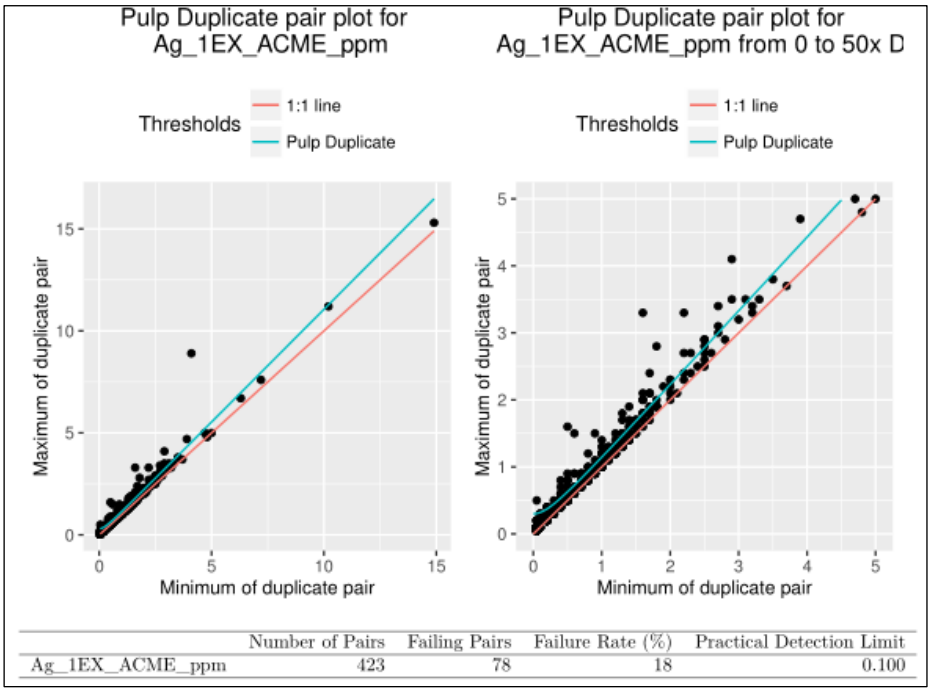

	Number of Pairs	Failing Pairs	Failure Rate (%)	Practical Detection Limit
Ag_1EX_ACME_ppm	423	78	18	0.100

The ALS MEICP61, MEMS61, and MEMS62 data have limited QA/QC, but the data that is extant shows no evidence of poor data. The MEMS62 data (see Figure 11-7) in particular is well supported by a comprehensive QA/QC program. There are nearly 1,000 MEMS61 data points that have no QA/QC support. Given the necessity for data in this Project and familiarity with the quality of data produced by ALS at this time on other projects, these data are to be retained in the database with a low priority. The higher detection limit ME-ICP61a data can be excluded with no consequence as it is always accompanied by a lower level analytical method.

Figure 11-7: Control Charts and Bias Plot for ALS MEMS62 Silver Data

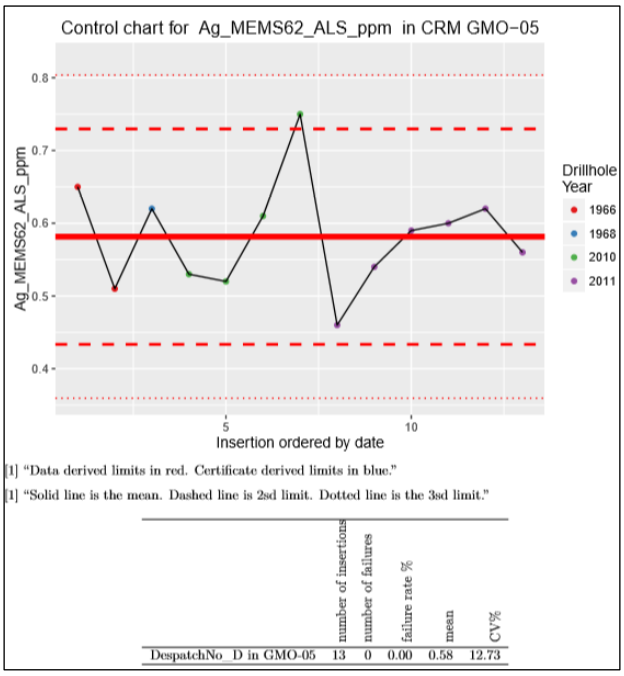

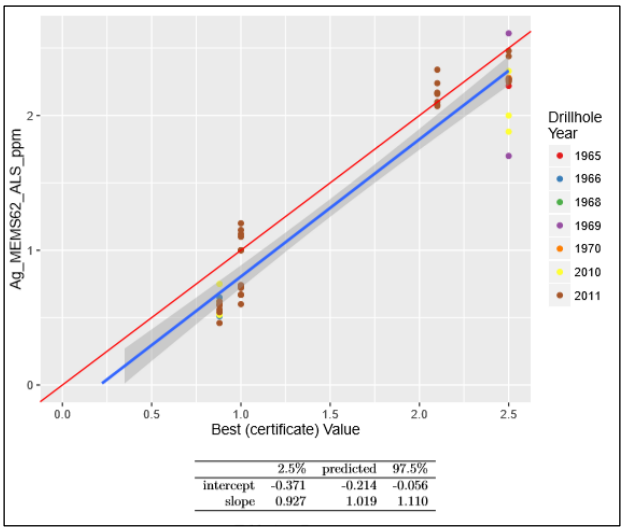

The Ag_FA_LOR_ppm data has a reported detection limit of 0.1 ppm, but is less precise than preferred. The CGS-3 data has a coefficient of variation (CV = standard deviation/mean) of 13 at 1.5 ppm, which strongly suggests that the practical detection limit was higher than 0.1 ppm. The certified reference materials used for this generation of data have no best value for silver, so there is no way to assess the accuracy of these data. The blanks show no evidence of contamination and the small population of duplicates make the assessment of quality tentative, but would technically be classified as unacceptable according to the strict criteria set by AMEC. However, one less failure would make the failure rate acceptable according to the recommendations of Simon (2014). Considering all these factors together, the recommendation is to include these data with a low priority.

The Ag_ICP_IPL_ppm data does not show acceptable precision on any of the certified reference materials (Figure 11-8). This suggests that at the range of concentration values for the standards (0 ppm to 2 ppm), the precision is poor. There is also no ability to assess accuracy as attempts to find certified values for the “STD-X” series has not been fruitful. This poor precision is a consequence of the 0.5 ppm detection limit, remembering that the median for the 1EX data was 0.4 ppm. There is a subset of samples in these data that were also analysed for the Ag 7TD assay package at ACME. While this assay data was itself not ideal for understanding the distribution of silver in deposit with a 2 ppm detection limit, CRMs show it to be unbiased at higher concentrations. Figure 11-9 shows that there is no bias between these datasets so it can therefore be inferred that the Ag_ICP_IPL_ppm data is most likely accurate. The duplicates are acceptable at a detection limit of 0.5 and there is no evidence of contamination. Therefore, the recommendation is to include these data in the final dataset with a low priority.

Figure 11-8: Control Chart for Ag_ICP_IPL_ppm for STD-A

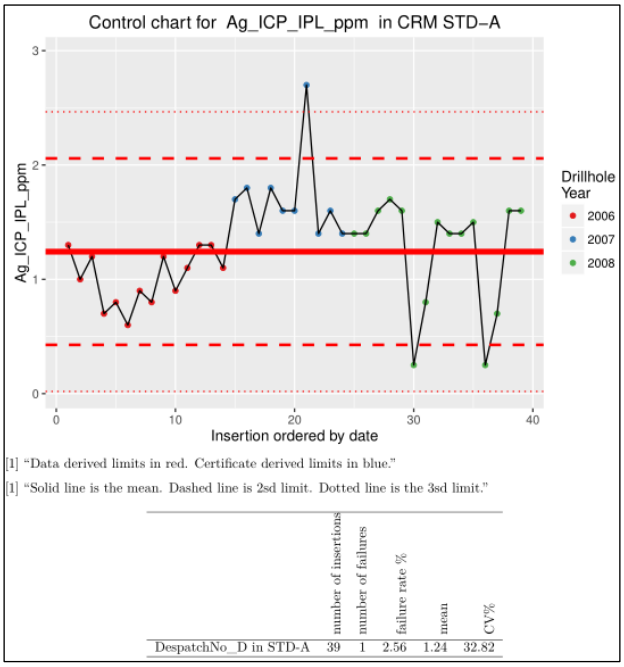

Figure 11-9: Correlation Between Ag_ICP_IPL_ppm and Ag_7RD_ACME_gpt Data for the Full Range of Points (and Right) Ranged From 0 to 25 ppm

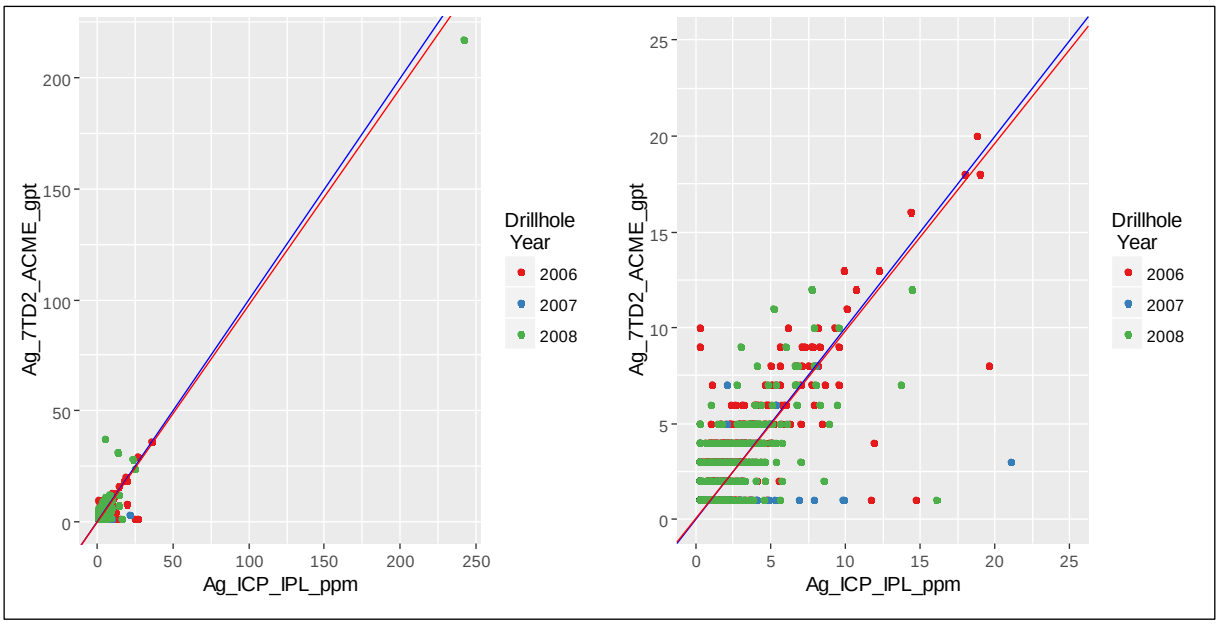

Also of note is the G612 gravimetric fire assay data for six analyses of four samples. These six analyses have such high silver that they appear inconsistent with the remainder of the silver datasets. The sample intervals that include G612 data should be checked in the geological logs to support their inclusion.

11.3.1.2 Arsenic

There are 15 arsenic methods in the database for arsenic, and like silver, there are variable detection limits and intended precisions. The methods and associated statistics are shown in Table 11-2. Like silver, in order to assess the suitability of various methods, a population that is most likely to be representative of the uncensored distribution of the dataset must be reviewed. Like silver, the best method for this will be the As_1EX_ACME_ppm data. There are critics of using mixed acid digestion data for arsenic because of potential volatility issues, but these issues are most pronounced in high total sulphide, low silicate geological matrices (it is a pronounced problem in NiS mines for instance) but is less of an issue for typical porphyry samples.

At the time of writing this Technical Report, arsenic was not intended to be included in the resource model, but should be reviewed given the potential penalty costs.

Table 11-2: Summary of the Available Arsenic Data in the Schaft Creek Database

Method	DL	No. Samples	No. > DL	No. > 3DL	No. in BESTEL	Standards + Blanks	Duplicates*
As_1DX1_ACME_ppm	0.5	2446	2323	1905	2114	107	208
As_1EX_ACME_ppm	1	8654	8105	5305	8654	1215	1636
As_1F04_ACME_ppm	0.1	111	111	111	111	0	0
As_1F06_ACME_ppm	0.1	10	10	10	10	0	3
As_7AR2_ACME_pct	100	37	0	0	1	3	3
As_7TD2_ACME_pct	200	21855	175	7	5574	1673	2865
As_AQ200_ppm	0.5	2110	1577	670	2110	204	101
As_AQ250_ppm	0.1	115	109	106	0	5	5
As_AQ252_ppm	0.1	28	25	24	5	0	0
As_ICP_IPL_ppm	5	7717	1058	701	6907	363	561
As_MA200_ppm	1	67	61	35	2	0	0
As_MA370_pct_ppm	200	2121	0	0	0	201	101
As_MEICP61_ALS_ppm	5	14	6	3	4	3	1
As_MEICP61a_ALS_ppm	50	922	81	8	586	67	18
As_MEMS61_ALS_ppm	0.2	926	914	899	877	0	0

The As_1EX_ACME_ppm data is presumed to be representative of the uncensored population as a whole. There is a median of 4 ppm, a 95th percentile of 36 ppm, and a 99th percentile of 107 ppm. The population density is shown in Figure 11-10. This suggests that the methods with detection limits of 100 ppm or greater are unsuitable for understanding the distribution of arsenic at Schaft Creek. In the event that arsenic is to be included in the resource model, the potential to use the few over-detection limit samples in the high detection limit assay methods should be reviewed in order to constrain high arsenic domains, but is not needed at this stage.

Figure 11-10: Population Density Plot for As_1EX_ACME_ppm, Presumed to be Representative of the Entire Population

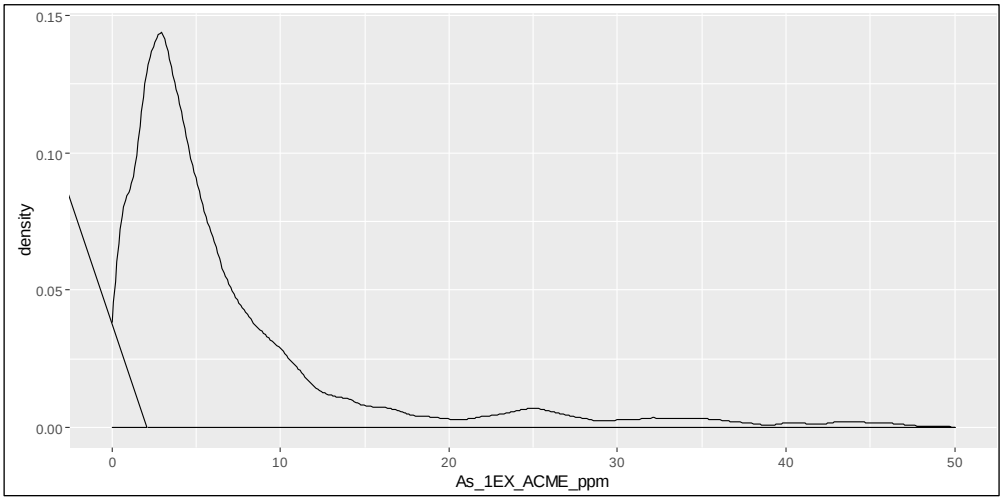

The ACME/BV data, which constitutes a substantial proportion of the samples in the dataset, both show sufficiently precise data to be considered acceptable (Figure 11-11), but both show a negative bias (Figure 11-12) presumably because of incomplete digestion in aqua regia and slight volatility in a mixed acid digestion. Like the silver data, the overall sample duplicates are acceptable, but the pulp duplicates have a higher failure rate than would generally be considered acceptable. Again, the implication of this is that the analytical imprecision makes a disproportionately high contribution to the overall variance (which is acceptable as a whole).

Figure 11-11: Control Charts for the 1DX and 1EX Methods for Arsenic

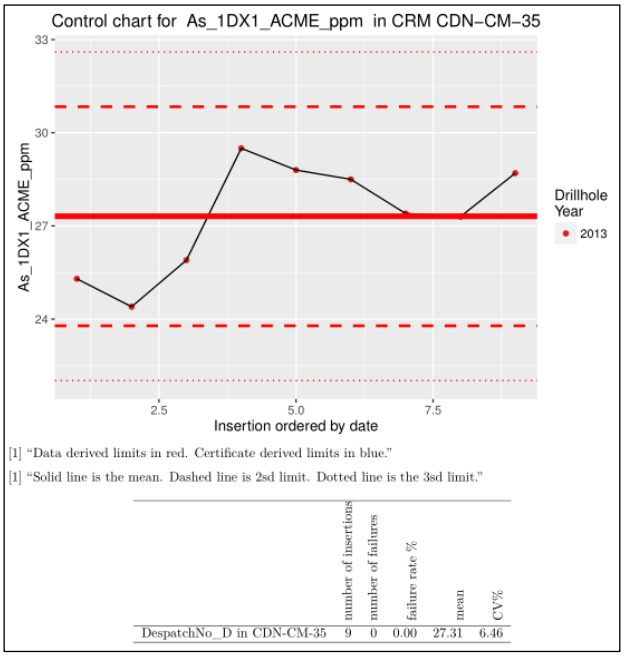

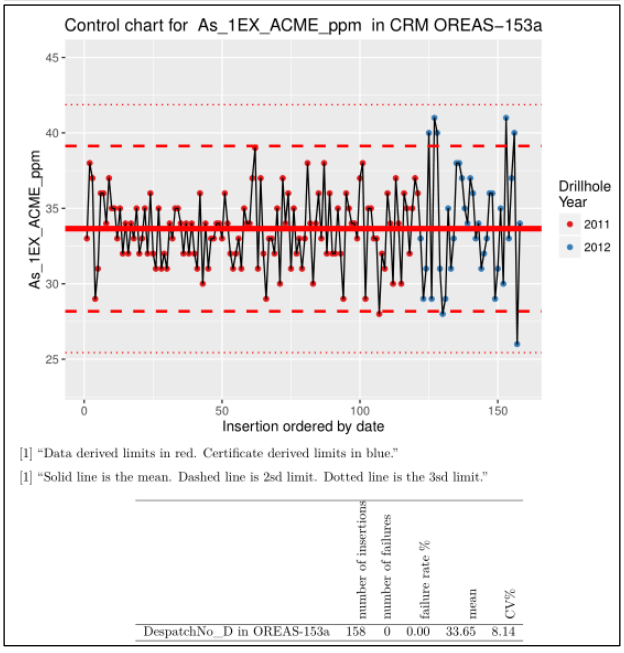

Figure 11-12: Bias Plot for the 1EX Data for Arsenic

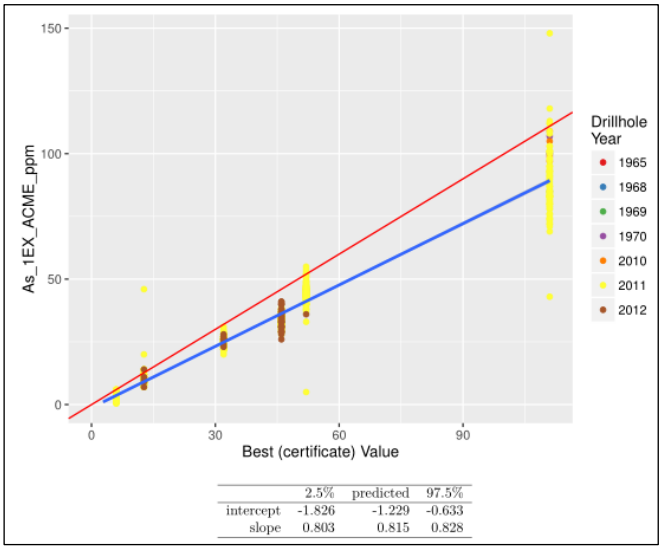

The As_ICP_IPL_ppm data, like the silver data, needs additional evaluation. The 7TD data for arsenic has a 200 ppm detection limit and is therefore unsuitable to make comparisons against, but there is a smaller subset of samples also with ALS MEICP61 data against which a comparison can be made (Figure 11-13). While these samples have insufficient CRMs to assess their accuracy, at the time ALS offered a reasonable data quality, whereas IPL were regarded as more questionable. The bimodal population for the IPL data is unrealistic given the populations indicated by other methods. The interpretation of these data is that there is some fundamental flaw in the arsenic IPL data. Therefore, the recommendation is not to include these data in the BESTEL arsenic column.

Figure 11-13: Scatter Plot of As_ICP_IPL_ppm Against As_MEMS61_ALS_ppm

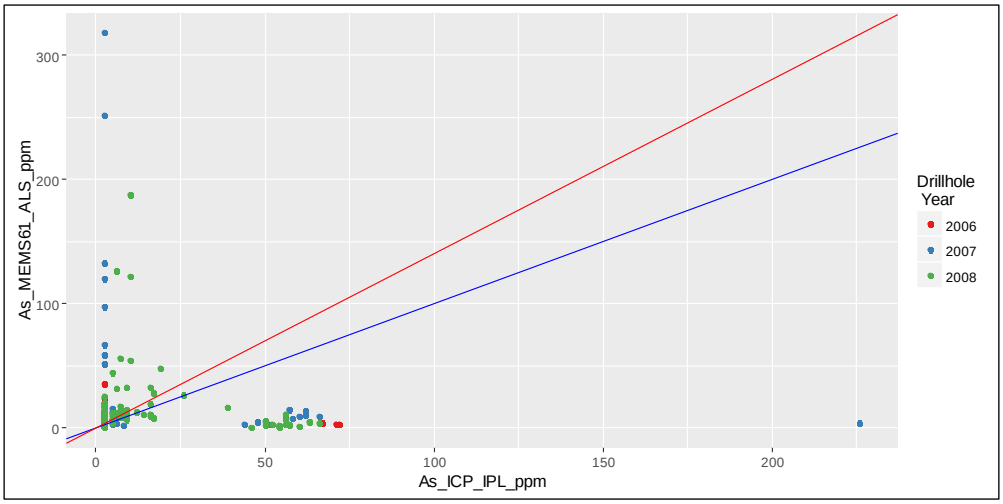

The two ALS methods at a low detection limit for arsenic have essentially no QA/QC support. The recommendation is to keep them in the database with a low priority.

11.3.1.3 Gold

There are 17 different gold methods (Table 11-3) in the Schaft Creek database. However, some of the methods that are included and which contribute to the BESTEL column, are grossly unsuitable for the quantification of gold. In particular, the 1DX1, 1EX, 1F04, AQ200, AQ250, and MA200 are all based on a < 1 g sample, and the AQ252 and 1F06 data are weak aqua regia digestions and not suitable for the quantification of gold either. The MA200 and 1EX data are 4-acid digestions, and it is extremely unusual for a laboratory to report gold by this method because it is strongly unsuitable. Therefore, approximately half the methods can immediately be removed from the QA/QC assessment. As an example of why these data are unsuitable, Figure 11-14 shows the control chart by gold reported by the 1EX, 0.25 g, mixed acid digestion method. The CV% far exceeds 5 and the data ranges far beyond the certificate limits for the CRM material.

The removal of all these methods removes only ~320 primary assays from the database, as the vast majority of samples have a high quality fire assay accompanying the multielement analysis that also reported gold. It, therefore, has a minor effect on the fidelity of the overall database for gold.

Table 11-3: Summary of the Available Au Data in the Schaft Creek Database

Method	DL	No. Samples	No. > DL	No. > 3DL	No. in BESTEL	Standards + Blanks	Duplicates*
Au_1DX1_ACME_ppb	0.0005	2446	2150	1934	84	107	208
Au_1EX_ACME_ppm	0.1	8654	2771	1272	373	1215	1663
Au_1F04_ACME_ppb	0.0002	111	106	102	0	0	0
Au_1F06_ACME_ppb	0.001	10	10	10	1	0	3
Au_AA26_ALS_gpt	0.01	640	521	365	642	65	17
Au_AQ200_ppb	0.0005	2110	1419	880	56	204	101
Au_AQ250_ppb	0.0004	115	113	110	0	5	5
Au_AQ252_ppb	0.0001	28	28	28	5	0	0
Au_FA_LOR_gpt	0.01	1089	1066	983	891	55	27
Au_FA430_ppm	0.005	2110	686	233	2110	205	101
Au_FAAAS_LOR_gpt	0.01	5734	5140	3827	1488	270	201
Au_G601_ACME_gpt	0.005	8425	6074	4792	8408	129	714
Au_G610_ACME_gpt	0.005	13447	10812	9220	12910	1544	2172
Au_G612_ACME_gpt	0.9	4	4	4	2	0	2
Au_ICP21_ALS_gpt	0.001	280	247	214	0	0	1
Au_MA200_ppm	0.1	67	29	15	2	0	0
Au_UNK_UNK_opt	0.003429	8808	8783	8528	8808	0	0

Figure 11-14: Control Chart for Gold Reported by the 1EX ACME Method

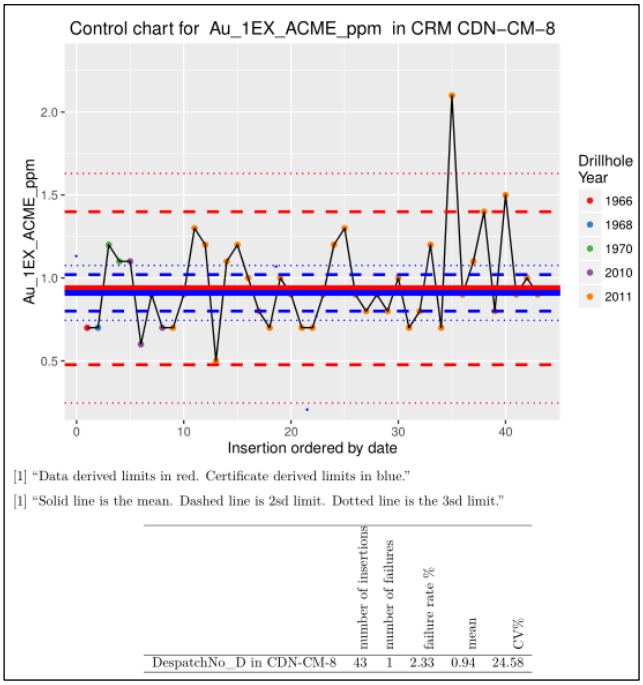

However, in all but the G612 ACME method, all fire assay methods provide precise (Figure 11-15) and accurate data (Figure 11-16). While there are occasional sample mix-ups, there are no other failures for gold by fire assay methods.

Figure 11-15: Control Charts for Gold for Two Selected CRMs

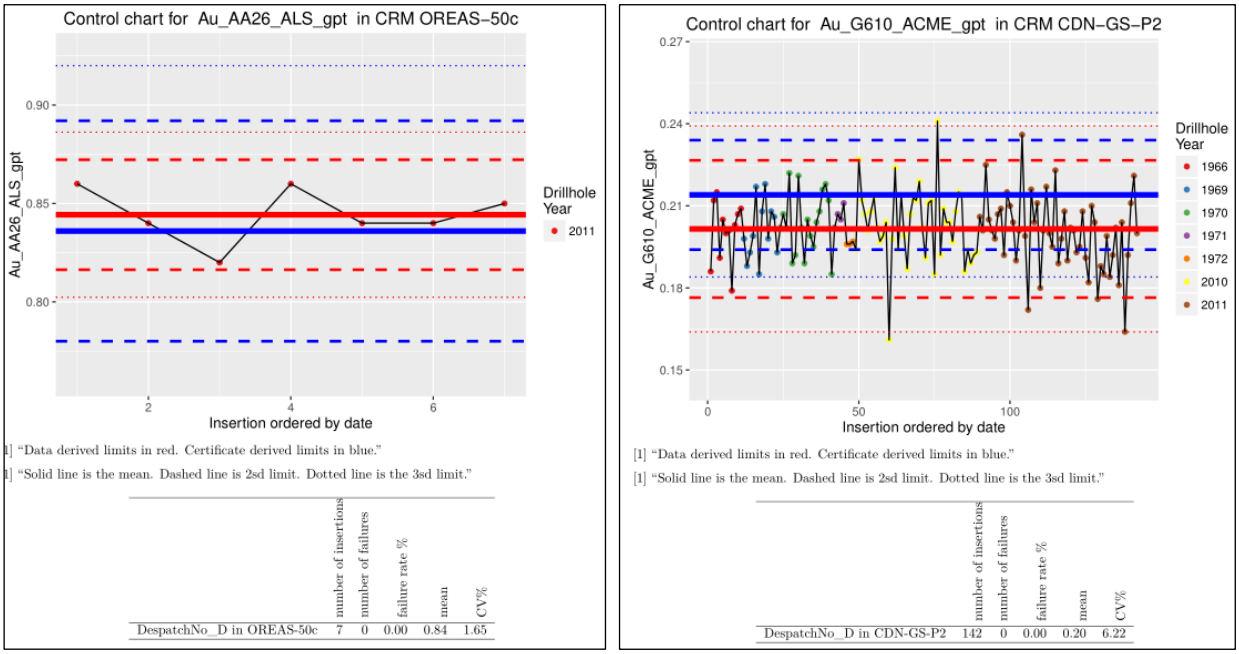

Figure 11-16: Bias Plots for the G610 ACME and AA26 ALS Data Fire Assay Methods

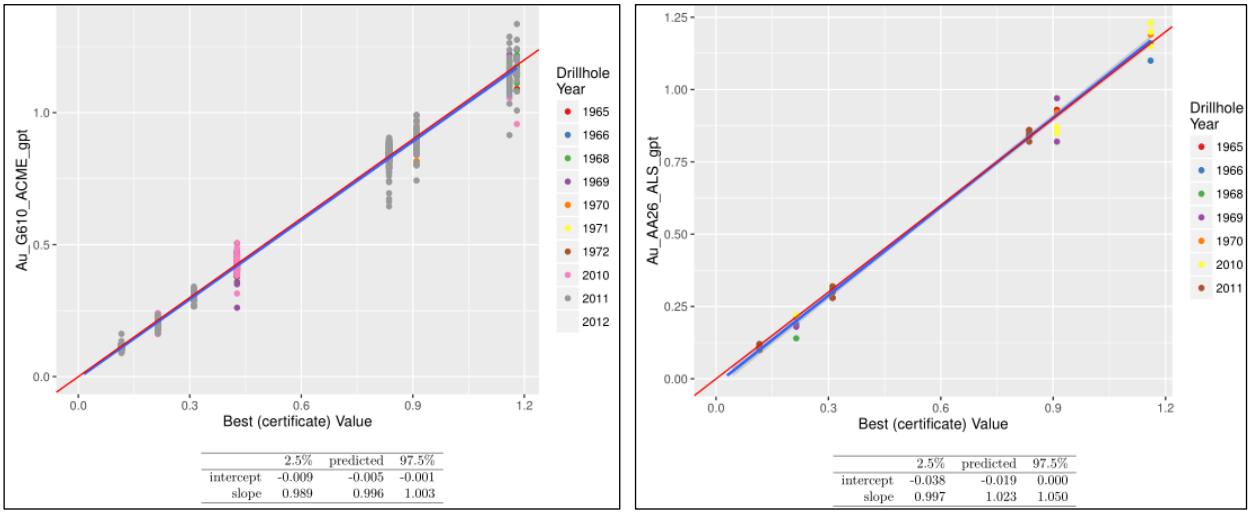

The only exception to the fire assay gold data quality is that Au_FAAAS_LOR_gpt does not have any CRMs with known values, so the accuracy of this method cannot be assessed.

Also of note is the G612 gravimetric fire assay data for four samples. These four samples have such high gold that they appear inconsistent with the remainder of the gold datasets. The sample intervals with a G612 data should be checked in the geological logs for a justification for their inclusion.

11.3.1.4 Copper

There are 20 copper methods in the database, including assay and geochemical methods, as well as mixed acid and aqua regia methods (Table 11-4). Again, there is variable QA/QC support for these methods.

Table 11-4: Summary of the Available Copper Data in the Schaft Creek Database

Method	DL	No. Samples	No. > DL	No. > 3DL	No. in BESTEL	Standards + Blanks	Duplicates*
Cu_1DX1_ACME_ppm	0.00001	2435	2435	2435	84	107	207
Cu_1EX_ACME_ppm	0.00001	8576	8574	8574	357	1203	1646
Cu_1F04_ACME_ppm	0.00001	111	111	111	0	0	0
Cu_1F06_ACME_ppm	0.00001	10	10	10	1	0	3
Cu_7AR2_ACME_pct	0.02	37	36	33	1	3	3
Cu_7TD2_ACME_pct	0.001	21855	20556	19466	21854	1673	2865
Cu_AQ200_ppm	0.00001	2106	2106	2098	57	204	101
Cu_AQ250_ppm	0.0001	115	115	115	0	5	5
Cu_AQ252_ppm	0.0001	27	27	27	0	0	0
Cu_ASY_IPL_Pct	0.01	1679	1345	1293	393	109	84
Cu_FA_LOR_pct	0.001	1089	1089	1089	846	55	27
Cu_ICP_IPL_ppm	0.0001	7693	7588	7447	1789	363	537
Cu_MA200_ppm	0.00076	63	62	62	2	0	0
Cu_MA370_pct	0.001	2121	1612	1260	2120	201	101
Cu_MEICP61_ALS_pct	0.001	14	14	12	4	3	1
Cu_MEICP61a_ALS_pct	0.001	642	634	608	80	67	17
Cu_MEICP61a_ALS_ppm	0.001	280	251	230	0	0	1
Cu_MEMS61_ALS_ppm	0.0001	926	926	925	275	0	0
Cu_OG62_ALS_pct	0.001	278	266	230	0	0	1
Cu_UNK_UNK_pct	0.001	18249	18224	18026	18282	0	0

There is a singular circumstance for copper in this dataset in that of the 20 methods available, there is not a strong justification to exclude the data from any one method. Some methods have more QA/QC support than others, but there is generally good quality data for copper in the entire database. Apart from the occasional insertion of the incorrect standard, all control charts show good precision in the data (Figure 11-17). These results also show no significant bias in any method (Figure 11-18).

Figure 11-17: Selected Control Charts for a Variety of Copper Methods in the Database

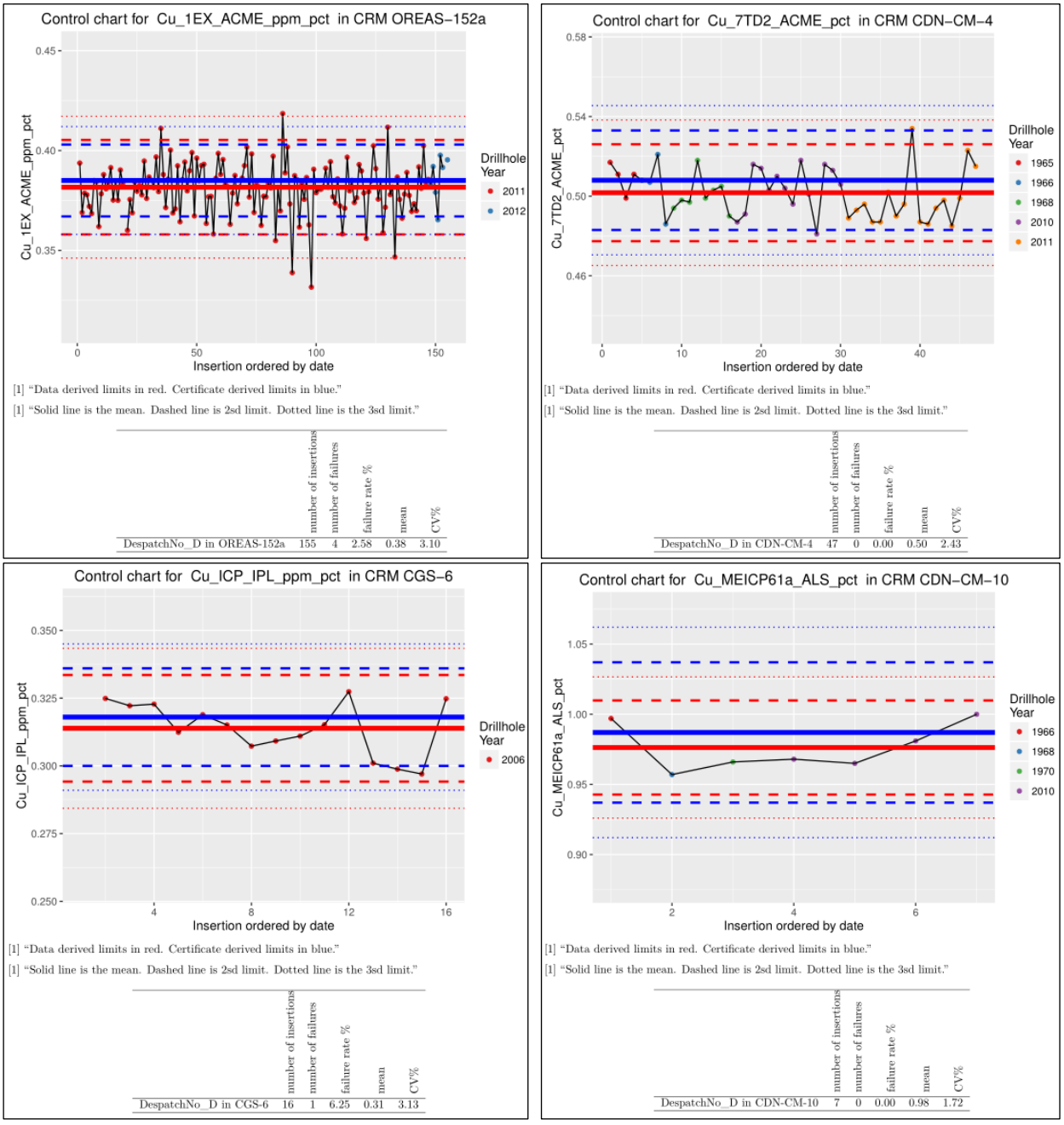

Figure 11-18: Selected Bias Plots for Cu

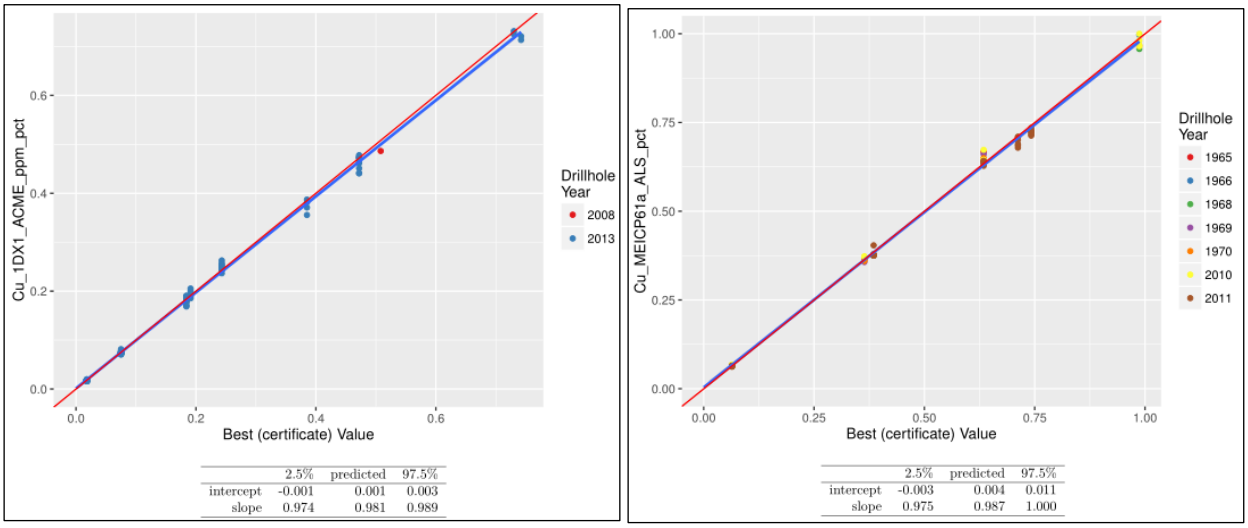

The blanks for copper show no or very minor contamination (Figure 11-19). In the right example plots in Figure 11-19, the null hypothesis that the slope is not different to 0 must be rejected, implying some systematic contamination, but the level of contamination is < 0.25% on average. This is therefore acceptable.

Figure 11-19: Selected Blank Plots for Cu

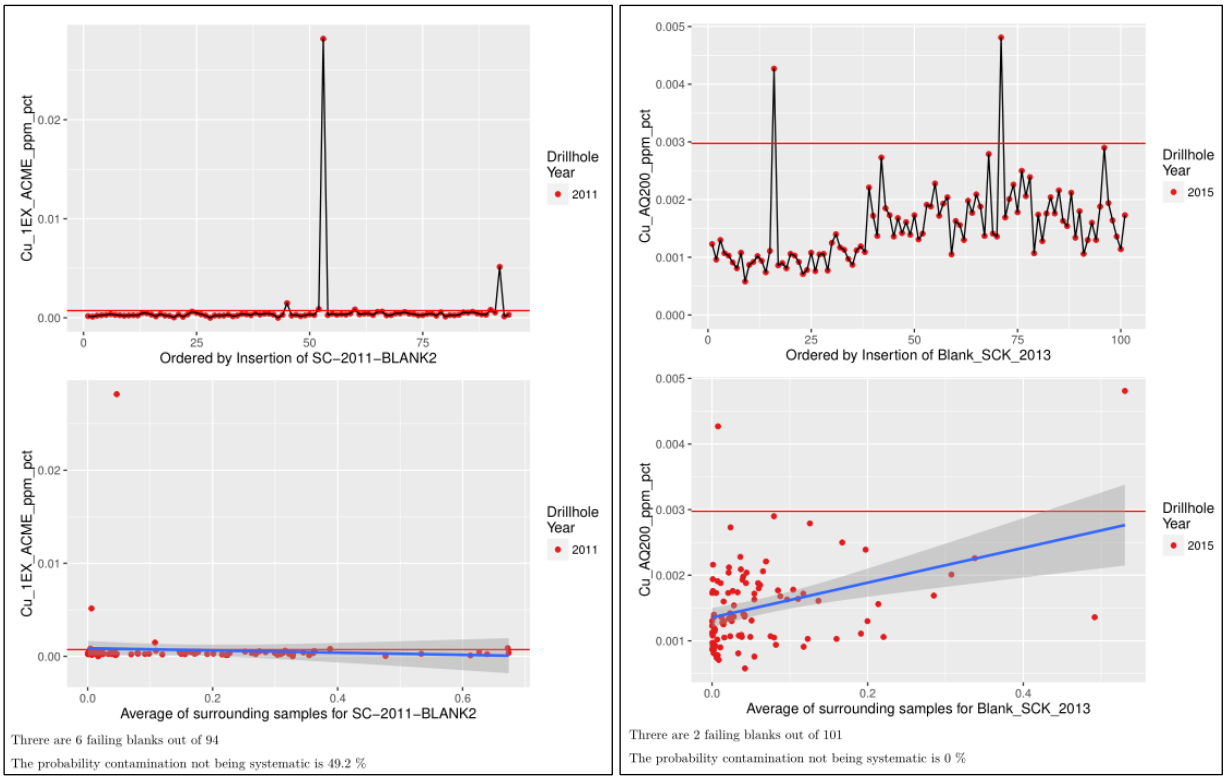

The duplicates show the only problem for the copper data (Figure 11-20). In several of the datasets, the overall sample duplicate failure rate exceeds 10%. However, in all the subsequent stages of sample reduction (crushing, pulverization, etc.) the duplicate failure rates are acceptable. This strongly suggests that the common practice of ¼ core sample duplicates is not suitable for Schaft Creek and this practice should be discontinued in the future. The copper data as a whole should nevertheless be considered acceptable.

Figure 11-20: Selected Duplicate Control Charts for Cu

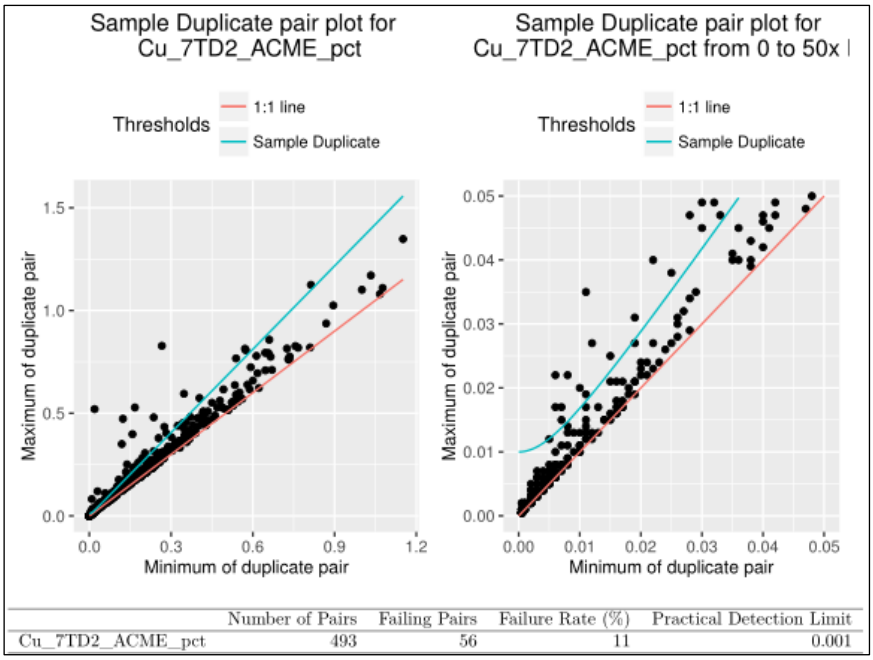

	Number of Pairs	Failing Pairs	Failure Rate (%)	Practical Detection Limit
Cu_7TD2_ACME_pct	493	56	11	0.001

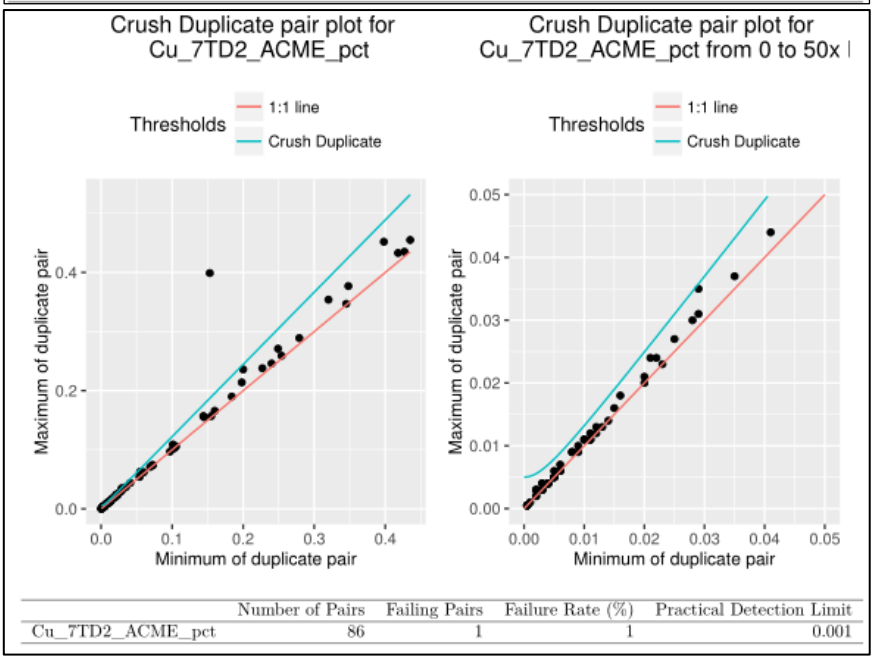

	Number of Pairs	Failing Pairs	Failure Rate (%)	Practical Detection Limit
Cu_7TD2_ACME_pct	86	1	1	0.001

11.3.1.5 Molybdenum

There are 20 molybdenum methods in the dataset, with a range of methods and precisions (Table 11-5). It is notable that there will be a methodological difference in the bias when comparing aqua regia and mixed acid digestion data. The molybdenum will not fully extract into aqua regia but is metastable in solution in an aqua regia, particularly after dilution for analysis. It is anticipated that the aqua regia data will demonstrate a negative bias.

Table 11-5: Summary of the Available Molybdenum Data in the Schaft Creek Database

Method	DL	No. Samples	No. > DL	No. > 3DL	No. in BESTEL	Standards + Blanks	Duplicates*
Mo_1DX1_ACME_ppm	0.00001	2445	2435	2201	84	107	280
Mo_1EX_ACME_ppm	0.00001	8650	8642	8387	8654	1215	1661
Mo_1F04_ACME_ppm	0.000001	111	106	79	0	0	0
Mo_1F06_ACME_ppm	0.000001	10	9	2	1	0	3
Mo_7AR2_ACME_pct	0.001	37	30	28	1	3	3
Mo_7TD2_ACME_pct	0.001	21855	13645	10803	13557	1673	2865
Mo_AQ200_ppm	0.00001	2108	2104	1840	57	204	101
Mo_AQ250_ppm	0.000001	115	109	105	0	5	5
Mo_AQ252_ppm	0.00001	28	27	25	0	0	0
Mo_ASY_IPL_pct	0.0006	1007	962	886	764	0	0
Mo_ICP_IPL_pct	0.0001	2292	2279	2133	214	116	152
Mo_ICP_IPL_ppm	0.0001	5404	5189	5014	1947	247	388
Mo_MA200_ppm	0.00001	67	65	58	2	0	0
Mo_MA370_pct	0.001	2121	371	185	2120	201	101
Mo_MEICP61_ALS_pct	0.0001	14	12	7	4	3	1
Mo_MEICP61a_ALS_pct	0.001	642	454	335	80	67	17
Mo_MEICP61a_ALS_ppm	0.001	280	157	115	0	0	1
Mo_MEMS61_ALS_ppm	0.000001	926	913	821	275	0	0
Mo_OG62_ALS_pct	0.001	278	163	115	0	0	1
Mo_UNK_UNK_pct	0.0001	18124	16909	13156	18135	0	0

The data for molybdenum is generally good as was the case for copper. While molybdenum exhibits a slightly higher CV% than was seen for copper, this is generally attributable to the concentration of the sample being nearer the detection limit for the method. There are no CRMs that are not performing at a level of precision that would indicate that it was unsuitable for resource estimation (Figure 11-21).

Figure 11-21: Control Charts for Selected Molybdenum Methods

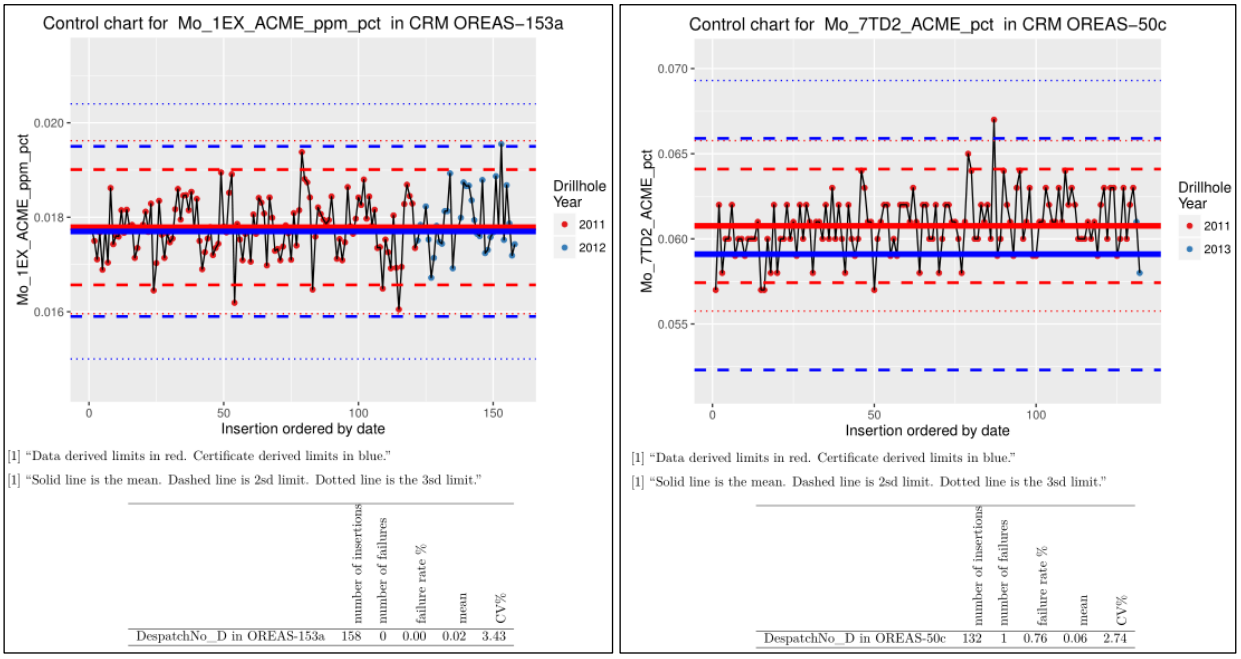

The aqua regia methods generally exhibit a negative bias of between 5% and 10% of the certified values (Figure 11-22). This is expected and is a function of the chemistry of the method. The 4-acid digestion data generally exhibits no or an acceptably small bias.

Figure 11-22: Bias Plots for an Aqua Regia Method (Left) and a 4-acid Digestion (Right)

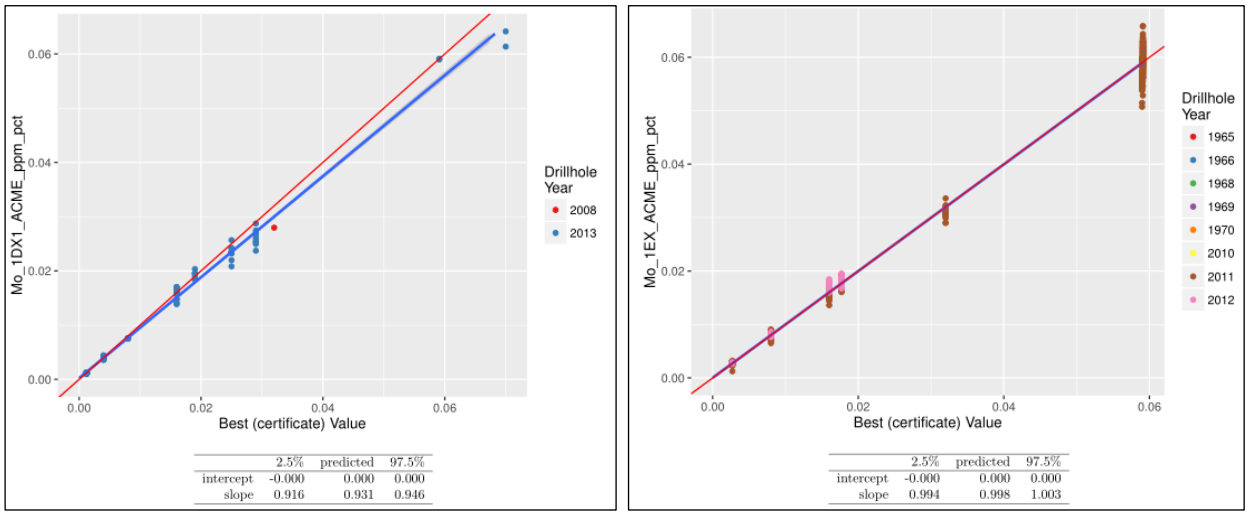

The blanks for molybdenum exhibit an acceptable failure rate and generally no evidence of systematic contamination. Where there is systematic contamination, it is generally a very low level of carryover. This is significant as molybdenite has a tendency to smear on the bowl during pulverization. The duplicate data is better for the assay data than for the geochemical methods (Figure 11-23). The 1EX data for instance has a higher failure rate than the 7TD data. The 1EX data has a failure rate of greater than 30%, which is alarming given that the assay data has an 8% failure rate. That suggests that the error is independent of the sampling. The subsequent stages of the 1EX digestion exhibit the same sort of failure rate, suggesting that the issue is related to subsampling at a late stage as the CRMs indicate that there is good analytical precision. Non-assay data should therefore be deprioritised relative to the assay data.

If the Schaft Creek JV was to remount a significant drill program, the source of this error should be determined, whether it is methodological or related to subsampling for digestion.

Figure 11-23: Selected Duplicate Plots for Selected Mo Methods

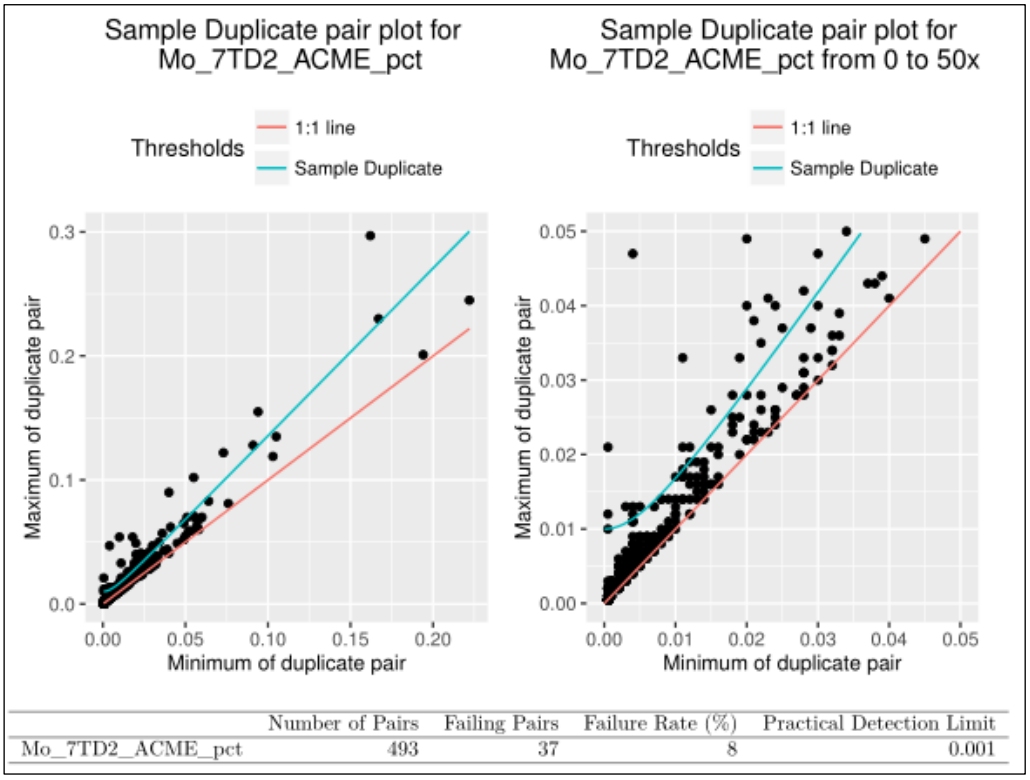

	Number of Pairs	Failing Pairs	Failure Rate (%)	Practical Detection Limit
Mo_7TD2_ACME_pct	493	37	8	0.001

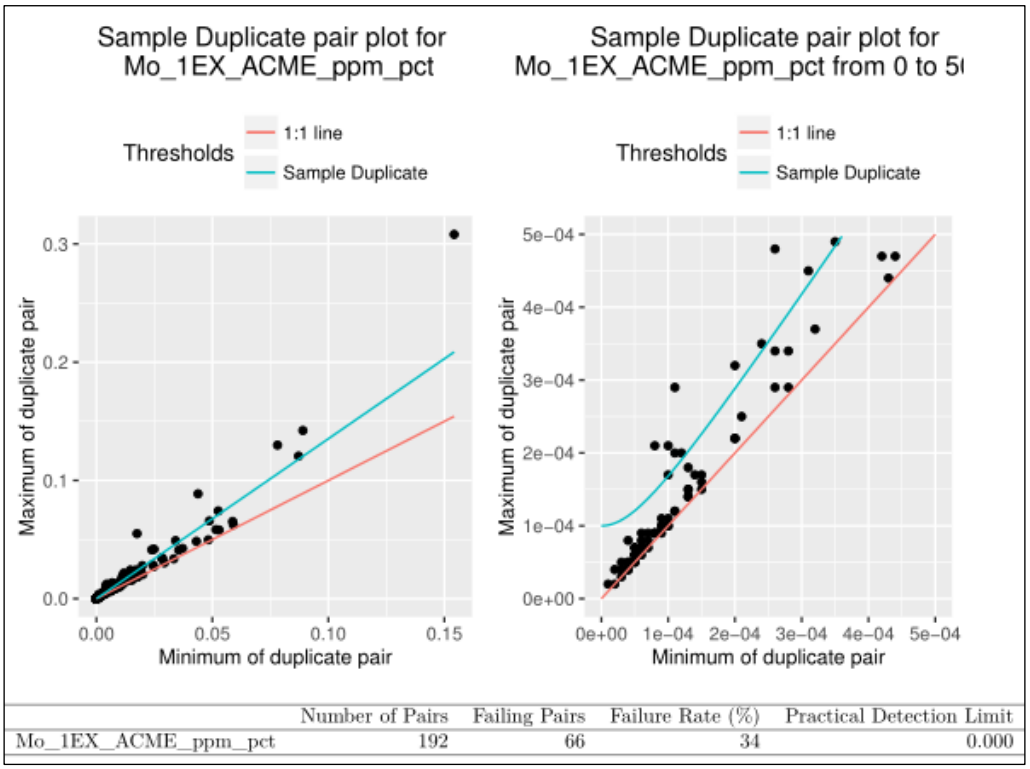

	Number of Pairs	Failing Pairs	Failure Rate (%)	Practical Detection Limit
Mo_1EX_ACME_ppm_pct	192	66	34	0.000

11.3.1.6 Rhenium

There is only a small subset of samples with a valid rhenium analysis (Table 11-6). There is also only one method with valid QA/QC included, which shows acceptable precision, but the standards for that method have no certification for rhenium (Figure 11-24). Therefore, there is no way of assessing the accuracy of the rhenium data.

At the time of this QA/QC review, there was no intention to include rhenium in the resource estimate, but an assessment of quality was requested.

Table 11-6: Summary of the Available Rhenium Data in the Schaft Creek Database

Method	DL	No. Samples	No. > DL	No. > 3DL	No. in BESTEL	Standards + Blanks	Duplicates*
Re_1F04_ACME_ppb	0.001	111	46	25	111	0	0
Re_1F06_ACME_ppb	0.001	10	5	2	10	0	3
Re_AQ200_ppb	0.01	2105	156	78	2105	201	101
Re_AQ250_ppb	0.001	115	114	104	0	5	5
Re_AQ252_ppb	0.001	28	22	21	28	0	0
Re_MA200_ppm	0.005	67	57	49	65	0	0
Re_MEMS61_ALS_ppm	0.002	926	699	569	906	0	0

Figure 11-24: Control Chart for Rhenium using the AQ200 Method

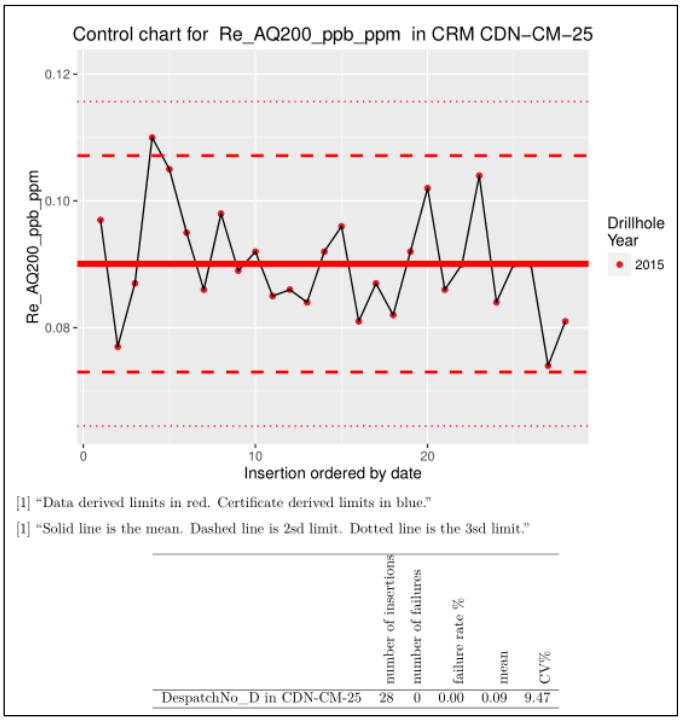

Note: This is the only CRM with more than a few insertions for rhenium in the entire database.

There is not enough blank or duplicate data to conclusively assess rhenium data quality, but the limited data suggests that it is not biased.

It is notable that there is generally a good correlation between molybdenum and rhenium for Mo < 0.2% (Figure 11-25). The statistics for the SMA shown in red are also provided below.

Figure 11-25: Correlation of Rhenium with Molybdenum for the Full Range of Data (Left) and Zoomed into Near the Origin (Right)

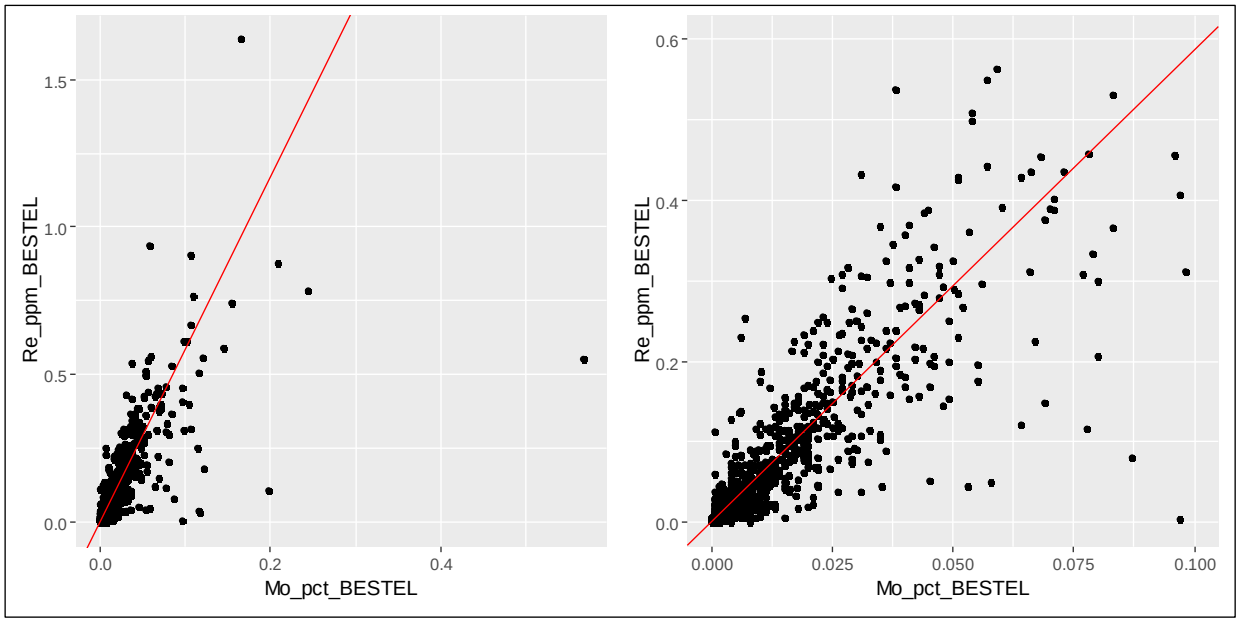

Note: SMA in red.

```
Coefficients:
                elevation    slope
estimate     -0.0004765358 5.884923
lower limit  -0.0020112563 5.782979
upper limit   0.0010581846 5.988665

H0 : variables uncorrelated
R-squared : 0.7443584
P-value : < 2.22e-16
```

11.3.1.7 Sulphur

There are 14 different sulphur methods (Table 11-7) in the dataset, but at present, only the "TOT_S" infrared combustion data are included in the BESTEL column. Most sulphates and sulphides will be dissolved in an aqua regia digestion or a 4-acid digestion. The latter may exhibit some volatility for sulphur but that is generally negligible in low total sulphur environments and can be evaluated. Some sulphates (barite in particular) have limited solubility, but there is little recorded evidence for their presence at Schaft Creek. If the sulphur by these methods can be validated, it provides an additional 30,000 valid analytical results.

At the time of writing this Technical Report, there was no indication that sulphur would be estimated into the block model.

Table 11-7: Summary of the Available Sulphur Data in the Schaft Creek Database

Method	DL	No. Samples	No. > DL	No. > 3DL	No. in BESTEL	Standards + Blanks	Duplicates*
S_1DX1_ACME_pct	0.05	2209	1781	1392	0	105	194
S_1EX_ACME_pct	0.1	8654	6364	4152	0	1215	1663
S_1F06_ACME_pct	0.1	10	4	1	0	0	3
S_7AR2_ACME_pct	0.05	37	34	33	0	0	0
S_7TD2_ACME_pct	0.05	21855	18231	14893	0	1674	2865
S_AQ200_pct	0.05	2105	483	229	0	201	101
S_MA200_pct	0.1	67	62	47	0	0	0
S_MA370_pct	0.05	2121	506	229	0	201	101
S_MEICP61_ALS_pct	0.04	14	13	12	0	3	1
S_MEICP61a_ALS_pct	0.05	922	860	621	0	67	18
S_MEMS61_ALS_ppm_pct	0.01	926	899	769	0	0	0
TotS_2A13_ACME_pct	0.02	15153	13697	12532	14913	1586	1705
TotS_IR08_ALS_pct	0.01	926	898	766	650	0	0
S_TC000_pct	0.02	2260	1095	575	0	209	106

The sulphur data shows excellent precision by all methods. The vast majority of CRMs show excellent precision (Figure 11-26) when above the detection limit, the exception being 7TD2_ACME_pct in CRM CDN−GS−P2, which has an atypically high CV%. The bias plots (Figure 11-27) also show no appreciable bias by any method (note that the 0.6% S point on the 7TD graph shown is a recommended value, not a certified value) and there is no evidence of contamination. Every duplicate population has < 10% failure rate at all levels of duplication.

There is no reason to exclude the additional 30,000 samples in the calculation of a _BESTEL column.

Figure 11-26: Control Charts for (Left) an Infrared Combustion Method and (Right) a Mixed Acid Digestion

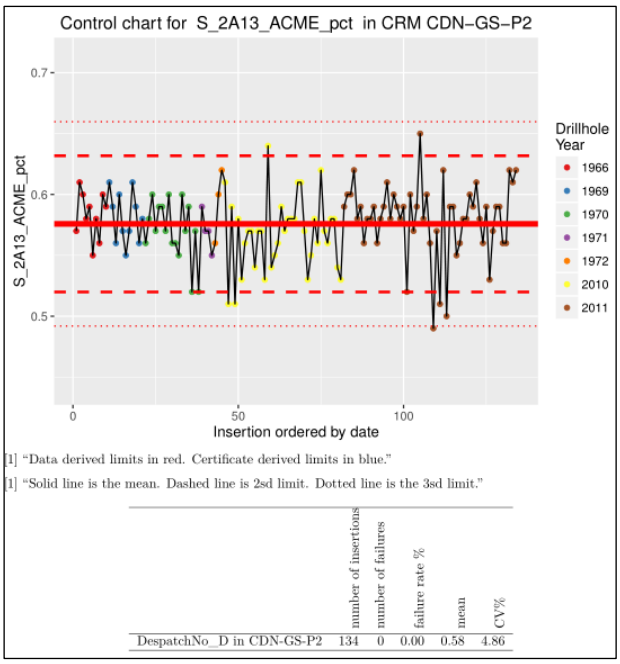

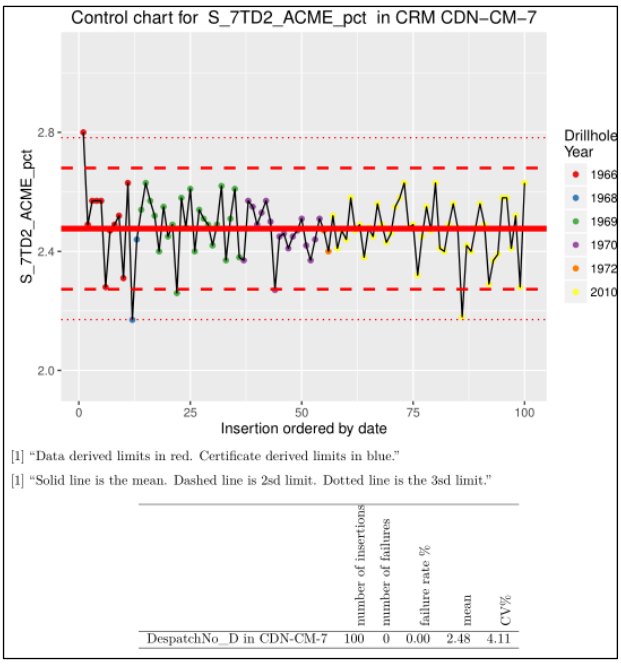

Figure 11-27: Bias Plots for S by (Left) a Total Digestion Method and (Right) an Aqua Regia Method

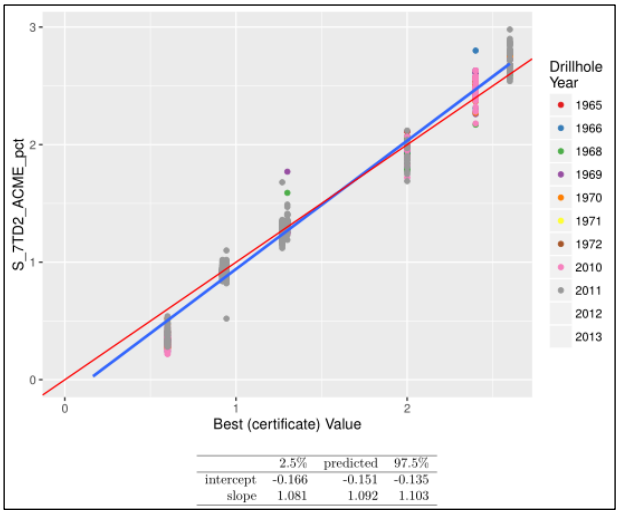

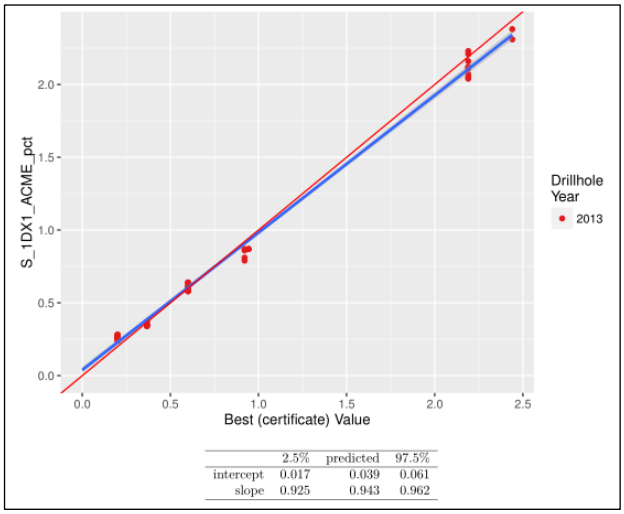

11.3.2 Historical Data

The Schaft Creek JV assessed the historical data by comparing results from twinned drill holes (drilled by Copper Fox) and nearest neighbour (NN) samples and from a small subset of reassays taken by Copper Fox on different sampling intervals compared to the original sampling. AMEC provided a set of 3 m composite samples from historical and modern drill holes and provided nearest sample comparisons. The distance between points ranged from < 1 m to > 100 m. For the purposes of this review, for a sample to be considered a twin, the maximum difference that could be considered was assumed to be 20 m but preferably a much closer sample spacing would be required for a twinned sample comparison. For each element and generation, plots and summary statistics were produced for a 5 m maximum distance, as well as a 10 m and 20 m maximum distance.

For each comparison, the Schaft Creek JV prepared three different plots. The top plot shows the number of sample pairs that are within a certain distance. The middle plot shows a scatterplot of historical data versus nearest modern data with the points coloured by distance. There is a 1:1 line shown in blue and the red line shows the SMA regression forced through the origin for the data limited to the maximum sample spacing. The thinner red lines show the 95% confidence interval in the slope of the SMA regression. The pink line shows the SMA when not forced through 0 and is more in line with the analysis performed by AMEC. The bottom plot shows the slope of the SMA correlation (forced through the origin) in red and the 95% confidence interval in the blue and green lines. If this range contains 1.0, at any sample spacing then at that distance, there is insufficient evidence the data is biased and that a correction needs to be made. Likewise, the purple line shows the probability that the data is no different from 1. When this line drops below 0.05, then the data is biased and there is good evidence that a correction needs to be made.

In addition to this, for each comparison, the SMA coefficients and uncertainties are printed firstly for the SMA forced through the origin, and subsequently for the SMA with the intercept also calculated. Both of these have the probability of a correlation shown and the probability that the slope =1 shown. In the event that AMEC recommended a correction to a historical dataset previously, then the probability that the same slope would be predicted was also evaluated.

In some cases, there are resampling and modern analyses on different sample intervals for a subset of historical holes. Quantile-quantile (QQ) plots are shown for these sampling intervals to allow for comparisons of the populations of data and an estimate of bias.

11.3.2.1 Asarco Data

The Asarco generation drilling has no primary data for silver or gold; however, the copper and molybdenum data were reviewed. AMEC previously recommended the correction below be applied to the molybdenum data and that no correction be made to the copper data.

Asarco

- Mo – correction y = (x - 0.0039) / 0.8605
  The correction is applied up to a maximum grade of 0.03% Mo. At higher grades, no correction is applied, as the corrected grades would be higher than the original grades.

Copper in the twinned samples shows that at nearly all spacings between 0 m and 20 m, there is insufficient evidence for the need of a correction (Figure 11-28). For a very small set of maximum sample distances between 4 m and 6 m, there is > 95% chance that the slope is not 1. At 4 m maximum sample spacing, there are more than 80 samples, and the SMA regression through this population is not statistically different to 1. At 6 m maximum sample spacing, there are 90 samples, and the SMA regression through this population is again not statistically different to 1; however, at 5 m, there is a suggestion of bias between the datasets. There is no industry standard on what constitutes a twinned sample but consensus seems to be between 5 m and 10 m as a maximum distance. Given that at most sample spacings < 10 m, there is a < 95% probability that the slope is not 1; there is no basis for a copper correction based on these data. This is in agreement with AMEC recommendations from the previous resource estimate.

However, the QQ plots for copper of the resampling completed by Copper Fox show that the populations match at low concentrations (up to 0.4% Cu), but that at higher concentration, there is a clear departure from the near-linear trend (Figure 11-31). This would affect some 1,500 assays across the entire dataset, with the bias becoming more pronounced at higher concentrations. This has been debated amongst the project team as it indicates a strong bias at high concentrations. However, there was at least 30 years between the original drilling and the resampling, during which time, the samples had been exposed to the atmosphere. It is possible that intense oxidation of the core may have resulted in a mass increase becoming more pronounced in higher sulphide material and in a higher bias in higher grade samples. Because the bias is not indicated in the twinned dataset, it has been concluded that there is no justification for a correction based on these data.

Figure 11-28: Summary Plots for Copper in the Asarco Data as Compared to the Copper Fox Data for Sample Pairs up to 20 m Apart

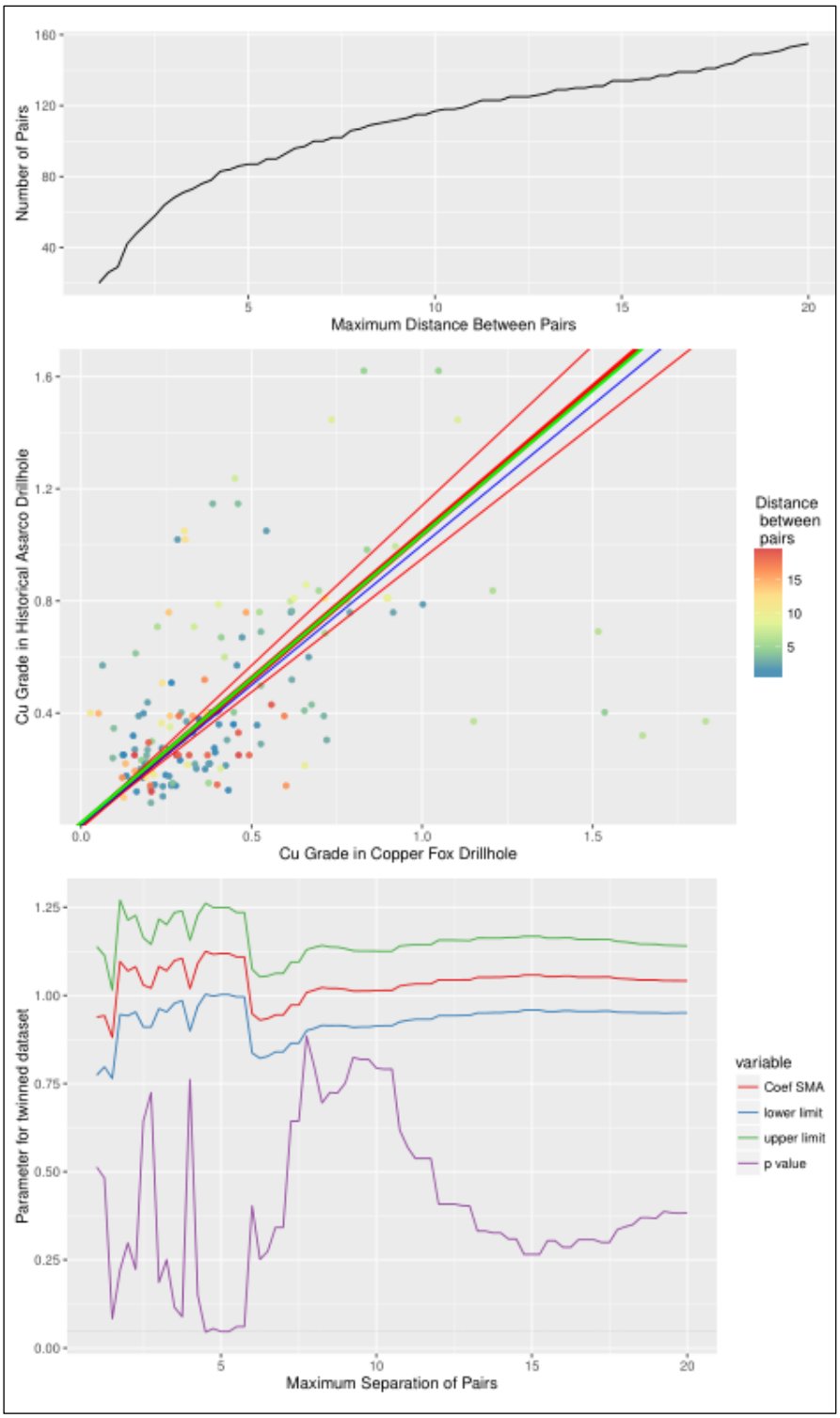

The molybdenum data is far more complicated (Figure 11-29 and Figure 11-30). At 5 m, there is a slope averaging around 0.8 but statistically different from 1, implying that a correction is warranted. However, at distances of 7.5 m and greater, there is no statistically different slope of the SMA regression from 1 and no correction is warranted. This raises questions about what the correct course of action should be. The AMEC correction slope is within error of the SMA coefficients at a 5 m sample spacing. The SMA coefficients are shown below for an unconstrained SMA (top) and an SMA forced through the origin (below).

```
Coefficients:
             elevation     slope
estimate    0.005936893 0.6337891
lower limit 0.003494934 0.5338013
upper limit 0.008378852 0.7525059

Coefficients (no intercept included):
            elevation     slope
estimate            0 0.8504140
lower limit        NA 0.7491039
upper limit        NA 0.9654255
```

The recommendation assumes that 90 pairs at 5 m is probably representative and that a correction for the slope should be used, but not the intercept in this case, as there is an issue for data around detection limit in the historical data. This makes the data around the intercept unreliable, and therefore, an intercept correction is not supported by the quantized data. The appropriate correction would therefore be to use the SMA forced through the origin:

Mo_Asarco = Mo_UNK_UNK_pct/0.8504.

However, this would result in an increased molybdenum grade, which AMEC was consistently reluctant to recommend historically. The QQ plots for the molybdenum data show the same bias as the twinned data and confirm the recommended correction, which is shown as a green line.

Figure 11-29: Summary Plots for Mo in the Asarco Data as Compared to the Copper Fox Data for Sample Pairs up to 5 m Apart

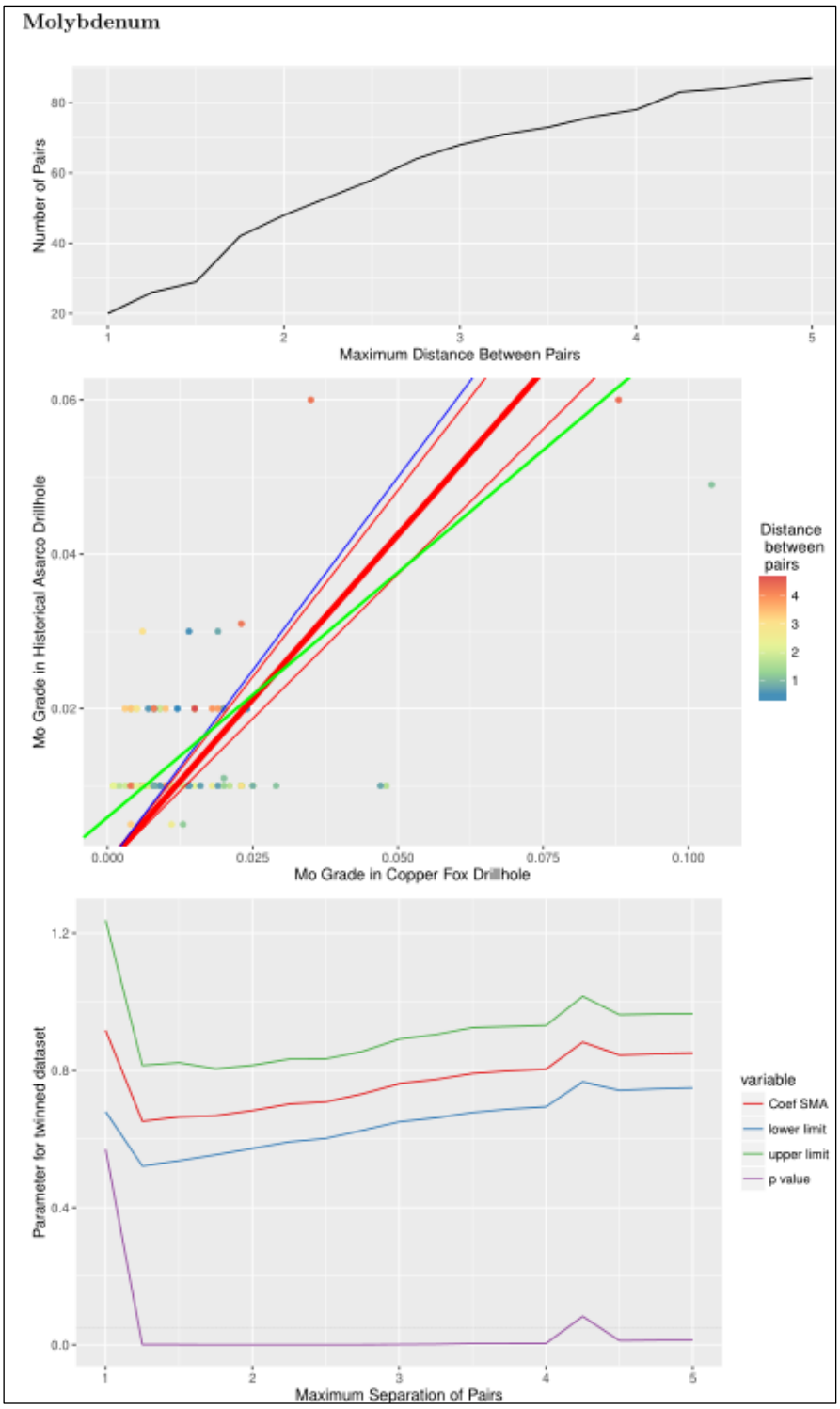

Figure 11-30: Summary Plots for Mo in the Asarco Data as Compared to the Copper Fox Data for Sample Pairs up to 20 m Apart

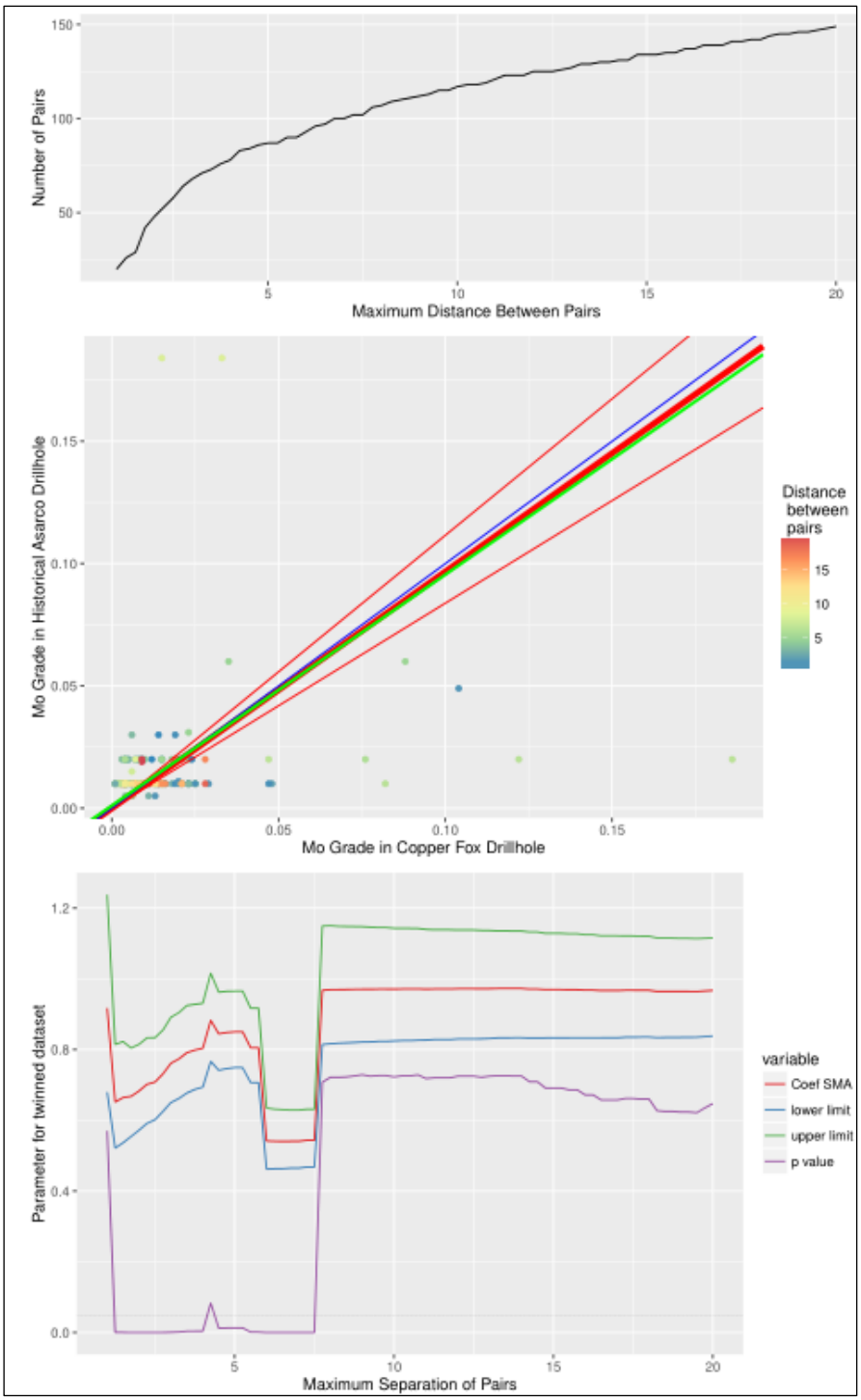

Figure 11-31: QQ plots for Resampling of Asarco Generation Drilling

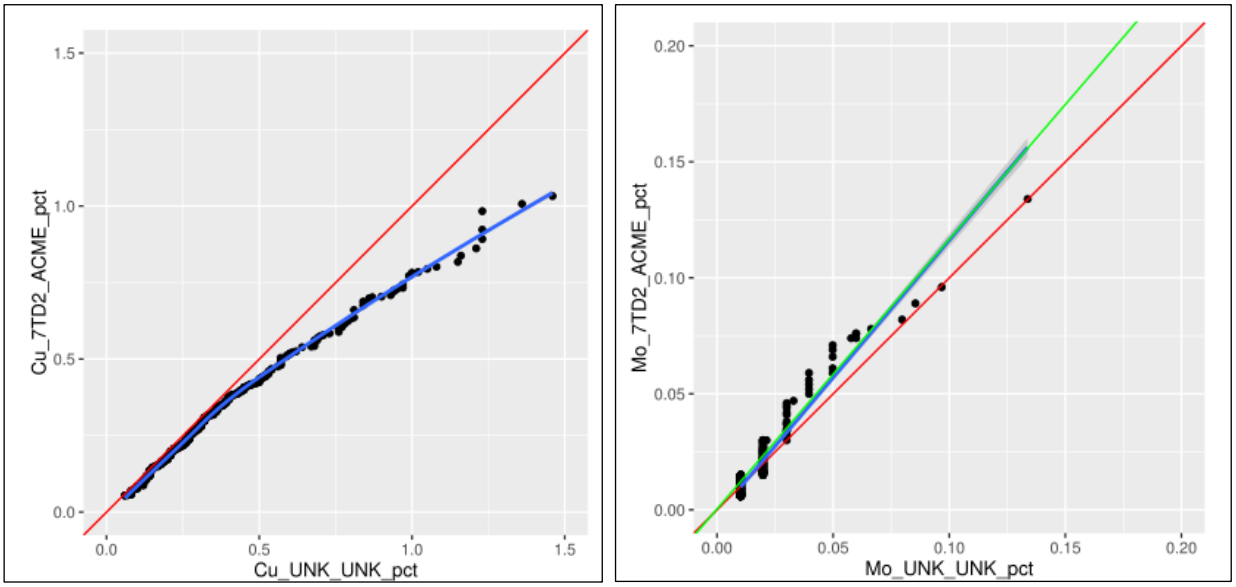

Note: The recommended correction is shown as a green line.

11.3.2.2 Hecla Data

AMEC compared silver, gold, copper, and molybdenum data from the Hecla drilling program in support of a previous resource estimate. There are more than 200 sample pairs within 5 m of each other and over 600 within 20 m. For the Hecla data, there are reassays using the 7TD2 assay method at ACME on recut intervals that were different to the primary assays. These reassays were not taken on barren material and only exist for six holes, but they can be used to compare populations of data for these elements, but for copper and molybdenum only. Where these data are not available, only the NN comparisons are relied upon. Previously, AMEC made the following recommendations for corrections to the raw data:

- Cu – correction y = (x+0.0114) / 1.0659
- Au –correction y = (x + 0.0022) / 1.1271
- Ag – correction y = (x – 0.2685) / 0.9418
  The correction is applied up to a maximum of 4.6 g/t Ag. At higher grades, no correction is applied as the corrected grades would be higher than the original grades. Grades below 0.27 g/t are re-set to zero.

The Schaft Creek JV's analysis of the twinned samples is that the silver comparison data does not support a correction, which is not in line with previous recommendations. The summary statistics for the SMA are shown below for sample comparisons at a maximum of 5 m. The origin lies within error of the elevation parameters, and there is a > 90% chance that the SMA slope is not different to 1. This observation that there is no apparent bias is mimicked at all potential sample spacings up 20 m (Figure 11-32).

```
Coefficients:
             elevation     slope
estimate     0.1776835 0.9935611
lower limit -0.2023746 0.8915230
upper limit  0.5577417 1.1072778

H0 : variables uncorrelated
R-squared : 0.0530017
P-value : 3.9208e-05

------------------------------------------------------------
H0 : slope not different from 1
Test statistic : r= -0.006638 with 311 degrees of freedom under H0
P-value : 0.90689
```

Figure 11-32: Paired Sample Comparison Plots for Silver in the Hecla Data for all Sample Spacings up to 20 m

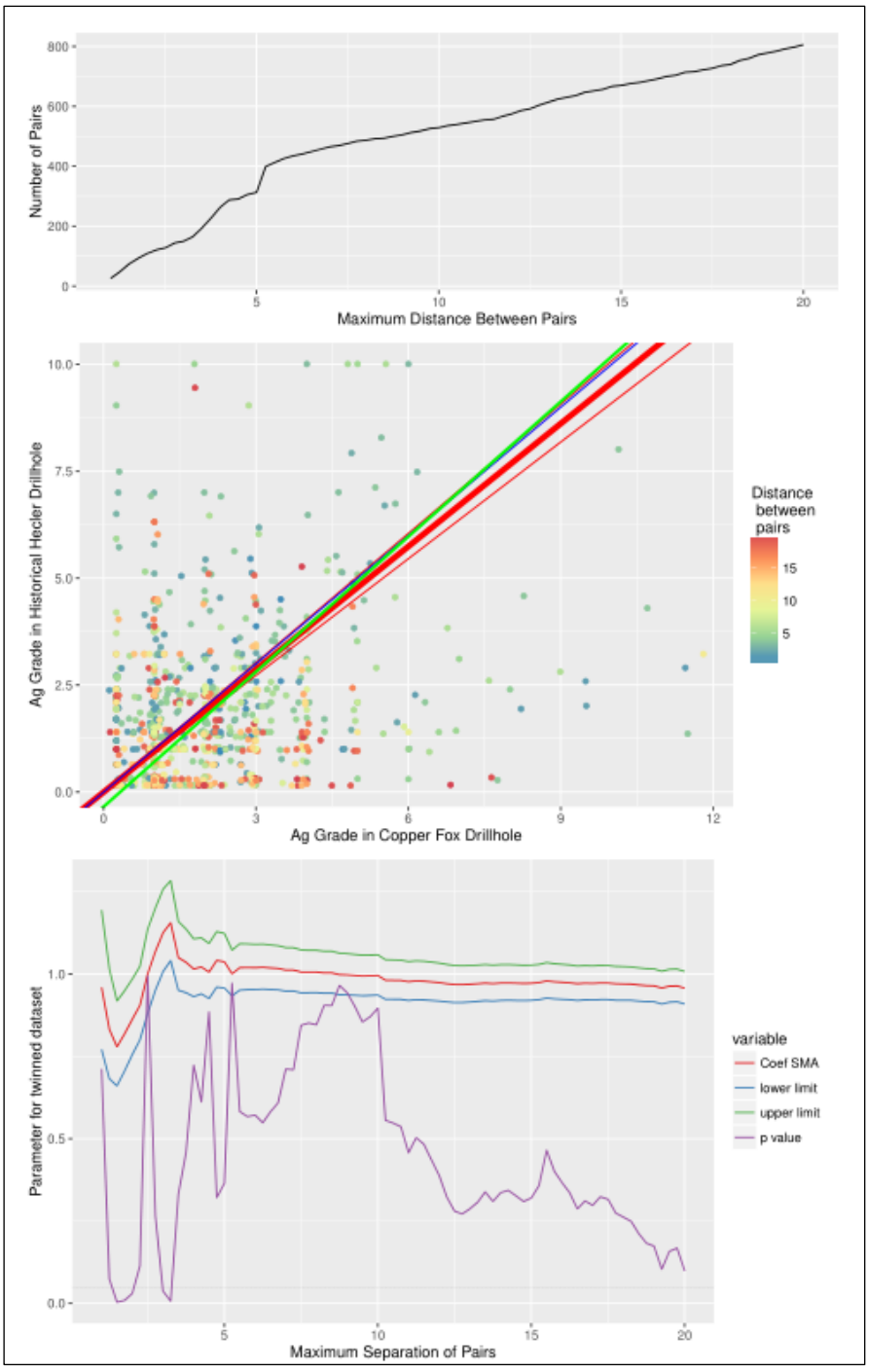

The gold comparison (Figure 11-33) data shows that sample pairs between 0 m and 5 m have a 3% probability of not being different to 1, so it would be typical to justify that a correction is warranted. The previous AMEC recommendation was for a correction of y = (x + 0.0022) / 1.1271. This can also be evaluated (below). There is a 64% probability that the slope is not different to the 1.1271 recommended by AMEC; however, there is a complication with the intercept. The lower and upper estimates for the intercept straddle 0 (i.e., there is not good evidence that the slope does not go through the origin).

```
Coefficients:
              elevation    slope
estimate    -0.01668429 1.103483
lower limit -0.07012727 1.007173
upper limit  0.03675869 1.209002

H0 : variables uncorrelated


R-squared : 0.3281777
P-value : < 2.22e-16

------------------------------------------------------------
H0 : slope not different from 1.1271
Test statistic : r= -0.02583 with 311 degrees of freedom under H0
P-value : 0.64895
```

Because of this, the Schaft Creek JV recommends that the slope forced through the origin is used for the correction. This still has a < 5% chance of accepting the null hypothesis that the slope is not different to 1 and is a simpler correction of:

Au_Hecla = Au_UNK_UNK_pct/1.0806.

```
Coefficients (no intercept included):
            elevation    slope
estimate            0 1.080614
lower limit        NA 1.006467
upper limit        NA 1.160224

H0 : variables uncorrelated
R-squared : 0.592102
P-value : < 2.22e-16

------------------------------------------------------------
H0 : slope not different from 1
Test statistic : r= 0.1206 with 311 degrees of freedom under H0
P-value : 0.032892
```

There is very little difference between this correction and the one recommended by AMEC in the previous resource estimate.

Figure 11-33: Paired Sample Comparison Plots for Gold in the Hecla Data for all Sample Spacings up to 20 m

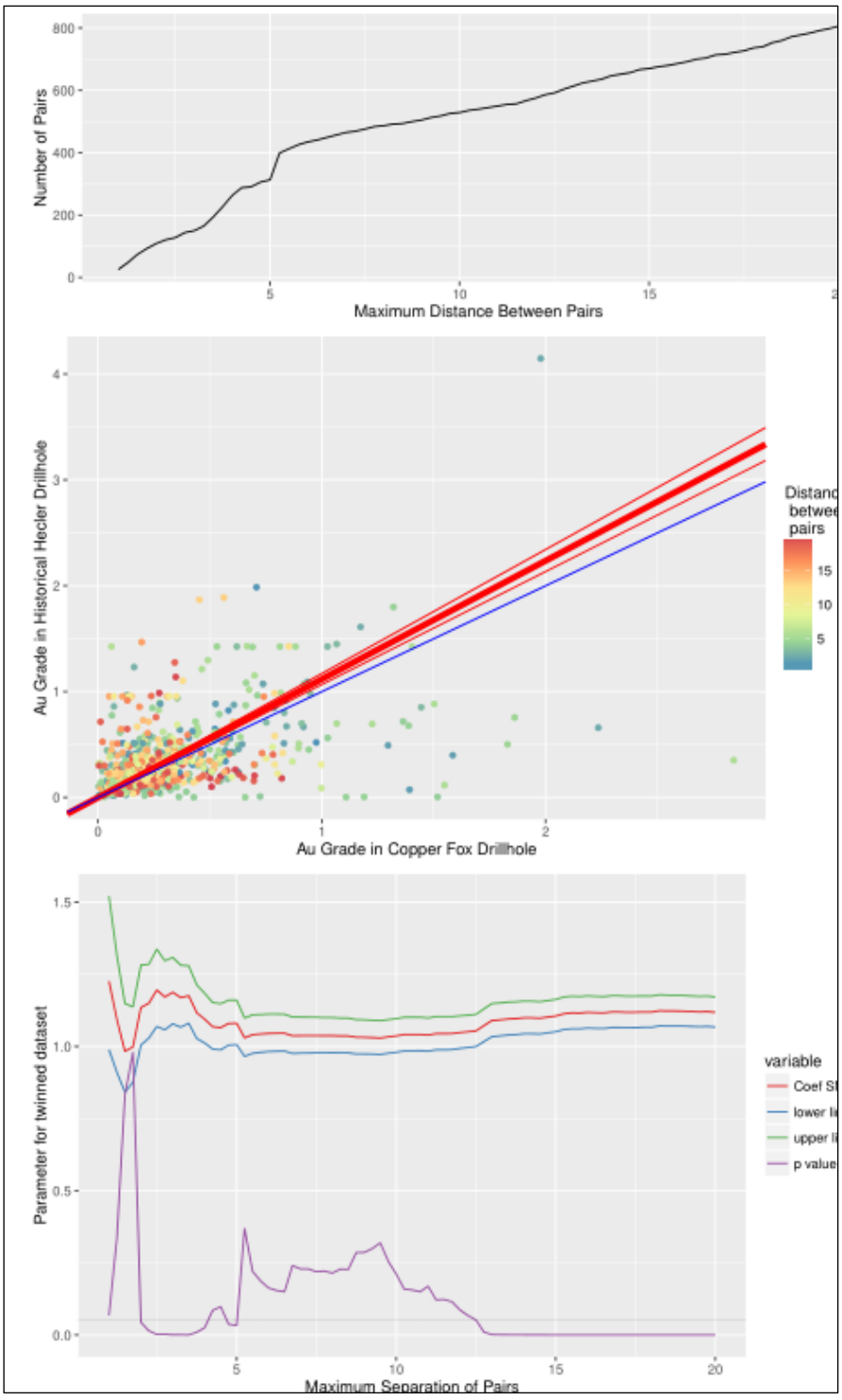

AMEC recommended a sample correction of around 6% to the data for copper. The QQ plot for the six holes with resampling shows no bias between assays and reassays (Figure 11-34).

When initially reviewing the NN data, it seems difficult to support the correction. If samples are limited to being within 5 m of each other. The slope of the SMA forced through the origin is predicted to be 1.33 and has a negligible probability not being different to either 1 or 1.06. This discrepancy is at least in part explained by the presence of regular high copper samples, which were removed from the dataset by AMEC as outliers. These outliers are clear in (Figure 11-35).

```
Coefficients (no intercept included):
            elevation    slope
estimate            0 1.325695
lower limit        NA 1.247355
upper limit        NA 1.408956

H0 : variables uncorrelated
R-squared : 0.6425972
P-value : < 2.22e-16

------------------------------------------------------------
H0 : slope not different from 1
Test statistic : r= 0.4312 with 371 degrees of freedom under H0
P-value : < 2.22e-16
```

Once the outliers are removed from the dataset, the SMA slope is much more reasonable and the results are almost identical to what AMEC recommended (Figure 11-36). The limitation, however, is that there is a 22% chance that the slope is not different to 1, which does not meet the standard 95% criteria for assessing certainty. In this case, it may not seem significant, but there seems to be insufficient evidence to support the correction and the data should be accepted as is.

```
Coefficients:
               elevation     slope
estimate    -0.008953563 1.0616166
lower limit -0.060094138 0.9636584
upper limit  0.042187012 1.1695325

H0 : variables uncorrelated
R-squared : 0.1223891
P-value : 6.8681e-12

------------------------------------------------------------
H0 : slope not different from 1
Test statistic : r= 0.06373 with 361 degrees of freedom under H0
P-value : 0.22576
```

On the other side of this argument is that it equally cannot be argued that the correction factor applied by AMEC is incorrect. Thus, if it was desired to maintain consistency, there is an argument for that also. This correction reduces the grade of the historical samples, so it does not run the risk of overestimating grade, and thus, does not have dire consequences.

However, the QQ plots of the resampled material show no bias between the primary assays and the resampled data (Figure 11-34). Therefore, the recommendation is to reject a correction of these data.

Figure 11-34: QQ Plots for Copper in the Resampled Hecla Holes

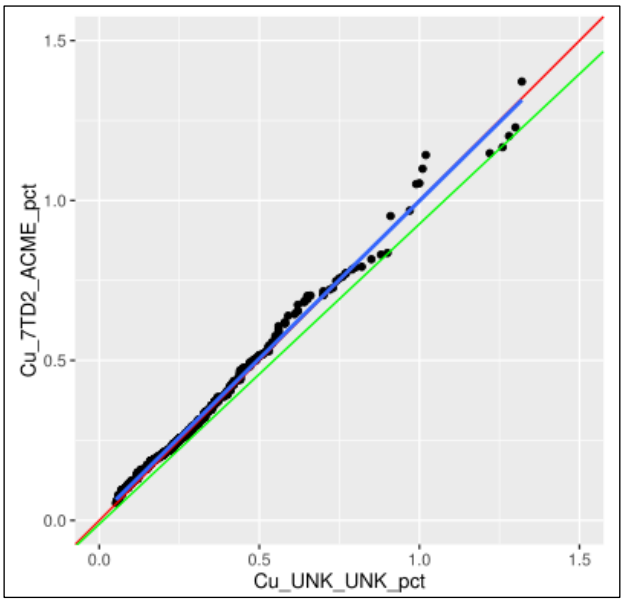

Figure 11-35: Uncensored Copper Duplicated Data

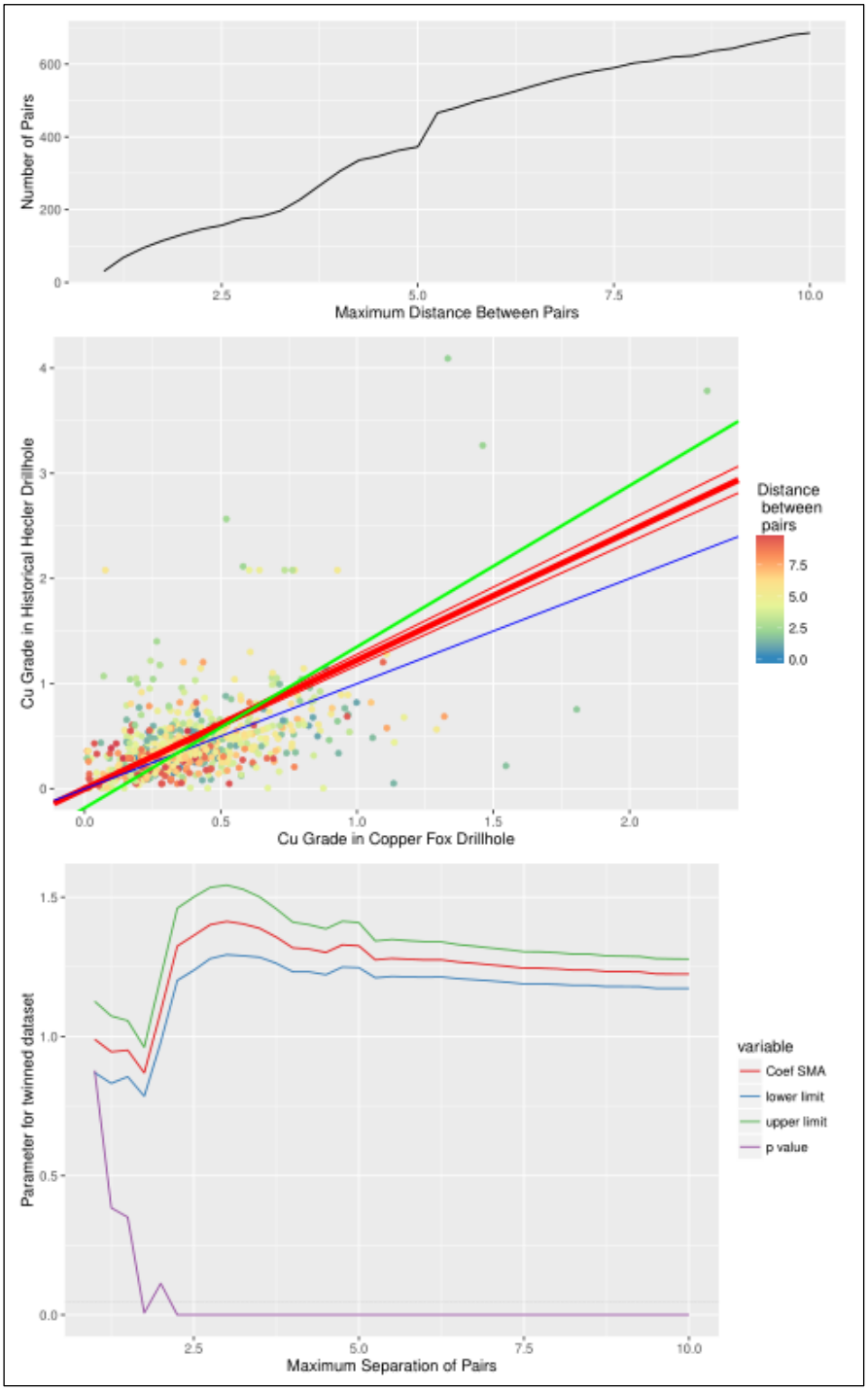

Note: There are regular samples > 2% Cu in the historical assays that are not reflected in the more modern assays.

Figure 11-36: Paired Sample Comparison Plots for Censored Copper in the Hecla Data for All Sample Spacings up to 5 m

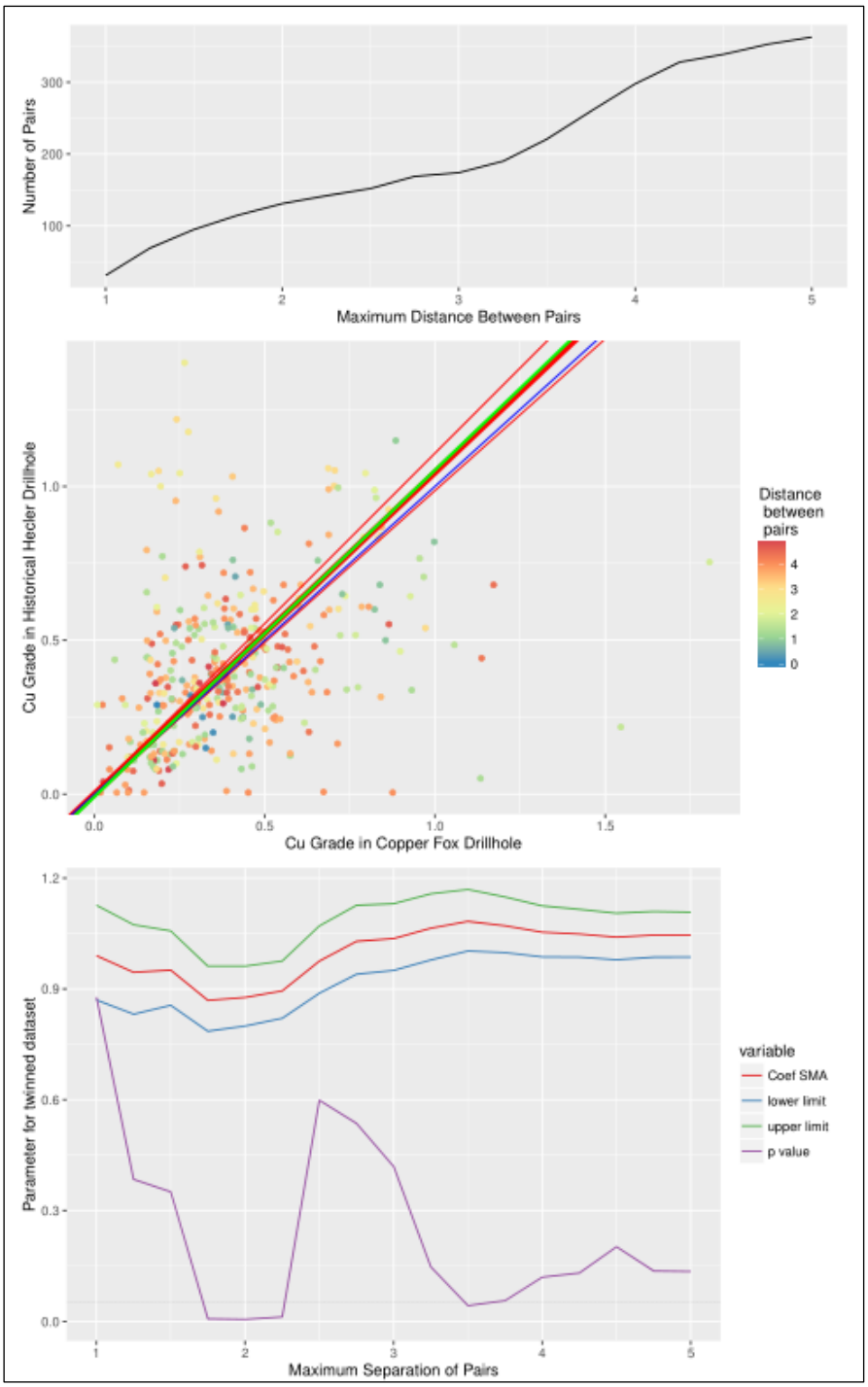

The molybdenum data once the outliers are removed from the historical datasets shows no bias between historical and modern data, which supports the AMEC recommendation to make no change to this dataset (Figure 11-37 and Figure 11-38).

```
Coefficients:
                elevation     slope
estimate    -0.0006118044 0.9869365
lower limit -0.0037741405 0.8954924
upper limit  0.0025505317 1.0877184

H0 : variables uncorrelated
R-squared : 0.1665657
P-value : 3.6905e-15

------------------------------------------------------------
H0 : slope not different from 1
Test statistic : r= -0.0144 with 340 degrees of freedom under H0
P-value : 0.79071
```

Figure 11-37: Paired Sample Comparison Plots for Censored Molybdenum in the Hecla Data for All Sample Spacings up to 5 m

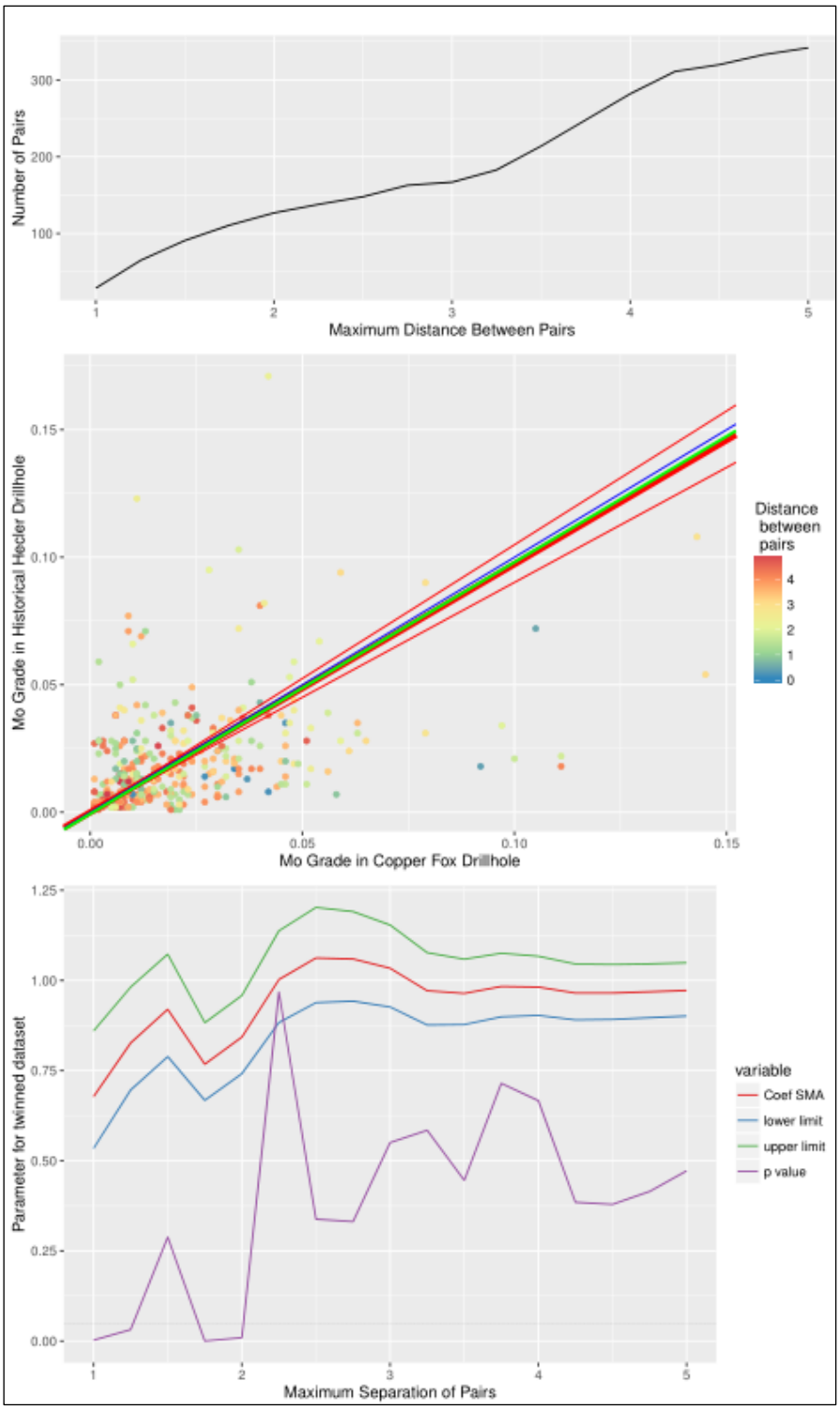

Figure 11-38: QQ Plots for Molybdenum in the Resampled Hecla Holes

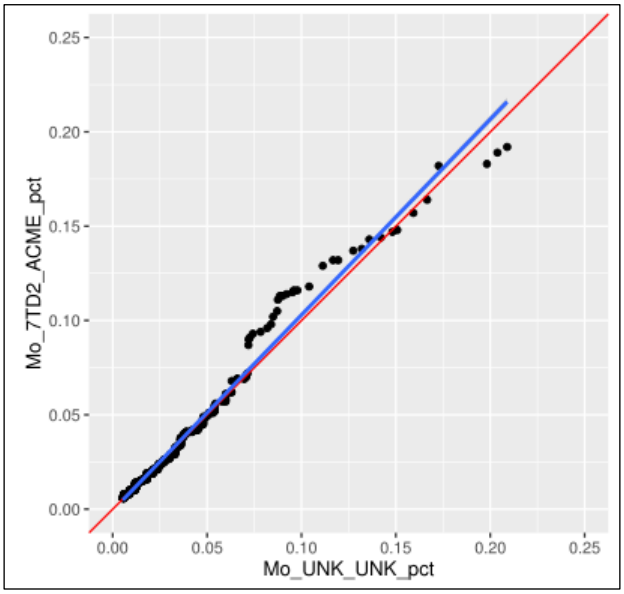

11.3.2.3 Paramount Data

There are no Paramount twinned samples within 20 m, thus there is no way to assess the accuracy of these data. A subset of Paramount holes were reassayed on different sample intervals by Copper Fox using the 7TD package from ACME. The QQ plots comparing these datasets show no bias in the historical assays for copper and a low bias in the historical molybdenum assays (Figure 11-39). In the first case, this can be used as evidence to support the inclusion of the historical copper assays in the final dataset. For molybdenum, the level of bias that is evident is typical of the difference between an aqua regia and a 4-acid digestion. This methodological difference has not been corrected for elsewhere in this dataset so it should not be corrected for here.

The QQ plots for silver and gold are based on more limited data but show general agreement between data sources. Accepting the historical data is a conservative course of action in these cases (Figure 11-40).

Figure 11-39: QQ plots for Primary Assays and Resampling of Cu and Mo Data From the Paramount Generation of Drilling

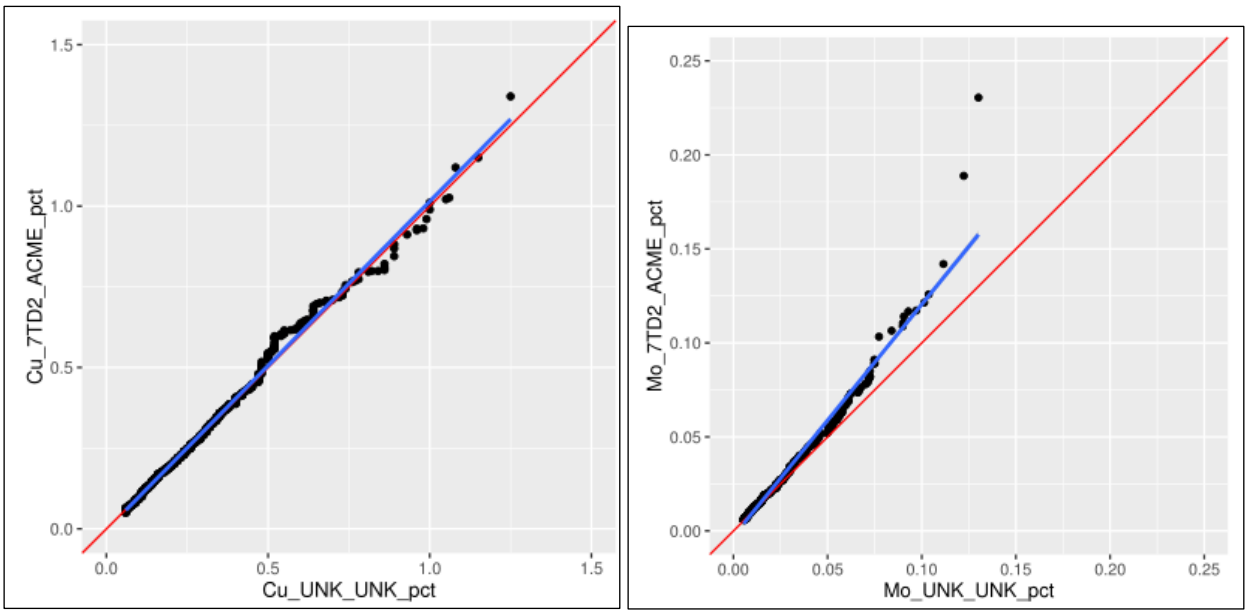

Figure 11-40: QQ Plots for Primary Assays and Resampling of Au and Ag Data From the Paramount Generation of Drilling

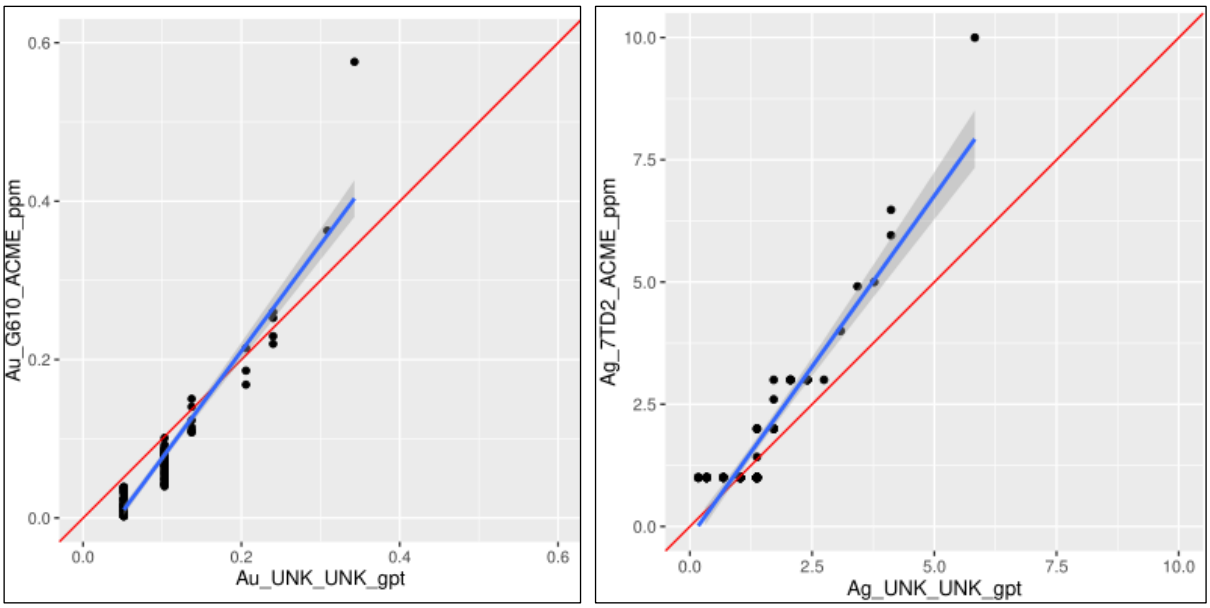

11.3.2.4 Silver Standard Data

There is no silver or gold data from Silver Standard campaign for comparison. Even within 20 m, there are only 20 NN points for comparison for copper and molybdenum, with none within 7 m. Because there are so few samples, the error in the slopes of the SMA are large. AMEC made no recommendations for corrections to these data.

In the case of copper, a slope and an error can be calculated that show that the slope is not statistically different to 1 (Figure 11-41). However, the crucial factor is that there is an 86% probability that the data are uncorrelated at both 10 m and 20 m sample spacing. If the null hypothesis that the data are uncorrelated is accepted, then nothing significant can be said about the slope. There cannot be any correction based on these data, and the modern data to support the accuracy of the Silver Standard copper data cannot be used.

```
Coefficients:
              elevation     slope
estimate     0.03080624 0.9527499
lower limit -0.07976738 0.6140723
upper limit  0.14137985 1.4782174

H0 : variables uncorrelated
R-squared : 0.001358712
P-value : 0.86739

------------------------------------------------------------
H0 : slope not different from 1
Test statistic : r= -0.0484 with 21 degrees of freedom under H0
P-value : 0.82642
```

Figure 11-41: Paired Sample Comparison Plots for Copper in the Silver Standard Data for All Sample Spacings up to 20 m

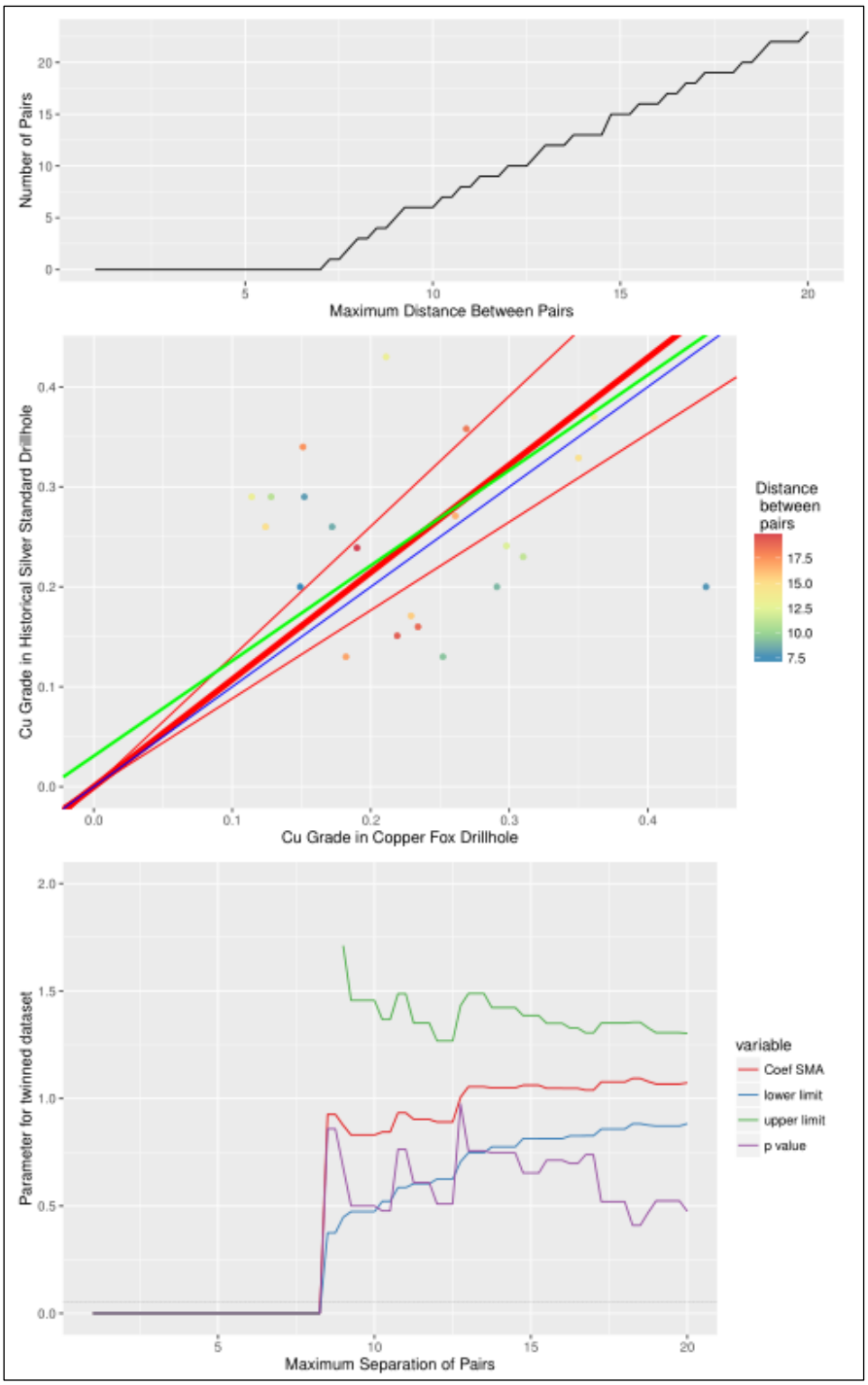

There is likewise no statistically significant correlation between the historical and modern molybdenum data. The molybdenum data has the added complication that the historical data is within error of the detection limit for all comparison points within 20 m (Figure 11-42).

Figure 11-42: Paired Sample Comparison Plots for Molybdenum in the Silver Standard Data for All Sample Spacings up to 20 m

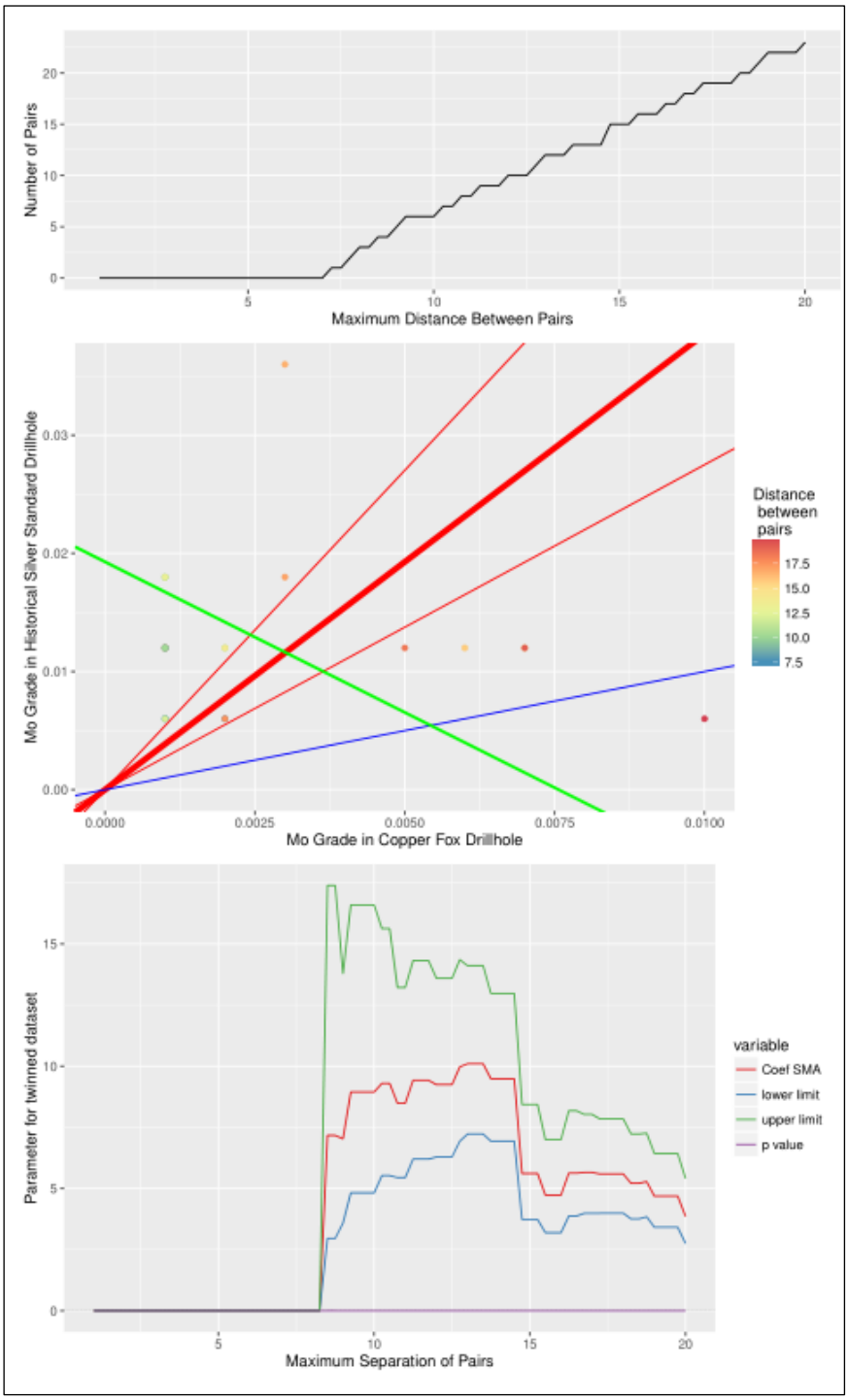

There are only two holes with modern reassays. They show no significant bias for copper or molybdenum (Figure 11-43). The slight high bias in historical assays for copper evident affects only approximately 10 samples in the Silver Standard dataset and can readily be ignored. It may well be that this is caused by the same oxidation as was evident in the Asarco generation data.

As was the case with the Paramount generation data, the bias in molybdenum is most readily explained by the historical use of aqua regia and the use of a mixed acid digestion in the reassays. It is recommended that these data can be accepted without correction in the resource estimate.

Figure 11-43: QQ Plots for Primary Assays and Resampling of Copper and Molybdenum From the Silver Standard Generation of Drilling

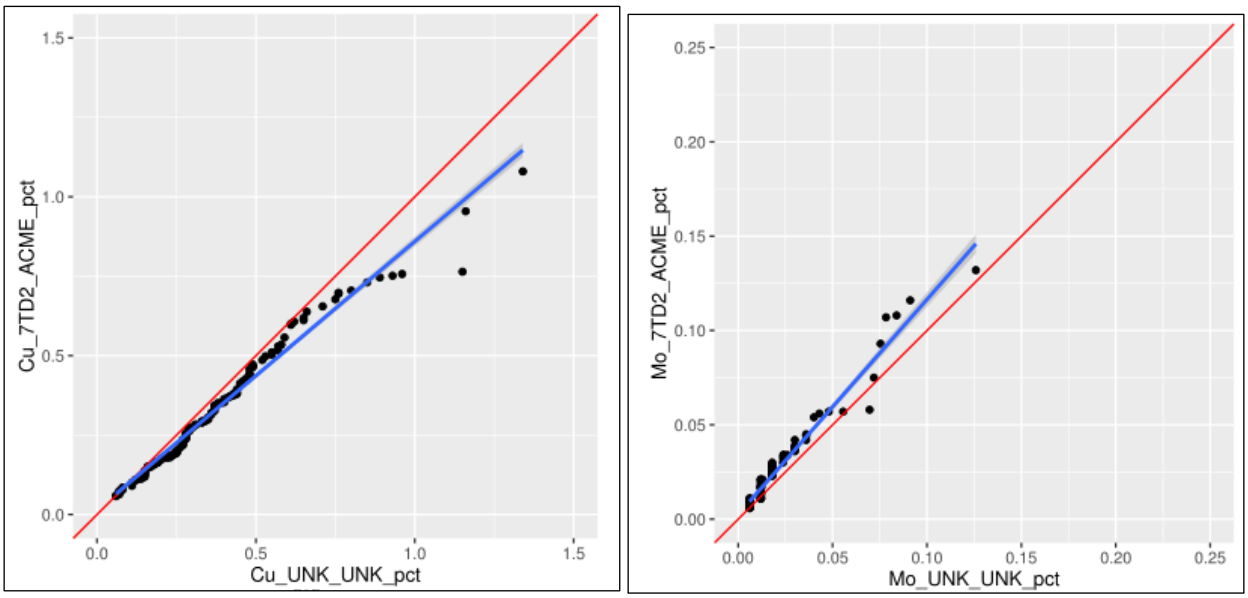

11.3.2.5 Teck Data (1980s data only)

The comparison of paired data with the older Teck data has no samples between 0 m and 3 m. There are approximately 80 samples within 5 m but more than 400 within 10 m. The only AMEC recommended change was for silver, as documented below. There was also no resampling of the historical core by Copper Fox, so consequently, no comparisons can be made with reassays.

- Ag – correction x = (y – 1.5064) / 0.5047
  The correction is applied up to a maximum of 3.04 g/t Ag. At higher grades, no correction is applied so that the corrected grades are not increased by applying the correction. Grades below 1.51 g/t Ag are re-set to zero.

The historical Teck silver data is so extremely poor that it should be discarded (Figure 11-44). A comparison of points within 5 m shows that there is a very high predicted intercept in the SMA data. The predicted intercept and slope are similar to but not in total agreement with the AMEC recommendation.

```
Coefficients:
            elevation     slope
estimate     1.413590 0.6279874
lower limit  1.144311 0.5142203
upper limit  1.682870 0.7669245

H0 : variables uncorrelated
R-squared : 0.08742958
P-value : 0.004433

------------------------------------------------------------
H0 : slope not different from 1
Test statistic : r= -0.4506 with 89 degrees of freedom under H0
P-value : 7.3904e-06
```

If the much larger 10 m sample dataset is used, a high intercept is maintained (below), but the predicted slope for the SMA correlation changes from 0.51 to 1.41. This drastic inconsistency tends to suggest that it is not understood what the historical Teck silver data is showing relative to twinned samples, and so, it cannot be corrected for. The Schaft Creek JV recommendation is to reject these data.

```
Coefficients:
            elevation    slope
estimate    1.0167188 1.410502
lower limit 0.7423447 1.288877
upper limit 1.2910929 1.543603

H0 : variables uncorrelated
R-squared : 0.1667533
P-value : < 2.22e-16

------------------------------------------------------------
H0 : slope not different from 1
Test statistic : r= 0.3587 with 395 degrees of freedom under H0
P-value : 1.692e-13
```

Figure 11-44: Paired Sample Comparison Plots for Silver in the Teck Data for All Sample Spacings up to 5 m

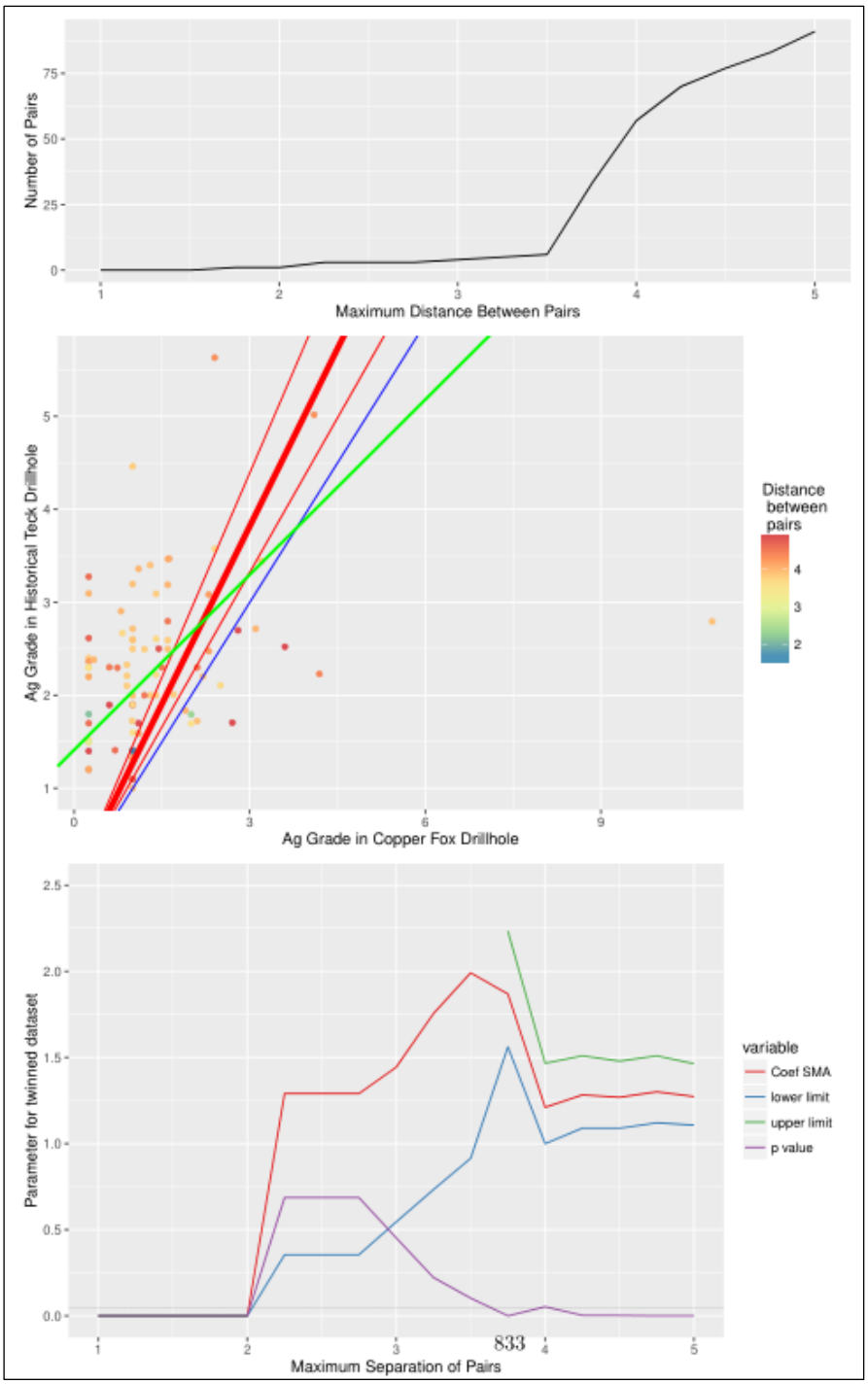

Gold in the historical data shows a reasonable correlation but with a bias. The unrestricted SMA shows a strong bias but that the intercept includes 0. Therefore, it is recommended to evaluate the bias using the SMA model forced through the intercept. If this is done (below), then the predicted slope correction is 0.9. However, this does not meet the 95% confidence that the slope is not different to 1. Therefore, the null hypothesis must be accepted and no correction made, in line with the previous recommendation from AMEC (Figure 11-45).

```
Coefficients (no intercept included):
            elevation     slope
estimate            0 0.9017426
lower limit        NA 0.8071517
upper limit        NA 1.0074188

H0 : variables uncorrelated
R-squared : 0.7188209
P-value : < 2.22e-16

------------------------------------------------------------
H0 : slope not different from 1
Test statistic : r= -0.1918 with 89 degrees of freedom under H0
P-value : 0.068569
```

Figure 11-45: Paired Sample Comparison Plots for Gold in the Teck Data for All Sample Spacings up to 5 m

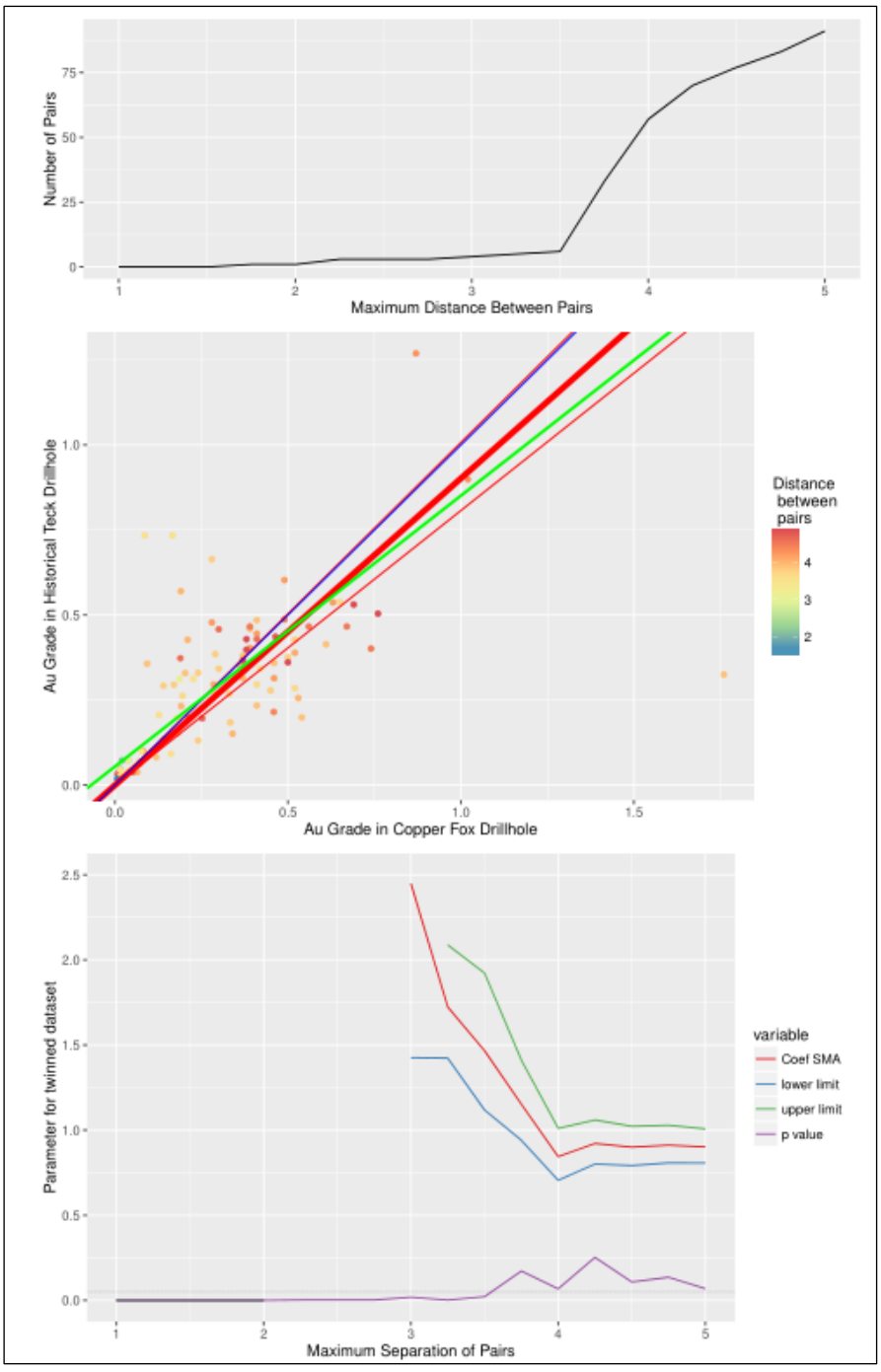

For copper, a similar chain of logic applies. If the SMA with no intercept is used, then it does not meet the 95% confidence limit that is required in the slope being different to 1 (Figure 11-46). The original data must be accepted. While it may appear somewhat biased, the data is of acceptable quality without correction.

```
Coefficients (no intercept included):
            elevation     slope
estimate            0 0.9265678
lower limit        NA 0.8432100
upper limit        NA 1.0181661

H0 : variables uncorrelated
R-squared : 0.7967488
P-value : < 2.22e-16

------------------------------------------------------------
H0 : slope not different from 1
Test statistic : r= -0.167 with 89 degrees of freedom under H0
P-value : 0.11366
```

Figure 11-46: Paired Sample Comparison Plots for Cu in the Teck Data for All Sample Spacings up to 5 m

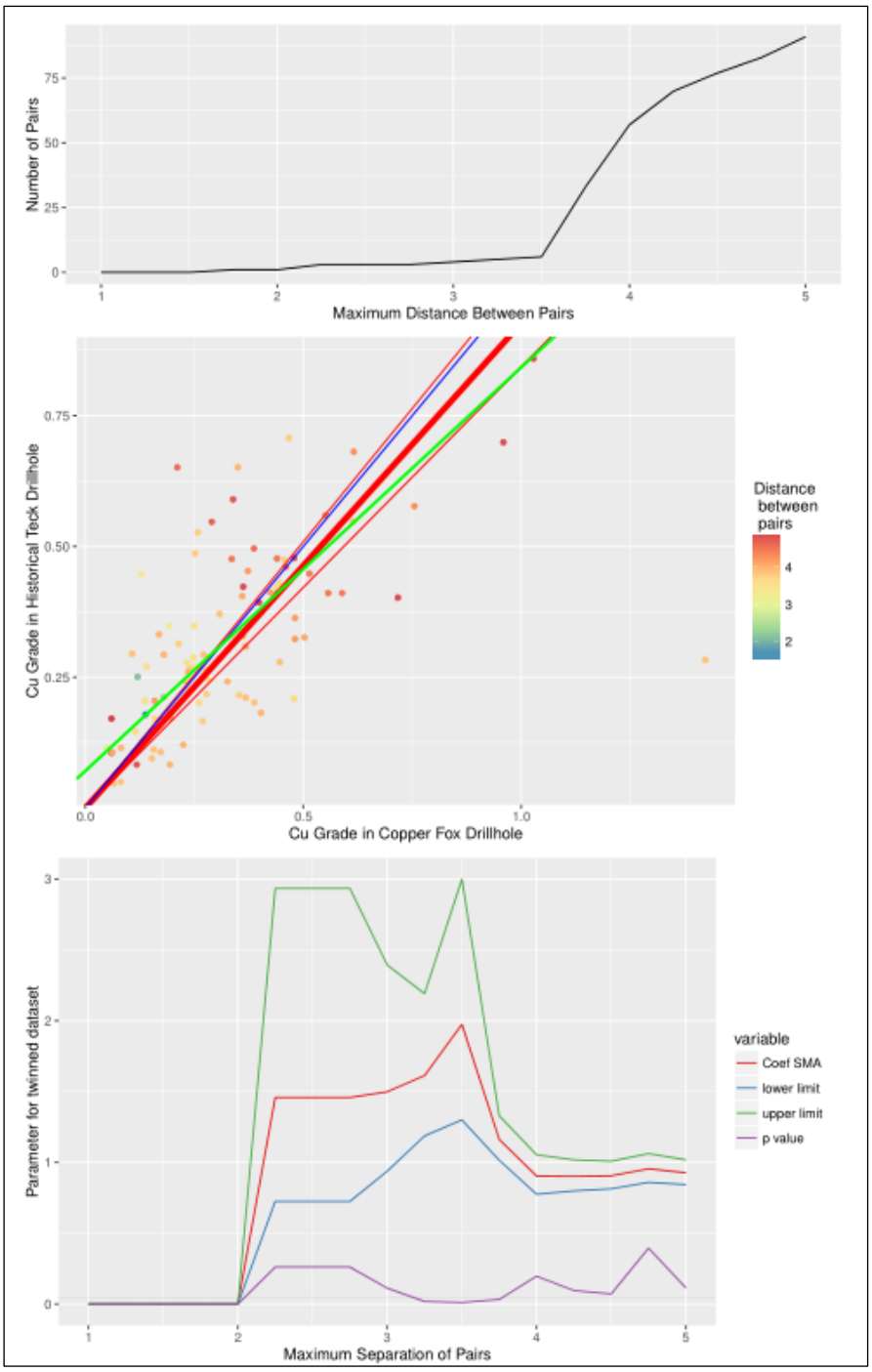

The molybdenum data (Figure 11-47) is virtually the same as for copper in the Teck 1980s data. In this case, the 10 m dataset was chosen because of a larger number of outliers in the 5 m dataset. The more robust dataset makes the effect of these outliers less significant. But again, the slope of regression fails to meet the 95% confidence interval that would suggest a correction should be made. Therefore, the data must be accepted as it is in line with AMEC's recommendations.

```
Coefficients (no intercept included):
            elevation     slope
estimate            0 0.9769554
lower limit        NA 0.9093472
upper limit        NA 1.0495901

H0 : variables uncorrelated
R-squared : 0.4466921
P-value : < 2.22e-16

------------------------------------------------------------
H0 : slope not different from 1
Test statistic : r= -0.03133 with 414 degrees of freedom under H0
P-value : 0.52396
```

Figure 11-47: Paired Sample Comparison Plots for Molybdenum in the Teck Data for All Sample Spacings up to 5 m

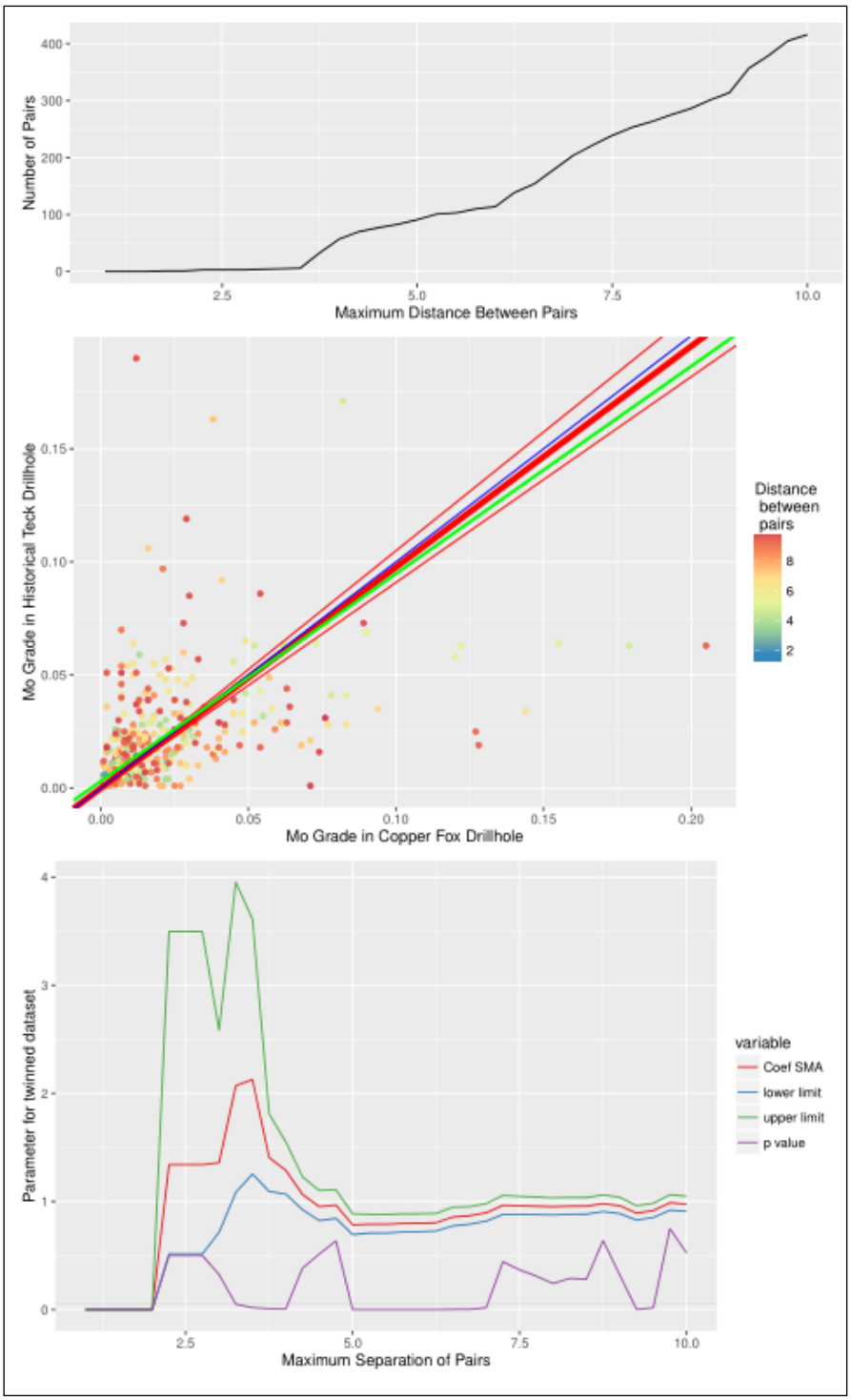

11.3.3 Recommendations for Further Work

There are two pieces of outstanding work to be completed for the next generation of study:

- The geological logs from samples listed in Table 11-8 need to be reviewed to see if there is any justification for the gravimetric fire assays on these samples that seem out of line with the remainder of the dataset.
- The Schaft Creek JV noted that in the Hecla drilling, there were multiple samples of very high copper grade that were not reflected in the NN samples from twinned drill holes. All these samples came from H72CH101 and H72CH091. A review of the drill logs, assays, and historical core for these holes would determine whether these samples were erroneous.

Table 11-8: Gravimetric Fire Assay Samples to be Validated

SAMPLEID	DUPLICATENO	HOLEID	DH_YEAR	RETURNDATE	SAMPFROM	SAMPTO	Ag_G613_ACME_gpt	Au_G612_ACME_gpt
611008	DUP	2010CF397	2010		47.8	49.8	662	
611008	PRIMARY	2010CF397	2010	3-Jan-11	47.8	49.8	686	
1053597	DUP	2011CF415	2011		75	77	2027	
1053597	PRIMARY	2011CF415	2011	7-Dec-11	75	77	2006	
1054879	PRIMARY	2011CF411	2011	19-Aug-11	206	209	1689	
1579183	PRIMARY	2012CF430	2012	14-Sep-12	130.75	132.15	414	
1053547	DUP	2011CF413	2011		560.5	562.5		18.6
1053547	PRIMARY	2011CF413	2011	23-Nov-11	560.5	562.5		20.2
1579000	DUP	2012CF427	2012		657	659		6.1
1579000	PRIMARY	2012CF427	2012	16-Aug-12	657	659		7.2

11.3.4 Corrections to Historical Data

There are a number of corrections recommended to be made in the exporting process for the acQuire database for the historical data in the Element_UNK_UNK_units columns for copper, molybdenum, silver, and gold. These are summarized below by each historic drilling program.

11.3.4.1 Asarco Generation Data

There are only primary copper and molybdenum data. No correction is recommended for copper (in line with previous resource estimates). The Schaft Creek JV recommends a correction for molybdenum that is slightly different to the previous AMEC recommendation.

Mo_corrected = Mo_UNK_UNK_pct/0.8504.

11.3.4.2 Hecla Generation Data

Previously, AMEC recommended a correction for silver, gold, and copper. The Schaft Creek JV recommends that there is insufficient evidence for a correction for silver or copper, both of which were relatively minor corrections in the AMEC dataset. The recommended correction for gold is marginally different to the correction recommended by AMEC.

Au_corrected = Au_UNK_UNK_pct/1.0806.

11.3.4.3 Paramount Generation Data

No correction is recommended in these data, in line with previous work.

11.3.4.4 Silver Standard Generation Data

No data exists for gold or silver. No correction to copper or molybdenum is warranted.

11.3.4.5 Teck 1980s Generation Data

As discussed, the Teck silver data is recommended for exclusion from the resource estimation process. This is inconsistent with the recommendations of AMEC used previously. No correction is warranted for copper, molybdenum, or gold.

11.3.5 BESTEL Comparisons

The new BESTEL column derives data from a different source compared to the previous _BESTEL calculations. Table 11-9 below shows the number of each method in the old and in the new _BESTEL calculations. The differences in total silver are due almost entirely to the exclusion of the 5312 Teck 1980s generation data.

Table 11-9: BESTEL Comparison

Method	DL	No. Samples	No. in old BESTEL	No. in new BESTEL
Ag_1DX1_ACME_ppm	0.1	2444	2091	2318
Ag_1EX_ACME_ppm	0.1	12368	12364	12368
Ag_1F04_ACME_ppb	0.002	111	111	0
Ag_1F06_ACME_ppb	0.002	10	10	1
Ag_7AR2_ACME_gpt	2	37	10	10
Ag_7TD2_ACME_gpt	2	21854	6922	2665
Ag_AQ200_ppm	0.1	2110	57	2004
Ag_AQ250_ppb	0.002	115	0	0
Ag_AQ252_ppb	0.002	28	28	5
Ag_FA_LOR_gpt	0.1	1089	1089	1089
Ag_G613_ACME_gpt	?	6	2	0
Ag_ICP_IPL_ppm	0.5	7717	2182	7258
Ag_MA200_ppm	0.1	67	2	5
Ag_MA370_gpt	2	2121	2115	0
Ag_MEICP61_ALS_gpt	0.5	14	0	0
Ag_MEICP61a_ALS_gpt	1	443	136	0
Ag_MEICP61a_ALS_ppm	1	479	285	0
Ag_MEMS61_ALS_ppm	0.02	926	612	639
Ag_MEMS62_ALS_ppm	0.02	642	0	154
Ag_OG62_ALS_gpt	1	278	0	0
Ag_UNK_UNK_opt	0.34286	8791	8795	3483
Total			36811	31999

table continues…

Method	DL	No. Samples	No. in old BESTEL	No. in new BESTEL
As_1DX1_ACME_ppm	0.5	2446	2114	2325
As_1EX_ACME_ppm	1	8654	8654	8654
As_1F04_ACME_ppm	0.1	111	111	0
As_1F06_ACME_ppm	0.1	10	10	10
As_7AR2_ACME_pct	100	37	1	0
As_7TD2_ACME_pct	200	21855	5574	0
As_AQ200_ppm	0.5	2110	2110	2004
As_AQ250_ppm	0.1	115	0	0
As_AQ252_ppm	0.1	28	5	5
As_ICP_IPL_ppm	5	7717	6907	0
As_MA200_ppm	1	67	2	5
As_MA370_pct_ppm	200	2121	0	0
As_MEICP61_ALS_ppm	5	14	4	4
As_MEICP61a_ALS_ppm	50	922	586	0
As_MEMS61_ALS_ppm	0.2	926	877	925
Total			26955	13932
Method	DL	No. Samples	No. in old BESTEL	No. in new BESTEL
Au_1DX1_ACME_ppb	0.0005	2446	84	0
Au_1EX_ACME_ppm	0.1	8654	373	0
Au_1F04_ACME_ppb	0.0002	111	0	0
Au_1F06_ACME_ppb	0.001	10	1	0
Au_AA26_ALS_gpt	0.01	640	642	88
Au_AQ200_ppb	0.0005	2110	56	0
Au_AQ250_ppb	0.0004	115	0	0
Au_AQ252_ppb	0.0001	28	5	0
Au_FA_LOR_gpt	0.01	1089	891	891
Au_FA430_ppm	0.005	2110	2110	2001
Au_FAAAS_LOR_gpt	0.01	5734	1488	1517
Au_G601_ACME_gpt	0.005	8425	8408	8425
Au_G610_ACME_gpt	0.005	13447	12910	13447
Au_G612_ACME_gpt	0.9	4	2	0
Au_ICP21_ALS_gpt	0.001	280	0	8
Au_MA200_ppm	0.1	67	2	0
Au_UNK_UNK_opt	0.003429	8808	8808	8808
Total			35780	35185

table continues…

Method	DL	No. Samples	No. in old BESTEL	No. in new BESTEL
Cu_1DX1_ACME_ppm	0.00001	2435	84	237
Cu_1EX_ACME_ppm	0.00001	8576	357	367
Cu_1F04_ACME_ppm	0.00001	111	0	0
Cu_1F06_ACME_ppm	0.00001	10	1	1
Cu_7AR2_ACME_pct	0.02	37	1	1
Cu_7TD2_ACME_pct	0.001	21855	21854	21855
Cu_AQ200_ppm	0.00001	2106	57	4
Cu_AQ250_ppm	0.0001	115	0	0
Cu_AQ252_ppm	0.0001	27	0	0
Cu_ASY_IPL_Pct	0.01	1679	393	394
Cu_FA_LOR_pct	0.001	1089	846	846
Cu_ICP_IPL_ppm	0.0001	7693	1789	1885
Cu_MA200_ppm	0.00076	63	2	5
Cu_MA370_pct	0.001	2121	2120	2005
Cu_MEICP61_ALS_pct	0.001	14	4	4
Cu_MEICP61a_ALS_pct	0.001	642	80	84
Cu_MEICP61a_ALS_ppm	0.001	280	0	0
Cu_MEMS61_ALS_ppm	0.0001	926	275	294
Cu_OG62_ALS_pct	0.001	278	0	8
Cu_UNK_UNK_pct	0.001	18249	18282	18249
Total			46145	46239
Method	DL	No. Samples	No. in old BESTEL	No. in new BESTEL
Mo_1DX1_ACME_ppm	0.00001	2445	84	237
Mo_1EX_ACME_ppm	0.00001	8650	8654	365
Mo_1F04_ACME_ppm	0.000022	111	0	0
Mo_1F06_ACME_ppm	0.000186	10	1	1
Mo_7AR2_ACME_pct	0.001	37	1	1
Mo_7TD2_ACME_pct	0.001	21855	13557	21855
Mo_AQ200_ppm	0.00001	2108	57	4
Mo_AQ250_ppm	0.000354	115	0	0
Mo_AQ252_ppm	0.000058	28	0	0
Mo_ASY_IPL_pct	0.0006	1007	764	809
Mo_ICP_IPL_pct	0.0001	2292	214	285
Mo_ICP_IPL_ppm	0.0001	5404	1947	2194
Mo_MA200_ppm	0.00006	67	2	5
Mo_MA370_pct	0.001	2121	2120	2005
Mo_MEICP61_ALS_pct	0.0001	14	4	0
Mo_MEICP61a_ALS_pct	0.001	642	80	88
Mo_MEICP61a_ALS_ppm	0.001	280	0	0
Mo_MEMS61_ALS_ppm	0.000042	926	275	19
Mo_OG62_ALS_pct	0.001	278	0	8
Mo_UNK_UNK_pct	0.0006	18124	18124	18124
Total			45884	46000

table continues…

Method	DL	No. Samples	No. in old BESTEL	No. in new BESTEL
Re_1F04_ACME_ppb	0.001	111	111	111
Re_1F06_ACME_ppb	0.001	10	10	9
Re_AQ200_ppb	0.01	2105	2105	2001
Re_AQ250_ppb	0.001	115	0	0
Re_AQ252_ppb	0.001	28	28	28
Re_MA200_ppm	0.005	67	65	67
Re_MEMS61_ALS_ppm	0.002	926	906	926
Total			3225	3142
Method	DL	No. Samples	No. in old BESTEL	No. in new BESTEL
S_1DX1_ACME_pct	0.05	2209	0	0
S_1EX_ACME_pct	0.1	8654	0	315
S_1F06_ACME_pct	0.42	10	0	1
S_7AR2_ACME_pct	0.05	37	0	1
S_7TD2_ACME_pct	0.05	21855	0	7988
S_AQ200_pct	0.05	2105	0	1
S_MA200_pct	0.1	67	0	5
S_MA370_pct	0.05	2121	0	2005
S_MEICP61_ALS_pct	0.04	14	0	0
S_MEICP61a_ALS_pct	0.05	922	0	96
S_MEMS61_ALS_ppm_pct	0.01	926	0	0
TotS_2A13_ACME_pct	0.02	15153	14913	15052
TotS_IR08_ALS_pct	0.01	926	650	294
S_TC000_pct	0.02	2260	0	0
Total			15563	25758

11.3.6 Assay Recommendations

Based on the findings detailed above, Table 11-10 contains the recommendation of which methods from the Copper Fox and more recent data should be accepted and with what order or rejected in the cascading _BESTEL calculations.

Table 11-10: Analytical Method Recommendations

Method	Status	Order
Ag_1DX1_ACME_ppm	Accept	1
Ag_AQ250_ppb	Accept	2
Ag_AQ200_ppm	Accept	3
Ag_1EX_ACME_ppm	Accept	4
Ag_MEMS62_ALS_ppm	Accept	5
Ag_FA_LOR_gpt	Accept	6
Ag_AQ252_ppb	Accept	7
Ag_1F04_ACME_ppb	Accept	8
Ag_1F06_ACME_ppb	Accept	9
Ag_MA200_ppm	Accept	10
Ag_MEICP61_ALS_gpt	Accept	11
Ag_MEMS61_ALS_ppm	Accept	12
Ag_ICP_IPL_ppm	Accept	13
Ag_7AR2_ACME_gpt	Partial Accept ≥ DL	14
Ag_7TD2_ACME_gpt	Partial Accept ≥ DL	15
Ag_UNK_UNK_opt	Corrections Needed	16
Ag_G613_ACME_gpt	Reject	
Ag_MA370_gpt	Reject	
Ag_MEICP61a_ALS_gpt	Reject	
Ag_MEICP61a_ALS_ppm	Reject	
Ag_OG62_ALS_gpt	Reject	

Method	Status	Order
As_1DX1_ACME_ppm	Accept	1
As_AQ200_ppm	Accept	2
As_1EX_ACME_ppm	Accept	3
As_AQ250_ppm	Accept	4
As_1F04_ACME_ppm	Accept	5
As_AQ252_ppm	Accept	6
As_1F06_ACME_ppm	Accept	7
As_MA200_ppm	Accept	8
As_MEMS61_ALS_ppm	Accept	9
As_MEICP61_ALS_ppm	Accept	10
As_7AR2_ACME_pct	Reject	
As_7TD2_ACME_pct	Reject	
As_ICP_IPL_ppm	Reject	
As_MA370_pct_ppm	Reject	
As_MEICP61a_ALS_ppm	Reject	

table continues…

Method	Status	Order
Au_G610_ACME_gpt	Accept	1
Au_G601_ACME_gpt	Accept	2
Au_AA26_ALS_gpt	Accept	3
Au_FA430_ppm	Accept	4
Au_FA_LOR_gpt	Accept	5
Au_FAAAS_LOR_gpt	Accept	6
Au_ICP21_ALS_gpt	Accept	7
Au_UNK_UNK_opt	Corrections Needed	8
Au_1DX1_ACME_ppb	Reject	
Au_1EX_ACME_ppm	Reject	
Au_1F04_ACME_ppb	Reject	
Au_1F06_ACME_ppb	Reject	
Au_AQ200_ppb	Reject	
Au_AQ250_ppb	Reject	
Au_AQ252_ppb	Reject	
Au_G612_ACME_gpt	Reject	
Au_MA200_ppm	Reject	

Method	Status	Order
Cu_MA370_pct	Accept	1
Cu_7TD2_ACME_pct	Accept	2
Cu_1EX_ACME_ppm	Accept	3
Cu_AQ200_ppm	Accept	4
Cu_AQ250_ppm	Accept	5
Cu_7AR2_ACME_pct	Accept	6
Cu_MEICP61a_ALS_pct	Accept	7
Cu_FA_LOR_pct	Accept	8
Cu_ASY_IPL_Pct	Accept	9
Cu_ICP_IPL_ppm	Accept	10
Cu_1DX1_ACME_ppm	Accept	11
Cu_OG62_ALS_pct	Accept	12
Cu_MA200_ppm	Accept	13
Cu_AQ252_ppm	Accept	14
Cu_1F04_ACME_ppm	Accept	15
Cu_1F06_ACME_ppm	Accept	16
Cu_MEICP61_ALS_pct	Accept	17
Cu_MEICP61a_ALS_ppm	Accept	18
Cu_MEMS61_ALS_ppm	Accept	19
Cu_UNK_UNK_pct	Accept	20

table continues…

Method	Status	Order
Mo_7TD2_ACME_pct	Accept	1
Mo_MA370_pct	Accept	2
Mo_1EX_ACME_ppm	Accept	3
Mo_7AR2_ACME_pct	Accept	4
Mo_1DX1_ACME_ppm	Accept	5
Mo_AQ200_ppm	Accept	6
Mo_MEICP61a_ALS_pct	Accept	7
Mo_ASY_IPL_pct	Accept	8
Mo_ICP_IPL_pct	Accept	9
Mo_ICP_IPL_ppm	Accept	10
Mo_MA200_ppm	Accept	11
Mo_1F04_ACME_ppm	Accept	12
Mo_1F06_ACME_ppm	Accept	13
Mo_AQ250_ppm	Accept	14
Mo_AQ252_ppm	Accept	15
Mo_OG62_ALS_pct	Accept	16
Mo_MEICP61a_ALS_ppm	Accept	17
Mo_MEICP61_ALS_pct	Accept	18
Mo_MEMS61_ALS_ppm	Accept	19
Mo_UNK_UNK_pct	Corrections Needed	20

Method	Status	Order
Re_MEMS61_ALS_ppm	Accept	1
Re_1F04_ACME_ppb	Accept	2
Re_1F06_ACME_ppb	Accept	3
Re_AQ250_ppb	Accept	4
Re_AQ252_ppb	Accept	5
Re_MA200_ppm	Accept	6
Re_AQ200_ppb	Accept	7

table continues…

Method	Status	Order
TotS_2A13_ACME_pct	Accept	1
S_1DX1_ACME_pct	Accept	2
S_7TD2_ACME_pct	Accept	3
S_MA370_pct	Accept	4
S_1EX_ACME_pct	Accept	5
S_AQ200_pct	Accept	6
S_TC000_pct	Accept	7
S_MEICP61a_ALS_pct	Accept	8
TotS_IR08_ALS_pct	Accept	9
S_7AR2_ACME_pct	Accept	10
S_MA200_pct	Accept	11
S_1F06_ACME_pct	Accept	12
S_MEICP61_ALS_pct	Accept	13
S_MEMS61_ALS_ppm_pct	Accept	14

It is recommended that two corrections be applied to the historical datasets based on either twinned samples, resampling, or both. AMEC recommended making a correction to both these subsets of data also. AMEC also recommended other corrections previously. A review of these corrections indicates that there is insufficient evidence to support their use. The recommended corrections are shown below:

- The Asarco generation data justifies a correction to molybdenum:
  - Mo_corrected = Mo_UNK_UNK_pct/0.8504.
- The Hecla generation data justifies a correction to gold:
  - Au_corrected = Au_UNK_UNK_pct/1.0806.

The Teck 1980s generation data for silver has no QA/QC and no correlation with twinned samples. There is no reason to assume that these data are correct and they should be excluded from the resource estimate.

The new cascading _BESTEL calculation has consequences for the number of samples available for resource estimation. In the case of silver, there are approximately 5,000 fewer samples available than previously. This is almost entirely a consequence of the removal of the Teck 1980s generation data. There is a reduction in the number of gold samples available, but only 600 samples (< 2% of the dataset) as a consequence of the removal of specific unsuitable methods. The number of available copper and molybdenum samples are essentially unchanged.

All recommendations for changes were implemented in acQuire.

11.4 Density

11.4.1 Density from Previous Programs

From Caron et al. (2012):

> Ninety-six samples of full diameter drill core were selected from drill holes 2011CF407 through to 2011CF425 for specific gravity determination, averaging about five samples per drill hole. Samples were between 13 cm and 20 cm long and were selected by the geologist responsible as being representative of lithology, alteration, or mineralization. Samples were collected roughly every 100 m throughout each drill hole, or as dictated by changes in lithology/alteration/mineralization. A labelled wooden reference block was inserted in the core box from where the sample was collected. Samples were assigned a unique sample ID number and sent to the Acme laboratory for specific gravity measurement according to criteria specified by Copper Fox.
>
> The specific gravity samples were processed according to Acme laboratory code G813-WAX as follows: The core was first dried and weighed, then covered in wax to seal any fractures and to eliminate the porous nature of the core. The waxed core was then re-weighed to note the amount of wax, and then weighed in water. The specific gravity was then calculated as a ratio of the sample weight in air and the sample weight in water.

The QP is satisfied that the density determination procedures are industry standard and appropriate to provide data suitable for in situ bulk density estimation.

12.0 DATA VERIFICATION

12.1 Historic versus Current Drill Sampling Comparisons

The QP compared subsets of drill sampling from historic (pre-2000) and current (since 2000) campaigns to assess the risk of bias using Leapfrog EDGE™ software.

Subsets of assay data were prepared by locating historic and drillhole segments within 10 m of each other. The sampling data for historic and current sets within this common volume was composited to 6 m lengths, and the resulting 546 NNs were compared by means of QQ plots for gold, copper, and molybdenum (Figure 12-1). The red points represent the data and a black line representing the ideal condition where historic and current sample populations would be identical is shown for convenience.

Figure 12-1: Quantile Plots for Gold, Copper, and Molybdenum (Clockwise) Comparing Historic and Current Sampling Results

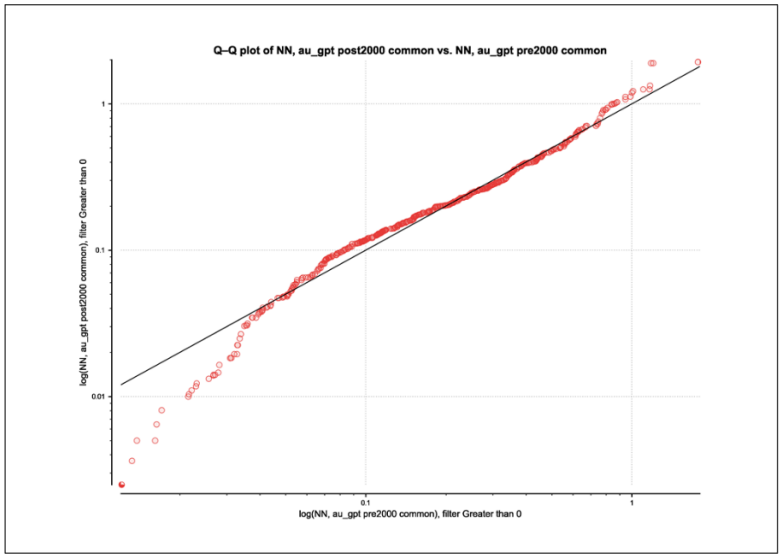

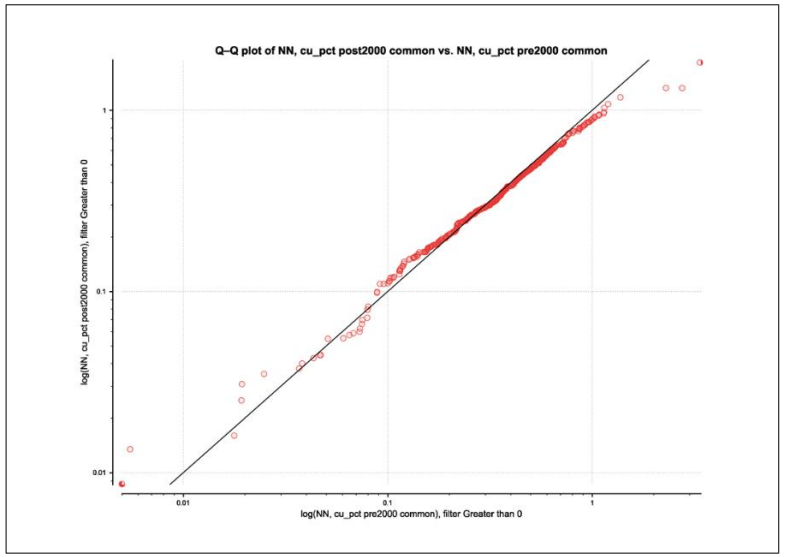

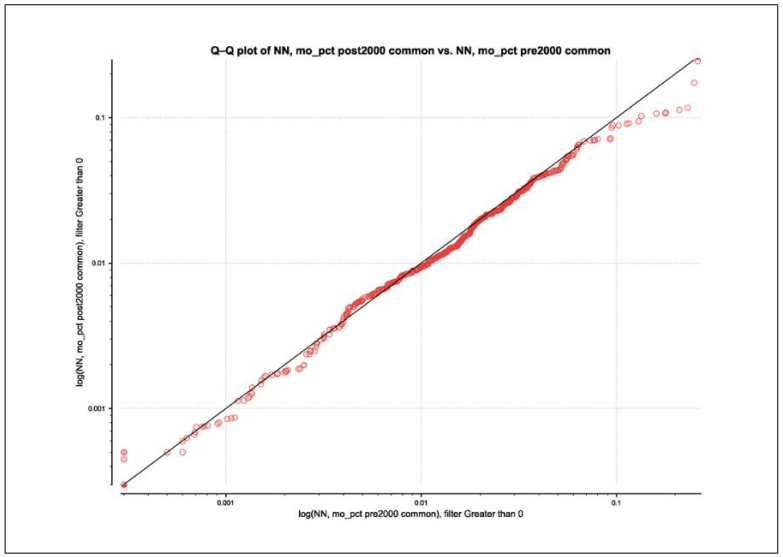

Historic and current sampling for all three elements within the comparable region appear to draw from the same populations with some statistical noise for low and very high-grade material. The QP is satisfied that there is no significant bias between the comparable historic and current sampling and assay data within the grade range of practical resource estimation for the assay data that has been retained in terms of the recommendations made in Section 11.3.6, “Assay Recommendations”.

12.2 Topography Verification

The provenance of the high definition topographic surface mesh (Dem_SCK) that was used for geological modelling and resource estimation is not documented. Tetra Tech compared this mesh with public domain data from NASA's Shuttle Radar Topography Mission (SRTM).

The difference between the high definition topographic surface mesh and the SRTM mesh over the area covered by the resource block model was estimated using Leapfrog Geo™. The difference is summarised in Figure 12-2.

Figure 12-2: Histogram of the Difference Between Dem_SCK and SRTM Topography Data

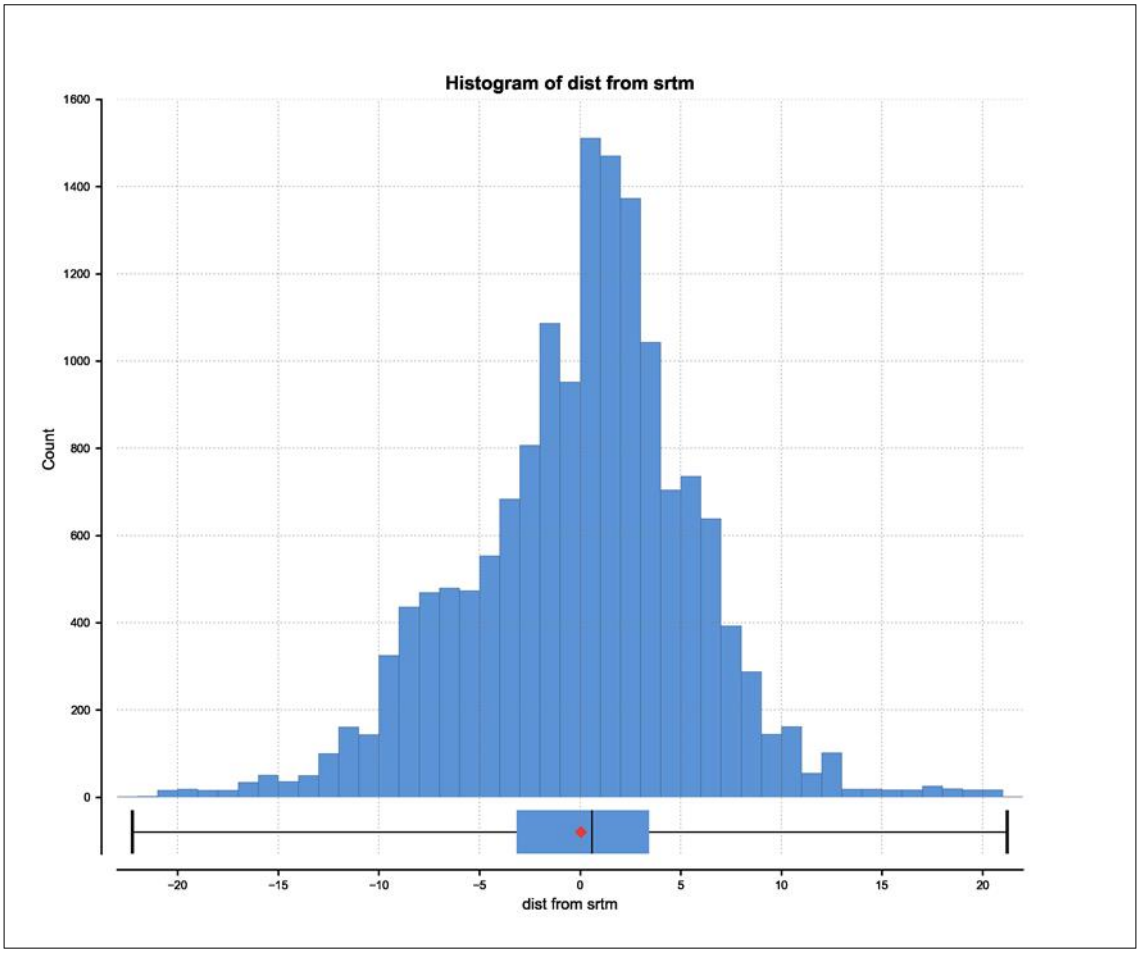

The average difference is 0.038 m, and 90% of differences fall between -13 m and 13 m. The resource block model vertical dimension is 15 m, so the QP believes that the uncertainty in topography data does not present a material risk to the Project.

12.3 Site Visit Verifications

The QP visited the site on Friday, October 30, 2020. The camp and core storage area appear to be in good order despite no site work for some time. A remote piloted aerial system (RPAS) was used for general photography of the site.

A general view of the core stacks and camp buildings is shown in Figure 12-3.

Figure 12-3: Schaft Creek Camp Looking Southwest Showing Camp Buildings and Core Stacks

A view of the deposit, with the network of drill roads and drill pads is shown in Figure 12-4.

Figure 12-4: Looking Northeast From Above the Camp Towards Mount LaCasse

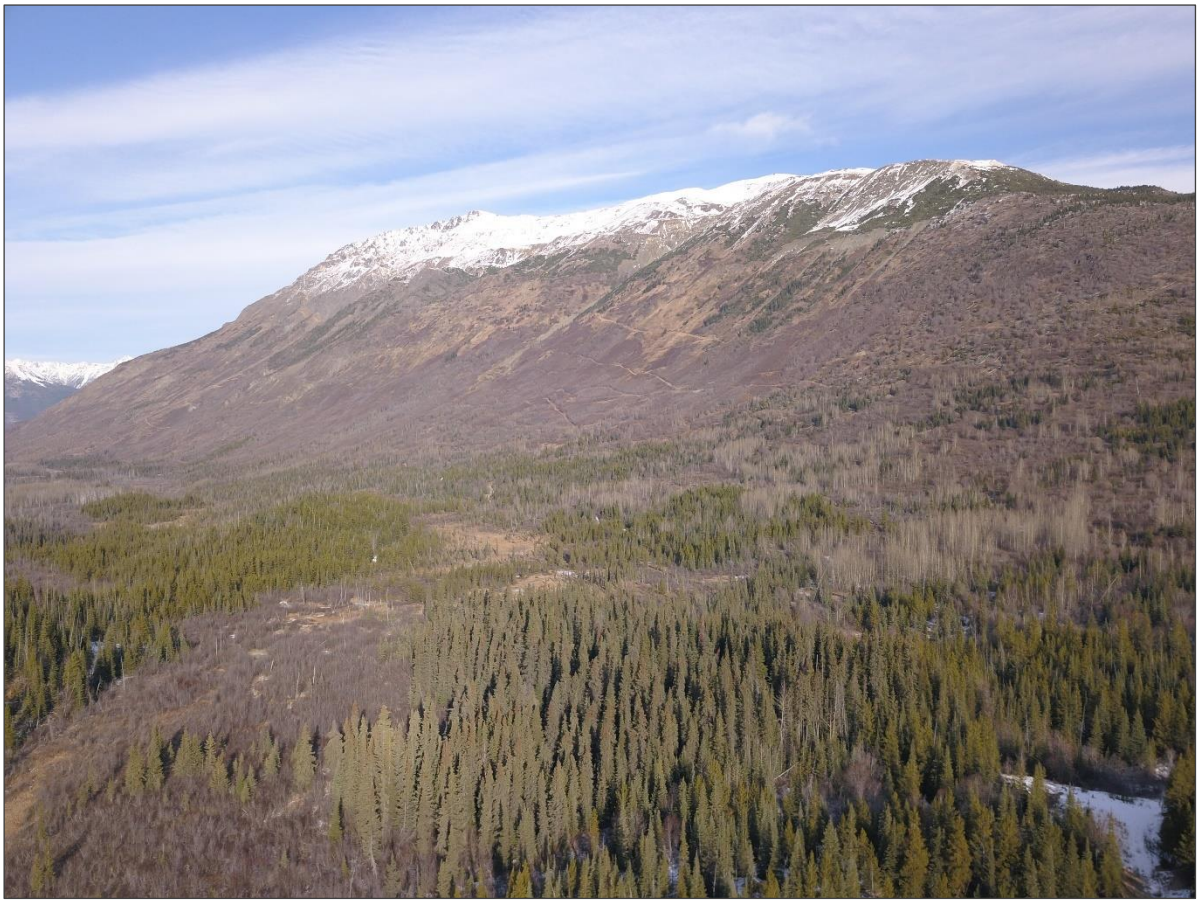

Note: The deposit including the Paramount and Liard Zones occupies the middle ground of the image. The breccia units occur along the foot of the slope and trend north-south along the valley. A network of drill access tracks can be made out on the lower slopes of the mountain.

Several boxes of core were temporarily removed from the stacks at the camp and reviewed. The information is summarized in Table 12-1.

Table 12-1: Core Reviewed On Site

Video File	Time	Hole	From	To	Remarks	Lithology	If_dom
DJI_0395	0	H-86-B15	297	312	Hole not found in database, old core, depths in feet?	Breccia	-
							
DJI_0396	2:03	07CF316	41.5	43	-	Porphyritic Lava	-
							

table continues…

Video File	Time	Hole	From	To	Remarks	Lithology	If_dom
DJI_0396	3:24	2010CF405B	125.58	128.94	Bornite, as it should ~1% Cu based on assays file.	Breccia	3200

table continues…

Video File	Time	Hole	From	To	Remarks	Lithology	If_dom
-	-	2011CF410B	141.62	144.37	Acme labs ticket 586862 – correct ticket in database.	Diorite or Monzonite	3301
							
DJI_0397	0:26	08CF369	147.5	150.1	In database, low copper grade.	Breccia	3200
							
DJI_0398	0:04	SCK-13-433	106.9	109.5	Assays copper ~0.15%.	-	-
							

table continues…

Video File	Time	Hole	From	To	Remarks	Lithology	If_dom
DJI_0398	2:41	SCK-15-440	180.1	182.7	Acme ticket 2307885 – ticket confirmed in database, negligible grades. Far north.	Andesite	-

The collar of inclined drill hole 07CF306 was located some 600 m north of the camp on the track to the main concentration of drill pads. Two GPS units, a Suunto Traverse Alpha and a Garmin GPSmap 66i) were used to measure the collar position.

Source	Easting	Northing	Elevation	Horiz Difference	Elev Difference
GPSmap 66i	379,087.0	6,358,929.6	937.0	3.4	45.0
Suunto Traverse Alpha	379,092.2	6,358,931.6	892.0	2.1	12.2
Collar Database	379,090.1	6,358,930.9	879.8	-	-

The database plan position of the collar was in reasonable agreement with the two GPS measurements, but the elevation measurements from the two GPS units were poor. The collar elevation in the database agrees closely with both the detailed topographic surface model (Dem_SCK) and the SRTM data, so the elevation measurements provided by the GPS units are likely to be at fault.

(Reference *Global Positioning System Standard Positioning Service Performance Standard*, 5th Edition April 2020, Office of the Department of Defense Chief Information Officer Attn: Assistant for GPS, Positioning and Navigation 6000 Defense Pentagon Washington, DC 20301-6000.)

12.4 Data Verification Conclusion

The QP is satisfied that the sampling and assay data, topographic information, and drill core management for this Project have been comprehensively verified and are suitable to be used for mineral resource estimation.

13.0 MINERAL PROCESSING AND METALLURGICAL TESTING

13.1 Introduction

The Schaft Creek deposit is a low-sulphidation, calc-alkalic, polymetallic (copper-molybdenum-gold-silver), porphyry deposit. Historically, the deposit has been divided into three mineralization zones: the Main (or Liard) Zone, the Paramount Zone, and the West Breccia Zone. The Liard Zone is the largest zone of mineralization; the Paramount Zone and the West Breccia Zone were combined into one zone at the end of the 2011 field season.

Limited test work was undertaken in the periods 1970 to 1971 and 1981 to 1982 and is not considered relevant. Thirteen test programs have been conducted since 2004. Laboratories that completed the test work are:

- Process Research Associates Ltd. (PRA), BC, Canada
- Hazen Research Inc. (Hazen), Golden, CO, USA
- Lehne & Associates Applied Mineralogy (Lehne), Germany
- Cominco Engineering Services Ltd. (CESL), BC, Canada
- Polysius AG (Polysius), Neubeckum, Germany
- G&T Metallurgical Services (G&T)/ALS Metallurgy Kamloops (ALS), Kamloops, BC, Canada.

The drill core samples used for the 2004 to 2012 test work were collected from historical drilling programs and from the 2005 to 2011 drilling programs completed by Copper Fox on the main mineralization zones (Figure 13-1). Test work conducted in the 2004 to 2012 period included mineralogical examinations and mineral liberation patterns; Bond crushing and grinding work indices (BWi, RWi, CWi), abrasion indices (Ai), JK SimMet drop weight breakage parameters (A x b, Ta), SMC breakage parameters, and high-pressure grind roll (HPGR) related hardness parameters; semi-autogenous grind (SAG) mills/ball mills/pebble crushers (SABC) circuit simulations; primary grind and regrind size tests; evaluation of reagent regimes; flotation, bulk flotation locked cycle, metallurgical variability, and pilot plant tests; copper and molybdenum separation tests; thickening and filtration tests; exploratory tests to investigate copper and gold hydrometallurgical extractions using the proprietary CESL method; and acid base accounting tests.

Figure 13-1: Schaft Creek Metallurgical 2004–2012 Test Work Drill Hole Location Map

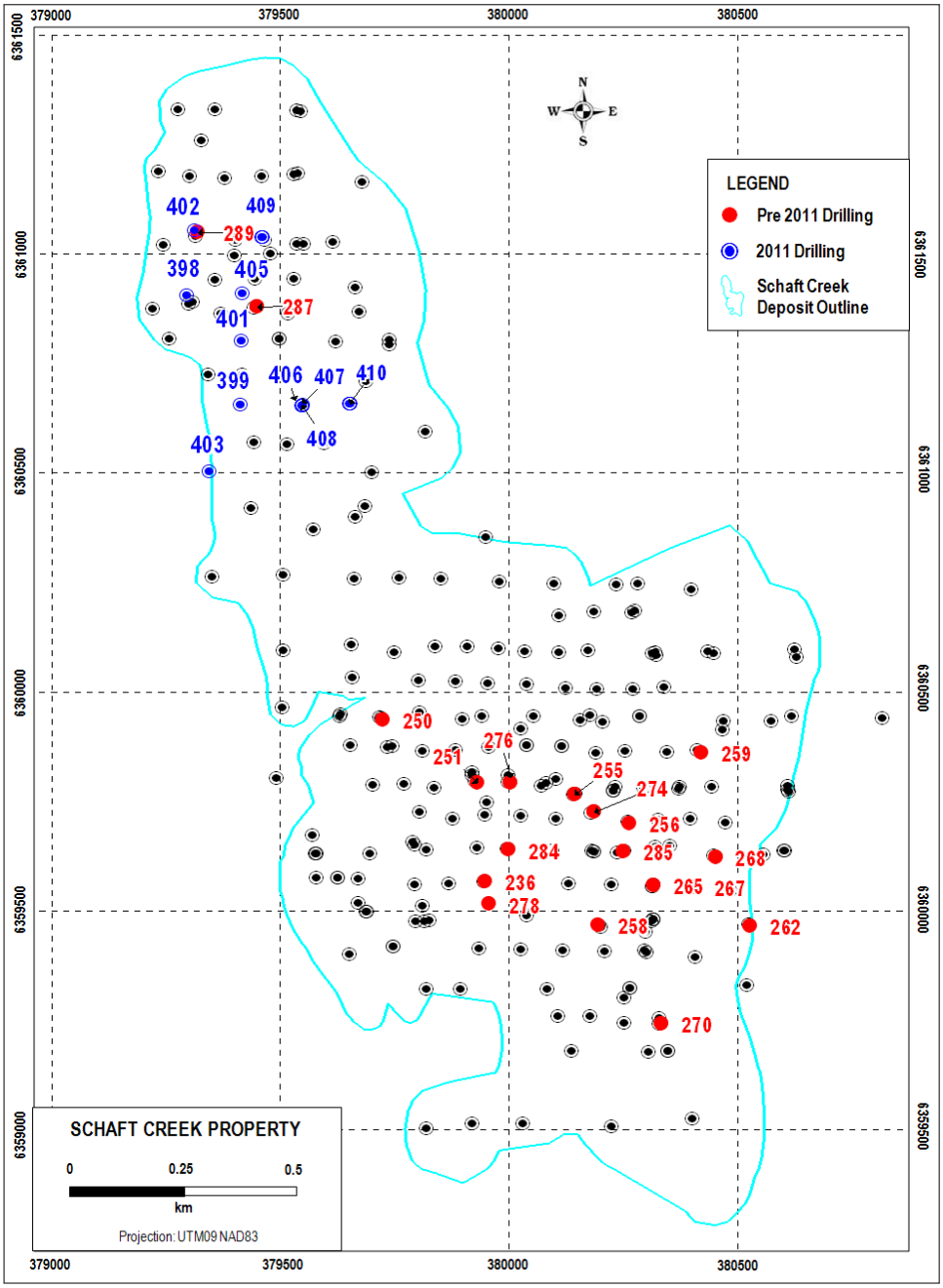

During 2015, the Schaft Creek JV completed a geometallurgical study focused on comminution using half or quarter core from historical drill holes. As part of the 2015 program, the Schaft Creek JV subdivided the mineralization into four rock types: volcanic, intrusive, porphyry, and breccias to characterize their grindability and update the comminution circuit design (the Schaft Creek 2015 GeoMet program). The main focuses of the 2015 GeoMet program were to evaluate the primary comminution circuits proposed by the 2012 study and investigate the comminution variability for updating the mill throughput projection.

Table 13-1 summarizes the major test work programs for the Project.

Table 13-1: Major Metallurgical Testing Programs

Year	Program ID	Laboratory	Mineralogy	Flotation	Grindability	Others
2015	KM4658	ALS			√	
2012	KM 3149	G&T	√	√	√	√
2010	KM 2291	G&T	√	√		√
2009	KM 2292	G&T		√		
2008	KM 2136	G&T	√	√	√	
2008	2337 3326	Polysius			√	
2008	10736	Hazen			√	
2007	-	CESL				√
2007	-	Lehne	√			
2007	PRA 0701301	PRA		√		
2007	10515	Hazen			√	
2006	PRA 0603303	PRA		√	√	
2005	PRA 0502002	PRA	√	√	√	
2004	PRA 0402903	PRA		√		√

Note: PRA Reports 0409111 were not available for the review.

13.2 Samples

The samples used for the 2004 to 2015 test work were collected from the following:

- Historical drilling programs
- The 2005 to 2011 drilling programs completed by Copper Fox
- The 2013 drill program by the Schaft Creek JV on the main mineralization zones
- The samples used for 2015 comminution test work were individual drill core samples, one lithology per sample.

13.3 Mineralogy

Several mineralogical examinations were conducted since 2005, including the analysis of the flotation product samples. The most recent and comprehensive mineralogical studies were conducted by G&T on the composite samples for KM2050 (2008), KM2291 (2010), and KM3149 (2012). The key findings of these studies are summarized below:

- Chalcopyrite was the dominant copper sulphide mineral, together with ancillary bornite and chalcocite.
- The other main non-copper sulphide mineral in the mineralization was pyrite. The pyrite contents in these mineral samples were relatively low, ranging from 0.04% to 0.15% in 2010 to 0.1% to 0.8% pyrite in the 2012 program. The pyrite content in the 2012 samples averaged 0.3%.
- Most of the iron minerals in the samples from the 2010 test program were in oxide forms, such as magnetite, hematite, goethite, and limonite.
- Feldspar was the dominant silicate mineral, ranging between 44% and 52% of the total minerals.
- Moderate amounts of quartz, micas, and chlorite were also detected in the samples.

The 2008 mineralogical study on variability samples showed that there is a significant variation in secondary copper minerals and pyrite contents. In some of the variability samples, the ratio of chalcopyrite to secondary copper minerals (bornite, chalcocite, and covellite) was low. On average, the ratio was 2.7:1. For the 2012 test program samples, the copper was primarily contained in chalcopyrite. Seventy-eight percent of the copper minerals occurred as chalcopyrite. These mineralogical studies indicated that the ratio of pyrite to copper minerals was low for all the samples tested.

G&T also estimated the percent of mineral liberation at a grind size of 80% passing approximately 100 µm for the 2008 samples and at a grind size of 80% passing approximately 150 µm for the 2010 samples. The data are summarized in Table 13-2.

Table 13-2: Mineral Liberation Estimate (Two Dimensions), 2008/2010 (G&T)

Sample	Test Program							
	KM2291 (2010)					KM2050 (2008)		
	Composite					Paramount	Liard	West Breccia
	1	2	3	4	5	Zone	Zone	Zone
Grind Size 80% passing (µm)								
-	161	156	153	153	145	111	117	89
Liberation Rate (%)								
Chalcopyrite	-	-	-	-	-	59	70	50
Bornite	-	-	-	-	-	83	81	64
Copper Sulphides	39	45	51	47	46	61	72	53
Molybdenite	52	38	55	58	57	73	62	70
Pyrite	57	56	69	83	61	71	80	77
Gangues	96	97	95	97	96	98	97	98

The 2012 test program showed liberation patterns similar to those recorded in the 2010 test program. When measured in two dimensions, approximately 47% of the copper sulphides were in liberation form at the nominal primary grind sizing of 80% passing 150 µm. Most of the interlocked copper sulphides were associated with non-sulphide gangue in binary structures. These particles, on average, contained approximately 14% copper sulphides and should be recoverable by flotation processes.

The 2008 test work included a mineralogical study to assess gold occurrence in the copper flotation concentrate. The samples tested were derived from the copper-molybdenum separation test work and used an Automated Digital Imaging System (ADIS) to scan the copper concentrate. The tests showed that approximately 80% of the gold observed was liberated. The remaining 20% was locked with copper minerals or multi-phase particles. The average observed gold grain size was 11 µm in equivalent circle diameter.

13.4 Hardness Test Results

The mineral sample hardness to crushing and grinding were determined by different laboratories in the different test programs. The parameters determined include BWi, RWi, CWi, JK SimMet Drop Weight breakage parameters, SMC test breakage parameters, and high-pressure grinding rolls (HPGR) related hardness parameters. The test results are summarized in the following sections.

13.4.1 Mineral Sample Hardness Parameters – Crushing and Ball/Rod Mill Milling

Four test programs conducted crushability and grindability tests on various samples collected for different test programs.

The low energy impact work indices (CWi) are relatively low, ranging from 6.3 kWh/t to 11.9 kWh/t. The grindability test results (Bond BWi and Bond RWi) indicates that the mineral samples exhibit a high grinding resistance to ball mill and rod mill grinding. There is a considerable variation in the grinding hardness among the samples tested. The BWi ranges from 13.7 kWh/t to 25.4 kWh/t, averaging 21.3 kWh/t. The RWi is slightly lower than the BWi, averaging 20.8 kWh/t. The average Ai is 0.25 g, fluctuating from 0.17 g to 0.57 g.

13.4.2 Mineral Sample Hardness Parameters and Simulations – SAG Mill Milling

Hazen conducted JK SimMet Drop Weight breakage tests and SMC tests on the samples collected for the 2007 and 2008 test programs. In 2012, G&T conducted further JK SimMet Drop Weight breakage tests and SMC tests on the 2012 test samples. JKTech Pty Ltd. analyzed the generated data. In 2015, the Schaft Creek JV program further investigated resistance to SAG mill and ball mill grinding using SMC test procedure. The 2015 results indicate that the samples are rated moderately hard to very hard for SAG mill milling. The key parameter (A x b) ranged from 27.4 to 44.7.

In 2007 and 2010, Contract Support Services conducted SAG mill / ball mill / pebble crusher circuit simulations for the Project. In 2012, more SABC simulations were conducted using the data generated from the 2012 test work and the historical test programs. These simulations were conducted at 120,000 t/d at an availability of 92% and 130,000 t/d at an availability of 94%.

In 2015, further JK SimMet simulations were conducted based on the data produced from the 2015 GeoMet program. The primary grinding circuit arrangement used in the simulations is the same as the SABC circuit in the 2013 feasibility study, which consists of two grinding lines, each line equipped with one 40 ft. x 23 ft. (effective grinding length [EGL]) SAG mill, two 26 ft. x 44.5 ft. (EGL) ball mills, and one MP1000 pebble crusher. The feed particle sizes used for the simulations range from 80% passing 89.6 mm to 106.3 mm. The hydrocyclone overflow particle size was 80% passing 150 µm.

13.4.3 Mineral Sample Hardness Parameters – HPGR Crushing

In June 2008, the Polysius Research and Development Centre carried out HPGR tests on a sample consisting of large pieces of split cores with a net weight of 700 kg from the Schaft Creek deposit. The tests included bench scale LABWAL HPGR tests and REGRO semi-industrial HPGR tests. The material was crushed to two different sizes, less than 31 mm for the REGRO test, and less than 12.5 mm for the LABWAL test.

The tests found that the mineral sample was amenable to HPGR process and the results indicated the following:

- A pressure of at least 4 N/mm² was needed to reduce the feed particle size to, on average, 80% passing 8 mm (50% passing 2 mm and 20% passing 0.25 mm).

- The optimum press force was found to be a little higher than 4.2 N/mm²; increasing pressure beyond this limit had minimal impact on size reduction.
- The moisture was not detrimental to the performance of the rolls.
- The specific throughputs were reasonably high, in a range of 210 ts/hm³ to 250 ts/hm³, under all the conditions tested.
- The average specific energy consumption was less than 2 kWh/t at 4 N/mm².
- The material after pressing did not form competent flakes, which implies that the HPGR product could be screened with a relatively high efficiency.
- The material was of low to medium abrasiveness, with an ATWAL wear index of 9.2 g/t at a moisture of 3%; wear life for HPGR rolls was estimated at 8,000 h.

Results obtained from the LABWAL unit were reproduced on the semi-industrial scale REGRO unit.

More ATWAL tests are recommended if the HPGR technology will be used for the Project.

13.5 Metallurgical Test Results

13.5.1 Copper/Molybdenum Bulk Flotation

13.5.1.1 Process Condition Development Tests

Various test programs were conducted between 2004 and 2012 to develop optimum process conditions, including primary grind size, regrind size, pulp pH, and various reagent regimes.

The 2012 tests used test conditions similar to those in the 2010 and 2008 test programs. The pH was elevated to approximately pH 9 using lime. Fuel oil was added in the grinding mill to collect molybdenum, while sodium ethyl xanthate was added as the copper collector. Four batch rougher flotation tests were completed on each of the six samples. On each sample, two tests were completed at a grind size of 80% passing 150 µm, and two were completed at a coarser sizing of approximately 80% passing 190 µm. The 2012 tests appear to show that the coarser primary grind sizing had only insignificant effects on copper, gold, and silver metallurgical performance; however, molybdenum performance appeared to deteriorate at the coarser sizing on all six samples. On average, molybdenum recovery dropped at the coarser primary grind sizing by approximately 7% at the same mass recovery.

The effect of regrind size on copper and molybdenum cleaner flotation was also investigated. The test results show that to obtain a high concentrate grade, the rougher concentrate should be reground prior to cleaner flotation. A finer regrinding appeared to benefit the molybdenum metallurgical performance. Ultra-fine regrinding is not required.

The test results indicate that pH did not significantly influence the copper rougher flotation at the pH range of between 8.1 and 9.5. The optimum bulk rougher flotation pH was in range of 9.0 to 9.5. The test program also investigated the effect of pulp pH on the copper-molybdenum bulk cleaner flotation.

The test results indicate that metal recoveries declined when the cleaner flotation was conducted at pH 12.

13.5.1.2 Variability Test Results

Two variability testing programs were conducted by PRA and G&T.

The variability test results show a significant variation in the metallurgical performances between the individual drill core interval samples. The variation can be traced to significant differences in mineralogy between the samples. The varying differences in the results have reflected a very poor correlation in the metallurgical performance among the samples tested. However, the master composites show much less variation in the metallurgical performance.

The copper grade and recovery results from the variability testing of KM2136 are shown in Table 13-3 and plotted in Figure 13-2 to Figure 13-6. Variability samples were selected with a wide range of feed grades from 0.16% Cu to 1.24% Cu, with an average feed grade of 0.55% Cu. The variability tests used the optimum test conditions developed at the time of these programs.

Table 13-3: Variability Test Result Summary, 2008, G&T

Test#	Sample ID	Head Grade	P_{80}	Rougher Conc			Cleaner Conc	
				MP	Grade	Recovery	Grade	Recovery
		% Cu	µm	%	% Cu	% Cu	% Cu	% Cu
KM2136-58	126712	0.16	143	2.5	5.4	81.6	51.2	69.5
KM2136-59	126720	0.17	144	2.8	4.8	82.9	42.6	69.8
KM2136-72	127121	0.17	141	9.8	1.6	93.1	25.6	80.1
KM2136-79	127348	0.17	142	4.5	3.4	87.7	32.0	80.2
KM2136-62	126768	0.21	118	4.2	4.4	88.8	49.9	79.4
KM2136-67	126865	0.21	143	5.8	3.6	97.3	27.2	91.5
KM2136-53	126649	0.22	137	5.5	3.5	87.2	34.2	81.7
KM2136-52	126644	0.28	147	8.1	2.2	64.2	46.5	53.1
KM2136-60	126725	0.29	155	3.9	6.5	89.6	37.5	81.3
KM2136-73	127126	0.29	135	6.1	4.6	97.7	32.9	94.8
KM2136-77	127321	0.29	157	4.4	6.4	94.5	30.7	89.4
KM2136-78	127337	0.37	158	9.0	4.0	97.3	28.7	93.7
KM2136-80	127352	0.37	142	8.5	4.0	93.7	26.5	90.1
KM2136-56	126705	0.38	152	3.7	8.7	85.2	51.9	78.5
KM2136-63	126777	0.40	137	7.4	5.0	94.1	29.2	89.6
KM2136-68	126876	0.40	153	9.2	4.1	95.4	36.9	85.9
KM2136-84	127573	0.47	146	6.6	6.5	91.1	37.7	85.5

table continues…

Test#	Sample ID	Head Grade	P_{80}	Rougher Conc			Cleaner Conc	
				MP	Grade	Recovery	Grade	Recovery
		% Cu	µm	%	% Cu	% Cu	% Cu	% Cu
KM2136-64	126785	0.50	153	7.4	6.2	93.3	36.3	86.8
KM2136-57	126710	0.51	141	3.8	11.5	87.4	54.6	81.6
KM2136-70	126882	0.55	162	10.8	4.8	93.2	39.9	88.5
KM2136-69	126881	0.61	143	6.1	9.4	94.0	41.7	88.0
KM2136-51	126636	0.63	152	9.6	5.4	82.7	40.2	76.5
KM2136-83	127378	0.68	104	11.5	5.4	91.1	26.7	86.0
KM2136-61	126737	0.74	199	6.4	10.9	94.0	30.0	90.7
KM2136-54	126694	0.76	132	6.4	10.9	91.8	53.5	86.4
KM2136-65	126787	0.80	141	6.8	11.2	94.2	38.5	88.7
KM2136-81	127376	0.81	151	10.8	6.7	88.7	23.6	83.7
KM2136-55	126702	0.90	114	8.0	10.7	94.9	50.2	89.8
KM2136-82	127377	0.95	133	11.6	7.5	90.8	23.3	86.3
KM2136-75	127151	0.98	135	11.7	8.3	98.8	28.0	97.3
KM2136-66	126799	1.02	158	10.0	9.4	91.5	30.9	87.0
KM2136-71	126927	1.07	136	12.4	8.0	92.8	30.8	88.8
KM2136-76	127197	1.15	162	10.1	11.1	97.0	35.5	92.3
KM2136-74	127145	1.24	147	9.2	13.3	98.7	32.6	97.1
Max		**1.24**		**12.4**	**13.3**	**98.8**	**54.6**	**97.3**
Min		**0.16**		**2.5**	**1.62**	**64.2**	**23.3**	**53.1**
Average		**0.55**		**7.49**	**6.74**	**91.1**	**36.4**	**85.0**

Figure 13-2: Copper Recovery vs. Copper Head Grade

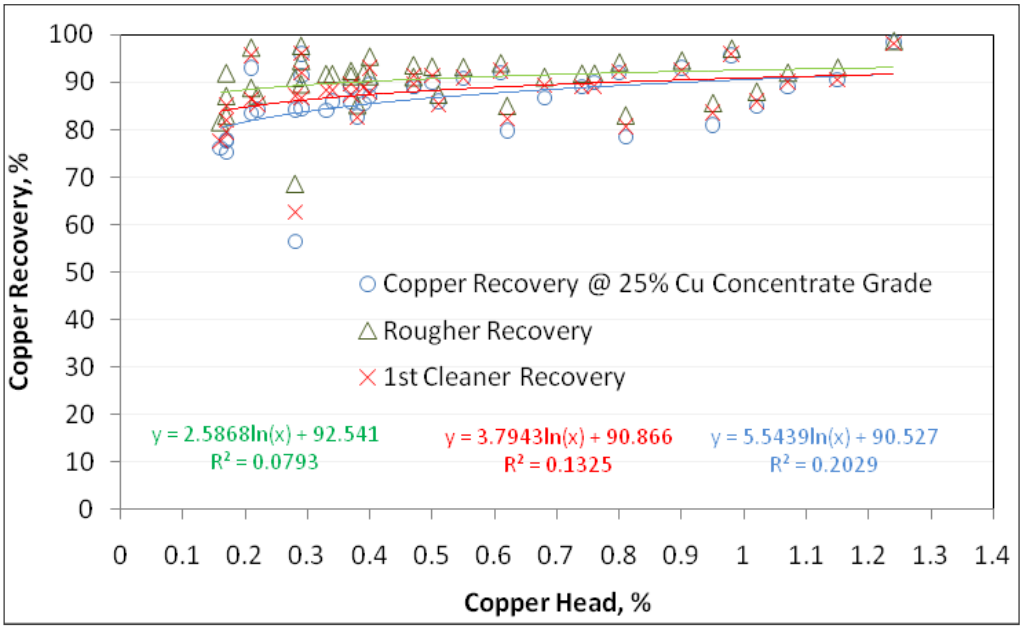

Figure 13-3: Gold Recovery vs. Gold Head Grade

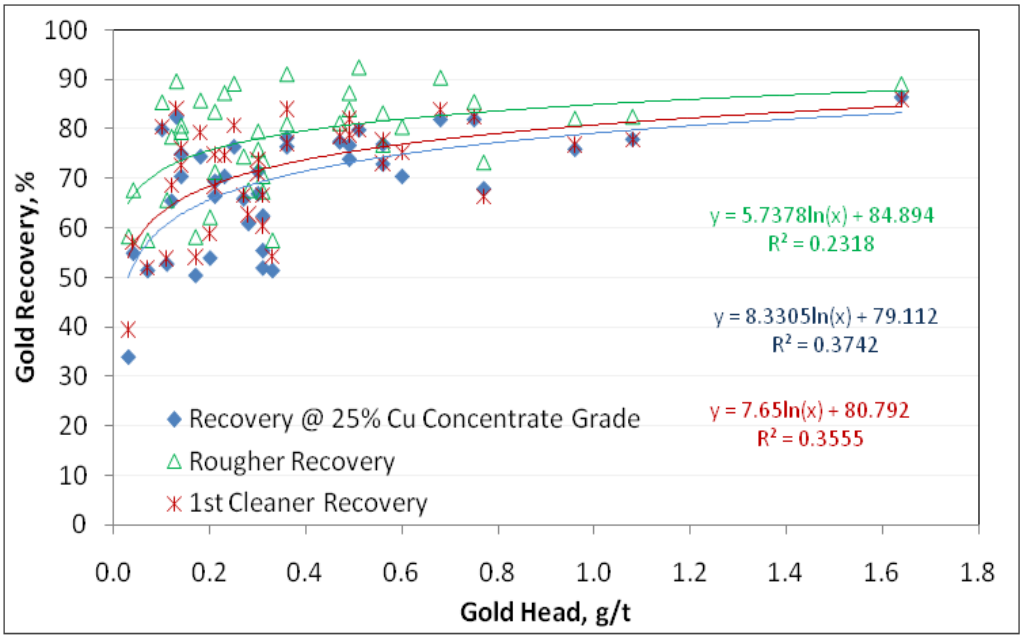

Figure 13-4: Silver Recovery vs. Silver Head Grade

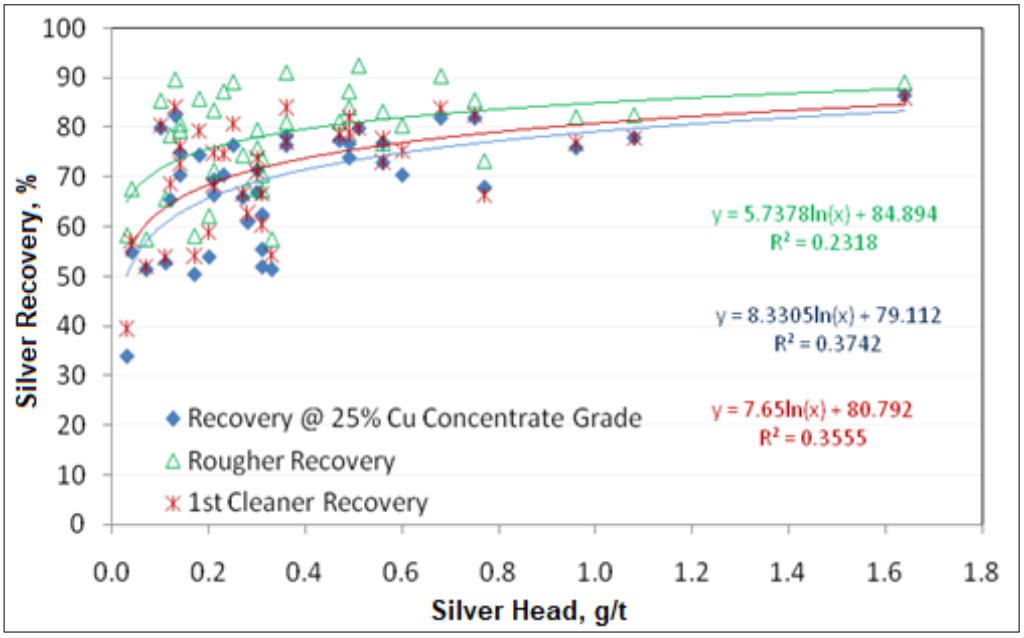

Figure 13-5: Molybdenum Recovery to First Cleaner Concentrate vs. Molybdenum Head Grade

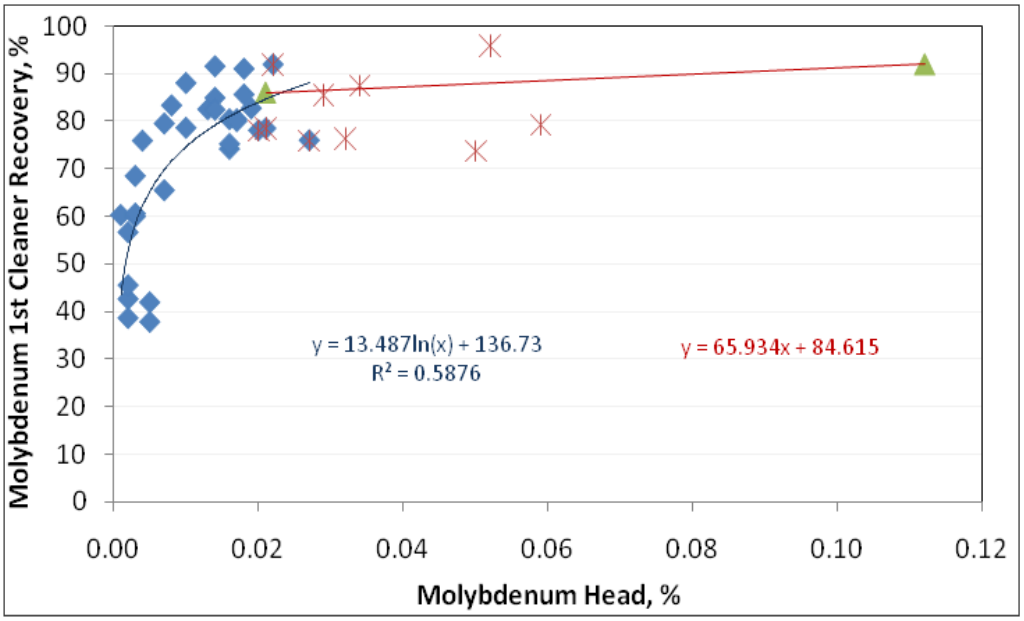

Figure 13-6: Copper Concentrate Grade vs. Copper Head Grade

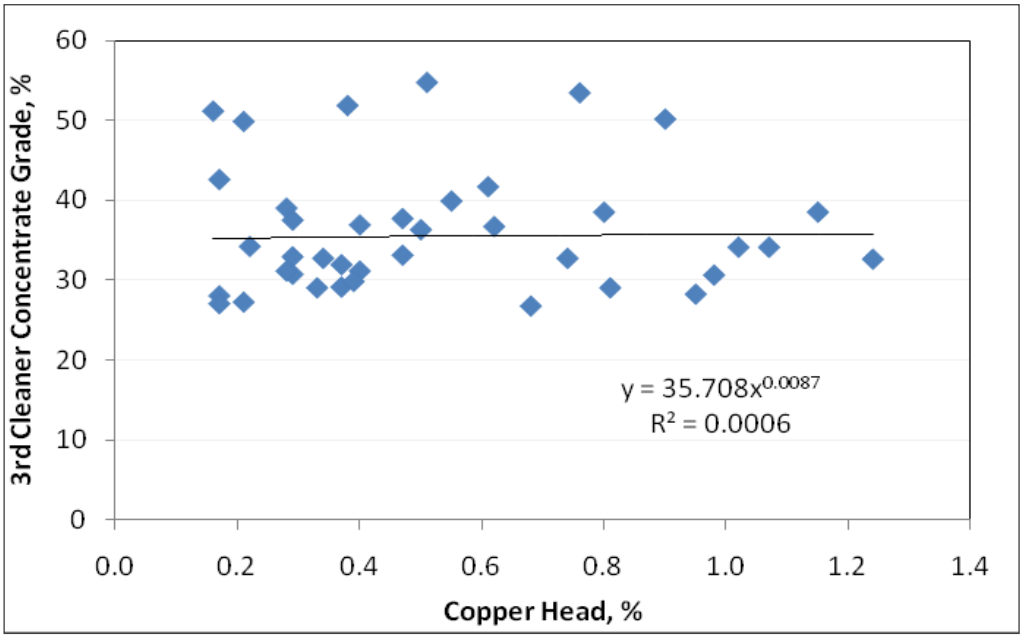

The test results indicate that the metal recoveries increase with an increase in head grades. There are more significant fluctuations in gold and silver recoveries in comparison with copper and molybdenum recoveries.

The copper grades of the third cleaner concentrates (open bench tests) varied from 26% to 55%, averaging at 36%. The copper grade of the cleaner concentrate is not related to the copper head grade. This indicates the significant effect of copper mineralogy on the copper concentrate grade. The results indicate that on average, the Project would be able to produce a high-grade copper concentrate due to a portion of the copper mineralization being present in the form of bornite and other copper minerals.

The variability test results show a significant variation in the metallurgical performances between the individual samples, which is not feed grade driven, but rather mineralogically driven. Locked cycle testing was not completed on the variability samples although batch cleaning stage test work was conducted to inform final grade predictions. Final concentrate grades that are significantly higher than 32% copper are indications that other copper minerals such as bornite are present in high levels. The results speak to the mineralogical variability within the mineralization body. Future variability test work consistent with spatial and material associations should be considered for higher level studies. Deposit geology with respect to variation in the distribution of copper minerals is an important factor to consider.

13.5.1.3 Locked Cycle Tests – Bulk Flotation

Six test programs conducted locked cycle tests to evaluate the flotation metallurgical performance of various composite samples since 2005. A summary of the bulk flotation locked cycle test results is presented in Table 13-4. This summary excludes the 2005 test results because the flowsheet used was significantly different from the optimum flowsheet that was used in more recent test programs. Duplicate locked cycle tests were done on the 2008 Master Composite sample (KM2136) at three different primary grind sizes, namely 80% passing approximately 109 µm, 142 µm, and 173 µm.

Table 13-4: Bulk Flotation Locked Cycle Test Results

Samples	Primary Grind (P80, µm)	Regrind (P80, µm)	Head				Concentrate Grade Copper	Recovery – To Bulk Concentrate				
			Cu	Mo	Ag	Au	Cu	Cu	Mo	Ag	Au	Mass
			(%)	(%)	(g/t)	(g/t)	(%)	(%)	(%)	(%)	(%)	(%)*
Master Composite 1 (2012)†	155	20	0.42	0.026	3.5	0.27	31.7	89.0	63.9	50.5	72.6	5.4
Sample 1 (2012)	154	21	0.18	0.01	3.0	0.18	27.6	82.6	60.2	23.9	56.1	6.0
Sample 2 (2012)	143	23	0.17	0.009	1.0	0.09	26.2	78.5	33.8	18.9	31.9	6.7
Sample 3 (2012)	159	28	0.32	0.014	2.0	0.2	30.1	90.2	68.2	48.3	58.8	7.5
Sample 4 (2012)	150	26	0.38	0.024	2.0.	0.11	28.8	86.3	42.7	64.5	76.9	7.8
Sample 5 (2012)	142	23	0.79	0.035	5.0	0.5	32.4	92.0	54.4	61.8	76.0	12.7
Sample 6 (2012)	140	24	0.70	0.053	4.0	0.59	34.8	90.2	65.7	71.7	74.1	9.4
Composite 1 (2010)	180	23	0.37	0.012	3.0	0.33	30.1	86.5	75.6	57.0	79.0	10.5
Composite 2 (2010)	154	24	0.33	0.018	2.0	0.32	31.0	83.2	67.2	50.8	63.9	12.3
Composite 3 (2010)	153	23	0.45	0.03	3.0	0.51	34.1	85.6	83.0	60.7	77.6	10.6
Composite 4 (2010)	153	25	0.33	0.021	2.0	0.2	27.2	84.3	86.2	63.4	83.8	12.3
Composite 5 (2010)	144	27	0.27	0.018	2.0	0.17	28.3	81.2	74.8	62.8	82.2	10.7
Paramount Zone Composite (2008)	109	14	0.27	0.016	3.2	0.22	26.2	77.8	75.2	48.2	70.3	-
Liard Zone Composite (2008)	102	12	0.3	0.015	2.3	0.23	29.8	84.7	86.5	73.6	76.2	-
West Breccia Zone Composite (2008)	96	17	0.69	0.026	6.2	0.38	29.9	86.9	61.4	81.1	85.1	-
Master Composite 1 (2008)‡	141	20	0.33	0.013	2.3	0.25	31.7	87.4	76.2	56.5	69.8	10.3

table continues…

Samples	Primary Grind (P80, µm)	Regrind (P80, µm)	Head				Concentrate Grade Copper	Recovery – To Bulk Concentrate				
			Cu	Mo	Ag	Au	Cu	Cu	Mo	Ag	Au	Mass
			(%)	(%)	(g/t)	(g/t)	(%)	(%)	(%)	(%)	(%)	(%)*
Master Composite 1 (2008)	109	21	0.32	0.014	2.0	0.26	32.7	88.3	66.6	59.9	58.9	7.9
Master Composite 1 (2008)	109	19	0.33	0.012	2.0	0.25	31.4	89.5	75.7	59.7	75.2	12.2
Master Composite 1 (2008)	142	19	0.33	0.014	2.0	0.25	33.0	86.4	65.3	48.6	68.7	8.4
Master Composite 1 (2008)	142	21	0.33	0.014	2.0	0.29	31.6	87.0	90.2	69.6	72.4	13.2
Master Composite 1 (2008)	173	18	0.33	0.011	3.0	0.23	31.2	86.4	84.3	51.2	71.1	7.9
Master Composite 1 (2008)	173	21	0.34	0.013	2.0	0.25	30.6	85.4	90.5	59.1	73.3	12.1
Master (2007)	101	20	0.39	0.017	2.1	0.29	25.4	85.4	76.2	68.5	81.6	25.1
Liard Zone (2007)	109	20	0.39	0.009	2.44	0.37	25.4	87.9	87.9	67.0	84.2	12.4
Paramount Zone (2007)	101	25	0.45	0.033	2.6	0.28	26.5	93.7	88.4	52.6	74.5	25.9
West Breccia Zone (2007)	107	20	0.41	0.02	2.34	0.28	27	93.2	83.4	42.8	86.0	27.6
MLS (2006)	139	19	0.45	0.018	2.0	0.28	25.1	83.9	81.4	61.2	84.3	14.1
WBZ (2006)	142	Unknown	0.41	0.027	2.3	0.2	22.1	82.9	80.0	70.2	72.6	14.7
WLZ (2006)	168	15	0.36	0.017	1.7	0.31	34.2	70.0	59.9	63.0	71.9	5.4
LNZ (2006)	157	14	0.34	0.024	1.96	0.31	29.8	80.6	80.0	66.6	76.6	9.7
PIT Composite (2006)	133	16	0.39	0.022	2.2	0.25	26.4	86.7	81.3	60.2	80	18.6

*Rougher flotation
†Two locked cycle test results average
‡Six locked cycle test results average

The bulk flotation locked cycle test results showed that the mineral samples tested responded well to a simple, conventional process: bulk sulphide flotation followed by fine regrinding on the bulk rougher concentrate and three stages of cleaner flotation.

In general, the master composite samples from the Liard Zone showed similar metallurgical responses between the various testing programs. However, the samples from the Paramount Zone and the West Breccia Zone yielded different metallurgical performances. The metallurgical performance results obtained from PRA and G&T for the two zones were conversely different. The reasons for the difference in the metallurgical performance are not clear. However, the overall average test results for the Paramount Zone and West Breccia Zone samples are similar to the data obtained from the Liard mineralization. The 2012 program covered a significant portion of the Paramount Zone and included different grade classes, as well as lithologies and alterations, showed similar metallurgical performances as the Liard mineralization. Further test work is suggested for a better understanding of the metallurgical performances of the mineralization in the Paramount Zone and the West Breccia Zone.

Locked cycle testing in program KM2291 was based on composites intended to represent the first five years of production as envisioned in the LOM at the time. While not mineralogically discrete, these results provide high quality information for this spatial area.

At an average primary grind size of 80% passing 151 µm, G&T test work data shows that on average, 86.2% of the copper was recovered from the head sample containing approximately 0.37% Cu. The other associated metal recoveries were 73.3% for gold, 55.7% for silver, and 71.9% for molybdenum. The average sample feed grades were approximately 0.27 g/t Au, 2.7 g/t Ag, and 0.019% Mo. The concentrate produced contained 30.9% Cu. The average data from G&T and PRA show that at the primary grind size of 80% passing 146 µm, 86.7% of the copper reported to the copper concentrate at a grade of 29.9% Cu. The gold, silver, and molybdenum recoveries to the concentrate were 74.7%, 56.9%, and 73.7%, respectively. Apart from lower-grade concentrates produced by PRA, the test results from the two laboratories were very comparable.

The test results from the KM2136 testing program on the master composite sample show that a finer primary grind size may be beneficial for copper and silver recovery, but detrimental for gold and molybdenum. It is not clear why the gold recovery decreased with a finer primary grind.

The 2012 test program also conducted locked cycle tests to investigate the metallurgical responses of the composite sample and various individual samples mainly collected from the lower part of Paramount Zone. In general, the samples produced results similar to those from the previous test programs. However, Sample 1 and Sample 2 had poorer performances than the other four samples, likely due to their lower copper contents in the head samples.

In general, the average metallurgical performances from the variability tests agree with the locked cycle test results.

13.5.1.4 Pilot Plant Tests

During October and November 2008, G&T conducted a pilot plant test campaign using 8,000 drill core interval samples from the Liard Zone. The main objective of the campaign was to produce a bulk copper-molybdenum concentrate sample for copper-molybdenum separation tests and smelter evaluation. Twelve pilot plant campaigns were conducted, including two grind size calibration trials. The flowsheet used was based on the previous locked cycle tests and is shown in Figure 13-7. The reagents used were lime as pH regulator and potassium ethyl xanthate (PEX) and fuel oil as collectors. The pH ranged from 7.8 to 9.6 for rougher flotation and from 10.5 to 11.1 for cleaner flotation.

Figure 13-7: Pilot Plant Test Flowsheet, KM2292, 2008 (G&T)

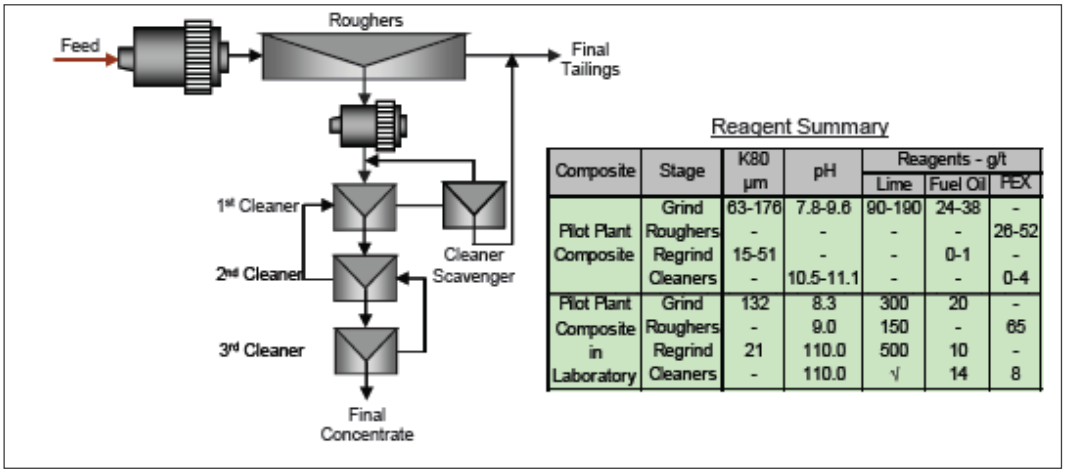

Reagent Summary

Composite	Stage	K80 µm	pH	Reagents - g/t		
				Lime	Fuel Oil	PEX
Pilot Plant Composite	Grind	63-176	7.8-9.6	90-190	24-38	-
	Roughers	-	-	-	-	26-52
	Regrind	15-51	-	-	0-1	-
	Cleaners	-	10.5-11.1	-	-	0-4
Pilot Plant Composite in Laboratory	Grind	132	8.3	300	20	-
	Roughers	-	9.0	150	-	65
	Regrind	21	110.0	500	10	-
	Cleaners	-	110.0	√	14	8

The test results from the pilot plant runs are shown in Table 13-5 and indicates that at a nominal primary grind size of 80% passing 160 µm, on average 78% of the copper was recovered into the bulk concentrate containing 27% Cu. 64% of the molybdenum was recovered to the concentrate. The metallurgical performance of the sample in the pilot plant tests was inferior to the results obtained from the locked cycle tests. G&T indicated that the inferior metallurgical performance was due to the elevated copper-oxide content in the sample. On average, the copper content of the sample was 0.32% and molybdenum grade was 0.016%. Approximately 11% of the total copper was present in non-sulphide form. It appears that the oxidation degree of the pilot plant test sample was higher than that of the sample used in the 2008 test program (KM2136) that contained approximately 7% of non-sulphide copper.

Table 13-5: Pilot Plant Test Results – Cu-Mo Bulk Concentrate – KM2292, 2008 G&T

Test Number	Sample ID	Primary Grind	Regrind	Feed Grade				Concentrate Grade	Recovery			
		P80,µm	P80, µm	% Cu	% Mo	g/t Ag	g/t Au	% Cu	% Cu	% Mo	% Ag	% Au
KM2292-7	Sample 1	146	21	0.39	0.025	2	0.30	26.0	80.9	80.0	57.3	80.0
	Sample 2	141	18	0.39	0.033	8	0.24	27.0	83.7	80.3	33.0	80.0
	Sample 3	130	20	0.35	0.019	4	0.25	27.9	80.7	73.4	28.6	76.1
KM2292-9	Sample 1	146	15	0.29	0.020	2	0.15	28.1	73.5	57.4	48.8	96.7
	Sample 2	137	16	0.36	0.026	2	0.19	29.1	73.6	57.0	54.9	97.3
	Sample 3	156	17	0.38	0.026	2	0.21	27.2	74.5	65.8	57.2	97.6
KM2292-10	Sample 1	189	24	0.32	0.013	2	0.25	28.0	75.5	62.8	51.9	68.4
	Sample 2	179	22	0.36	0.013	3	0.28	27.9	78.3	62.2	39.6	68.0
	Sample 3	191	24	0.31	0.012	3	0.24	29.5	77.0	65.7	36.0	70.8
KM2292-11	Sample 1	155	20	0.30	0.022	2	0.15	25.3	68.6	58.4	50.5	88.4
	Sample 2	172	17	0.38	0.026	2	0.21	28.8	80.4	64.6	57.8	85.9
	Sample 3	177	18	0.35	0.025	2	0.21	28.5	80.5	57.8	56.4	80.1
	Sample 4	184	19	0.32	0.022	2	0.20	29.2	75.8	48.3	50.4	66.9
	Sample 5	188	18	0.39	0.025	2	0.23	28.3	82.7	63.1	59.1	81.2
KM2292-12	Sample 1	176	22	0.31	0.020	3	0.21	27.6	75.4	68.2	33.4	85.9
	Sample 2	170	23	0.36	0.020	2	0.30	29.0	76.5	73.0	52.9	56.2
	Sample 3	174	18	0.36	0.021	3	0.26	27.9	81.7	69.7	37.9	70.9

A separate open batch test for the 2008 pilot plant tests produced a 30.7% Cu copper-molybdenum bulk concentrate. The copper and molybdenum reporting to the bulk cleaner concentrate were 81% and 55%, respectively. The two metals reported to the bulk rougher concentrate were 88.2% for copper and 80.0% for molybdenum. The data indicates that the 2008 pilot plant tests were not conducted at the optimum conditions developed from the bench scale tests.

In 2007, G&T conducted pilot plant campaigns on three composite samples generated from the Paramount, Liard, and West Breccia Zones. The composite samples were identified as PZ Composite, LZ Composite, and WZ Composite. The objective of the pilot plant tests was to generate sufficient bulk concentrates for copper-molybdenum separation tests. The pilot plant test results are summarized in Table 13-6. The primary grind size varied between 80% passing 82 µm and 119 µm, excluding the first run. The copper recoveries ranged from 62% for the PZ composite to 80% for the WZ composite. Molybdenum recoveries were higher than copper recoveries, ranging from 75% for the PZ composite to 85% for the WZ composite. Possibly due to difficulty maintaining control in small-scale pilot plant runs, the results produced were not as promising as those obtained from the locked cycle tests.

Table 13-6: Pilot Plant Test Results – Copper-Molybdenum Bulk Concentrate, KM2050 2007 G&T

Sample	Grade (%)		Recovery (%)		
	Cu	Mo	Mass	Cu	Mo
LZ Composite*	25.2	1.84	0.87	73	77
PZ Composite†	26.5	2.22	0.78	62	75
WZ Composite‡	28.0	1.06	1.8	80	85

*The data for LZ composite is average data from Run 4.
†The data for PZ composite is average data from Runs 5 and 7.
‡The data for WZ composite is average data from Run 8 (8:30 to 10:30) and Run 11 (8:30 to 11:00).

In the 2006 PRA test program, one pilot plant test was conducted on 1,600 kg of assay rejects and 2005 drill cores. The test was expected to generate copper-molybdenum bulk concentrate for molybdenum-copper separation tests. However, the molybdenum concentrates produced from the bulk concentrate contained elevated levels of carbon, which was identified as graphite. It was suspected that the tested sample was contaminated by foreign graphite. No detailed data were reported.

It is evident that pilot plant results are consistently lower than the locked cycle flotation test results. Factors contributing to the lower recoveries achieved in pilot plant runs include:

- The pilot plant objective was to create a product for further processing, not circuit optimization.
- There is no automatic control nor automated circuit monitoring, resulting in difficulty in achieving process stabilization.
- The pilot plant was run in dayshift batch cycles rather than continuous round the clock campaigns, resulting in shorter periods of stable and optimized performance.

Accordingly, it is believed that the pilot plant results do not properly reflect the achievable grades and recoveries for the project due to the above listed factors and the data was therefore not taken into consideration in the metallurgical performance projections.

13.5.2 Copper-Molybdenum Separation

Both PRA and G&T conducted copper and molybdenum separation tests using the samples generated from pilot plant campaigns. PRA conducted molybdenum and copper separation tests on the samples from the 2006 pilot plant test. Because the bulk concentrate produced from the pilot plant test was believed to have been contaminated by foreign graphite, no detailed test results were available for the review.

The 2008 mineralogical examination indicates that at the regrind size of 80% passing 20 µm, the sulphide minerals were very well liberated, although the liberation degree of molybdenite was lower than the copper minerals. Also, approximately 26% of the gangue minerals were associated with sulphide minerals, mainly with chalcopyrite and pyrite.

The bulk concentrate used for the 2010 molybdenum-copper separation from the KM2292 pilot plant campaign was coarse in particle size. The averaged particle size was 80% passing 54 µm. Compared to the 2008 test sample, the 2010 sample had a lower liberation degree. A mineralogical analysis of the concentrate was completed prior to the copper-molybdenum separation testing. The mineralogical composition and degree of mineral liberation are shown in Table 13-7. The molybdenum liberation constraints indicate that regrinding will be required to recover and upgrade molybdenum sufficiently as a final salable product.

Table 13-7: Liberation and Composition – Bulk Concentrate – KM2291, 2010 G&T

Item	Mineral Liberation or Composition (%)			
	Copper Sulphides	Molybdenite	Pyrite	Gangues
Liberated	84.5	75.4	71.8	47.2
Binary with				
Copper Sulphides	-	8.1	9.2	48.6
Molybdenite	0.1	-	0	1
Pyrite	0.2	0	-	1.9
Gangues	14.9	11.3	15.1	-
Multiphases	0.3	5.2	3.9	1.3

Prior to locked cycle testing, open circuit evaluation of reagent requirements, regrind sizing, and cleaner circuit configuration was completed.

The separation used sodium hydrosulphide to depress copper minerals under nitrogen atmosphere. Although other reagent schemes, such as Nokes (D-910) and sodium cyanide were used as ancillary reagents to selectively suppress copper minerals, they did not improve the separation.

The test results showed that the regrinding of molybdenum rougher flotation concentrate improved the separation efficiency. The 2010 tests show that the molybdenum concentrate grade improved from 38% to 47% Mo when the molybdenum rougher concentrate was reground from 80% passing 43 µm to approximately 30 µm.

Five copper-molybdenum separation locked cycle tests were performed on the bulk concentrates generated from the pilot plant tests. The separation tests results are presented in Table 13-8.

Table 13-8: Copper-Molybdenum Separation Test Results

Test ID	Product	Grade		Recovery		
		Cu	Mo	Cu	Mo	Wt
		(%)	(%)	(%)	(%)	(%)
KM2050/Test 31	Bulk Concentrate	26.6	1.45	100	100	100
	Molybdenum Concentrate	1.63	44.6	0.2	87.6	2.8
	Molybdenum Rougher Tailings	27.4	0.18	99.8	12.4	97.2
KM2050/Test 32	Bulk Concentrate	26.7	1.44	100	100	100
	Molybdenum Concentrate	1.16	50.0	0.1	67.9	2.0
	Molybdenum First Cleaner Tailings	22.7	2.62	10	21.3	11.7
	Molybdenum Rougher Tailings	27.8	0.18	90	10.8	86.3
KM2050/Test 33	Bulk Concentrate	26.6	1.5	100	100	100
	Molybdenum Concentrate	1.19	46.4	0.1	74.5	2.4
	Molybdenum First Cleaner Tailings	20.3	2.47	8.0	17.2	10.5
	Molybdenum Rougher Tailings	28.1	0.14	91.9	8.3	87.1
KM2291/Test 59	Bulk Concentrate	24.5	1.55	100	100	100
	Molybdenum Concentrate	3.48	44.7	0.3	69.8	2.4
	Molybdenum First Cleaner Tailings	25.8	3.52	9.7	20.9	9.2
	Molybdenum Rougher Tailings	24.9	0.16	90.0	9.2	88.4
KM2291/Test 61	Bulk Concentrate	24.9	1.36	100	100	100
	Molybdenum Concentrate	3.63	44.2	0.3	69.3	2.1
	Molybdenum First Cleaner Tailings	26.5	3.09	9.9	21.1	9.3
	Molybdenum Rougher Tailings	25.3	0.15	89.8	9.5	88.4

The molybdenum recovery to molybdenum concentrate ranged from 67% to 88%. On average, 73.1% of the molybdenum was recovered to the molybdenum concentrates. The molybdenum concentrate grades fluctuated from 44% to 50% molybdenum. Approximately 0.2% of the copper in the bulk concentrate was lost to the molybdenum concentrate. The locked cycle testing completed by the KM2291 program was completed at a molybdenum rougher concentrate regrind size of 80% passing coarser than 22 µm, which is expected to be too coarse for proper molybdenum and copper separation. This regrind target size discrepancy may have significantly contributed to issues in achieving molybdenum concentrate grade and reducing copper loss into the molybdenum concentrate (approximately 0.2% of the copper in the bulk copper-molybdenum concentrate was lost in the molybdenum concentrate). Further locked cycle testing is recommended for higher level studies to refine both the molybdenum separation process conditions and improve molybdenum concentrate grade.

13.5.3 Other Tests

A variety of auxiliary testing have been conducted over the life of the project. This information is informative, and the data are deemed appropriate for the level of study. Further tests should be conducted to update and verify the auxiliary testing information on appropriate samples during higher-level study work.

Thickening and filtration tests were completed on the concentrate and tailings samples generated from the early project history.

13.5.3.1 Thickening Test

In 2007, G&T conducted three thickening tests on copper concentrate (molybdenum flotation tailings) using a standard cylinder settling method. The tests used A130 as flocculant. The test results and the unit settling rates estimated by G&T are summarized in Table 13-9. At a 60% underflow density, a unit area requirement produced was between 0.24 m^2/d/t and 0.28 m^2/d/t depending on flocculant dosage.

Table 13-9: Settling Test Results, 2007 G&T

Test	Flocculant Dosage (g/t)	Unit Area (m^2/d/t)	Underflow Solids (%)
1	25.2	0.24	60
2	26.5	0.26	60
3	28.0	0.28	60

13.5.3.2 Filtration Test

The 2007 test program conducted a filtration test using a laboratory scale vacuum filter leaf. The test results are shown in Table 13-10. Only vacuum filtration testing was completed with an 18.2% final moisture achieved. Pressure filtration will be required to treat the concentrates.

Table 13-10: Filtration Test Results, 2007 G&T

Parameter	Unit	Value
Solid SG	-	3.94
Particle Size, 80% passing	µ	33
Filtration Rate	ml/sec	11
Vacuum	in Hg	60
Filtrate Clarity	-	Good
Final Cake Moisture	%	18.2

13.5.3.3 Copper and Gold Hydrometallurgical Extraction from Concentrates

In 2007, CESL conducted exploratory tests to investigate copper and gold hydrometallurgical extractions. The tests used the CESL proprietary leaching technology, including pressure oxidation of the copper concentrate followed by pressure cyanidation of the copper leach residue. Two-thirds cleaner bulk copper-molybdenum concentrates produced from the PRA test work, assaying 26.3% and 24.9% Cu, were used for the testing. The preliminary tests produced high copper extractions in the range of 96% to 98%, indicating that Schaft Creek copper concentrates were amenable to the CESL process. These copper extractions were achieved at 15 to 30 minutes of retention time as compared to a typical requirement of 60 minutes normally required for a chalcopyrite concentrate.

Pressure cyanidation tests extracted between 89% and 92% of the gold and between 81% and 88% of the silver from the copper leach residue. Sodium cyanide consumption was approximately 3 kg/t due to the high thiocyanate and other metal cyanate compounds formed.

13.5.3.4 Acid Base Accounting Tests

In 2004, PRA conducted acid base accounting tests on 16 selected drill core interval samples. The data are summarized as Table 13-11.

Table 13-11: ABA Test Results, 2004 PRA

Item	S(-2) (%)	Paste (pH)	AP	NP	NP/AP	(NP-AP)
Average	0.43	8.8	13.4	75.5	7.36	62.2
Range	0.1 to 0.9	7.5 to 9.3	3.4 to 28.6	53 to 114	3.0 to 16.9	45 to 91

Notes: AP = acid generation potential, expressed as kilograms of its CaCO3 equivalent per tonne of sample;
NP = neutralization potential

13.5.4 Concentrate Multi-Element Assay

Concentrate produced from locked cycle test programs was subjected to multi-element analysis to evaluate concentrate product quality. Concentrate quality impacts potential economic penalties specific to the contract terms negotiated with smelters. As no specific contracts for Schaft Creek concentrates have been negotiated, the evaluation of potential penalty elements is based on broad industry knowledge. However, fluorine levels in some of the bulk and copper concentrates are approaching these thresholds and may attract penalties.

Molybdenum concentrates produced during the KM2291 locked cycle test program failed to achieve concentrate grades and may attract penalties. However, it should be noted that these locked cycle tests did not achieve the projected target regrind. This regrind is likely to impact the achievable molybdenum grade and copper rejection. Based on the separation testing completed to date, the copper content of the molybdenum concentrate could be higher than the penalty thresholds outlined by most molybdenum smelters. To mitigate the penalty, the molybdenum concentrate should be leached by ferric chloride to reduce the copper level, which would increase molybdenum grade as well.

In the 2006 testing program, an 18.4% molybdenum concentrate generated from Test F75 by the 2006 PRA test program contained 181 ppm rhenium. Mineralogical examination of the concentrate indicated that rhenium occurred as discrete particles intimately associated with the molybdenite. Because the concentrate was diluted by the contaminated foreign graphite, the rhenium concentration in the 48% to 50% Mo concentrate is expected to be higher than 400 ppm. It is possible that the rhenium may be recoverable if the smelter chosen to treat the molybdenum is equipped with a rhenium recovery system.

The multi-element assay data on concentrates generated from the locked cycle tests are provided in Table 13-12.

Table 13-12: Concentrate Multi-element Assay

			KM2050		KM2291 – Bulk Cu-Mo Concentrate					KM3149 – Bulk Cu-Mo Concentrate
			Mo	Cu	Composite					Conc. Master
Element	Symbol	Units	Conc.	Conc.	1	2	3	4	5	Composite 1 [IV-Vi]
Aluminum	Al	%	0.50	1.25	1.24	1.70	0.93	1.27	1.63	0.88
Antimony	Sb	g/t	234	228	24	15	52	32	25	100
Arsenic	As	g/t	3.17	30.5	124	125	143	181	182	85
Barium	Ba	g/t	76	71	-	-	-	-	-	-
Bismuth	Bi	g/t	212	238	53	57	107	57	55	170
Cadmium	Cd	g/t	10	12	8	8	24	8	8	16

table continues…

Element	Symbol	Units	KM2050		KM2291 – Bulk Cu-Mo Concentrate					KM3149 – Bulk Cu-Mo Concentrate
			Mo	Cu	Composite					Conc. Master
			Conc.	Conc.	1	2	3	4	5	Composite 1 [IV-Vi]
Calcium	Ca	%	0.30	0.77	0.56	0.73	0.33	0.46	0.67	0.34
Carbon	C	%	2.12	0.18	-	-	-	-	-	0.15
Chromium	Cr	g/t	226	73	-	-	-	-	-	-
Cobalt	Co	g/t	110	140	56	72	88	96	88	98
Copper	Cu	%	1.27	28.2	32.1	28.6	34.8	30.5	30.3	31.3
Fluorine	F	g/t	-	-	102	145	96	116	130	110
Iron	Fe	%	4.02	28.7	23.2	18.5	24.5	23.7	23.0	25.6
Lead	Pb	%	0.06	0.04	0.02	0.02	0.1	0.01	0.01	0.03
Magnesium	Mg	%	0.15	0.26	0.51	0.89	0.36	0.47	0.59	0.46
Manganese	Mn	%	0.01	<0.01	0.01	0.02	0.01	0.01	0.01	0.004
Mercury	Hg	g/t	<1	<1	<1	<1	<1	<1	<1	<1
Molybdenum	Mo	%	49.6	0.7	0.99	1.37	2.37	2.2	1.91	1.29
Nickel	Ni	%	0.007	0.007	28	56	24	40	56	96
Phosphorus	P	g/t	<1	<1	90	126	70	103	106	73
Potassium	K	g/t	<1	<1	-	-	-	-	-	-
Selenium	Se	g/t	317	150	110	99	103	84	103	134
Silica	SiO2	%	2.76	7.42	3	5	2	3	4	2.12
Silver	Ag	g/t	181	147	131	137	199	131	176	131
Sulphur	S	%	36.7	29.4	26.6	24.7	27.2	26.2	25	32.8
Zinc	Zn	%	0.01	0.03	0.05	0.02	0.16	0.11	0.03	0.08

Note: Copper concentrate is in fact the molybdenum rougher tailings produced during the copper-molybdenum separation process.

13.6 Projected Metallurgical Performance

The metallurgical test work program completed between 2004 and 2015 have provided information on metallurgical performance on various samples collected from within the Liard, Paramount, and West Breccia Zones. This data and interpretation of the results is sufficient to inform a metallurgical performance for the Schaft Creek deposit.

The metallurgical performance projection is same as the previous study competed in 2013. On average, the metal recoveries are expected to be 86.6% for copper, 73.0% for gold, 58.8% for molybdenum, and 48.3% for silver.

To advance the metallurgical performance and variability of the Schaft Creek deposit, further metallurgical test work is recommended to optimize the previous test work results considering the geometallurgical domains identified in 2015 and the mineralogical variability across the Schaft Creek deposit.

14.0 MINERAL RESOURCE ESTIMATES

14.1 Introduction

In 2018, the Schaft Creek JV geologists developed the three dimensional (3D) electronic geological model for the Schaft Creek deposit using Leapfrog Geo software. In 2020, the QP imported the triangulated surfaces and wireframes to be used as mineral resource estimation domains into Leapfrog Geo 6.0.3 software. The domains and drillhole assay data were verified in Leapfrog Geo by the QP and independent estimates were made using Leapfrog Edge by the QP.

14.2 Geological Models

During 2017 and 2018, original paper cross sections were scanned and imported into Leapfrog by the Schaft Creek JV personnel and projected in 3D space to guide the initial placement of lithological and structural domains in the 3D geological model. Once sections were imported into Leapfrog, volumes from interval data and interpreted linework were interpolated by Leapfrog software and additional structural guides were added by Schaft Creek JV geologists to ensure volumes were geologically reasonable in orientation and magnitude.

Grade shell interpolants were created to domain mineralization within the host Stuhini Group volcanic and sedimentary rocks (grouped for simplicity as “Andesites” [AN]).

A major fault unit, the Basal Fault, was modelled as a mineralization hard boundary. A practical bottom limit to mineralization in the footwall of the Basal Fault was generated by creating a surface conforming to the general shape of the Basal Fault plane which was interpreted to lie 25 m below the end of drill hole traces. Other modelled faults are shown in Figure 14-1.

Figure 14-1: Schematic View Showing Modelled Structural Zones

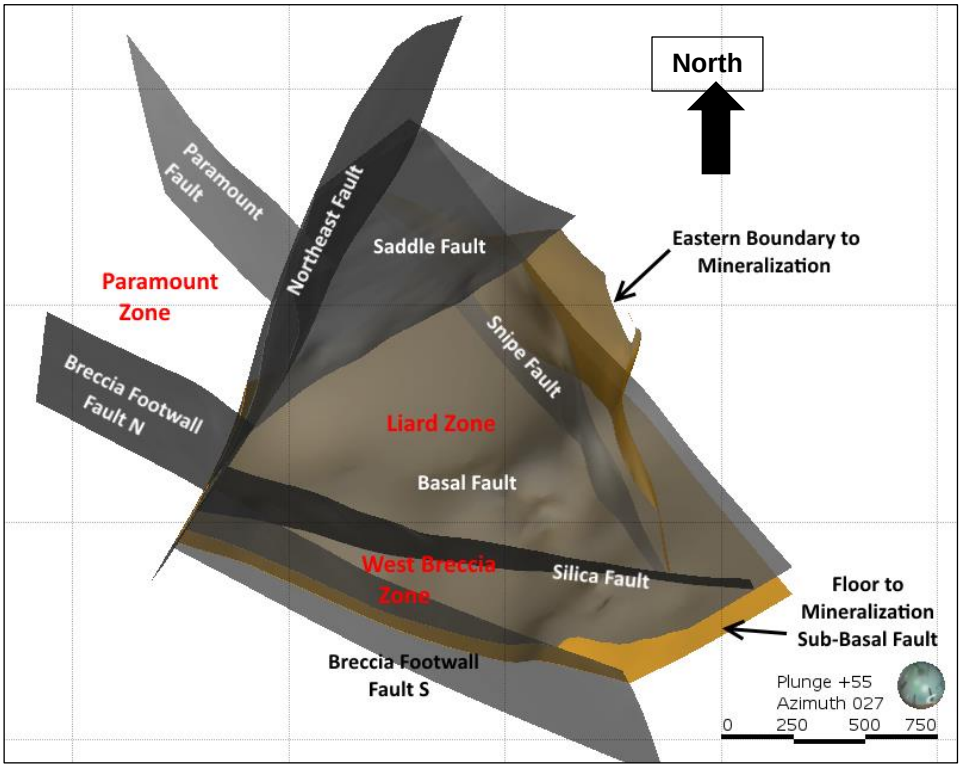

Source: Schaft Creek JV (2019)

In late 2020 the QP imported and validated the Leapfrog wireframes for lithological boundaries and fault blocks using Leapfrog Geo v6.0.3 software. The geological model meshes are the basis for the resource grade estimation domains.

The resource estimation domains are shown in Figure 14-2.

Figure 14-2: Perspective Diagram of Estimation Domains (Conceptual Pit Shown as 15 m contours)

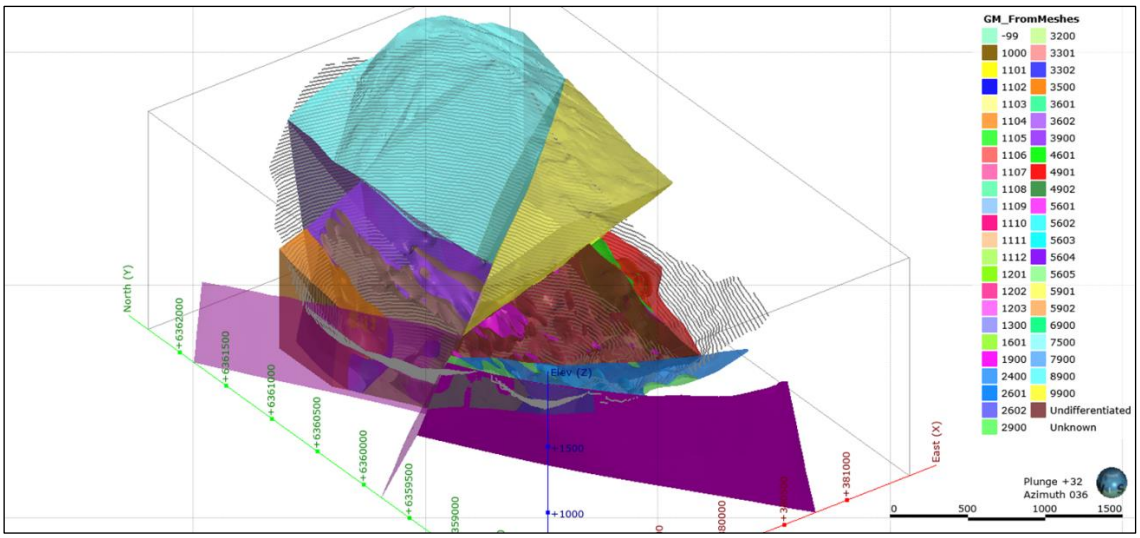

Source: Red Pennant (2021)

A block model was created by the QP and the wireframe surfaces were used to define estimation domains. The model has a parent block size of 20 x 20 x 15 m with 5 x 5 x 5 m sub-blocks.

Grade domains were defined in Leapfrog using the resource estimation domains. Copper, molybdenum, silver and gold were all estimated using the same domains.

The domains are identified by a four-digit code. The first two digits identify the structural block and the third digit represent lithology type. The fourth digit is used to identify individual blocks of similar lithology within the same structural block.

The domains are coded as shown in Table 14-1.

Table 14-1: Domain Coding

	Lithology	Syn Mineral porph	Paramount Breccia	Quartz Monzonite	West Breccia	Granodiorite	Mineralized Andesite	Andesite	Overburden
Structural Block		100	200	300	400	500	600	900	1000
Liard	1000	**1100**	**1200**	**1300**	1400	1500	**1600**	**1900**	**1000**
West Breccia	2000	2100	2200	2300	**2400**	2500	**2600**	**2900**	
Paramount	3000	3100	**3200**	**3300**	3400	**3500**	**3600**	**3900**	
Snipe Wedge	4000	4100	4200	4300	4400	4500	**4600**	**4900**	
Basal Fault Footwall	5000	5100	5200	5300	5400	5500	**5600**	**5900**	
South West of Breccia Footwall	6000	6100	6200	6300	6400	6500	6600	**6900**	
West Wedge Paramount	7000	7100	7200	7300	7400	**7500**	7600	**7900**	
East Wedge Paramount	8000	8100	8200	8300	8400	8500	8600	**8900**	
Saddle Wedge	9000	9100	9200	9300	9400	9500	9600	**9900**	

Notes:
estimation domains

combination
combination
combination

split

In some instances individual volumes have been combined to simplify estimation based on geological and statistical similarities.

Resource estimation domains are listed in Table 14-2.

Table 14-2: Resource Estimation Domains

1000	11_12_13_16	32_33_36	1900
2400	2601	2602	2900
3500	3900	4601	4901
5601	5602	5603	5604
5605	5901_5902	6900_7500	7900
8900	9900	1000	

In Table 14-1, the bolded codes indicate combinations of structural block and lithology that are valid domains for estimation. Three groups were estimated as combination (yellow) 1100, 1200, 1300 and 1600; (orange) 3200, 3300 and (blue) 3600; 6900 and 7500. Units 2660, 5600 and 5900 (green) are split into contiguous subunits for estimation.

14.3 Exploratory Data Analysis

Exploratory data analysis included review of histograms, scatter plots, sample statistics, and mean versus standard deviation plots. Results (see Table 14-3) included:

- Breccia domains have the highest average grades for all four metals of interest (Cu, Au, Mo, and Ag) and the highest variances along with the syn-mineralisation porphyry; mineralised porphyry domains have moderate average grades and moderate variances; granodiorite domains generally have low average grades and variances;
- Generally the correlation between copper and molybdenum is poor. The correlation with copper and gold is reasonable in all domains. The correlations between copper and silver vary by domain; good for the breccia, monzodiorite, and the waste andesite domains but poor for the mineralized andesite.

Table 14-3: Length-weighted Raw Sample Grade Statistics

Domain	Metal	Count	Length	Mean Grade	SD	CV	Variance	Minimum	Q1	Q2	Q3	Maximum
1000	Ag (g/t)	349	544.766	0.769	1.157	1.504	1.338	0.020	0.250	0.250	1.115	12.000
11_12_13_16	Ag (g/t)	15278	42951.59	1.274	2.105	1.653	4.430	0.000	0.600	1.086	1.512	208.100
32_33_36	Ag (g/t)	8515	19404.07	1.557	4.241	2.723	17.989	0.050	0.483	1.100	1.800	200.000
1900	Ag (g/t)	1122	2668.089	0.439	0.444	1.012	0.197	0.000	0.250	0.370	0.532	9.600
2400	Ag (g/t)	711	1996.902	2.146	2.593	1.209	6.725	0.050	0.900	1.371	2.632	40.000
2601	Ag (g/t)	721	1817.01	0.892	0.691	0.774	0.477	0.020	0.400	0.847	1.138	7.543
2602	Ag (g/t)	67	167.891	2.006	2.680	1.336	7.184	0.100	0.807	1.056	2.000	14.400
2900	Ag (g/t)	737	2054.875	0.411	0.250	0.607	0.062	0.040	0.250	0.302	0.552	2.329
3500	Ag (g/t)	443	1311.077	0.766	0.513	0.670	0.263	0.098	0.399	0.700	1.015	5.880
3900	Ag (g/t)	1095	2532.15	0.692	8.422	12.167	70.926	0.030	0.100	0.250	0.435	241.800
4601	Ag (g/t)	663	1873.085	0.835	0.423	0.507	0.179	0.100	0.546	0.831	1.095	3.000
4901	Ag (g/t)	444	1167.962	0.422	0.238	0.563	0.057	0.040	0.250	0.380	0.552	2.300
5601	Ag (g/t)	133	344.675	1.117	1.624	1.454	2.637	0.171	0.667	0.886	1.172	20.000
5602	Ag (g/t)	60	173.351	0.708	0.310	0.437	0.096	0.171	0.552	0.763	0.847	1.416
5603	Ag (g/t)	27	58.641	0.677	0.245	0.362	0.060	0.200	0.526	0.683	0.859	1.065
5604	Ag (g/t)	5	10.67	1.615	1.409	0.872	1.984	0.717	0.717	1.115	1.371	4.114
5605	Ag (g/t)	24	74.077	1.160	0.271	0.234	0.074	0.717	0.992	1.144	1.251	1.942
5901_5902	Ag (g/t)	1194	3054.849	0.354	0.416	1.175	0.173	0.000	0.200	0.250	0.452	5.143
6900_7500	Ag (g/t)	931	2598.507	0.448	1.466	3.275	2.150	0.010	0.250	0.250	0.435	40.900

table continues…

Domain	Metal	Count	Length	Mean Grade	SD	CV	Variance	Minimum	Q1	Q2	Q3	Maximum
7900	Ag (g/t)	468	1237.834	0.568	0.440	0.775	0.193	0.050	0.300	0.500	0.736	4.000
8900	Ag (g/t)	585	1270.012	0.568	5.268	9.270	27.755	0.030	0.050	0.100	0.250	100.000
9900	Ag (g/t)	651	1732.11	0.423	1.243	2.938	1.546	0.010	0.209	0.250	0.250	21.100
1000	Au (g/t)	349	544.766	0.094	0.150	1.592	0.023	0.003	0.017	0.040	0.113	1.025
11_12_13_16	Au (g/t)	15278	42951.59	0.202	0.273	1.355	0.075	0.002	0.079	0.147	0.249	19.304
32_33_36	Au (g/t)	8515	19404.07	0.170	0.325	1.918	0.106	0.002	0.028	0.079	0.211	10.834
1900	Au (g/t)	1122	2668.089	0.033	0.061	1.862	0.004	0.002	0.010	0.022	0.037	1.157
2400	Au (g/t)	711	1996.902	0.124	0.264	2.138	0.070	0.003	0.049	0.086	0.143	6.179
2601	Au (g/t)	721	1817.01	0.086	0.081	0.949	0.007	0.003	0.032	0.067	0.111	0.781
2602	Au (g/t)	67	167.891	0.138	0.149	1.083	0.022	0.005	0.069	0.105	0.172	1.020
2900	Au (g/t)	737	2054.875	0.027	0.027	1.029	0.001	0.003	0.008	0.017	0.038	0.417
3500	Au (g/t)	443	1311.077	0.069	0.096	1.395	0.009	0.003	0.017	0.042	0.075	1.354
3900	Au (g/t)	1095	2532.15	0.026	0.046	1.788	0.002	0.003	0.003	0.014	0.032	1.035
4601	Au (g/t)	663	1873.085	0.074	0.062	0.845	0.004	0.003	0.034	0.058	0.093	0.588
4901	Au (g/t)	444	1167.962	0.030	0.058	1.916	0.003	0.003	0.011	0.024	0.039	1.073
5601	Au (g/t)	133	344.675	0.102	0.083	0.816	0.007	0.003	0.055	0.088	0.127	0.794
5602	Au (g/t)	60	173.351	0.082	0.062	0.756	0.004	0.010	0.048	0.069	0.099	0.422
5603	Au (g/t)	27	58.641	0.072	0.088	1.214	0.008	0.009	0.019	0.048	0.065	0.394
5604	Au (g/t)	5	10.67	0.100	0.060	0.597	0.004	0.032	0.062	0.111	0.127	0.177

table continues…

Domain	Metal	Count	Length	Mean Grade	SD	CV	Variance	Minimum	Q1	Q2	Q3	Maximum
5605	Au (g/t)	24	74.077	0.139	0.055	0.397	0.003	0.062	0.105	0.132	0.153	0.311
5901_5902	Au (g/t)	1194	3054.849	0.024	0.045	1.893	0.002	0.002	0.006	0.012	0.028	0.583
6900_7500	Au (g/t)	931	2598.507	0.028	0.097	3.504	0.009	0.001	0.003	0.008	0.024	1.829
7900	Au (g/t)	468	1237.834	0.036	0.075	2.105	0.006	0.003	0.015	0.028	0.045	3.177
8900	Au (g/t)	585	1270.012	0.008	0.028	3.453	0.001	0.003	0.003	0.003	0.007	0.656
9900	Au (g/t)	651	1732.11	0.013	0.023	1.807	0.001	0.002	0.003	0.007	0.013	0.214
1000	Cu (%)	349	544.766	0.139	0.158	1.135	0.025	0.001	0.024	0.082	0.214	0.945
11_12_13_16	Cu (%)	15278	42951.59	0.290	0.202	0.695	0.041	0.001	0.153	0.250	0.376	3.472
32_33_36	Cu (%)	8515	19404.07	0.284	0.245	0.863	0.060	0.001	0.118	0.233	0.388	3.628
1900	Cu (%)	1122	2668.089	0.039	0.067	1.710	0.004	0.001	0.010	0.023	0.043	2.828
2400	Cu (%)	711	1996.902	0.365	0.457	1.252	0.209	0.007	0.140	0.230	0.390	4.503
2601	Cu (%)	721	1817.01	0.211	0.164	0.776	0.027	0.001	0.104	0.170	0.280	2.091
2602	Cu (%)	67	167.891	0.321	0.279	0.870	0.078	0.050	0.120	0.184	0.456	1.200
2900	Cu (%)	737	2054.875	0.040	0.049	1.226	0.002	0.001	0.010	0.029	0.050	0.870
3500	Cu (%)	443	1311.077	0.106	0.112	1.059	0.013	0.001	0.022	0.072	0.160	0.820
3900	Cu (%)	1095	2532.15	0.040	0.066	1.661	0.004	0.001	0.006	0.019	0.049	0.870
4601	Cu (%)	663	1873.085	0.165	0.121	0.734	0.015	0.004	0.080	0.139	0.216	1.260
4901	Cu (%)	444	1167.962	0.035	0.039	1.119	0.002	0.001	0.010	0.026	0.046	0.410
5601	Cu (%)	133	344.675	0.168	0.212	1.262	0.045	0.005	0.060	0.110	0.201	2.158

table continues…

Domain	Metal	Count	Length	Mean Grade	SD	CV	Variance	Minimum	Q1	Q2	Q3	Maximum
5602	Cu (%)	60	173.351	0.136	0.117	0.860	0.014	0.026	0.060	0.090	0.170	0.590
5603	Cu (%)	27	58.641	0.093	0.039	0.424	0.002	0.036	0.061	0.087	0.116	0.168
5604	Cu (%)	5	10.67	0.145	0.096	0.662	0.009	0.060	0.070	0.150	0.180	0.280
5605	Cu (%)	24	74.077	0.208	0.115	0.550	0.013	0.070	0.140	0.190	0.230	0.590
5901_5902	Cu (%)	1194	3054.849	0.031	0.061	1.983	0.004	0.001	0.005	0.010	0.031	0.933
6900_7500	Cu (%)	931	2598.507	0.050	0.117	2.350	0.014	0.000	0.003	0.011	0.046	2.117
7900	Cu (%)	468	1237.834	0.069	0.089	1.287	0.008	0.001	0.019	0.039	0.082	0.601
8900	Cu (%)	585	1270.012	0.017	0.069	4.007	0.005	0.001	0.002	0.005	0.010	1.909
9900	Cu (%)	651	1732.11	0.018	0.048	2.650	0.002	0.001	0.003	0.006	0.013	0.643
1000	Mo (%)	349	544.766	0.0055	0.0128	2.3388	0.0002	0.0001	0.0005	0.0015	0.0072	0.1653
11_12_13_16	Mo (%)	15264	42908.3	0.0159	0.0265	1.6674	0.0007	0.0002	0.0040	0.0090	0.0186	2.8720
32_33_36	Mo (%)	8515	19404.07	0.0219	0.0308	1.4050	0.0009	0.0003	0.0040	0.0122	0.0290	0.5875
1900	Mo (%)	1122	2668.089	0.0032	0.0097	3.0553	0.0001	0.0003	0.0003	0.0006	0.0020	0.1679
2400	Mo (%)	709	1992.642	0.0191	0.0316	1.6487	0.0010	0.0003	0.0042	0.0102	0.0228	0.3477
2601	Mo (%)	713	1796.848	0.0092	0.0170	1.8391	0.0003	0.0003	0.0012	0.0040	0.0114	0.3110
2602	Mo (%)	67	167.891	0.0075	0.0085	1.1282	0.0001	0.0003	0.0018	0.0048	0.0114	0.0468
2900	Mo (%)	731	2042.947	0.0019	0.0037	1.9580	0.0000	0.0001	0.0003	0.0005	0.0012	0.0288
3500	Mo (%)	443	1311.077	0.0070	0.0134	1.9020	0.0002	0.0003	0.0012	0.0024	0.0072	0.1150
3900	Mo (%)	1095	2532.15	0.0018	0.0061	3.3730	0.0000	0.0003	0.0005	0.0005	0.0010	0.1260

table continues…

Domain	Metal	Count	Length	Mean Grade	SD	CV	Variance	Minimum	Q1	Q2	Q3	Maximum
4601	Mo (%)	663	1873.085	0.0050	0.0111	2.2092	0.0001	0.0003	0.0006	0.0018	0.0050	0.1481
4901	Mo (%)	441	1160.073	0.0015	0.0028	1.8620	0.0000	0.0001	0.0003	0.0003	0.0012	0.0120
5601	Mo (%)	133	344.675	0.0070	0.0155	2.2263	0.0002	0.0003	0.0003	0.0012	0.0048	0.0923
5602	Mo (%)	60	173.351	0.0098	0.0057	0.5843	0.0000	0.0003	0.0056	0.0120	0.0120	0.0233
5603	Mo (%)	27	58.641	0.0050	0.0055	1.1031	0.0000	0.0003	0.0012	0.0040	0.0070	0.0240
5604	Mo (%)	5	10.67	0.0294	0.0254	0.8668	0.0006	0.0018	0.0018	0.0288	0.0378	0.0659
5605	Mo (%)	24	74.077	0.0023	0.0033	1.4142	0.0000	0.0003	0.0003	0.0012	0.0024	0.0144
5901_5902	Mo (%)	1157	2944.868	0.0023	0.0074	3.2198	0.0001	0.0001	0.0003	0.0005	0.0012	0.1570
6900_7500	Mo (%)	925	2582.193	0.0017	0.0031	1.8370	0.0000	0.0002	0.0005	0.0005	0.0012	0.0240
7900	Mo (%)	468	1237.834	0.0022	0.0040	1.8075	0.0000	0.0003	0.0003	0.0005	0.0018	0.0324
8900	Mo (%)	585	1270.012	0.0009	0.0033	3.6713	0.0000	0.0005	0.0005	0.0005	0.0005	0.0650
9900	Mo (%)	651	1732.11	0.0011	0.0033	2.9448	0.0000	0.0003	0.0005	0.0005	0.0008	0.0570

The composited grades for the 6 m length composites are summarized by estimation domain in Table 14-4.

Table 14-4: Composite Statistics (6 metre lengths)

Domain	Metal	Composites	Length	Mean Grade	SD	CV	Variance	Minimum	Q1	Q2	Q3	Maximum
1000	Ag (g/t)	86	523.4	0.79	0.95	1.19	0.90	0.050	0.250	0.414	1.139	6.273
11_12_13_16	Ag (g/t)	7150	42952.6	1.27	1.44	1.13	2.07	0.050	0.691	1.116	1.520	82.494
1900	Ag (g/t)	429	2542.3	0.44	0.30	0.69	0.09	0.050	0.250	0.388	0.524	3.266
2400	Ag (g/t)	335	1996.5	2.14	2.07	0.97	4.30	0.250	0.989	1.481	2.603	18.158
2601	Ag (g/t)	300	1805.6	0.89	0.56	0.62	0.31	0.070	0.522	0.895	1.110	5.143
2602	Ag (g/t)	128	383.3	2.24	1.94	0.87	3.76	0.250	1.007	1.872	2.529	12.393
2900	Ag (g/t)	343	2035.1	0.41	0.22	0.53	0.05	0.100	0.250	0.341	0.568	1.432
32_33_36	Ag (g/t)	3237	19435.8	1.56	2.62	1.68	6.87	0.050	0.589	1.179	1.827	68.956
3500	Ag (g/t)	218	1311.4	0.77	0.43	0.56	0.18	0.098	0.438	0.707	1.012	3.451
3900	Ag (g/t)	424	2521.9	0.69	6.02	8.68	36.23	0.050	0.133	0.250	0.484	123.097
4601	Ag (g/t)	313	1875.6	0.84	0.38	0.46	0.14	0.171	0.621	0.857	1.077	2.064
4901	Ag (g/t)	197	1169.7	0.42	0.20	0.47	0.04	0.113	0.250	0.417	0.549	1.136
5601	Ag (g/t)	105	621.7	0.86	0.94	1.09	0.88	0.050	0.487	0.714	0.959	8.675
5602	Ag (g/t)	45	268.7	0.65	0.27	0.41	0.07	0.171	0.457	0.702	0.864	1.255
5603	Ag (g/t)	21	125.3	0.74	0.28	0.37	0.08	0.238	0.547	0.720	0.942	1.236
5604	Ag (g/t)	12	71.5	1.74	1.51	0.87	2.28	0.402	0.871	1.085	3.750	4.866
5605	Ag (g/t)	16	96.3	1.00	0.37	0.37	0.14	0.250	0.722	1.014	1.226	1.774

table continues…

Domain	Metal	Composites	Length	Mean Grade	SD	CV	Variance	Minimum	Q1	Q2	Q3	Maximum
5901_5902	Ag (g/t)	504	3042.4	0.35	0.37	1.03	0.13	0.000	0.209	0.285	0.437	4.904
6900_7500	Ag (g/t)	427	2569.2	0.45	1.00	2.22	1.01	0.050	0.235	0.250	0.495	18.543
7900	Ag (g/t)	207	1241.0	0.57	0.37	0.65	0.14	0.050	0.327	0.526	0.710	2.663
8900	Ag (g/t)	310	1863.0	0.43	2.20	5.15	4.85	0.050	0.051	0.095	0.190	28.604
9900	Ag (g/t)	328	1972.7	0.41	0.75	1.83	0.56	0.050	0.206	0.250	0.324	9.240
1000	Au (g/t)	86	523.4	0.09	0.14	1.49	0.02	0.003	0.017	0.047	0.102	0.947
11_12_13_16	Au (g/t)	7150	42952.6	0.20	0.22	1.07	0.05	0.002	0.090	0.155	0.253	9.897
1900	Au (g/t)	429	2542.3	0.03	0.04	1.25	0.00	0.002	0.012	0.024	0.038	0.375
2400	Au (g/t)	335	1996.5	0.12	0.16	1.27	0.02	0.008	0.057	0.092	0.145	2.018
2601	Au (g/t)	300	1805.6	0.09	0.06	0.74	0.00	0.005	0.039	0.073	0.117	0.396
2602	Au (g/t)	128	383.3	0.16	0.16	1.01	0.03	0.012	0.072	0.107	0.167	0.946
2900	Au (g/t)	343	2035.1	0.03	0.02	0.82	0.00	0.002	0.010	0.021	0.040	0.160
32_33_36	Au (g/t)	3237	19435.8	0.17	0.25	1.46	0.06	0.003	0.036	0.091	0.222	5.584
3500	Au (g/t)	218	1311.4	0.07	0.08	1.11	0.01	0.003	0.023	0.044	0.083	0.740
3900	Au (g/t)	424	2521.9	0.03	0.04	1.37	0.00	0.002	0.006	0.015	0.033	0.327
4601	Au (g/t)	313	1875.6	0.07	0.05	0.70	0.00	0.007	0.039	0.058	0.093	0.364
4901	Au (g/t)	197	1169.7	0.03	0.04	1.24	0.00	0.003	0.013	0.026	0.040	0.470
5601	Au (g/t)	105	621.7	0.08	0.06	0.76	0.00	0.008	0.037	0.062	0.100	0.351
5602	Au (g/t)	45	268.7	0.07	0.05	0.71	0.00	0.010	0.034	0.061	0.091	0.228
5603	Au (g/t)	21	125.3	0.07	0.05	0.73	0.00	0.012	0.034	0.056	0.112	0.213

table continues…

Domain	Metal	Composites	Length	Mean Grade	SD	CV	Variance	Minimum	Q1	Q2	Q3	Maximum
5604	Au (g/t)	12	71.5	0.08	0.04	0.56	0.00	0.016	0.025	0.086	0.122	0.144
5605	Au (g/t)	16	96.3	0.12	0.06	0.54	0.00	0.011	0.065	0.109	0.148	0.271
5901_5902	Au (g/t)	504	3042.4	0.02	0.04	1.54	0.00	0.002	0.007	0.014	0.029	0.434
6900_7500	Au (g/t)	427	2569.2	0.03	0.08	2.77	0.01	0.001	0.003	0.009	0.028	1.181
7900	Au (g/t)	207	1241.0	0.04	0.04	1.23	0.00	0.003	0.019	0.031	0.045	0.694
8900	Au (g/t)	310	1863.0	0.01	0.02	2.06	0.00	0.003	0.003	0.003	0.007	0.220
9900	Au (g/t)	328	1972.7	0.01	0.02	1.66	0.00	0.002	0.003	0.007	0.014	0.201
1000	Cu (%)	86	523.4	0.14	0.15	1.11	0.02	0.000	0.030	0.092	0.216	0.722
11_12_13_16	Cu (%)	7150	42952.6	0.29	0.18	0.61	0.03	0.001	0.167	0.260	0.374	1.560
1900	Cu (%)	429	2542.3	0.04	0.05	1.36	0.00	0.001	0.014	0.026	0.042	0.538
2400	Cu (%)	335	1996.5	0.37	0.40	1.11	0.16	0.018	0.155	0.239	0.404	3.824
2601	Cu (%)	300	1805.6	0.21	0.13	0.61	0.02	0.040	0.116	0.180	0.272	0.836
2602	Cu (%)	128	383.3	0.48	0.43	0.90	0.19	0.037	0.190	0.370	0.632	2.912
2900	Cu (%)	343	2035.1	0.04	0.04	0.98	0.00	0.001	0.014	0.032	0.054	0.310
32_33_36	Cu (%)	3237	19435.8	0.28	0.21	0.73	0.04	0.001	0.139	0.245	0.381	2.538
3500	Cu (%)	218	1311.4	0.11	0.09	0.90	0.01	0.001	0.028	0.080	0.158	0.432
3900	Cu (%)	424	2521.9	0.04	0.05	1.35	0.00	0.001	0.007	0.023	0.052	0.378
4601	Cu (%)	313	1875.6	0.17	0.10	0.60	0.01	0.011	0.098	0.142	0.215	0.771
4901	Cu (%)	197	1169.7	0.04	0.03	0.85	0.00	0.001	0.013	0.029	0.047	0.184

table continues…

Domain	Metal	Composites	Length	Mean Grade	SD	CV	Variance	Minimum	Q1	Q2	Q3	Maximum
5601	Cu (%)	105	621.7	0.13	0.14	1.14	0.02	0.005	0.043	0.093	0.150	1.090
5602	Cu (%)	45	268.7	0.13	0.13	1.00	0.02	0.015	0.054	0.090	0.140	0.658
5603	Cu (%)	21	125.3	0.12	0.07	0.56	0.00	0.025	0.077	0.110	0.152	0.246
5604	Cu (%)	12	71.5	0.11	0.07	0.59	0.00	0.022	0.048	0.108	0.170	0.216
5605	Cu (%)	16	96.3	0.17	0.12	0.69	0.01	0.008	0.076	0.147	0.221	0.495
5901_5902	Cu (%)	504	3042.4	0.03	0.05	1.54	0.00	0.000	0.007	0.018	0.036	0.503
6900_7500	Cu (%)	427	2569.2	0.05	0.09	1.78	0.01	0.000	0.005	0.017	0.058	0.838
7900	Cu (%)	207	1241.0	0.07	0.07	1.03	0.00	0.001	0.026	0.045	0.084	0.376
8900	Cu (%)	310	1863.0	0.01	0.04	2.59	0.00	0.000	0.004	0.007	0.012	0.378
9900	Cu (%)	328	1972.7	0.02	0.05	2.19	0.00	0.001	0.004	0.007	0.015	0.334
1000	Mo (%)	86	523.4	0.01	0.01	2.02	0.00	0.0001	0.0005	0.0015	0.0071	0.0897
11_12_13_16	Mo (%)	7142	42902.2	0.0159	0.0199	1.2513	0.0004	0.0003	0.0051	0.0105	0.0196	0.3186
1900	Mo (%)	429	2542.3	0.0032	0.0075	2.3401	0.0001	0.0003	0.0005	0.0009	0.0028	0.0801
2400	Mo (%)	334	1991.5	0.0191	0.0282	1.4800	0.0008	0.0004	0.0056	0.0111	0.0230	0.3106
2601	Mo (%)	297	1785.4	0.0093	0.0133	1.4371	0.0002	0.0003	0.0013	0.0044	0.0119	0.0997
2602	Mo (%)	128	383.3	0.0135	0.0190	1.4012	0.0004	0.0005	0.0029	0.0061	0.0180	0.1133
2900	Mo (%)	342	2028.8	0.0019	0.0035	1.8894	0.0000	0.0002	0.0003	0.0005	0.0012	0.0233
32_33_36	Mo (%)	3237	19435.8	0.0219	0.0236	1.0797	0.0006	0.0003	0.0057	0.0146	0.0302	0.2460
3500	Mo (%)	218	1311.4	0.0070	0.0105	1.5029	0.0001	0.0003	0.0012	0.0029	0.0089	0.0697

table continues…

Domain	Metal	Composites	Length	Mean Grade	SD	CV	Variance	Minimum	Q1	Q2	Q3	Maximum
3900	Mo (%)	424	2521.9	0.0018	0.0041	2.2742	0.0000	0.0003	0.0005	0.0005	0.0012	0.0525
4601	Mo (%)	313	1875.6	0.0050	0.0084	1.6814	0.0001	0.0003	0.0011	0.0023	0.0053	0.0782
4901	Mo (%)	196	1163.4	0.0015	0.0028	1.8476	0.0000	0.0003	0.0003	0.0005	0.0009	0.0120
5601	Mo (%)	105	621.7	0.0047	0.0096	2.0626	0.0001	0.0003	0.0005	0.0009	0.0030	0.0530
5602	Mo (%)	45	268.7	0.0080	0.0055	0.6852	0.0000	0.0003	0.0008	0.0103	0.0120	0.0177
5603	Mo (%)	21	125.3	0.0064	0.0039	0.6136	0.0000	0.0003	0.0040	0.0060	0.0089	0.0165
5604	Mo (%)	12	71.5	0.0202	0.0160	0.7953	0.0003	0.0035	0.0068	0.0087	0.0367	0.0476
5605	Mo (%)	16	96.3	0.0020	0.0022	1.1174	0.0000	0.0003	0.0007	0.0008	0.0026	0.0077
5901_5902	Mo (%)	486	2932.8	0.0023	0.0056	2.4233	0.0000	0.0001	0.0003	0.0005	0.0011	0.0549
6900_7500	Mo (%)	424	2549.0	0.0017	0.0029	1.7061	0.0000	0.0003	0.0005	0.0005	0.0013	0.0198
7900	Mo (%)	207	1241.0	0.0022	0.0033	1.4687	0.0000	0.0003	0.0005	0.0009	0.0024	0.0238
8900	Mo (%)	310	1863.0	0.0008	0.0020	2.5394	0.0000	0.0005	0.0005	0.0005	0.0005	0.0222
9900	Mo (%)	328	1972.7	0.0014	0.0034	2.5328	0.0000	0.0003	0.0005	0.0005	0.0009	0.0384

14.3.1 Gold and Silver Values Calculated by Regression

The dataset (a total of 37,616 samples) contains samples with missing values for silver and gold. This is due to some samples not being assayed for these elements (silver and gold) and also because some poor-quality assay values were removed from the dataset. In 2018, 13,009 silver and 8,180 gold samples were replaced with a value calculated from copper-related regressions based on the more recent and reliable silver and gold assays.

All three variables (silver, gold, and copper) display a lognormal distribution. Natural logs were calculated for each variable and used in the estimation. The correlation coefficient shows the relationship between variables, where 0 is no relationship and 1 is a direct relationship. The correlation coefficients for the 6 m composite log data for all domains combined is displayed in Table 14-5, and the relationship is shown with scatter plots in Figure 14-3.

The natural log of the grades for the variables were plotted and a regression line was fitted to the data. The R-squared values gives an indication of the variance of the data from the regression line (the success of the fit).

Figure 14-3: Scatter Plots for Log Transformed Gold and Silver by Copper

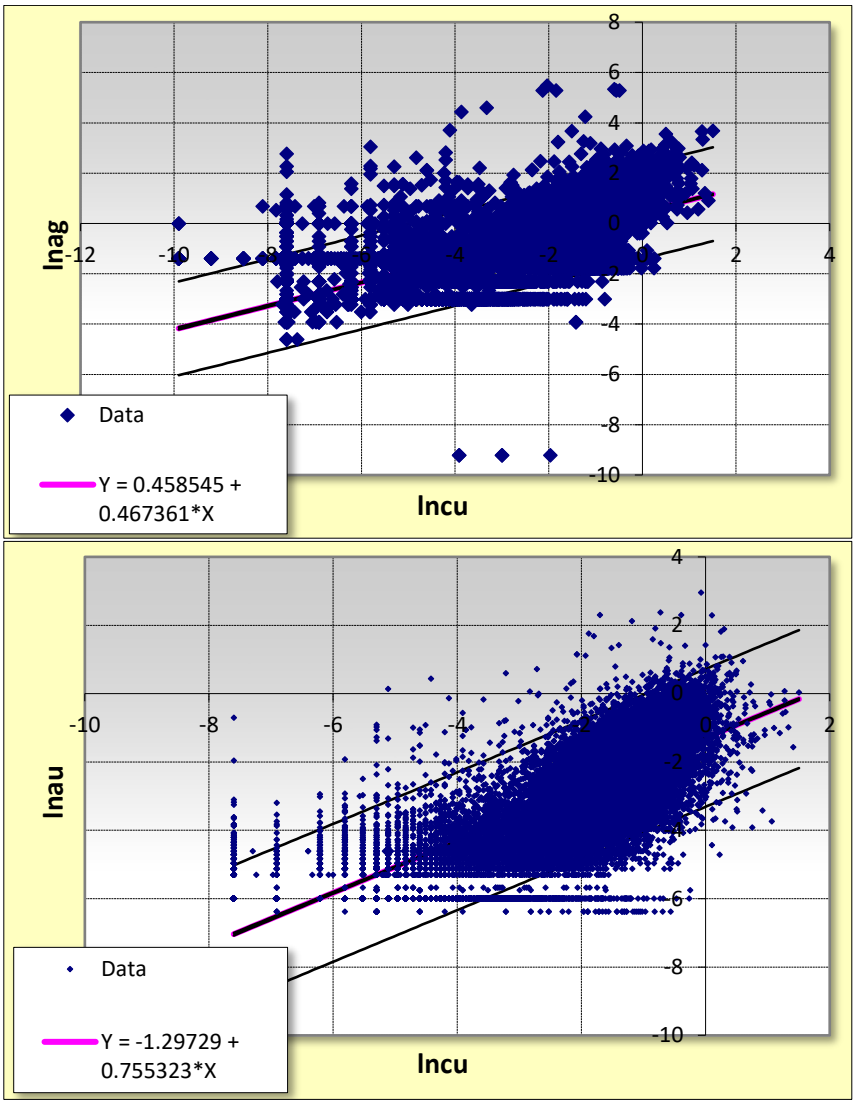

Source: Schaft Creek JV (2018)

The equation of the line gives a prediction of the LnAg or LnAu in relation to LnCu in the format of Y = A + B*X. A value was assigned for each missing LnAg and LnAu value using the following formulas:

$$\text{LnAg} = 0.458545031 + 0.647360968 * \text{LnCu}$$

$$\text{LnAu} = \text{-}1.297289347 + 0.755323121 * \text{LnCu}$$

In order to calculate the silver and gold values from the natural log prediction, the predicted LnAg and LnAu values are back-transformed by taking the antilog with a minor correction to account for the difference between the geometric and arithmetic mean. The mean of the back-transformed data is calculated from the variance of the LnAg and LnAu and the R-squared.

To calculate any value of silver or gold is the same as calculating the mean value using:

$$m = e^{\alpha + \beta 2/2}$$

Where

$$\beta^2 = \sigma^2.(1 - R^2)$$

The back calculated predicted silver and gold values are summarised in Table 14-5.

Table 14-5: Summary of Statistics for the Prediction of Gold and Silver from Regression with Copper

	Ag	Au
Correlation with LnCu	0.714	0.815
R-squared	0.509769	0.664
Variance (σ^2)	1.844	3.145
$\beta^2 = (\sigma^2.(1 - R^2))$	0.903985	1.05672
m = ($e^{\alpha + \beta 2/2}$)	Exp (LnCu+0.45199)	Exp (LnCu+0.52836)

The resulting data has the following median and mean values (Table 14-6).

Table 14-6: Summary of Statistics of Gold and Silver Calculated by Regression

	Original Data			Grade Calculated from Regression		
	Number	Median	Mean	Number	Median	Mean
Cu%	38494	0.150	0.205	0	-	-
Mo %	38368	0.005	0.012	0	-	-
Ag g/t	24607	0.040	1.119	13009	0.965	0.977
Au g/t	29436	0.064	0.143	8180	0.052	0.079

The QP considers that this is a reasonable approach to reduce the risk posed by potentially inaccurate historic assay data

14.4 Domain Estimation Boundaries

Grade estimates in domains were either estimated as discrete (“hard” boundary estimation) units with no data used outside the domains, or as gradational (“soft” boundary) units with limited data used adjacent to and outside the domain. Contact analysis and structural context was used to determine which domains could be combined for resource estimation and where hard or soft boundaries should be used.

14.5 Density Assignment

Bulk density was applied to the model by assigning the average value of 2.69 g/cm^3 for all domains except overburden (domain 1000), which has an assigned grade of 2.0 g/cm^3.

14.6 Grade Capping/Outlier Restrictions

Top cuts were applied where necessary. The application of a grade cap and threshold value were determined by analysis of histograms, log histograms and mean variance plots for each domain. Capping values are shown in the statistical summary tables for composites.

The data are mostly sampled at 3 m or 2 m intervals, with smaller intervals being used around geological boundaries and some larger samples being taken. The data were composited to 6 m intervals, broken at geological boundaries.

Samples remaining at the base of the domain of <6 m were treated as residuals. Residuals <3 m were merged with the composite sample above. The QP regards the compositing strategy as reasonable to provide equivalent volumetric support for estimation.

14.7 Variography

Variogram modelling was undertaken using Leapfrog EDGE. Variograms were modelled for copper, molybdenum, silver and gold using normal scores transformed data to reduce the masking effects of extreme values.

Traditional variograms with spherical models were used to model the data in all cases. In all cases, nugget values were estimated using the downhole variogram, with 6 m lag spacing to match the composite length. Lag spacing for the directional variograms was generally set to multiples of the 6 m composite length and the angular tolerance was adjusted where necessary to develop experimental variograms.

The direction of continuity varies by domain. Variograms were modelled with a nugget and either one or two spherical structures. The variograms are robust for the major domains.

A local orientation model (see Figure 14-4) for variography and search was developed using Leapfrog Geo and Leapfrog EDGE from the orientations of the copper variogram models. The orientations of the variogram models were used to build smoothed and nested form interpolants using leapfrog Geo. The orientations of form interpolants were projected to each block in the block model and used to orientate the search and variogram ellipsoids during for weighting composite grades during inverse distance and kriging estimation.

The variogram model parameters used for Kriging estimates are summarized in Table 14-7.

Table 14-7: Variogram Parameters

General	Direction							Structure 1							Structure 2						
Variogram Name	Dip	Dip Azimuth	Pitch	Model Space	Variance	Nugget	Normalised Nugget	Sill	Normalised Sill	Structure	Alpha	Major	Semi-major	Minor	Sill	Normalised Sill	Structure	Alpha	Major	Semi-major	Minor
ag2_gt 1000: Model	27.7	249.8	65.2	data	0.878	0.689	0.784	0.189	0.215	Spherical		82.7	49.2	25.5							
ag2_gt 1000: Model	27.7	249.8	65.2	normal score	0.997	0.690		0.308		Spherical		82.7	49.2	25.5							
ag2_gt 11_12_13_16: Model	26.0	262.0	107.8	data	2.069	0.443	0.214	0.997	0.482	Spherical		25.7	32.8	39.4	0.625	0.302	Spherical		139.3	160.5	162.9
ag2_gt 11_12_13_16: Model	26.0	262.0	107.8	normal score	1.000	0.146		0.419		Spherical		25.7	32.8	39.4	0.431		Spherical		139.3	160.5	162.9
ag2_gt 1900: Model	17.0	288.9	138.0	data	0.082	0.042	0.508	0.017	0.205	Spherical		56.2	39.2	24.6	0.023	0.285	Spherical		222.4	242.4	63.2
ag2_gt 1900: Model	17.0	288.9	138.0	normal score	0.999	0.392		0.188		Spherical		56.2	39.2	24.6	0.417		Spherical		222.4	242.4	63.2
ag2_gt 2400: Model	17.0	288.9	147.5	data	4.293	1.397	0.325	2.069	0.482	Spherical		22.6	11.9	14.2	0.828	0.193	Spherical		128.9	57.8	77.0
ag2_gt 2400: Model	17.0	288.9	147.5	normal score	0.999	0.233		0.478		Spherical		22.6	11.9	14.2	0.290		Spherical		128.9	57.8	77.0
ag2_gt 2601: Model	17.0	288.9	154.2	data	0.311	0.153	0.491	0.092	0.297	Spherical		69.4	67.7	28.3	0.066	0.211	Spherical		186.3	152.0	63.0
ag2_gt 2601: Model	17.0	288.9	154.2	normal score	0.999	0.376		0.296		Spherical		69.4	67.7	28.3	0.325		Spherical		186.3	152.0	63.0
ag2_gt 2602: Model	83.8	79.8	4.6	data	3.754	1.626	0.433	0.672	0.179	Spherical		62.4	29.2	14.3	1.441	0.384	Spherical		206.4	166.9	139.0
ag2_gt 2602: Model	83.8	79.8	4.6	normal score	0.998	0.324		0.122		Spherical		62.4	29.2	14.3	0.548		Spherical		206.4	166.9	139.0
ag2_gt 2900: Model	11.5	344.8	67.1	data	0.048	0.014	0.286	0.019	0.392	Spherical		54.2	29.2	22.6	0.015	0.322	Spherical		247.3	238.6	123.7
ag2_gt 2900: Model	11.5	344.8	67.1	normal score	0.999	0.201		0.337		Spherical		54.2	29.2	22.6	0.462		Spherical		247.3	238.6	123.7
ag2_gt 32_33_36: Model	44.9	73.7	69.1	normal score	1.000	0.157		0.355		Spherical		21.3	29.2	32.9	0.485		Spherical		161.2	123.4	111.8
ag2_gt 32_33_36: Model	44.9	73.7	69.1	data	6.873	1.573	0.229	2.865	0.417	Spherical		21.3	29.2	32.9	2.424	0.353	Spherical		161.2	123.4	111.8
ag2_gt 3500: Model	21.4	231.4	24.9	normal score	0.999	0.160		0.239		Spherical		30.0	92.5	15.7	0.599		Spherical		204.1	199.5	114.8
ag2_gt 3500: Model	21.4	231.4	24.9	data	0.183	0.042	0.232	0.058	0.315	Spherical		30.0	92.5	15.7	0.083	0.452	Spherical		204.1	199.5	114.8
ag2_gt 3900: Model	44.3	85.5	170.1	data	35.921	11.455	0.319	10.489	0.292	Spherical		30.2	15.0	27.1	13.916	0.387	Spherical		138.1	142.0	139.9
ag2_gt 3900: Model	44.3	85.5	170.1	normal score	0.999	0.227		0.230		Spherical		30.2	15.0	27.1	0.540		Spherical		138.1	142.0	139.9

table continues…

General	Direction							Structure 1							Structure 2						
Variogram Name	Dip	Dip Azimuth	Pitch	Model Space	Variance	Nugget	Normalised Nugget	Sill	Normalised Sill	Structure	Alpha	Major	Semi-major	Minor	Sill	Normalised Sill	Structure	Alpha	Major	Semi-major	Minor
ag2_gt 4601: Model	87.9	281.2	14.7	data	0.145	0.041	0.283	0.041	0.284	Spherical		62.4	12.0	30.4	0.062	0.430	Spherical		161.0	91.8	60.7
ag2_gt 4601: Model	87.9	281.2	14.7	normal score	0.999	0.199		0.173		Spherical		62.4	12.0	30.4	0.624		Spherical		161.0	91.8	60.7
ag2_gt 4901: Model	78.8	95.6	111.5	data	0.038	0.011	0.296	0.013	0.341	Spherical		17.5	32.4	25.5	0.014	0.362	Spherical		116.5	78.2	73.4
ag2_gt 4901: Model	78.8	95.6	111.5	normal score	0.999	0.209		0.291		Spherical		17.5	32.4	25.5	0.500		Spherical		116.5	78.2	73.4
ag2_gt 5601: Model	17.5	355.3	109.8	data	0.878	0.194	0.221	0.682	0.776	Spherical		151.3	121.6	54.0							
ag2_gt 5601: Model	17.5	355.3	109.8	normal score	0.997	0.152		0.844		Spherical		151.3	121.6	54.0							
ag2_gt 5602: Model	17.5	355.3	108.2	normal score	0.994	0.162		0.831		Spherical		141.5	121.6	54.0							
ag2_gt 5602: Model	17.5	355.3	108.2	data	0.000	0.000	0.235	0.000	0.761	Spherical		141.5	121.6	54.0							
ag2_gt 5603: Model	17.5	355.3	77.8	data	0.076	0.010	0.136	0.065	0.856	Spherical		141.5	121.6	54.0							
ag2_gt 5603: Model	17.5	355.3	77.8	normal score	0.988	0.090		0.897		Spherical		141.5	121.6	54.0							
ag2_gt 5604: Model	17.5	355.3	85.0	data	2.262	0.838	0.370	1.396	0.617	Spherical		141.5	121.6	54.0							
ag2_gt 5604: Model	17.5	355.3	85.0	normal score	0.981	0.270		0.710		Spherical		141.5	121.6	54.0							
ag2_gt 5605: Model	17.5	355.3	92.3	normal score	0.985	0.294		0.689		Spherical		141.5	121.6	54.0							
ag2_gt 5605: Model	17.5	355.3	92.3	data	0.000	0.000	0.400	0.000	0.590	Spherical		141.5	121.6	54.0							
ag2_gt 5901_5902: Model	19.6	324.9	110.1	data	0.134	0.047	0.348	0.025	0.188	Spherical		62.4	29.2	14.6	0.062	0.463	Spherical		143.3	203.3	119.7
ag2_gt 5901_5902: Model	19.6	324.9	110.1	normal score	0.999	0.251		0.069		Spherical		62.4	29.2	14.6	0.677		Spherical		143.3	203.3	119.7
ag2_gt 6900_7500: Model	6.1	31.7	23.4	data	1.010	0.345	0.341	0.253	0.250	Spherical		62.4	29.2	15.9	0.413	0.409	Spherical		211.1	203.3	99.5
ag2_gt 6900_7500: Model	6.1	31.7	23.4	normal score	0.999	0.246		0.174		Spherical		62.4	29.2	15.9	0.581		Spherical		211.1	203.3	99.5
ag2_gt 7900: Model	74.2	77.7	104.7	data	0.140	0.031	0.221	0.055	0.391	Spherical		30.0	20.8	40.0	0.055	0.390	Spherical		260.5	240.0	80.5
ag2_gt 7900: Model	74.2	77.7	104.7	normal score	0.999	0.152		0.324		Spherical		30.0	20.8	40.0	0.527		Spherical		260.5	240.0	80.5
ag2_gt 8900: Model	15.5	205.0	63.8	normal score	0.999	0.447		0.198		Spherical		30.0	25.0	19.6	0.355		Spherical		278.9	227.2	63.1
ag2_gt 8900: Model	15.5	205.0	63.8	data	7.323	4.138	0.565	1.386	0.189	Spherical		30.0	25.0	19.6	1.801	0.246	Spherical		278.9	227.2	63.1

table continues…

General	Direction							Structure 1							Structure 2						
Variogram Name	Dip	Dip Azimuth	Pitch	Model Space	Variance	Nugget	Normalised Nugget	Sill	Normalised Sill	Structure	Alpha	Major	Semi-major	Minor	Sill	Normalised Sill	Structure	Alpha	Major	Semi-major	Minor
ag2_gt 9900: Model	15.5	205.0	63.8	normal score	0.999	0.310		0.107		Spherical		30.0	25.0	13.6	0.578		Spherical		184.2	120.3	47.2
ag2_gt 9900: Model	15.5	205.0	63.8	data	0.625	0.261	0.418	0.093	0.148	Spherical		30.0	25.0	13.6	0.269	0.431	Spherical		184.2	120.3	47.2
ag2_gt: Model	5.3	225.6	35.8	normal score	1.000	0.079		0.202		Spherical		34.0	26.0	19.7	0.520		Spherical		275.0	108.1	149.1
ag2_gt: Model	5.3	225.6	35.8	data	4.066	0.374	0.092	0.931	0.229	Spherical		34.0	26.0	19.7	2.043	0.502	Spherical		275.0	108.1	149.1
au2_gt 1000: Model	27.7	249.8	65.2	data	0.021	0.016	0.784	0.005	0.215	Spherical		82.7	49.2	25.5							
au2_gt 1000: Model	27.7	249.8	65.2	normal score	0.997	0.690		0.308		Spherical		82.7	49.2	25.5							
au2_gt 11_12_13_16: Model	15.4	342.5	0.0	data	0.047	0.010	0.214	0.013	0.273	Spherical		29.4	13.9	19.7	0.020	0.417	Spherical		112.5	170.5	129.0
au2_gt 11_12_13_16: Model	15.4	342.5	0.0	normal score	1.000	0.146		0.186		Spherical		29.4	13.9	19.7	0.518		Spherical		112.5	170.5	129.0
au2_gt 1900: Model	17.0	288.9	138.0	normal score	0.999	0.278		0.201		Spherical		54.2	29.2	14.2	0.523		Spherical		266.4	182.3	57.6
au2_gt 1900: Model	17.0	288.9	138.0	data	0.002	0.001	0.381	0.000	0.247	Spherical		54.2	29.2	14.2	0.001	0.374	Spherical		266.4	182.3	57.6
au2_gt 2400: Model	17.0	288.9	138.0	data	0.024	0.010	0.400	0.007	0.304	Spherical		53.1	29.2	26.6	0.007	0.294	Spherical		134.7	72.9	121.7
au2_gt 2400: Model	17.0	288.9	138.0	normal score	0.999	0.295		0.257		Spherical		53.1	29.2	26.6	0.445		Spherical		134.7	72.9	121.7
au2_gt 2601: Model	17.0	288.9	138.0	data	0.004	0.002	0.465	0.001	0.148	Spherical		62.4	29.2	14.3	0.002	0.384	Spherical		206.4	166.9	139.0
au2_gt 2601: Model	17.0	288.9	138.0	normal score	0.999	0.352		0.094		Spherical		62.4	29.2	14.3	0.549		Spherical		206.4	166.9	139.0
au2_gt 2602: Model	83.8	79.8	4.6	data	0.026	0.013	0.519	0.002	0.093	Spherical		62.4	29.2	14.3	0.010	0.384	Spherical		206.4	166.9	139.0
au2_gt 2602: Model	83.8	79.8	4.6	normal score	0.998	0.402		0.043		Spherical		62.4	29.2	14.3	0.548		Spherical		206.4	166.9	139.0
au2_gt 2900: Model	11.5	344.8	67.1	data	0.000	0.000	0.380	0.000	0.247	Spherical		54.2	29.2	14.2	0.000	0.368	Spherical		256.1	106.1	139.3
au2_gt 2900: Model	11.5	344.8	67.1	normal score	0.999	0.278		0.201		Spherical		54.2	29.2	14.2	0.514		Spherical		256.1	106.1	139.3
au2_gt 32_33_36: Model	44.9	73.7	174.3	normal score	1.000	0.138		0.259		Spherical		19.6	29.2	40.3	0.604		Spherical		235.6	179.7	122.4
au2_gt 32_33_36: Model	44.9	73.7	174.3	data	0.061	0.012	0.203	0.020	0.329	Spherical		19.6	29.2	40.3	0.028	0.469	Spherical		235.6	179.7	122.4
au2_gt 3500: Model	21.4	231.4	32.6	normal score	0.999	0.201		0.146		Spherical		30.0	29.2	19.9	0.648		Spherical		213.9	173.5	129.2
au2_gt 3500: Model	21.4	231.4	32.6	data	0.006	0.002	0.286	0.001	0.210	Spherical		30.0	29.2	19.9	0.003	0.502	Spherical		213.9	173.5	129.2

table continues…

General	Direction							Structure 1							Structure 2						
Variogram Name	Dip	Dip Azimuth	Pitch	Model Space	Variance	Nugget	Normalised Nugget	Sill	Normalised Sill	Structure	Alpha	Major	Semi-major	Minor	Sill	Normalised Sill	Structure	Alpha	Major	Semi-major	Minor
au2_gt 3900: Model	44.3	85.5	170.1	normal score	0.999	0.138		0.119		Spherical		30.2	42.8	12.1	0.739		Spherical		300.2	300.2	79.3
au2_gt 3900: Model	44.3	85.5	170.1	data	0.001	0.000	0.203	0.000	0.188	Spherical		30.2	42.8	12.1	0.001	0.606	Spherical		300.2	300.2	79.3
au2_gt 4601: Model	87.9	281.2	0.8	normal score	0.999	0.295		0.259		Spherical		35.7	15.1	25.5	0.449		Spherical		160.7	257.9	60.5
au2_gt 4601: Model	87.9	281.2	0.8	data	0.003	0.001	0.400	0.001	0.290	Spherical		35.7	15.1	25.5	0.001	0.311	Spherical		160.7	257.9	60.5
au2_gt 4901: Model	78.8	95.6	176.7	data	0.001	0.000	0.296	0.001	0.443	Spherical		62.4	31.3	25.5	0.000	0.258	Spherical		162.1	150.8	131.7
au2_gt 4901: Model	78.8	95.6	176.7	normal score	0.999	0.209		0.393		Spherical		62.4	31.3	25.5	0.393		Spherical		162.1	150.8	131.7
au2_gt 5601: Model	17.5	355.3	99.1	normal score	0.997	0.138		0.858		Spherical		151.3	121.6	54.0							
au2_gt 5601: Model	17.5	355.3	99.1	data	0.020	0.004	0.202	0.016	0.795	Spherical		151.3	121.6	54.0							
au2_gt 5602: Model	17.5	355.3	87.4	normal score	0.994	0.521		0.472		Spherical		141.5	121.6	54.0							
au2_gt 5602: Model	17.5	355.3	87.4	data	0.002	0.002	0.637	0.001	0.359	Spherical		141.5	121.6	54.0							
au2_gt 5603: Model	17.5	355.3	77.8	normal score	0.988	0.266		0.721		Spherical		141.5	121.6	54.0							
au2_gt 5603: Model	17.5	355.3	77.8	data	0.003	0.001	0.366	0.002	0.626	Spherical		141.5	121.6	54.0							
au2_gt 5604: Model	17.5	355.3	85.0	normal score	0.981	0.336		0.644		Spherical		141.5	121.6	54.0							
au2_gt 5604: Model	17.5	355.3	85.0	data	0.002	0.001	0.447	0.001	0.541	Spherical		141.5	121.6	54.0							
au2_gt 5605: Model	17.5	355.3	92.3	normal score	0.985	0.136		0.847		Spherical		141.5	121.6	54.0							
au2_gt 5605: Model	17.5	355.3	92.3	data	0.004	0.001	0.200	0.003	0.790	Spherical		141.5	121.6	54.0							
au2_gt 5901_5902: Model	19.6	324.9	65.3	data	0.001	0.000	0.256	0.000	0.215	Spherical		62.4	29.2	10.1	0.001	0.525	Spherical		220.5	165.5	126.5
au2_gt 5901_5902: Model	19.6	324.9	65.3	normal score	0.999	0.178		0.105		Spherical		62.4	29.2	10.1	0.711		Spherical		220.5	165.5	126.5
au2_gt 6900_7500: Model	6.1	31.7	23.4	normal score	0.999	0.138		0.148		Spherical		62.4	29.2	15.3	0.711		Spherical		252.3	203.3	136.2
au2_gt 6900_7500: Model	6.1	31.7	23.4	data	0.006	0.001	0.203	0.002	0.263	Spherical		62.4	29.2	15.3	0.003	0.533	Spherical		252.3	203.3	136.2
au2_gt 7900: Model	74.2	77.7	6.7	normal score	0.999	0.321		0.069		Spherical		30.0	24.4	40.0	0.608		Spherical		278.9	401.9	122.7
au2_gt 7900: Model	74.2	77.7	6.7	data	0.003	0.001	0.430	0.000	0.100	Spherical		30.0	24.4	40.0	0.001	0.469	Spherical		278.9	401.9	122.7

table continues…

General	Direction							Structure 1							Structure 2						
Variogram Name	Dip	Dip Azimuth	Pitch	Model Space	Variance	Nugget	Normalised Nugget	Sill	Normalised Sill	Structure	Alpha	Major	Semi-major	Minor	Sill	Normalised Sill	Structure	Alpha	Major	Semi-major	Minor
au2_gt 8900: Model	15.5	205.0	63.8	data	0.000	0.000	0.354	0.000	0.380	Spherical		30.0	25.0	14.2	0.000	0.266	Spherical		278.9	227.2	40.6
au2_gt 8900: Model	15.5	205.0	63.8	normal score	0.999	0.256		0.364		Spherical		30.0	25.0	14.2	0.379		Spherical		278.9	227.2	40.6
au2_gt 9900: Model	15.5	205.0	63.8	normal score	0.999	0.256		0.262		Spherical		30.0	25.0	18.0	0.478		Spherical		278.9	227.2	112.8
au2_gt 9900: Model	15.5	205.0	63.8	data	0.000	0.000	0.354	0.000	0.294	Spherical		30.0	25.0	18.0	0.000	0.350	Spherical		278.9	227.2	112.8
cu_pct 1000: Model	27.7	249.8	65.2	normal score	0.997	0.690		0.308		Spherical		82.7	49.2	25.5							
cu_pct 1000: Model	27.7	249.8	65.2	data	0.023	0.018	0.784	0.005	0.215	Spherical		82.7	49.2	25.5							
cu_pct 11_12_13_16: Model	34.6	250.2	12.8	normal score	1.000	0.138		0.299		Spherical		94.7	41.4	22.4	0.563		Spherical		306.9	341.7	177.5
cu_pct 11_12_13_16: Model	17.0	288.9	138.0	data	0.032	0.006	0.203	0.011	0.344	Spherical		62.4	29.2	25.5	0.012	0.376	Spherical		269.2	203.3	131.7
cu_pct 11_12_13_16: Model	17.0	288.9	138.0	normal score	1.000	0.138		0.260		Spherical		62.4	29.2	25.5	0.481		Spherical		269.2	203.3	131.7
cu_pct 11_12_13_16: Model	34.6	250.2	12.8	data	0.032	0.006	0.203	0.013	0.405	Spherical		94.7	41.4	22.4	0.012	0.392	Spherical		306.9	341.7	177.5
cu_pct 1900: Model	17.0	288.9	138.0	normal score	0.999	0.278		0.201		Spherical		54.2	29.2	14.2	0.519		Spherical		266.4	192.5	75.9
cu_pct 1900: Model	87.8	262.8	167.3	normal score	0.999	0.300		0.249		Spherical		94.7	39.0	44.9	0.449		Spherical		316.9	185.3	108.0
cu_pct 1900: Model	87.8	262.8	167.3	data	0.003	0.001	0.407	0.001	0.288	Spherical		94.7	39.0	44.9	0.001	0.305	Spherical		316.9	185.3	108.0
cu_pct 1900: Model	17.0	288.9	138.0	data	0.003	0.001	0.381	0.001	0.247	Spherical		54.2	29.2	14.2	0.001	0.372	Spherical		266.4	192.5	75.9
cu_pct 2400: Model	17.0	288.9	138.0	normal score	0.999	0.324		0.228		Spherical		53.1	29.2	26.6	0.441		Spherical		188.0	109.4	146.7
cu_pct 2400: Model	17.0	288.9	138.0	data	0.165	0.072	0.434	0.043	0.260	Spherical		53.1	29.2	26.6	0.050	0.302	Spherical		188.0	109.4	146.7
cu_pct 24_26: Model	67.4	88.3	65.8	normal score	1.000	0.240		0.485		Spherical		42.8	77.0	35.4	0.275		Spherical		119.8	102.9	74.2
cu_pct 24_26: Model	67.4	88.3	65.8	data	0.098	0.033	0.335	0.048	0.489	Spherical		42.8	77.0	35.4	0.017	0.176	Spherical		119.8	102.9	74.2
cu_pct 2601: Model	17.0	288.9	138.0	data	0.017	0.007	0.434	0.003	0.179	Spherical		62.4	29.2	14.3	0.007	0.384	Spherical		206.4	166.9	139.0
cu_pct 2601: Model	17.0	288.9	138.0	normal score	0.999	0.324		0.122		Spherical		62.4	29.2	14.3	0.549		Spherical		206.4	166.9	139.0
cu_pct 2602: Model	83.8	79.8	4.6	normal score	0.998	0.324		0.121		Spherical		62.4	29.2	14.3	0.544		Spherical		206.4	166.9	139.0
cu_pct 2602: Model	83.8	79.8	4.6	data	0.052	0.023	0.431	0.009	0.178	Spherical		62.4	29.2	14.3	0.020	0.383	Spherical		206.4	166.9	139.0

table continues…

General	Direction							Structure 1							Structure 2						
Variogram Name	Dip	Dip Azimuth	Pitch	Model Space	Variance	Nugget	Normalised Nugget	Sill	Normalised Sill	Structure	Alpha	Major	Semi-major	Minor	Sill	Normalised Sill	Structure	Alpha	Major	Semi-major	Minor
cu_pct 2900: Model	11.5	344.8	67.1	data	0.002	0.001	0.380	0.000	0.247	Spherical		54.2	29.2	14.2	0.001	0.373	Spherical		266.4	192.5	64.5
cu_pct 2900: Model	11.5	344.8	67.1	normal score	0.999	0.278		0.201		Spherical		54.2	29.2	14.2	0.522		Spherical		266.4	192.5	64.5
cu_pct 32_33_36: Model	44.9	73.7	174.3	data	0.042	0.009	0.203	0.018	0.427	Spherical		19.6	29.2	43.1	0.016	0.368	Spherical		278.9	227.2	152.0
cu_pct 32_33_36: Model	44.9	73.7	174.3	normal score	1.000	0.138		0.365		Spherical		19.6	29.2	43.1	0.494		Spherical		278.9	227.2	152.0
cu_pct 3500: Model	21.4	231.4	32.6	data	0.009	0.003	0.380	0.002	0.184	Spherical		30.0	29.2	19.3	0.004	0.434	Spherical		213.9	192.5	92.8
cu_pct 3500: Model	21.4	231.4	32.6	normal score	0.999	0.278		0.141		Spherical		30.0	29.2	19.3	0.578		Spherical		213.9	192.5	92.8
cu_pct 3900: Model	44.3	85.5	170.1	normal score	0.999	0.138		0.097		Spherical		30.2	42.8	21.6	0.766		Spherical		300.2	300.2	95.4
cu_pct 3900: Model	44.3	85.5	170.1	data	0.003	0.001	0.203	0.001	0.165	Spherical		30.2	42.8	21.6	0.002	0.633	Spherical		300.2	300.2	95.4
cu_pct 4601: Model	87.9	281.2	0.8	normal score	0.999	0.378		0.311		Spherical		62.4	17.5	25.5	0.298		Spherical		211.9	116.3	60.5
cu_pct 4601: Model	87.9	281.2	0.8	data	0.010	0.005	0.493	0.003	0.303	Spherical		62.4	17.5	25.5	0.002	0.196	Spherical		211.9	116.3	60.5
cu_pct 4901: Model	78.8	95.6	176.7	data	0.001	0.000	0.296	0.001	0.503	Spherical		62.4	17.5	25.5	0.000	0.198	Spherical		162.1	150.8	131.7
cu_pct 4901: Model	78.8	95.6	176.7	normal score	0.999	0.209		0.479		Spherical		62.4	17.5	25.5	0.307		Spherical		162.1	150.8	131.7
cu_pct 5601: Model	17.5	355.3	99.1	normal score	0.997	0.138		0.858		Spherical		151.3	121.6	54.0							
cu_pct 5601: Model	17.5	355.3	99.1	data	0.020	0.004	0.202	0.016	0.795	Spherical		151.3	121.6	54.0							
cu_pct 5602: Model	17.5	355.3	87.4	normal score	0.994	0.137		0.855		Spherical		141.5	121.6	54.0							
cu_pct 5602: Model	17.5	355.3	87.4	data	0.017	0.003	0.202	0.014	0.794	Spherical		141.5	121.6	54.0							
cu_pct 5603: Model	17.5	355.3	77.8	normal score	0.988	0.136		0.850		Spherical		141.5	121.6	54.0							
cu_pct 5603: Model	17.5	355.3	77.8	data	0.004	0.001	0.201	0.004	0.791	Spherical		141.5	121.6	54.0							
cu_pct 5604: Model	17.5	355.3	85.0	normal score	0.981	0.135		0.834		Spherical		141.5	121.6	54.0							
cu_pct 5604: Model	17.5	355.3	85.0	data	0.005	0.001	0.197	0.004	0.783	Spherical		141.5	121.6	54.0							
cu_pct 5605: Model	17.5	355.3	92.3	normal score	0.985	0.136		0.846		Spherical		141.5	121.6	54.0							
cu_pct 5605: Model	17.5	355.3	92.3	data	0.013	0.003	0.200	0.010	0.789	Spherical		141.5	121.6	54.0							

table continues…

General	Direction							Structure 1							Structure 2						
Variogram Name	Dip	Dip Azimuth	Pitch	Model Space	Variance	Nugget	Normalised Nugget	Sill	Normalised Sill	Structure	Alpha	Major	Semi-major	Minor	Sill	Normalised Sill	Structure	Alpha	Major	Semi-major	Minor
cu_pct 5901_5902: Model	22.2	311.6	151.5	normal score	0.999	0.154		0.411		Spherical		94.7	39.0	24.1	0.436		Spherical		316.9	136.1	65.7
cu_pct 5901_5902: Model	19.6	324.9	110.1	normal score	0.999	0.138		0.278		Spherical		62.4	29.2	12.2	0.578		Spherical		252.3	203.3	64.4
cu_pct 5901_5902: Model	19.6	324.9	110.1	data	0.002	0.000	0.203	0.001	0.377	Spherical		62.4	29.2	12.2	0.001	0.417	Spherical		252.3	203.3	64.4
cu_pct 5901_5902: Model	22.2	311.6	151.5	data	0.002	0.001	0.225	0.001	0.482	Spherical		94.7	39.0	24.1	0.001	0.294	Spherical		316.9	136.1	65.7
cu_pct 6900_7500: Model	6.1	31.7	23.4	normal score	0.999	0.138		0.248		Spherical		62.4	29.2	26.3	0.611		Spherical		252.3	203.3	134.7
cu_pct 6900_7500: Model	6.1	31.7	23.4	data	0.008	0.002	0.203	0.003	0.351	Spherical		62.4	29.2	26.3	0.004	0.444	Spherical		252.3	203.3	134.7
cu_pct 7900: Model	74.2	77.7	6.7	normal score	0.999	0.152		0.351		Spherical		30.0	30.0	40.0	0.491		Spherical		278.9	227.2	122.7
cu_pct 7900: Model	74.2	77.7	6.7	data	0.005	0.001	0.221	0.002	0.413	Spherical		30.0	30.0	40.0	0.002	0.362	Spherical		278.9	227.2	122.7
cu_pct 8900: Model	15.5	205.0	63.8	normal score	0.999	0.256		0.239		Spherical		30.0	25.0	17.0	0.505		Spherical		278.9	227.2	78.8
cu_pct 8900: Model	15.5	205.0	63.8	data	0.002	0.001	0.354	0.001	0.274	Spherical		30.0	25.0	17.0	0.001	0.372	Spherical		278.9	227.2	78.8
cu_pct 9900: Model	15.5	205.0	63.8	normal score	0.999	0.256		0.239		Spherical		30.0	25.0	17.0	0.505		Spherical		278.9	227.2	78.8
cu_pct 9900: Model	15.5	205.0	63.8	data	0.002	0.001	0.354	0.000	0.274	Spherical		30.0	25.0	17.0	0.001	0.372	Spherical		278.9	227.2	78.8
cu_pct in GM_FromMeshes: 2601: Model	64.5	239.2	167.0	normal score	0.999	0.340		0.320		Spherical		200.0	60.0	35.0	0.340		Spherical		1140.0	450.0	80.0
cu_pct in GM_FromMeshes: 3200: Model	88.7	90.5	153.9	normal score	1.000	0.100		0.520		Spherical		46.8	16.0	55.0	0.380		Spherical		425.0	290.0	110.0
cu_pct in GM_FromMeshes: 3301: Model	45.1	81.4	168.6	data	0.023	0.003	0.143	0.010	0.412	Spherical		50.0	85.0	25.0	0.010	0.446	Spherical		255.0	265.0	110.0
mo_pct 1000: Model	27.7	249.8	65.2	data	0.000	0.000	0.784	0.000	0.215	Spherical		82.7	49.2	25.5							
mo_pct 1000: Model	27.7	249.8	65.2	normal score	0.997	0.690		0.308		Spherical		82.7	49.2	25.5							
mo_pct 11_12_13_16: Model	17.0	288.9	154.3	normal score	1.000	0.168		0.193		Spherical		33.3	35.7	17.8	0.640		Spherical		303.8	240.2	151.7
mo_pct 11_12_13_16: Model	17.0	288.9	154.3	data	0.000	0.000	0.243	0.000	0.259	Spherical		33.3	35.7	17.8	0.000	0.498	Spherical		303.8	240.2	151.7
mo_pct 1900: Model	17.0	288.9	138.0	data	0.000	0.000	0.215	0.000	0.471	Spherical		56.2	39.2	32.2	0.000	0.316	Spherical		222.4	192.5	96.3
mo_pct 1900: Model	17.0	288.9	138.0	normal score	0.999	0.147		0.397		Spherical		56.2	39.2	32.2	0.458		Spherical		222.4	192.5	96.3

table continues…

General	Direction							Structure 1							Structure 2						
Variogram Name	Dip	Dip Azimuth	Pitch	Model Space	Variance	Nugget	Normalised Nugget	Sill	Normalised Sill	Structure	Alpha	Major	Semi-major	Minor	Sill	Normalised Sill	Structure	Alpha	Major	Semi-major	Minor
mo_pct 2400: Model	17.0	288.9	147.5	data	0.001	0.000	0.325	0.000	0.306	Spherical		54.0	45.4	37.4	0.000	0.368	Spherical		158.5	134.7	165.0
mo_pct 2400: Model	17.0	288.9	147.5	normal score	0.999	0.233		0.230		Spherical		54.0	45.4	37.4	0.537		Spherical		158.5	134.7	165.0
mo_pct 2601: Model	17.0	288.9	154.2	data	0.000	0.000	0.176	0.000	0.335	Spherical		62.4	16.2	28.3	0.000	0.490	Spherical		186.3	129.8	154.7
mo_pct 2601: Model	17.0	288.9	154.2	normal score	0.999	0.118		0.195		Spherical		62.4	16.2	28.3	0.688		Spherical		186.3	129.8	154.7
mo_pct 2602: Model	83.8	79.8	4.6	data	0.000	0.000	0.433	0.000	0.179	Spherical		62.4	29.2	14.3	0.000	0.384	Spherical		206.4	166.9	139.0
mo_pct 2602: Model	83.8	79.8	4.6	normal score	0.998	0.324		0.122		Spherical		62.4	29.2	14.3	0.548		Spherical		206.4	166.9	139.0
mo_pct 2900: Model	11.5	344.8	67.1	normal score	0.999	0.278		0.190		Spherical		54.2	29.2	49.8	0.528		Spherical		303.5	278.2	197.0
mo_pct 2900: Model	11.5	344.8	67.1	data	0.000	0.000	0.380	0.000	0.234	Spherical		54.2	29.2	49.8	0.000	0.384	Spherical		303.5	278.2	197.0
mo_pct 32_33_36: Model	44.9	73.7	69.1	data	0.001	0.000	0.229	0.000	0.332	Spherical		22.6	29.2	32.9	0.000	0.437	Spherical		181.6	177.1	175.4
mo_pct 32_33_36: Model	44.9	73.7	69.1	normal score	1.000	0.157		0.261		Spherical		22.6	29.2	32.9	0.577		Spherical		181.6	177.1	175.4
mo_pct 3500: Model	21.4	231.4	24.9	normal score	0.999	0.126		0.173		Spherical		30.0	92.5	38.6	0.701		Spherical		393.0	346.3	209.2
mo_pct 3500: Model	21.4	231.4	24.9	data	0.000	0.000	0.186	0.000	0.243	Spherical		30.0	92.5	38.6	0.000	0.571	Spherical		393.0	346.3	209.2
mo_pct 3900: Model	44.3	85.5	170.1	normal score	0.999	0.227		0.134		Spherical		30.2	9.2	8.5	0.640		Spherical		138.1	221.8	58.5
mo_pct 3900: Model	44.3	85.5	170.1	data	0.000	0.000	0.319	0.000	0.209	Spherical		30.2	9.2	8.5	0.000	0.473	Spherical		138.1	221.8	58.5
mo_pct 4601: Model	87.9	281.2	14.7	normal score	0.999	0.188		0.183		Spherical		62.4	12.0	30.4	0.630		Spherical		216.7	154.2	85.3
mo_pct 4601: Model	87.9	281.2	14.7	data	0.000	0.000	0.270	0.000	0.281	Spherical		62.4	12.0	30.4	0.000	0.451	Spherical		216.7	154.2	85.3
mo_pct 4901: Model	78.8	95.6	23.7	data	0.000	0.000	0.296	0.000	0.252	Spherical		62.4	32.4	25.5	0.000	0.451	Spherical		209.6	185.8	89.7
mo_pct 4901: Model	78.8	95.6	23.7	normal score	0.999	0.209		0.158		Spherical		62.4	32.4	25.5	0.631		Spherical		209.6	185.8	89.7
mo_pct 5601: Model	17.5	355.3	109.8	normal score	0.997	0.152		0.844		Spherical		151.3	121.6	54.0							
mo_pct 5601: Model	17.5	355.3	109.8	data	0.000	0.000	0.221	0.000	0.776	Spherical		151.3	121.6	54.0							
mo_pct 5602: Model	17.5	355.3	108.2	data	0.000	0.000	0.235	0.000	0.761	Spherical		141.5	121.6	54.0							
mo_pct 5602: Model	17.5	355.3	108.2	normal score	0.994	0.162		0.831		Spherical		141.5	121.6	54.0							

table continues…

General	Direction							Structure 1							Structure 2						
Variogram Name	Dip	Dip Azimuth	Pitch	Model Space	Variance	Nugget	Normalised Nugget	Sill	Normalised Sill	Structure	Alpha	Major	Semi-major	Minor	Sill	Normalised Sill	Structure	Alpha	Major	Semi-major	Minor
mo_pct 5603: Model	17.5	355.3	77.8	data	0.000	0.000	0.136	0.000	0.856	Spherical		141.5	121.6	54.0							
mo_pct 5603: Model	17.5	355.3	77.8	normal score	0.988	0.090		0.897		Spherical		141.5	121.6	54.0							
mo_pct 5604: Model	17.5	355.3	85.0	data	0.005	0.001	0.197	0.004	0.783	Spherical		141.5	121.6	54.0							
mo_pct 5604: Model	17.5	355.3	85.0	normal score	0.981	0.135		0.834		Spherical		141.5	121.6	54.0							
mo_pct 5605: Model	17.5	355.3	92.3	normal score	0.985	0.294		0.689		Spherical		141.5	121.6	54.0							
mo_pct 5605: Model	17.5	355.3	92.3	data	0.000	0.000	0.400	0.000	0.590	Spherical		141.5	121.6	54.0							
mo_pct 5901_5902: Model	19.6	324.9	110.1	data	0.000	0.000	0.348	0.000	0.280	Spherical		62.4	29.2	8.9	0.000	0.371	Spherical		252.3	203.3	127.9
mo_pct 5901_5902: Model	19.6	324.9	110.1	normal score	0.999	0.251		0.222		Spherical		62.4	29.2	8.9	0.525		Spherical		252.3	203.3	127.9
mo_pct 6900_7500: Model	6.1	31.7	23.4	data	0.000	0.000	0.203	0.000	0.351	Spherical		62.4	29.2	26.3	0.000	0.444	Spherical		252.3	203.3	134.7
mo_pct 6900_7500: Model	6.1	31.7	23.4	normal score	0.999	0.138		0.248		Spherical		62.4	29.2	26.3	0.611		Spherical		252.3	203.3	134.7
mo_pct 7900: Model	74.2	77.7	6.7	data	0.000	0.000	0.221	0.000	0.438	Spherical		30.0	28.6	40.0	0.000	0.340	Spherical		278.9	275.9	122.7
mo_pct 7900: Model	74.2	77.7	6.7	normal score	0.999	0.152		0.379		Spherical		30.0	28.6	40.0	0.467		Spherical		278.9	275.9	122.7
mo_pct 8900: Model	15.5	205.0	63.8	normal score	0.999	0.447		0.346		Spherical		30.0	25.0	21.1	0.207		Spherical		278.9	227.2	63.1
mo_pct 8900: Model	15.5	205.0	63.8	data	0.000	0.000	0.565	0.000	0.300	Spherical		30.0	25.0	21.1	0.000	0.135	Spherical		278.9	227.2	63.1
mo_pct 9900: Model	15.5	205.0	63.8	data	0.000	0.000	0.418	0.000	0.209	Spherical		30.0	25.0	17.0	0.000	0.373	Spherical		278.9	227.2	78.8
mo_pct 9900: Model	15.5	205.0	63.8	normal score	0.999	0.310		0.184		Spherical		30.0	25.0	17.0	0.505		Spherical		278.9	227.2	78.8
mo_pct Blk1: Model	26.0	262.0	107.8	normal score	0.999	0.146		0.419		Spherical		25.7	32.8	39.4	0.431		Spherical		139.3	160.5	162.9
mo_pct Blk1: Model	26.0	262.0	107.8	data	2.069	0.443	0.214	0.997	0.482	Spherical		25.7	32.8	39.4	0.625	0.302	Spherical		139.3	160.5	162.9
mo_pct: Model	5.3	225.6	35.8	data	0.000	0.000	0.062	0.000	0.264	Spherical		28.8	26.0	14.3	0.000	0.528	Spherical		408.9	227.1	177.6
mo_pct: Model	5.3	225.6	35.8	normal score	1.000	0.053		0.222		Spherical		28.8	26.0	14.3	0.536		Spherical		408.9	227.1	177.6

Figure 14-4: Development of Local Orientation Model

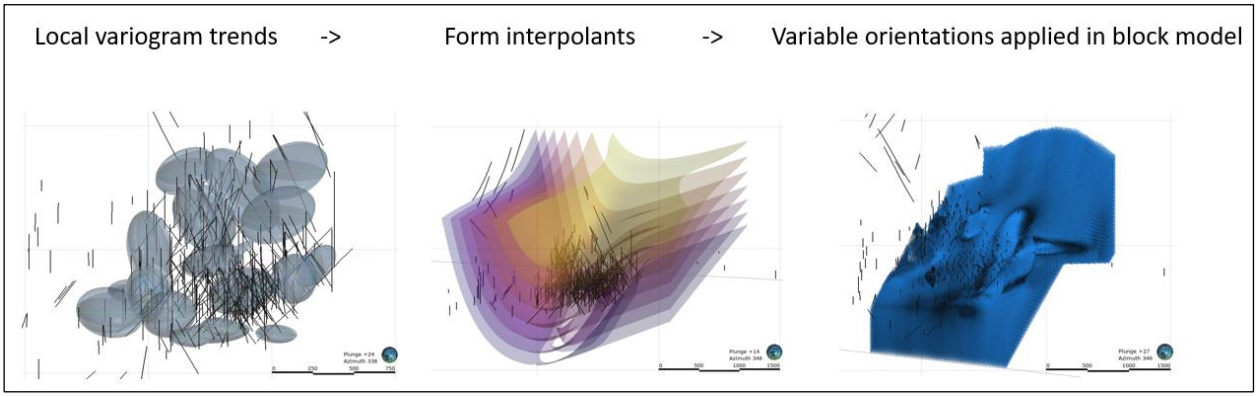

Source: Red Pennant (2021)

14.8 Estimation/Interpolation Methods

Copper, molybdenum, silver and gold were estimated using ordinary kriging (OK) with inverse distance and nearest neighbour estimates generated for validation (see Table 14-8). Search parameters are detailed in Table 14-9.

Table 14-8: Grade Interpolant Parameters

General				Value Capping		
Name	Domain	Values	Estimate Name	Lower Bound	Upper Bound	Estimate Type
ID, ag2_gt 1000	GM_Consolidated_from_meshes: 1000	ag2_gt	ag2_gt 1000	0.001	2.500	IDW
ID, ag2_gt 11_12_13_16	GM_Consolidated_from_meshes: 11_12_13_16	ag2_gt	ag2_gt 11_12_13_16	0.001	20.000	IDW
ID, ag2_gt 1900	GM_FromMeshes: 1900	ag2_gt	ag2_gt 1900	0.001	2.000	IDW
ID, ag2_gt 2400	GM_FromMeshes: 2400	ag2_gt	ag2_gt 2400	0.001	12.000	IDW
ID, ag2_gt 2601	GM_FromMeshes: 2601	ag2_gt	ag2_gt 2601	0.001	3.000	IDW
ID, ag2_gt 2602	GM_FromMeshes: 2602	ag2_gt	ag2_gt 2602	0.001	6.000	IDW
ID, ag2_gt 2900	GM_FromMeshes: 2900	ag2_gt	ag2_gt 2900	0.001	1.100	IDW
ID, ag2_gt 32_33_36	GM_Consolidated_from_meshes: 32_33_36	ag2_gt	ag2_gt 32_33_36	0.001	30.000	IDW
ID, ag2_gt 3500	GM_FromMeshes: 3500	ag2_gt	ag2_gt 3500	0.001	2.000	IDW
ID, ag2_gt 3900	GM_Consolidated_from_meshes: 3900	ag2_gt	ag2_gt 3900	0.001	10.000	IDW
ID, ag2_gt 4601	GM_FromMeshes: 4601	ag2_gt	ag2_gt 4601	0.001	2.000	IDW
ID, ag2_gt 4901	GM_FromMeshes: 4901	ag2_gt	ag2_gt 4901	0.001	1.000	IDW
ID, ag2_gt 5601	GM_FromMeshes: 5601	ag2_gt	ag2_gt 5601	0.001	3.000	IDW
ID, ag2_gt 5602	GM_FromMeshes: 5602	ag2_gt	ag2_gt 5602	0.001	0.900	IDW
ID, ag2_gt 5603	GM_FromMeshes: 5603	ag2_gt	ag2_gt 5603	0.001	1.236	IDW
ID, ag2_gt 5604	GM_FromMeshes: 5604	ag2_gt	ag2_gt 5604	0.001	4.866	IDW
ID, ag2_gt 5605	GM_FromMeshes: 5605	ag2_gt	ag2_gt 5605			IDW
ID, ag2_gt 5901_5902	GM_Consolidated_from_meshes: 5901	ag2_gt	ag2_gt 5901_5902	0.001	4.000	IDW

table continues…

General			Estimate Name	Value Capping		Estimate Type
Name	Domain	Values		Lower Bound	Upper Bound	
ID, ag2_gt 6900_7500	GM_Consolidated_from_meshes: 6900_7500	ag2_gt	ag2_gt 6900_7500	0.001	3.000	IDW
ID, ag2_gt 7900	GM_Consolidated_from_meshes: 7900	ag2_gt	ag2_gt 7900	0.001	2.000	IDW
ID, ag2_gt 8900	GM_FromMeshes: 8900	ag2_gt	ag2_gt 8900	0.001	4.000	IDW
ID, ag2_gt 9900	GM_FromMeshes: 9900	ag2_gt	ag2_gt 9900	0.001	6.000	IDW
ID, au2_gt 1000	GM_Consolidated_from_meshes: 1000	au2_gt	au2_gt 1000	0.001	0.600	IDW
ID, au2_gt 11_12_13_16	GM_Consolidated_from_meshes: 11_12_13_16	au2_gt	au2_gt 11_12_13_16	0.001	3.000	IDW
ID, au2_gt 1900	GM_FromMeshes: 1900	au2_gt	au2_gt 1900	0.001	0.270	IDW
ID, au2_gt 2400	GM_FromMeshes: 2400	au2_gt	au2_gt 2400	0.001	1.000	IDW
ID, au2_gt 2601	GM_FromMeshes: 2601	au2_gt	au2_gt 2601	0.001	0.300	IDW
ID, au2_gt 2602	GM_FromMeshes: 2602	au2_gt	au2_gt 2602	0.001	0.700	IDW
ID, au2_gt 2900	GM_FromMeshes: 2900	au2_gt	au2_gt 2900	0.001	0.120	IDW
ID, au2_gt 32_33_36	GM_Consolidated_from_meshes: 32_33_36	au2_gt	au2_gt 32_33_36	0.001	3.000	IDW
ID, au2_gt 3500	GM_FromMeshes: 3500	au2_gt	au2_gt 3500	0.001	0.400	IDW
ID, au2_gt 3900	GM_Consolidated_from_meshes: 3900	au2_gt	au2_gt 3900	0.001	0.250	IDW
ID, au2_gt 4601	GM_FromMeshes: 4601	au2_gt	au2_gt 4601	0.001	0.250	IDW
ID, au2_gt 4901	GM_FromMeshes: 4901	au2_gt	au2_gt 4901	0.001	0.200	IDW
ID, au2_gt 5601	GM_FromMeshes: 5601	au2_gt	au2_gt 5601	0.001	0.300	IDW
ID, au2_gt 5602	GM_FromMeshes: 5602	au2_gt	au2_gt 5602	0.001	0.200	IDW

table continues…

General			Estimate Name	Value Capping		Estimate Type
Name	Domain	Values		Lower Bound	Upper Bound	
ID, au2_gt 5603	GM_FromMeshes: 5603	au2_gt	au2_gt 5603	0.001	0.150	IDW
ID, au2_gt 5604	GM_FromMeshes: 5604	au2_gt	au2_gt 5604	0.001	0.140	IDW
ID, au2_gt 5605	GM_FromMeshes: 5605	au2_gt	au2_gt 5605	0.001	0.250	IDW
ID, au2_gt 5901_5902	GM_Consolidated_from_meshes: 5901	au2_gt	au2_gt 5901_5902	0.001	0.250	IDW
ID, au2_gt 6900_7500	GM_Consolidated_from_meshes: 6900_7500	au2_gt	au2_gt 6900_7500	0.001	0.300	IDW
ID, au2_gt 7900	GM_Consolidated_from_meshes: 7900	au2_gt	au2_gt 7900	0.001	0.200	IDW
ID, au2_gt 8900	GM_FromMeshes: 8900	au2_gt	au2_gt 8900	0.001	0.100	IDW
ID, au2_gt 9900	GM_FromMeshes: 9900	au2_gt	au2_gt 9900	0.001	0.100	IDW
ID, cu_pct 1000	GM_Consolidated_from_meshes: 1000	cu_pct	cu_pct 1000	0.001	0.500	IDW
ID, cu_pct 11_12_13_16	GM_Consolidated_from_meshes: 11_12_13_16	cu_pct	cu_pct 11_12_13_16	0.001	1.300	IDW
ID, cu_pct 1900	GM_FromMeshes: 1900	cu_pct	cu_pct 1900	0.001	0.383	IDW
ID, cu_pct 2400	GM_FromMeshes: 2400	cu_pct	cu_pct 2400	0.001	2.000	IDW
ID, cu_pct 2601	GM_FromMeshes: 2601	cu_pct	cu_pct 2601	0.001	0.650	IDW
ID, cu_pct 2602	GM_FromMeshes: 2602	cu_pct	cu_pct 2602	0.001	2.000	IDW
ID, cu_pct 2900	GM_FromMeshes: 2900	cu_pct	cu_pct 2900	0.001	0.310	IDW
ID, cu_pct 32_33_36	GM_Consolidated_from_meshes: 32_33_36	cu_pct	cu_pct 32_33_36	0.001	1.300	IDW
ID, cu_pct 3500	GM_FromMeshes: 3500	cu_pct	cu_pct 3500	0.001	0.310	IDW
ID, cu_pct 3900	GM_Consolidated_from_meshes: 3900	cu_pct	cu_pct 3900	0.001	0.320	IDW

table continues…

General				Value Capping		
Name	Domain	Values	Estimate Name	Lower Bound	Upper Bound	Estimate Type
ID, cu_pct 4601	GM_FromMeshes: 4601	cu_pct	cu_pct 4601	0.001	0.600	IDW
ID, cu_pct 4901	GM_FromMeshes: 4901	cu_pct	cu_pct 4901	0.001	0.184	IDW
ID, cu_pct 5601	GM_FromMeshes: 5601	cu_pct	cu_pct 5601	0.001	1.090	IDW
ID, cu_pct 5602	GM_FromMeshes: 5602	cu_pct	cu_pct 5602	0.001	0.658	IDW
ID, cu_pct 5603	GM_FromMeshes: 5603	cu_pct	cu_pct 5603	0.001	0.246	IDW
ID, cu_pct 5604	GM_FromMeshes: 5604	cu_pct	cu_pct 5604	0.001	0.216	IDW
ID, cu_pct 5605	GM_FromMeshes: 5605	cu_pct	cu_pct 5605	0.001	0.495	IDW
ID, cu_pct 5901_5902	GM_Consolidated_from_meshes: 5901	cu_pct	cu_pct 5901_5902	0.001	0.400	IDW
ID, cu_pct 6900_7500	GM_Consolidated_from_meshes: 6900_7500	cu_pct	cu_pct 6900_7500	0.001	0.400	IDW
ID, cu_pct 7900	GM_Consolidated_from_meshes: 7900	cu_pct	cu_pct 7900	0.001	0.310	IDW
ID, cu_pct 8900	GM_FromMeshes: 8900	cu_pct	cu_pct 8900	0.001	0.200	IDW
ID, cu_pct 9900	GM_FromMeshes: 9900	cu_pct	cu_pct 9900	0.001	0.200	IDW
ID, mo_pct 1000	GM_Consolidated_from_meshes: 1000	mo_pct	mo_pct 1000	0.001	0.030	IDW
ID, mo_pct 11_12_13_16	GM_Consolidated_from_meshes: 11_12_13_16	mo_pct	mo_pct 11_12_13_16	0.001	0.300	IDW
ID, mo_pct 1900	GM_FromMeshes: 1900	mo_pct	mo_pct 1900	0.001	0.050	IDW
ID, mo_pct 2400	GM_FromMeshes: 2400	mo_pct	mo_pct 2400	0.001	0.200	IDW
ID, mo_pct 2601	GM_FromMeshes: 2601	mo_pct	mo_pct 2601	0.001	0.060	IDW
ID, mo_pct 2602	GM_FromMeshes: 2602	mo_pct	mo_pct 2602	0.001	2.000	IDW

table continues…

General			Estimate Name	Value Capping		Estimate Type
Name	Domain	Values		Lower Bound	Upper Bound	
ID, mo_pct 2900	GM_FromMeshes: 2900	mo_pct	mo_pct 2900	0.001	0.015	IDW
ID, mo_pct 32_33_36	GM_Consolidated_from_meshes: 32_33_36	mo_pct	mo_pct 32_33_36	0.001	0.200	IDW
ID, mo_pct 3500	GM_FromMeshes: 3500	mo_pct	mo_pct 3500	0.001	0.055	IDW
ID, mo_pct 3900	GM_Consolidated_from_meshes: 3900	mo_pct	mo_pct 3900	0.001	0.025	IDW
ID, mo_pct 4601	GM_FromMeshes: 4601	mo_pct	mo_pct 4601	0.001	0.050	IDW
ID, mo_pct 4901	GM_FromMeshes: 4901	mo_pct	mo_pct 4901	0.001	0.008	IDW
ID, mo_pct 5601	GM_FromMeshes: 5601	mo_pct	mo_pct 5601	0.001	0.040	IDW
ID, mo_pct 5602	GM_FromMeshes: 5602	mo_pct	mo_pct 5602	0.001	0.018	IDW
ID, mo_pct 5603	GM_FromMeshes: 5603	mo_pct	mo_pct 5603	0.001	0.014	IDW
ID, mo_pct 5604	GM_FromMeshes: 5604	mo_pct	mo_pct 5604	0.001	0.216	IDW
ID, mo_pct 5605	GM_FromMeshes: 5605	mo_pct	mo_pct 5605	0.001	0.008	IDW
ID, mo_pct 5901_5902	GM_Consolidated_from_meshes: 5901	mo_pct	mo_pct 5901_5902	0.001	0.030	IDW
ID, mo_pct 6900_7500	GM_Consolidated_from_meshes: 6900_7500	mo_pct	mo_pct 6900_7500	0.001	0.015	IDW
ID, mo_pct 7900	GM_Consolidated_from_meshes: 7900	mo_pct	mo_pct 7900	0.001	0.020	IDW
ID, mo_pct 8900	GM_FromMeshes: 8900	mo_pct	mo_pct 8900	0.001	0.015	IDW
ID, mo_pct 9900	GM_FromMeshes: 9900	mo_pct	mo_pct 9900	0.001	0.015	IDW
Kr, ag2_gt	GM_Consolidated_from_meshes: Boundary	ag2_gt	ag2_gt			K
Kr, ag2_gt 1000	GM_Consolidated_from_meshes: 1000	ag2_gt	ag2_gt 1000	0.001	2.500	K

table continues…

General			Estimate Name	Value Capping		Estimate Type
Name	Domain	Values		Lower Bound	Upper Bound	
Kr, ag2_gt 11_12_13_16	GM_Consolidated_from_meshes: 11_12_13_16	ag2_gt	ag2_gt 11_12_13_16	0.001	20.000	K
Kr, ag2_gt 1900	GM_FromMeshes: 1900	ag2_gt	ag2_gt 1900	0.001	2.000	K
Kr, ag2_gt 2400	GM_FromMeshes: 2400	ag2_gt	ag2_gt 2400	0.001	12.000	K
Kr, ag2_gt 2601	GM_FromMeshes: 2601	ag2_gt	ag2_gt 2601	0.001	3.000	K
Kr, ag2_gt 2602	GM_FromMeshes: 2602	ag2_gt	ag2_gt 2602	0.001	6.000	K
Kr, ag2_gt 2900	GM_FromMeshes: 2900	ag2_gt	ag2_gt 2900	0.001	1.100	K
Kr, ag2_gt 32_33_36	GM_Consolidated_from_meshes: 32_33_36	ag2_gt	ag2_gt 32_33_36	0.001	30.000	K
Kr, ag2_gt 3500	GM_FromMeshes: 3500	ag2_gt	ag2_gt 3500	0.001	2.000	K
Kr, ag2_gt 3900	GM_Consolidated_from_meshes: 3900	ag2_gt	ag2_gt 3900	0.001	10.000	K
Kr, ag2_gt 4601	GM_FromMeshes: 4601	ag2_gt	ag2_gt 4601	0.001	2.000	K
Kr, ag2_gt 4901	GM_FromMeshes: 4901	ag2_gt	ag2_gt 4901	0.001	1.000	K
Kr, ag2_gt 5601	GM_FromMeshes: 5601	ag2_gt	ag2_gt 5601	0.001	3.000	K
Kr, ag2_gt 5602	GM_FromMeshes: 5602	ag2_gt	ag2_gt 5602	0.001	0.900	K
Kr, ag2_gt 5603	GM_FromMeshes: 5603	ag2_gt	ag2_gt 5603	0.001	1.236	K
Kr, ag2_gt 5604	GM_FromMeshes: 5604	ag2_gt	ag2_gt 5604	0.001	4.866	K
Kr, ag2_gt 5605	GM_FromMeshes: 5605	ag2_gt	ag2_gt 5605			K
Kr, ag2_gt 5901_5902	GM_Consolidated_from_meshes: 5901	ag2_gt	ag2_gt 5901_5902	0.001	4.000	K
Kr, ag2_gt 6900_7500	GM_Consolidated_from_meshes: 6900_7500	ag2_gt	ag2_gt 6900_7500	0.001	3.000	K

table continues…

General				Value Capping		
Name	Domain	Values	Estimate Name	Lower Bound	Upper Bound	Estimate Type
Kr, ag2_gt 7900	GM_Consolidated_from_meshes: 7900	ag2_gt	ag2_gt 7900	0.001	2.000	K
Kr, ag2_gt 8900	GM_FromMeshes: 8900	ag2_gt	ag2_gt 8900	0.001	4.000	K
Kr, ag2_gt 9900	GM_FromMeshes: 9900	ag2_gt	ag2_gt 9900	0.001	6.000	K
Kr, au2_gt	GM_Consolidated_from_meshes: Boundary	au2_gt	au2_gt			K
Kr, au2_gt 1000	GM_Consolidated_from_meshes: 1000	au2_gt	au2_gt 1000	0.001	0.600	K
Kr, au2_gt 11_12_13_16	GM_Consolidated_from_meshes: 11_12_13_16	au2_gt	au2_gt 11_12_13_16	0.001	3.000	K
Kr, au2_gt 1900	GM_FromMeshes: 1900	au2_gt	au2_gt 1900	0.001	0.270	K
Kr, au2_gt 2400	GM_FromMeshes: 2400	au2_gt	au2_gt 2400	0.001	1.000	K
Kr, au2_gt 2601	GM_FromMeshes: 2601	au2_gt	au2_gt 2601	0.001	0.300	K
Kr, au2_gt 2602	GM_FromMeshes: 2602	au2_gt	au2_gt 2602	0.001	0.700	K
Kr, au2_gt 2900	GM_FromMeshes: 2900	au2_gt	au2_gt 2900	0.001	0.120	K
Kr, au2_gt 32_33_36	GM_Consolidated_from_meshes: 32_33_36	au2_gt	au2_gt 32_33_36	0.001	3.000	K
Kr, au2_gt 3500	GM_FromMeshes: 3500	au2_gt	au2_gt 3500	0.001	0.400	K
Kr, au2_gt 3900	GM_Consolidated_from_meshes: 3900	au2_gt	au2_gt 3900	0.001	0.250	K
Kr, au2_gt 4601	GM_FromMeshes: 4601	au2_gt	au2_gt 4601	0.001	0.250	K
Kr, au2_gt 4901	GM_FromMeshes: 4901	au2_gt	au2_gt 4901	0.001	0.200	K
Kr, au2_gt 5601	GM_FromMeshes: 5601	au2_gt	au2_gt 5601	0.001	0.300	K
Kr, au2_gt 5602	GM_FromMeshes: 5602	au2_gt	au2_gt 5602	0.001	0.200	K

table continues…

General			Estimate Name	Value Capping		Estimate Type
Name	Domain	Values		Lower Bound	Upper Bound	
Kr, au2_gt 5603	GM_FromMeshes: 5603	au2_gt	au2_gt 5603	0.001	0.150	K
Kr, au2_gt 5604	GM_FromMeshes: 5604	au2_gt	au2_gt 5604	0.001	0.140	K
Kr, au2_gt 5605	GM_FromMeshes: 5605	au2_gt	au2_gt 5605	0.001	0.250	K
Kr, au2_gt 5901_5902	GM_Consolidated_from_meshes: 5901	au2_gt	au2_gt 5901_5902	0.001	0.250	K
Kr, au2_gt 6900_7500	GM_Consolidated_from_meshes: 6900_7500	au2_gt	au2_gt 6900_7500	0.001	0.300	K
Kr, au2_gt 7900	GM_Consolidated_from_meshes: 7900	au2_gt	au2_gt 7900	0.001	0.200	K
Kr, au2_gt 8900	GM_FromMeshes: 8900	au2_gt	au2_gt 8900	0.001	0.100	K
Kr, au2_gt 9900	GM_FromMeshes: 9900	au2_gt	au2_gt 9900	0.001	0.100	K
Kr, au2_gt Blk1	GM_Faults fault block 1: Unknown	au2_gt	au2_gt Blk1	0.001	20.000	K
Kr, cu_pct 1000	GM_Consolidated_from_meshes: 1000	cu_pct	cu_pct 1000	0.001	0.500	K
Kr, cu_pct 11_12_13_16	GM_Consolidated_from_meshes: 11_12_13_16	cu_pct	cu_pct 11_12_13_16	0.001	1.300	K
Kr, cu_pct 1900	GM_FromMeshes: 1900	cu_pct	cu_pct 1900	0.001	0.383	K
Kr, cu_pct 2400	GM_FromMeshes: 2400	cu_pct	cu_pct 2400	0.001	2.000	K
Kr, cu_pct 24_26	GM_Consolidated_from_meshes: 24_26	cu_pct	cu_pct 24_26			K
Kr, cu_pct 2601	GM_FromMeshes: 2601	cu_pct	cu_pct 2601	0.001	0.650	K
Kr, cu_pct 2601 P1	GM_FromMeshes: 2601	cu_pct	cu_pct in GM_FromMeshes: 2601			K
Kr, cu_pct 2601 P2	GM_FromMeshes: 2601	cu_pct	cu_pct in GM_FromMeshes: 2601			K
Kr, cu_pct 2601 P3	GM_FromMeshes: 2601	cu_pct	cu_pct in GM_FromMeshes: 2601			K

table continues…

General				Value Capping		
Name	Domain	Values	Estimate Name	Lower Bound	Upper Bound	Estimate Type
Kr, cu_pct 2602	GM_FromMeshes: 2602	cu_pct	cu_pct 2602	0.001	2.000	K
Kr, cu_pct 2900	GM_FromMeshes: 2900	cu_pct	cu_pct 2900	0.001	0.310	K
Kr, cu_pct 3200 P1	GM_FromMeshes: 3200	cu_pct	cu_pct in GM_FromMeshes: 3200			K
Kr, cu_pct 3200 P2	GM_FromMeshes: 3200	cu_pct	cu_pct in GM_FromMeshes: 3200			K
Kr, cu_pct 3200 P3	GM_FromMeshes: 3200	cu_pct	cu_pct in GM_FromMeshes: 3200			K
Kr, cu_pct 32_33_36	GM_Consolidated_from_meshes: 32_33_36	cu_pct	cu_pct 32_33_36	0.001	1.300	K
Kr, cu_pct 3500	GM_FromMeshes: 3500	cu_pct	cu_pct 3500	0.001	0.310	K
Kr, cu_pct 3900	GM_Consolidated_from_meshes: 3900	cu_pct	cu_pct 3900	0.001	0.320	K
Kr, cu_pct 4601	GM_FromMeshes: 4601	cu_pct	cu_pct 4601	0.001	0.600	K
Kr, cu_pct 4901	GM_FromMeshes: 4901	cu_pct	cu_pct 4901	0.001	0.184	K
Kr, cu_pct 5601	GM_FromMeshes: 5601	cu_pct	cu_pct 5601	0.001	1.090	K
Kr, cu_pct 5602	GM_FromMeshes: 5602	cu_pct	cu_pct 5602	0.001	0.658	K
Kr, cu_pct 5603	GM_FromMeshes: 5603	cu_pct	cu_pct 5603	0.001	0.246	K
Kr, cu_pct 5604	GM_FromMeshes: 5604	cu_pct	cu_pct 5604	0.001	0.216	K
Kr, cu_pct 5605	GM_FromMeshes: 5605	cu_pct	cu_pct 5605	0.001	0.495	K
Kr, cu_pct 5901_5902	GM_Consolidated_from_meshes: 5901	cu_pct	cu_pct 5901_5902	0.001	0.400	K
Kr, cu_pct 6900_7500	GM_Consolidated_from_meshes: 6900_7500	cu_pct	cu_pct 6900_7500	0.001	0.400	K
Kr, cu_pct 7900	GM_Consolidated_from_meshes: 7900	cu_pct	cu_pct 7900	0.001	0.310	K

table continues…

General				Value Capping		
Name	Domain	Values	Estimate Name	Lower Bound	Upper Bound	Estimate Type
Kr, cu_pct 8900	GM_FromMeshes: 8900	cu_pct	cu_pct 8900	0.001	0.200	K
Kr, cu_pct 9900	GM_FromMeshes: 9900	cu_pct	cu_pct 9900	0.001	0.200	K
Kr, mo_pct 1000	GM_Consolidated_from_meshes: 1000	mo_pct	mo_pct 1000	0.001	0.030	K
Kr, mo_pct 11_12_13_16	GM_Consolidated_from_meshes: 11_12_13_16	mo_pct	mo_pct 11_12_13_16	0.001	0.300	K
Kr, mo_pct 1900	GM_FromMeshes: 1900	mo_pct	mo_pct 1900	0.001	0.050	K
Kr, mo_pct 2400	GM_FromMeshes: 2400	mo_pct	mo_pct 2400	0.001	0.200	K
Kr, mo_pct 2601	GM_FromMeshes: 2601	mo_pct	mo_pct 2601	0.001	0.060	K
Kr, mo_pct 2602	GM_FromMeshes: 2602	mo_pct	mo_pct 2602	0.001	2.000	K
Kr, mo_pct 2900	GM_FromMeshes: 2900	mo_pct	mo_pct 2900	0.001	0.015	K
Kr, mo_pct 32_33_36	GM_Consolidated_from_meshes: 32_33_36	mo_pct	mo_pct 32_33_36	0.001	0.200	K
Kr, mo_pct 3500	GM_FromMeshes: 3500	mo_pct	mo_pct 3500	0.001	0.055	K
Kr, mo_pct 3900	GM_Consolidated_from_meshes: 3900	mo_pct	mo_pct 3900	0.001	0.025	K
Kr, mo_pct 4601	GM_FromMeshes: 4601	mo_pct	mo_pct 4601	0.001	0.050	K
Kr, mo_pct 4901	GM_FromMeshes: 4901	mo_pct	mo_pct 4901	0.001	0.008	K
Kr, mo_pct 5601	GM_FromMeshes: 5601	mo_pct	mo_pct 5601	0.001	0.040	K
Kr, mo_pct 5602	GM_FromMeshes: 5602	mo_pct	mo_pct 5602	0.001	0.018	K
Kr, mo_pct 5603	GM_FromMeshes: 5603	mo_pct	mo_pct 5603	0.001	0.014	K
Kr, mo_pct 5604	GM_FromMeshes: 5604	mo_pct	mo_pct 5604	0.001	0.048	K

table continues…

General			Estimate Name	Value Capping		Estimate Type
Name	Domain	Values		Lower Bound	Upper Bound	
Kr, mo_pct 5605	GM_FromMeshes: 5605	mo_pct	mo_pct 5605	0.001	0.008	K
Kr, mo_pct 5901_5902	GM_Consolidated_from_meshes: 5901	mo_pct	mo_pct 5901_5902	0.001	0.030	K
Kr, mo_pct 6900_7500	GM_Consolidated_from_meshes: 6900_7500	mo_pct	mo_pct 6900_7500	0.001	0.015	K
Kr, mo_pct 7900	GM_Consolidated_from_meshes: 7900	mo_pct	mo_pct 7900	0.001	0.020	K
Kr, mo_pct 8900	GM_FromMeshes: 8900	mo_pct	mo_pct 8900	0.001	0.015	K
Kr, mo_pct 9900	GM_FromMeshes: 9900	mo_pct	mo_pct 9900	0.001	0.015	K
NN, ag2_gt 1000	GM_Consolidated_from_meshes: 1000	ag2_gt	ag2_gt 1000	0.001	2.500	NN
NN, ag2_gt 11_12_13_16	GM_Consolidated_from_meshes: 11_12_13_16	ag2_gt	ag2_gt 11_12_13_16	0.001	20.000	NN
NN, ag2_gt 1900	GM_FromMeshes: 1900	ag2_gt	ag2_gt 1900	0.001	2.000	NN
NN, ag2_gt 2400	GM_FromMeshes: 2400	ag2_gt	ag2_gt 2400	0.001	12.000	NN
NN, ag2_gt 2601	GM_FromMeshes: 2601	ag2_gt	ag2_gt 2601	0.001	3.000	NN
NN, ag2_gt 2602	GM_FromMeshes: 2602	ag2_gt	ag2_gt 2602	0.001	6.000	NN
NN, ag2_gt 2900	GM_FromMeshes: 2900	ag2_gt	ag2_gt 2900	0.001	1.100	NN
NN, ag2_gt 32_33_36	GM_Consolidated_from_meshes: 32_33_36	ag2_gt	ag2_gt 32_33_36	0.001	30.000	NN
NN, ag2_gt 3500	GM_FromMeshes: 3500	ag2_gt	ag2_gt 3500	0.001	2.000	NN
NN, ag2_gt 3900	GM_Consolidated_from_meshes: 3900	ag2_gt	ag2_gt 3900	0.001	10.000	NN
NN, ag2_gt 4601	GM_FromMeshes: 4601	ag2_gt	ag2_gt 4601	0.001	2.000	NN
NN, ag2_gt 4901	GM_FromMeshes: 4901	ag2_gt	ag2_gt 4901	0.001	1.000	NN

table continues…

General				Value Capping		
Name	Domain	Values	Estimate Name	Lower Bound	Upper Bound	Estimate Type
NN, ag2_gt 5601	GM_FromMeshes: 5601	ag2_gt	ag2_gt 5601	0.001	3.000	NN
NN, ag2_gt 5602	GM_FromMeshes: 5602	ag2_gt	ag2_gt 5602	0.001	0.900	NN
NN, ag2_gt 5603	GM_FromMeshes: 5603	ag2_gt	ag2_gt 5603	0.001	1.236	NN
NN, ag2_gt 5604	GM_FromMeshes: 5604	ag2_gt	ag2_gt 5604	0.001	4.866	NN
NN, ag2_gt 5605	GM_FromMeshes: 5605	ag2_gt	ag2_gt 5605			NN
NN, ag2_gt 5901_5902	GM_Consolidated_from_meshes: 5901	ag2_gt	ag2_gt 5901_5902	0.001	4.000	NN
NN, ag2_gt 6900_7500	GM_Consolidated_from_meshes: 6900_7500	ag2_gt	ag2_gt 6900_7500	0.001	3.000	NN
NN, ag2_gt 7900	GM_Consolidated_from_meshes: 7900	ag2_gt	ag2_gt 7900	0.001	2.000	NN
NN, ag2_gt 8900	GM_FromMeshes: 8900	ag2_gt	ag2_gt 8900	0.001	4.000	NN
NN, ag2_gt 9900	GM_FromMeshes: 9900	ag2_gt	ag2_gt 9900	0.001	6.000	NN
NN, au2_gt 1000	GM_Consolidated_from_meshes: 1000	au2_gt	au2_gt 1000	0.001	0.600	NN
NN, au2_gt 11_12_13_16	GM_Consolidated_from_meshes: 11_12_13_16	au2_gt	au2_gt 11_12_13_16	0.001	3.000	NN
NN, au2_gt 1900	GM_FromMeshes: 1900	au2_gt	au2_gt 1900	0.001	0.270	NN
NN, au2_gt 2400	GM_FromMeshes: 2400	au2_gt	au2_gt 2400	0.001	1.000	NN
NN, au2_gt 2601	GM_FromMeshes: 2601	au2_gt	au2_gt 2601	0.001	0.300	NN
NN, au2_gt 2602	GM_FromMeshes: 2602	au2_gt	au2_gt 2602	0.001	0.700	NN
NN, au2_gt 2900	GM_FromMeshes: 2900	au2_gt	au2_gt 2900	0.001	0.120	NN
NN, au2_gt 32_33_36	GM_Consolidated_from_meshes: 32_33_36	au2_gt	au2_gt 32_33_36	0.001	3.000	NN

table continues…

General			Estimate Name	Value Capping		Estimate Type
Name	Domain	Values		Lower Bound	Upper Bound	
NN, au2_gt 3500	GM_FromMeshes: 3500	au2_gt	au2_gt 3500	0.001	0.400	NN
NN, au2_gt 3900	GM_Consolidated_from_meshes: 3900	au2_gt	au2_gt 3900	0.001	0.250	NN
NN, au2_gt 4601	GM_FromMeshes: 4601	au2_gt	au2_gt 4601	0.001	0.250	NN
NN, au2_gt 4901	GM_FromMeshes: 4901	au2_gt	au2_gt 4901	0.001	0.200	NN
NN, au2_gt 5601	GM_FromMeshes: 5601	au2_gt	au2_gt 5601	0.001	0.300	NN
NN, au2_gt 5602	GM_FromMeshes: 5602	au2_gt	au2_gt 5602	0.001	0.200	NN
NN, au2_gt 5603	GM_FromMeshes: 5603	au2_gt	au2_gt 5603	0.001	0.150	NN
NN, au2_gt 5604	GM_FromMeshes: 5604	au2_gt	au2_gt 5604	0.001	0.140	NN
NN, au2_gt 5605	GM_FromMeshes: 5605	au2_gt	au2_gt 5605	0.001	0.250	NN
NN, au2_gt 5901_5902	GM_Consolidated_from_meshes: 5901	au2_gt	au2_gt 5901_5902	0.001	0.250	NN
NN, au2_gt 6900_7500	GM_Consolidated_from_meshes: 6900_7500	au2_gt	au2_gt 6900_7500	0.001	0.300	NN
NN, au2_gt 7900	GM_Consolidated_from_meshes: 7900	au2_gt	au2_gt 7900	0.001	0.200	NN
NN, au2_gt 8900	GM_FromMeshes: 8900	au2_gt	au2_gt 8900	0.001	0.100	NN
NN, au2_gt 9900	GM_FromMeshes: 9900	au2_gt	au2_gt 9900	0.001	0.100	NN
NN, cu_pct 1000	GM_Consolidated_from_meshes: 1000	cu_pct	cu_pct 1000	0.001	0.500	NN
NN, cu_pct 11_12_13_16	GM_Consolidated_from_meshes: 11_12_13_16	cu_pct	cu_pct 11_12_13_16	0.001	1.300	NN
NN, cu_pct 1900	GM_FromMeshes: 1900	cu_pct	cu_pct 1900	0.001	0.383	NN
NN, cu_pct 2400	GM_FromMeshes: 2400	cu_pct	cu_pct 2400	0.001	2.000	NN

table continues…

General				Value Capping		
Name	Domain	Values	Estimate Name	Lower Bound	Upper Bound	Estimate Type
NN, cu_pct 2601	GM_FromMeshes: 2601	cu_pct	cu_pct 2601	0.001	0.650	NN
NN, cu_pct 2602	GM_FromMeshes: 2602	cu_pct	cu_pct 2602	0.001	2.000	NN
NN, cu_pct 2900	GM_FromMeshes: 2900	cu_pct	cu_pct 2900	0.001	0.310	NN
NN, cu_pct 32_33_36	GM_Consolidated_from_meshes: 32_33_36	cu_pct	cu_pct 32_33_36	0.001	1.300	NN
NN, cu_pct 3500	GM_FromMeshes: 3500	cu_pct	cu_pct 3500	0.001	0.310	NN
NN, cu_pct 3900	GM_Consolidated_from_meshes: 3900	cu_pct	cu_pct 3900	0.001	0.320	NN
NN, cu_pct 4601	GM_FromMeshes: 4601	cu_pct	cu_pct 4601	0.001	0.600	NN
NN, cu_pct 4901	GM_FromMeshes: 4901	cu_pct	cu_pct 4901	0.001	0.184	NN
NN, cu_pct 5601	GM_FromMeshes: 5601	cu_pct	cu_pct 5601	0.001	1.090	NN
NN, cu_pct 5602	GM_FromMeshes: 5602	cu_pct	cu_pct 5602	0.001	0.658	NN
NN, cu_pct 5603	GM_FromMeshes: 5603	cu_pct	cu_pct 5603	0.001	0.246	NN
NN, cu_pct 5604	GM_FromMeshes: 5604	cu_pct	cu_pct 5604	0.001	0.216	NN
NN, cu_pct 5605	GM_FromMeshes: 5605	cu_pct	cu_pct 5605	0.001	0.495	NN
NN, cu_pct 5901_5902	GM_Consolidated_from_meshes: 5901	cu_pct	cu_pct 5901_5902	0.001	0.400	NN
NN, cu_pct 6900_7500	GM_Consolidated_from_meshes: 6900_7500	cu_pct	cu_pct 6900_7500	0.001	0.400	NN
NN, cu_pct 7900	GM_Consolidated_from_meshes: 7900	cu_pct	cu_pct 7900	0.001	0.310	NN
NN, cu_pct 8900	GM_FromMeshes: 8900	cu_pct	cu_pct 8900	0.001	0.200	NN
NN, cu_pct 9900	GM_FromMeshes: 9900	cu_pct	cu_pct 9900	0.001	0.200	NN

table continues…

General			Estimate Name	Value Capping		Estimate Type
Name	Domain	Values		Lower Bound	Upper Bound	
NN, mo_pct 1000	GM_Consolidated_from_meshes: 1000	mo_pct	mo_pct 1000	0.001	0.030	NN
NN, mo_pct 11_12_13_16	GM_Consolidated_from_meshes: 11_12_13_16	mo_pct	mo_pct 11_12_13_16	0.001	0.300	NN
NN, mo_pct 1900	GM_FromMeshes: 1900	mo_pct	mo_pct 1900	0.001	0.050	NN
NN, mo_pct 2400	GM_FromMeshes: 2400	mo_pct	mo_pct 2400	0.001	0.200	NN
NN, mo_pct 2601	GM_FromMeshes: 2601	mo_pct	mo_pct 2601	0.001	0.060	NN
NN, mo_pct 2602	GM_FromMeshes: 2602	mo_pct	mo_pct 2602	0.001	2.000	NN
NN, mo_pct 2900	GM_FromMeshes: 2900	mo_pct	mo_pct 2900	0.001	0.015	NN
NN, mo_pct 32_33_36	GM_Consolidated_from_meshes: 32_33_36	mo_pct	mo_pct 32_33_36	0.001	0.200	NN
NN, mo_pct 3500	GM_FromMeshes: 3500	mo_pct	mo_pct 3500	0.001	0.055	NN
NN, mo_pct 3900	GM_Consolidated_from_meshes: 3900	mo_pct	mo_pct 3900	0.001	0.025	NN
NN, mo_pct 4601	GM_FromMeshes: 4601	mo_pct	mo_pct 4601	0.001	0.050	NN
NN, mo_pct 4901	GM_FromMeshes: 4901	mo_pct	mo_pct 4901	0.001	0.008	NN
NN, mo_pct 5601	GM_FromMeshes: 5601	mo_pct	mo_pct 5601	0.001	0.040	NN
NN, mo_pct 5602	GM_FromMeshes: 5602	mo_pct	mo_pct 5602	0.001	0.018	NN
NN, mo_pct 5603	GM_FromMeshes: 5603	mo_pct	mo_pct 5603	0.001	0.014	NN
NN, mo_pct 5604	GM_FromMeshes: 5604	mo_pct	mo_pct 5604	0.001	0.048	NN
NN, mo_pct 5605	GM_FromMeshes: 5605	mo_pct	mo_pct 5605	0.001	0.008	NN
NN, mo_pct 5901_5902	GM_Consolidated_from_meshes: 5901	mo_pct	mo_pct 5901_5902	0.001	0.030	NN

table continues…

General			Estimate Name	Value Capping		Estimate Type
Name	Domain	Values		Lower Bound	Upper Bound	
NN, mo_pct 6900_7500	GM_Consolidated_from_meshes: 6900_7500	mo_pct	mo_pct 6900_7500	0.001	0.015	NN
NN, mo_pct 7900	GM_Consolidated_from_meshes: 7900	mo_pct	mo_pct 7900	0.001	0.020	NN
NN, mo_pct 8900	GM_FromMeshes: 8900	mo_pct	mo_pct 8900	0.001	0.015	NN
NN, mo_pct 9900	GM_FromMeshes: 9900	mo_pct	mo_pct 9900	0.001	0.015	NN

The estimation was done in a single pass. Search ellipses for copper, molybdenum, silver and gold interpolation assumed ranges up to twice the maximum range of the variogram for the second structure. A block discretization of 5 x 5 x 3 steps (X, Y, Z) was used. Search parameters are shown in Table 14-9.

Table 14-9: Estimation Search Parameters

General			Ellipsoid Ranges			Ellipsoid Directions				Number of Samples	
Name	Domain	Values	Maximum	Intermediate	Minimum	Dip	Dip Azimuth	Pitch	Variable Orientation	Minimum	Maximum
ID, ag2_gt 1000	GM_Consolidated_from_meshes: 1000	ag2_gt	160	100	50				Variable Topo	5	11
ID, ag2_gt 11_12_13_16	GM_Consolidated_from_meshes: 11_12_13_16	ag2_gt	270	320	320				Variable Orientation	7	11
ID, ag2_gt 1900	GM_FromMeshes: 1900	ag2_gt	440	480	120				Variable Orientation	7	11
ID, ag2_gt 2400	GM_FromMeshes: 2400	ag2_gt	250	120	150				Variable Orientation	7	11
ID, ag2_gt 2601	GM_FromMeshes: 2601	ag2_gt	370	300	120				Variable Orientation	7	11
ID, ag2_gt 2602	GM_FromMeshes: 2602	ag2_gt	400	300	220				Variable Orientation	7	11
ID, ag2_gt 2900	GM_FromMeshes: 2900	ag2_gt	500	470	250				Variable Orientation	7	11
ID, ag2_gt 32_33_36	GM_Consolidated_from_meshes: 32_33_36	ag2_gt	320	240	220				Variable Orientation	7	11
ID, ag2_gt 3500	GM_FromMeshes: 3500	ag2_gt	400	400	200				Variable Orientation	7	11
ID, ag2_gt 3900	GM_Consolidated_from_meshes: 3900	ag2_gt	270	280	280				Variable Orientation	7	11
ID, ag2_gt 4601	GM_FromMeshes: 4601	ag2_gt	320	180	120				Variable Orientation	7	11
ID, ag2_gt 4901	GM_FromMeshes: 4901	ag2_gt	230	150	150				Variable Orientation	7	11
ID, ag2_gt 5601	GM_FromMeshes: 5601	ag2_gt	300	240	110				Variable Orientation	7	11
ID, ag2_gt 5602	GM_FromMeshes: 5602	ag2_gt	280	240	110				Variable Orientation	7	11
ID, ag2_gt 5603	GM_FromMeshes: 5603	ag2_gt	280	240	110				Variable Orientation	7	11
ID, ag2_gt 5604	GM_FromMeshes: 5604	ag2_gt	280	240	110				Variable Orientation	4	11
ID, ag2_gt 5605	GM_FromMeshes: 5605	ag2_gt	280	240	110				Variable Orientation	5	11
ID, ag2_gt 5901_5902	GM_Consolidated_from_meshes: 5901	ag2_gt	280	400	240				Variable Orientation	7	11
ID, ag2_gt 6900_7500	GM_Consolidated_from_meshes: 6900_7500	ag2_gt	420	400	200				Variable Orientation	7	11
ID, ag2_gt 7900	GM_Consolidated_from_meshes: 7900	ag2_gt	520	480	160				Variable Orientation	7	11
ID, ag2_gt 8900	GM_FromMeshes: 8900	ag2_gt	500	450	140				Variable Orientation	7	11
ID, ag2_gt 9900	GM_FromMeshes: 9900	ag2_gt	360	240	100				Variable Orientation	7	11
ID, au2_gt 1000	GM_Consolidated_from_meshes: 1000	au2_gt	160	100	50				Variable Topo	5	11
ID, au2_gt 11_12_13_16	GM_Consolidated_from_meshes: 11_12_13_16	au2_gt	225	340	260				Variable Orientation	7	11
ID, au2_gt 1900	GM_FromMeshes: 1900	au2_gt	500	360	120				Variable Orientation	7	11

table continues…

General			Ellipsoid Ranges			Ellipsoid Directions				Number of Samples	
Name	Domain	Values	Maximum	Intermediate	Minimum	Dip	Dip Azimuth	Pitch	Variable Orientation	Minimum	Maximum
ID, au2_gt 2400	GM_FromMeshes: 2400	au2_gt	260	140	240				Variable Orientation	7	11
ID, au2_gt 2601	GM_FromMeshes: 2601	au2_gt	400	300	240				Variable Orientation	7	11
ID, au2_gt 2602	GM_FromMeshes: 2602	au2_gt	400	300	220				Variable Orientation	7	11
ID, au2_gt 2900	GM_FromMeshes: 2900	au2_gt	500	200	270				Variable Orientation	7	11
ID, au2_gt 32_33_36	GM_Consolidated_from_meshes: 32_33_36	au2_gt	470	360	240				Variable Orientation	7	11
ID, au2_gt 3500	GM_FromMeshes: 3500	au2_gt	400	350	250				Variable Orientation	7	11
ID, au2_gt 3900	GM_Consolidated_from_meshes: 3900	au2_gt	550	550	150				Variable Orientation	7	11
ID, au2_gt 4601	GM_FromMeshes: 4601	au2_gt	320	500	120				Variable Orientation	7	11
ID, au2_gt 4901	GM_FromMeshes: 4901	au2_gt	320	300	260				Variable Orientation	7	11
ID, au2_gt 5601	GM_FromMeshes: 5601	au2_gt	300	240	110				Variable Orientation	7	11
ID, au2_gt 5602	GM_FromMeshes: 5602	au2_gt	280	240	110				Variable Orientation	7	11
ID, au2_gt 5603	GM_FromMeshes: 5603	au2_gt	280	240	110				Variable Orientation	7	11
ID, au2_gt 5604	GM_FromMeshes: 5604	au2_gt	280	240	110				Variable Orientation	4	11
ID, au2_gt 5605	GM_FromMeshes: 5605	au2_gt	280	240	110				Variable Orientation	5	11
ID, au2_gt 5901_5902	GM_Consolidated_from_meshes: 5901	au2_gt	440	330	250				Variable Orientation	7	11
ID, au2_gt 6900_7500	GM_Consolidated_from_meshes: 6900_7500	au2_gt	500	400	270				Variable Orientation	7	11
ID, au2_gt 7900	GM_Consolidated_from_meshes: 7900	au2_gt	550	800	240				Variable Orientation	7	11
ID, au2_gt 8900	GM_FromMeshes: 8900	au2_gt	550	450	80				Variable Orientation	7	11
ID, au2_gt 9900	GM_FromMeshes: 9900	au2_gt	550	450	220				Variable Orientation	7	11
ID, cu_pct 1000	GM_Consolidated_from_meshes: 1000	cu_pct	160	100	50				Variable Topo	5	11
ID, cu_pct 11_12_13_16	GM_Consolidated_from_meshes: 11_12_13_16	cu_pct	269.2	203.3	131.7				Variable Orientation	7	11
ID, cu_pct 1900	GM_FromMeshes: 1900	cu_pct	500	400	150				Variable Orientation	7	11
ID, cu_pct 2400	GM_FromMeshes: 2400	cu_pct	188	109.4	146.7				Variable Orientation	7	11
ID, cu_pct 2601	GM_FromMeshes: 2601	cu_pct	400	300	240				Variable Orientation	7	11
ID, cu_pct 2602	GM_FromMeshes: 2602	cu_pct	400	300	220				Variable Orientation	7	11
ID, cu_pct 2900	GM_FromMeshes: 2900	cu_pct	500	400	120				Variable Orientation	7	11
ID, cu_pct 32_33_36	GM_Consolidated_from_meshes: 32_33_36	cu_pct	550	450	300				Variable Orientation	7	11
ID, cu_pct 3500	GM_FromMeshes: 3500	cu_pct	400	380	180				Variable Orientation	7	11

table continues…

General			Ellipsoid Ranges			Ellipsoid Directions				Number of Samples	
Name	Domain	Values	Maximum	Intermediate	Minimum	Dip	Dip Azimuth	Pitch	Variable Orientation	Minimum	Maximum
ID, cu_pct 3900	GM_Consolidated_from_meshes: 3900	cu_pct	550	550	180				Variable Orientation	7	11
ID, cu_pct 4601	GM_FromMeshes: 4601	cu_pct	400	230	120				Variable Orientation	7	11
ID, cu_pct 4901	GM_FromMeshes: 4901	cu_pct	300	300	250				Variable Orientation	7	11
ID, cu_pct 5601	GM_FromMeshes: 5601	cu_pct	300	240	110				Variable Orientation	7	11
ID, cu_pct 5602	GM_FromMeshes: 5602	cu_pct	280	240	110				Variable Orientation	7	11
ID, cu_pct 5603	GM_FromMeshes: 5603	cu_pct	280	240	110				Variable Orientation	7	11
ID, cu_pct 5604	GM_FromMeshes: 5604	cu_pct	280	240	110				Variable Orientation	4	11
ID, cu_pct 5605	GM_FromMeshes: 5605	cu_pct	280	240	110				Variable Orientation	5	11
ID, cu_pct 5901_5902	GM_Consolidated_from_meshes: 5901	cu_pct	500	400	120				Variable Orientation	7	11
ID, cu_pct 6900_7500	GM_Consolidated_from_meshes: 6900_7500	cu_pct	500	400	250				Variable Orientation	7	11
ID, cu_pct 7900	GM_Consolidated_from_meshes: 7900	cu_pct	500	450	240				Variable Orientation	7	11
ID, cu_pct 8900	GM_FromMeshes: 8900	cu_pct	550	450	150				Variable Orientation	7	11
ID, cu_pct 9900	GM_FromMeshes: 9900	cu_pct	550	450	150				Variable Orientation	7	11
ID, mo_pct 1000	GM_Consolidated_from_meshes: 1000	mo_pct	160	100	50				Variable Topo	5	11
ID, mo_pct 11_12_13_16	GM_Consolidated_from_meshes: 11_12_13_16	mo_pct	600	480	300				Variable Orientation	7	11
ID, mo_pct 1900	GM_FromMeshes: 1900	mo_pct	440	400	200				Variable Orientation	7	11
ID, mo_pct 2400	GM_FromMeshes: 2400	mo_pct	300	260	330				Variable Orientation	7	11
ID, mo_pct 2601	GM_FromMeshes: 2601	mo_pct	350	260	300				Variable Orientation	7	11
ID, mo_pct 2602	GM_FromMeshes: 2602	mo_pct	400	300	220				Variable Orientation	7	11
ID, mo_pct 2900	GM_FromMeshes: 2900	mo_pct	600	550	400				Variable Orientation	7	11
ID, mo_pct 32_33_36	GM_Consolidated_from_meshes: 32_33_36	mo_pct	360	350	350				Variable Orientation	7	11
ID, mo_pct 3500	GM_FromMeshes: 3500	mo_pct	780	700	400				Variable Orientation	7	11
ID, mo_pct 3900	GM_Consolidated_from_meshes: 3900	mo_pct	270	440	120				Variable Orientation	7	11
ID, mo_pct 4601	GM_FromMeshes: 4601	mo_pct	430	300	170				Variable Orientation	7	11
ID, mo_pct 4901	GM_FromMeshes: 4901	mo_pct	400	360	200				Variable Orientation	7	11
ID, mo_pct 5601	GM_FromMeshes: 5601	mo_pct	300	240	110				Variable Orientation	7	11
ID, mo_pct 5602	GM_FromMeshes: 5602	mo_pct	280	240	110				Variable Orientation	7	11
ID, mo_pct 5603	GM_FromMeshes: 5603	mo_pct	280	240	110				Variable Orientation	7	11

table continues…

General			Ellipsoid Ranges			Ellipsoid Directions				Number of Samples	
Name	Domain	Values	Maximum	Intermediate	Minimum	Dip	Dip Azimuth	Pitch	Variable Orientation	Minimum	Maximum
ID, mo_pct 5604	GM_FromMeshes: 5604	mo_pct	280	240	110				Variable Orientation	4	11
ID, mo_pct 5605	GM_FromMeshes: 5605	mo_pct	280	240	110				Variable Orientation	5	11
ID, mo_pct 5901_5902	GM_Consolidated_from_meshes: 5901	mo_pct	500	400	250				Variable Orientation	7	11
ID, mo_pct 6900_7500	GM_Consolidated_from_meshes: 6900_7500	mo_pct	500	400	260				Variable Orientation	7	11
ID, mo_pct 7900	GM_Consolidated_from_meshes: 7900	mo_pct	500	500	250				Variable Orientation	7	11
ID, mo_pct 8900	GM_FromMeshes: 8900	mo_pct	500	450	140				Variable Orientation	7	11
ID, mo_pct 9900	GM_FromMeshes: 9900	mo_pct	550	450	150				Variable Orientation	7	11
Kr, ag2_gt 1000	GM_Consolidated_from_meshes: 1000	ag2_gt	160	100	50				Variable Topo	5	11
Kr, ag2_gt 11_12_13_16	GM_Consolidated_from_meshes: 11_12_13_16	ag2_gt	270	320	320				Variable Orientation	7	11
Kr, ag2_gt 1900	GM_FromMeshes: 1900	ag2_gt	440	480	120				Variable Orientation	7	11
Kr, ag2_gt 2400	GM_FromMeshes: 2400	ag2_gt	250	120	150				Variable Orientation	7	11
Kr, ag2_gt 2601	GM_FromMeshes: 2601	ag2_gt	370	300	120				Variable Orientation	7	11
Kr, ag2_gt 2602	GM_FromMeshes: 2602	ag2_gt	400	300	220				Variable Orientation	7	11
Kr, ag2_gt 2900	GM_FromMeshes: 2900	ag2_gt	500	470	250				Variable Orientation	7	11
Kr, ag2_gt 32_33_36	GM_Consolidated_from_meshes: 32_33_36	ag2_gt	320	240	220				Variable Orientation	7	11
Kr, ag2_gt 3500	GM_FromMeshes: 3500	ag2_gt	400	400	200				Variable Orientation	7	11
Kr, ag2_gt 3900	GM_Consolidated_from_meshes: 3900	ag2_gt	270	280	280				Variable Orientation	7	11
Kr, ag2_gt 4601	GM_FromMeshes: 4601	ag2_gt	320	180	120				Variable Orientation	7	11
Kr, ag2_gt 4901	GM_FromMeshes: 4901	ag2_gt	230	150	150				Variable Orientation	7	11
Kr, ag2_gt 5601	GM_FromMeshes: 5601	ag2_gt	300	240	110				Variable Orientation	7	11
Kr, ag2_gt 5602	GM_FromMeshes: 5602	ag2_gt	280	240	110				Variable Orientation	7	11
Kr, ag2_gt 5603	GM_FromMeshes: 5603	ag2_gt	280	240	110				Variable Orientation	7	11
Kr, ag2_gt 5604	GM_FromMeshes: 5604	ag2_gt	280	240	110				Variable Orientation	4	11
Kr, ag2_gt 5605	GM_FromMeshes: 5605	ag2_gt	280	240	110				Variable Orientation	5	11
Kr, ag2_gt 5901_5902	GM_Consolidated_from_meshes: 5901	ag2_gt	280	400	240				Variable Orientation	7	11
Kr, ag2_gt 6900_7500	GM_Consolidated_from_meshes: 6900_7500	ag2_gt	420	400	200				Variable Orientation	7	11
Kr, ag2_gt 7900	GM_Consolidated_from_meshes: 7900	ag2_gt	520	480	160				Variable Orientation	7	11
Kr, ag2_gt 8900	GM_FromMeshes: 8900	ag2_gt	500	450	140				Variable Orientation	7	11

table continues…

General			Ellipsoid Ranges			Ellipsoid Directions				Number of Samples	
Name	Domain	Values	Maximum	Intermediate	Minimum	Dip	Dip Azimuth	Pitch	Variable Orientation	Minimum	Maximum
Kr, ag2_gt 9900	GM_FromMeshes: 9900	ag2_gt	360	240	100				Variable Orientation	7	11
Kr, au2_gt 1000	GM_Consolidated_from_meshes: 1000	au2_gt	160	100	50				Variable Topo	5	11
Kr, au2_gt 11_12_13_16	GM_Consolidated_from_meshes: 11_12_13_16	au2_gt	225	340	260				Variable Orientation	7	11
Kr, au2_gt 1900	GM_FromMeshes: 1900	au2_gt	500	360	120				Variable Orientation	7	11
Kr, au2_gt 2400	GM_FromMeshes: 2400	au2_gt	260	1.4	240				Variable Orientation	7	11
Kr, au2_gt 2601	GM_FromMeshes: 2601	au2_gt	400	300	240				Variable Orientation	7	11
Kr, au2_gt 2602	GM_FromMeshes: 2602	au2_gt	400	300	220				Variable Orientation	7	11
Kr, au2_gt 2900	GM_FromMeshes: 2900	au2_gt	500	200	270				Variable Orientation	7	11
Kr, au2_gt 32_33_36	GM_Consolidated_from_meshes: 32_33_36	au2_gt	470	360	240				Variable Orientation	7	11
Kr, au2_gt 3500	GM_FromMeshes: 3500	au2_gt	400	350	250				Variable Orientation	7	11
Kr, au2_gt 3900	GM_Consolidated_from_meshes: 3900	au2_gt	550	550	150				Variable Orientation	7	11
Kr, au2_gt 4601	GM_FromMeshes: 4601	au2_gt	320	500	120				Variable Orientation	7	11
Kr, au2_gt 4901	GM_FromMeshes: 4901	au2_gt	320	300	260				Variable Orientation	7	11
Kr, au2_gt 5601	GM_FromMeshes: 5601	au2_gt	300	240	110				Variable Orientation	7	11
Kr, au2_gt 5602	GM_FromMeshes: 5602	au2_gt	280	240	110				Variable Orientation	7	11
Kr, au2_gt 5603	GM_FromMeshes: 5603	au2_gt	280	240	110				Variable Orientation	7	11
Kr, au2_gt 5604	GM_FromMeshes: 5604	au2_gt	280	240	110				Variable Orientation	4	11
Kr, au2_gt 5605	GM_FromMeshes: 5605	au2_gt	280	240	110				Variable Orientation	5	11
Kr, au2_gt 5901_5902	GM_Consolidated_from_meshes: 5901	au2_gt	440	330	250				Variable Orientation	7	11
Kr, au2_gt 6900_7500	GM_Consolidated_from_meshes: 6900_7500	au2_gt	500	400	270				Variable Orientation	7	11
Kr, au2_gt 7900	GM_Consolidated_from_meshes: 7900	au2_gt	550	800	240				Variable Orientation	7	11
Kr, au2_gt 8900	GM_FromMeshes: 8900	au2_gt	550	450	80				Variable Orientation	7	11
Kr, au2_gt 9900	GM_FromMeshes: 9900	au2_gt	550	450	220				Variable Orientation	7	11
Kr, cu_pct 1000	GM_Consolidated_from_meshes: 1000	cu_pct	160	100	50				Variable Topo	5	11
Kr, cu_pct 11_12_13_16	GM_Consolidated_from_meshes: 11_12_13_16	cu_pct	269.2	203.3	131.7				Variable Orientation	7	11
Kr, cu_pct 1900	GM_FromMeshes: 1900	cu_pct	500	400	150				Variable Orientation	7	11
Kr, cu_pct 2400	GM_FromMeshes: 2400	cu_pct	188	109.4	146.7	17.0	288.9	138.0		7	11
Kr, cu_pct 24_26	GM_Consolidated_from_meshes: 24_26	cu_pct	218.2	130.9	43.6	0.0	0.0	90.0		4	20

table continues…

General			Ellipsoid Ranges			Ellipsoid Directions				Number of Samples	
Name	Domain	Values	Maximum	Intermediate	Minimum	Dip	Dip Azimuth	Pitch	Variable Orientation	Minimum	Maximum
Kr, cu_pct 2601	GM_FromMeshes: 2601	cu_pct	400	300	240				Variable Orientation	7	11
Kr, cu_pct 2601 P1	GM_FromMeshes: 2601	cu_pct	80	80	25	64.5	234.7	167.0		7	11
Kr, cu_pct 2601 P2	GM_FromMeshes: 2601	cu_pct	200	80	90	64.5	234.7	167.0		4	11
Kr, cu_pct 2601 P3	GM_FromMeshes: 2601	cu_pct	400	160	180	64.5	234.7	167.0		2	11
Kr, cu_pct 2602	GM_FromMeshes: 2602	cu_pct	400	300	220				Variable Orientation	7	11
Kr, cu_pct 2900	GM_FromMeshes: 2900	cu_pct	500	400	120				Variable Orientation	7	11
Kr, cu_pct 3200 P1	GM_FromMeshes: 3200	cu_pct	140	100	55	59.9	90.5	156.9		7	11
Kr, cu_pct 3200 P2	GM_FromMeshes: 3200	cu_pct	300	100	200	59.9	90.5	156.9		4	11
Kr, cu_pct 3200 P3	GM_FromMeshes: 3200	cu_pct	600	200	400	59.9	90.5	156.9		2	11
Kr, cu_pct 32_33_36	GM_Consolidated_from_meshes: 32_33_36	cu_pct	278.9	227.2	152				Variable Orientation	7	11
Kr, cu_pct 3500	GM_FromMeshes: 3500	cu_pct	400	380	180				Variable Orientation	7	11
Kr, cu_pct 3900	GM_Consolidated_from_meshes: 3900	cu_pct	550	550	180				Variable Orientation	7	11
Kr, cu_pct 4601	GM_FromMeshes: 4601	cu_pct	400	230	120				Variable Orientation	7	11
Kr, cu_pct 4901	GM_FromMeshes: 4901	cu_pct	162.1	150.8	131.7				Variable Orientation	7	11
Kr, cu_pct 5601	GM_FromMeshes: 5601	cu_pct	300	240	110				Variable Orientation	7	11
Kr, cu_pct 5602	GM_FromMeshes: 5602	cu_pct	280	240	110				Variable Orientation	7	11
Kr, cu_pct 5603	GM_FromMeshes: 5603	cu_pct	280	240	110				Variable Orientation	7	11
Kr, cu_pct 5604	GM_FromMeshes: 5604	cu_pct	280	240	110				Variable Orientation	4	11
Kr, cu_pct 5605	GM_FromMeshes: 5605	cu_pct	280	240	110				Variable Orientation	5	11
Kr, cu_pct 5901_5902	GM_Consolidated_from_meshes: 5901	cu_pct	500	400	120				Variable Orientation	7	11
Kr, cu_pct 6900_7500	GM_Consolidated_from_meshes: 6900_7500	cu_pct	500	400	240				Variable Orientation	7	11
Kr, cu_pct 7900	GM_Consolidated_from_meshes: 7900	cu_pct	500	450	240				Variable Orientation	7	11
Kr, cu_pct 8900	GM_FromMeshes: 8900	cu_pct	550	450	150				Variable Orientation	7	11
Kr, cu_pct 9900	GM_FromMeshes: 9900	cu_pct	550	450	150				Variable Orientation	7	11
Kr, mo_pct 1000	GM_Consolidated_from_meshes: 1000	mo_pct	160	100	50				Variable Topo	5	11
Kr, mo_pct 11_12_13_16	GM_Consolidated_from_meshes: 11_12_13_16	mo_pct	600	480	300				Variable Orientation	7	11
Kr, mo_pct 1900	GM_FromMeshes: 1900	mo_pct	440	400	200				Variable Orientation	7	11
Kr, mo_pct 2400	GM_FromMeshes: 2400	mo_pct	300	260	330				Variable Orientation	7	11

table continues…

General			Ellipsoid Ranges			Ellipsoid Directions				Number of Samples	
Name	Domain	Values	Maximum	Intermediate	Minimum	Dip	Dip Azimuth	Pitch	Variable Orientation	Minimum	Maximum
Kr, mo_pct 2601	GM_FromMeshes: 2601	mo_pct	360	260	300				Variable Orientation	7	11
Kr, mo_pct 2602	GM_FromMeshes: 2602	mo_pct	400	300	220				Variable Orientation	7	11
Kr, mo_pct 2900	GM_FromMeshes: 2900	mo_pct	600	550	400				Variable Orientation	7	11
Kr, mo_pct 32_33_36	GM_Consolidated_from_meshes: 32_33_36	mo_pct	360	350	350				Variable Orientation	7	11
Kr, mo_pct 3500	GM_FromMeshes: 3500	mo_pct	780	700	400				Variable Orientation	7	11
Kr, mo_pct 3900	GM_Consolidated_from_meshes: 3900	mo_pct	270	440	120				Variable Orientation	7	11
Kr, mo_pct 4601	GM_FromMeshes: 4601	mo_pct	430	300	170				Variable Orientation	7	11
Kr, mo_pct 4901	GM_FromMeshes: 4901	mo_pct	400	360	200				Variable Orientation	7	11
Kr, mo_pct 5601	GM_FromMeshes: 5601	mo_pct	300	240	110				Variable Orientation	7	11
Kr, mo_pct 5602	GM_FromMeshes: 5602	mo_pct	280	240	110				Variable Orientation	7	11
Kr, mo_pct 5603	GM_FromMeshes: 5603	mo_pct	280	240	110				Variable Orientation	7	11
Kr, mo_pct 5604	GM_FromMeshes: 5604	mo_pct	280	240	110				Variable Orientation	4	11
Kr, mo_pct 5605	GM_FromMeshes: 5605	mo_pct	280	240	110				Variable Orientation	5	11
Kr, mo_pct 5901_5902	GM_Consolidated_from_meshes: 5901	mo_pct	500	400	250				Variable Orientation	7	11
Kr, mo_pct 6900_7500	GM_Consolidated_from_meshes: 6900_7500	mo_pct	500	400	260				Variable Orientation	7	11
Kr, mo_pct 7900	GM_Consolidated_from_meshes: 7900	mo_pct	500	500	250				Variable Orientation	7	11
Kr, mo_pct 8900	GM_FromMeshes: 8900	mo_pct	500	450	140				Variable Orientation	7	11
Kr, mo_pct 9900	GM_FromMeshes: 9900	mo_pct	550	450	150				Variable Orientation	7	11
NN, ag2_gt 1000	GM_Consolidated_from_meshes: 1000	ag2_gt	160	100	50	27.7	249.8	65.2			
NN, ag2_gt 11_12_13_16	GM_Consolidated_from_meshes: 11_12_13_16	ag2_gt	270	320	320	26.0	262.0	107.8			
NN, ag2_gt 1900	GM_FromMeshes: 1900	ag2_gt	440	480	120	17.0	288.9	138.0			
NN, ag2_gt 2400	GM_FromMeshes: 2400	ag2_gt	250	120	150	17.0	288.9	147.5			
NN, ag2_gt 2601	GM_FromMeshes: 2601	ag2_gt	370	300	120	17.0	288.9	154.2			
NN, ag2_gt 2602	GM_FromMeshes: 2602	ag2_gt	400	300	220	83.8	79.8	4.6			
NN, ag2_gt 2900	GM_FromMeshes: 2900	ag2_gt	500	470	250	11.5	344.8	67.1			
NN, ag2_gt 32_33_36	GM_Consolidated_from_meshes: 32_33_36	ag2_gt	320	240	220	44.9	73.7	69.1			
NN, ag2_gt 3500	GM_FromMeshes: 3500	ag2_gt	400	400	200	21.4	231.4	24.9			
NN, ag2_gt 3900	GM_Consolidated_from_meshes: 3900	ag2_gt	270	280	280	44.3	85.5	170.1			

table continues…

General			Ellipsoid Ranges			Ellipsoid Directions				Number of Samples	
Name	Domain	Values	Maximum	Intermediate	Minimum	Dip	Dip Azimuth	Pitch	Variable Orientation	Minimum	Maximum
NN, ag2_gt 4601	GM_FromMeshes: 4601	ag2_gt	320	180	120	87.9	281.2	14.7			
NN, ag2_gt 4901	GM_FromMeshes: 4901	ag2_gt	230	150	150	78.8	95.6	23.7			
NN, ag2_gt 5601	GM_FromMeshes: 5601	ag2_gt	300	240	110	17.5	355.3	109.8			
NN, ag2_gt 5602	GM_FromMeshes: 5602	ag2_gt	280	240	110	17.5	355.3	108.2			
NN, ag2_gt 5603	GM_FromMeshes: 5603	ag2_gt	280	240	110	17.5	355.3	77.8			
NN, ag2_gt 5604	GM_FromMeshes: 5604	ag2_gt	280	240	110	17.5	355.3	85.0			
NN, ag2_gt 5605	GM_FromMeshes: 5605	ag2_gt	280	240	110	17.0	288.9	138.0			
NN, ag2_gt 5901_5902	GM_Consolidated_from_meshes: 5901	ag2_gt	280	400	240	19.6	324.9	110.1			
NN, ag2_gt 6900_7500	GM_Consolidated_from_meshes: 6900_7500	ag2_gt	420	400	200	6.1	31.7	23.4			
NN, ag2_gt 7900	GM_Consolidated_from_meshes: 7900	ag2_gt	520	480	160	74.2	77.7	104.7			
NN, ag2_gt 8900	GM_FromMeshes: 8900	ag2_gt	500	450	140	74.2	77.7	6.7			
NN, ag2_gt 9900	GM_FromMeshes: 9900	ag2_gt	360	240	100	15.5	205.0	63.8			
NN, au2_gt 1000	GM_Consolidated_from_meshes: 1000	au2_gt	160	100	50	27.7	249.8	65.2			
NN, au2_gt 11_12_13_16	GM_Consolidated_from_meshes: 11_12_13_16	au2_gt	225	340	260	15.4	342.5	0.0			
NN, au2_gt 1900	GM_FromMeshes: 1900	au2_gt	500	360	120	17.0	288.9	138.0			
NN, au2_gt 2400	GM_FromMeshes: 2400	au2_gt	260	140	240	17.0	288.9	138.0			
NN, au2_gt 2601	GM_FromMeshes: 2601	au2_gt	400	300	240	17.0	288.9	138.0			
NN, au2_gt 2602	GM_FromMeshes: 2602	au2_gt	400	300	220	83.8	79.8	4.6			
NN, au2_gt 2900	GM_FromMeshes: 2900	au2_gt	500	200	270	11.5	344.8	67.1			
NN, au2_gt 32_33_36	GM_Consolidated_from_meshes: 32_33_36	au2_gt	470	360	240	44.9	73.7	174.3			
NN, au2_gt 3500	GM_FromMeshes: 3500	au2_gt	400	350	250	21.4	231.4	32.6			
NN, au2_gt 3900	GM_Consolidated_from_meshes: 3900	au2_gt	550	550	150	44.3	85.5	170.1			
NN, au2_gt 4601	GM_FromMeshes: 4601	au2_gt	320	500	120	87.9	281.2	0.8			
NN, au2_gt 4901	GM_FromMeshes: 4901	au2_gt	320	300	260	78.8	95.6	176.7			
NN, au2_gt 5601	GM_FromMeshes: 5601	au2_gt	300	240	110	17.0	288.9	138.0			
NN, au2_gt 5602	GM_FromMeshes: 5602	au2_gt	280	240	110	17.5	355.3	87.4			
NN, au2_gt 5603	GM_FromMeshes: 5603	au2_gt	280	240	110	17.5	355.3	77.8			
NN, au2_gt 5604	GM_FromMeshes: 5604	au2_gt	280	240	110	17.5	355.3	85.0			

table continues…

General			Ellipsoid Ranges			Ellipsoid Directions			Variable Orientation	Number of Samples	
Name	Domain	Values	Maximum	Intermediate	Minimum	Dip	Dip Azimuth	Pitch		Minimum	Maximum
NN, au2_gt 5605	GM_FromMeshes: 5605	au2_gt	280	240	110	17.5	355.3	92.3			
NN, au2_gt 5901_5902	GM_Consolidated_from_meshes: 5901	au2_gt	440	330	250	19.6	324.9	65.3			
NN, au2_gt 6900_7500	GM_Consolidated_from_meshes: 6900_7500	au2_gt	500	400	270	6.1	31.7	23.4			
NN, au2_gt 7900	GM_Consolidated_from_meshes: 7900	au2_gt	550	800	240	74.2	77.7	6.7			
NN, au2_gt 8900	GM_FromMeshes: 8900	au2_gt	550	450	80	74.2	77.7	6.7			
NN, au2_gt 9900	GM_FromMeshes: 9900	au2_gt	550	450	220	15.5	205.0	63.8			
NN, cu_pct 1000	GM_Consolidated_from_meshes: 1000	cu_pct	160	100	50	27.7	249.8	65.2			
NN, cu_pct 11_12_13_16	GM_Consolidated_from_meshes: 11_12_13_16	cu_pct	269.2	203.3	131.7	17.0	288.9	138.0			
NN, cu_pct 1900	GM_FromMeshes: 1900	cu_pct	500	400	150	17.0	288.9	138.0			
NN, cu_pct 2400	GM_FromMeshes: 2400	cu_pct	188	109.4	146.7	17.0	288.9	138.0			
NN, cu_pct 2601	GM_FromMeshes: 2601	cu_pct	400	300	240	17.0	288.9	138.0			
NN, cu_pct 2602	GM_FromMeshes: 2602	cu_pct	400	300	220	83.8	79.8	4.6			
NN, cu_pct 2900	GM_FromMeshes: 2900	cu_pct	500	400	120	11.5	344.8	67.1			
NN, cu_pct 32_33_36	GM_Consolidated_from_meshes: 32_33_36	cu_pct	550	450	300	44.9	73.7	174.3			
NN, cu_pct 3500	GM_FromMeshes: 3500	cu_pct	400	380	180	21.4	231.4	32.6			
NN, cu_pct 3900	GM_Consolidated_from_meshes: 3900	cu_pct	550	550	180	44.3	85.5	170.1			
NN, cu_pct 4601	GM_FromMeshes: 4601	cu_pct	400	230	120	87.9	281.2	0.8			
NN, cu_pct 4901	GM_FromMeshes: 4901	cu_pct	300	300	250	78.8	95.6	176.7			
NN, cu_pct 5601	GM_FromMeshes: 5601	cu_pct	300	240	110	17.0	288.9	138.0			
NN, cu_pct 5602	GM_FromMeshes: 5602	cu_pct	280	240	110	17.5	355.3	87.4			
NN, cu_pct 5603	GM_FromMeshes: 5603	cu_pct	280	240	110	17.5	355.3	77.8			
NN, cu_pct 5604	GM_FromMeshes: 5604	cu_pct	280	240	110	17.5	355.3	85.0			
NN, cu_pct 5605	GM_FromMeshes: 5605	cu_pct	280	240	110	17.5	355.3	92.3			
NN, cu_pct 5901_5902	GM_Consolidated_from_meshes: 5901	cu_pct	500	400	120	19.6	324.9	110.1			
NN, cu_pct 6900_7500	GM_Consolidated_from_meshes: 6900_7500	cu_pct	500	400	240	6.1	31.7	23.4			
NN, cu_pct 7900	GM_Consolidated_from_meshes: 7900	cu_pct	500	450	240	74.2	77.7	6.7			
NN, cu_pct 8900	GM_FromMeshes: 8900	cu_pct	550	450	150	74.2	77.7	6.7			
NN, cu_pct 9900	GM_FromMeshes: 9900	cu_pct	550	450	150	15.5	205.0	63.8			

table continues…

General			Ellipsoid Ranges			Ellipsoid Directions			Variable Orientation	Number of Samples	
Name	Domain	Values	Maximum	Intermediate	Minimum	Dip	Dip Azimuth	Pitch		Minimum	Maximum
NN, mo_pct 1000	GM_Consolidated_from_meshes: 1000	mo_pct	160	100	50	27.7	249.8	65.2			
NN, mo_pct 11_12_13_16	GM_Consolidated_from_meshes: 11_12_13_16	mo_pct	600	480	300	17.0	288.9	154.3			
NN, mo_pct 1900	GM_FromMeshes: 1900	mo_pct	440	400	200	17.0	288.9	138.0			
NN, mo_pct 2400	GM_FromMeshes: 2400	mo_pct	300	260	330	17.0	288.9	147.5			
NN, mo_pct 2601	GM_FromMeshes: 2601	mo_pct	360	260	300	17.0	288.9	154.2			
NN, mo_pct 2602	GM_FromMeshes: 2602	mo_pct	400	300	220	83.8	79.8	4.6			
NN, mo_pct 2900	GM_FromMeshes: 2900	mo_pct	600	550	400	11.5	344.8	67.1			
NN, mo_pct 32_33_36	GM_Consolidated_from_meshes: 32_33_36	mo_pct	360	350	350	44.9	73.7	69.1			
NN, mo_pct 3500	GM_FromMeshes: 3500	mo_pct	780	700	400	21.4	231.4	24.9			
NN, mo_pct 3900	GM_Consolidated_from_meshes: 3900	mo_pct	270	440	120	44.3	85.5	170.1			
NN, mo_pct 4601	GM_FromMeshes: 4601	mo_pct	430	300	170	87.9	281.2	14.7			
NN, mo_pct 4901	GM_FromMeshes: 4901	mo_pct	400	360	200	78.8	95.6	23.7			
NN, mo_pct 5601	GM_FromMeshes: 5601	mo_pct	300	240	110	17.5	355.3	109.8			
NN, mo_pct 5602	GM_FromMeshes: 5602	mo_pct	280	240	110	17.5	355.3	108.2			
NN, mo_pct 5603	GM_FromMeshes: 5603	mo_pct	280	240	110	17.5	355.3	77.8			
NN, mo_pct 5604	GM_FromMeshes: 5604	mo_pct	280	240	110	17.5	355.3	85.0			
NN, mo_pct 5605	GM_FromMeshes: 5605	mo_pct	280	240	110	17.5	355.3	92.3			
NN, mo_pct 5901_5902	GM_Consolidated_from_meshes: 5901	mo_pct	500	400	250	19.6	324.9	110.1			
NN, mo_pct 6900_7500	GM_Consolidated_from_meshes: 6900_7500	mo_pct	500	400	260	6.1	31.7	23.4			
NN, mo_pct 7900	GM_Consolidated_from_meshes: 7900	mo_pct	500	500	250	74.2	77.7	6.7			
NN, mo_pct 8900	GM_FromMeshes: 8900	mo_pct	500	450	140	74.2	77.7	6.7			
NN, mo_pct 9900	GM_FromMeshes: 9900	mo_pct	550	450	150	15.5	205.0	63.8			

14.9 Block Model Validation

Several validation techniques have been utilised to ensure that the estimates are reasonable.

- Swath plots comparing composite grade to the kriged estimate in corridors in the X, Y and Z directions. Comparison was also made with inverse distance to the second power (ID2) estimates and nearest neighbour (NN) estimates (representing declustered composite grades). (Examples are shown in Figure 14-5 to Figure 14-7.)
- Comparison with block estimates from the previous mineral resource estimates in 2011 and 2018.
- Visual comparisons on section and in plan. (Examples are shown in Figure 14-8 to Figure 14-11.)
- Comparison of grade–tonnage curves for the kriged estimates and the previous mineral resource estimates and the inverse distance estimates (see Figure 14-12 to Figure 14-15).

Figure 14-5: Copper Eastings Swathplot Example (All Estimated Blocks, Bars Represent Number of Blocks)

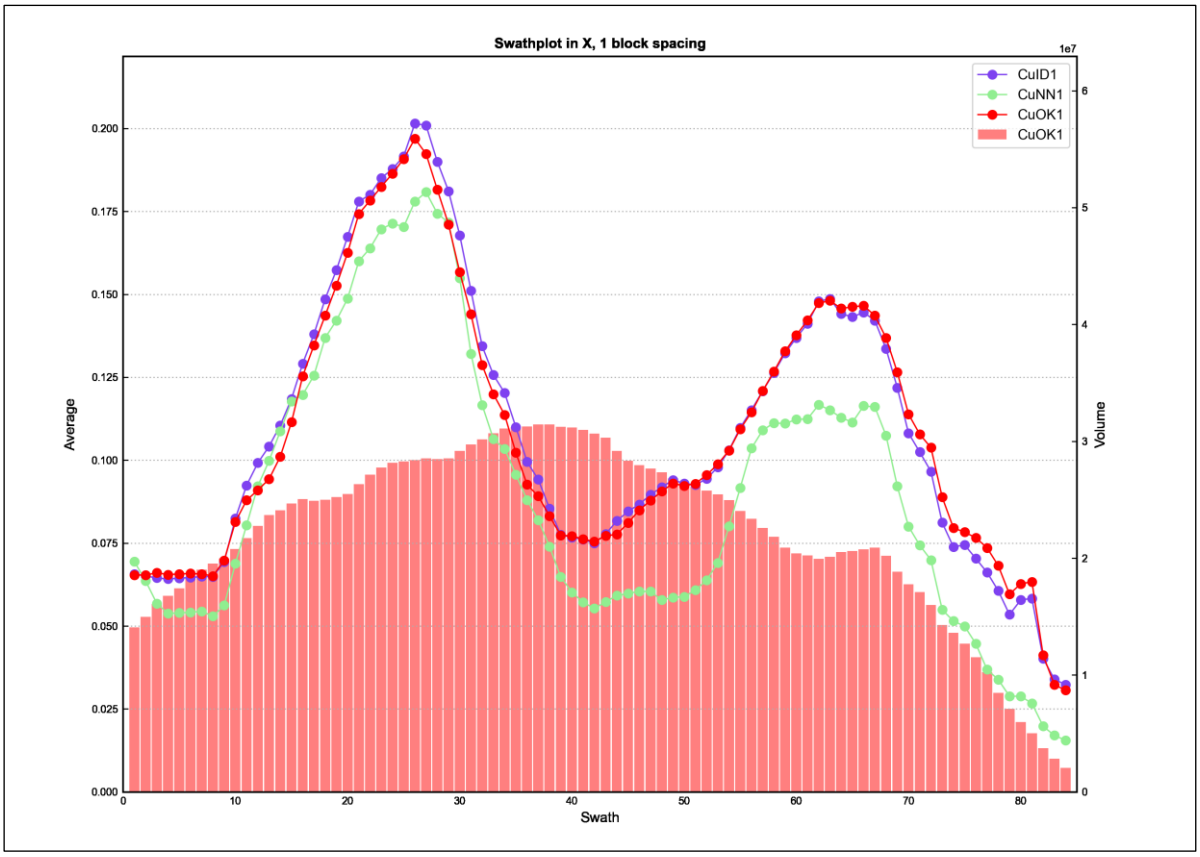

Source: Red Pennant

Figure 14-6: Copper Northings Swathplot Example

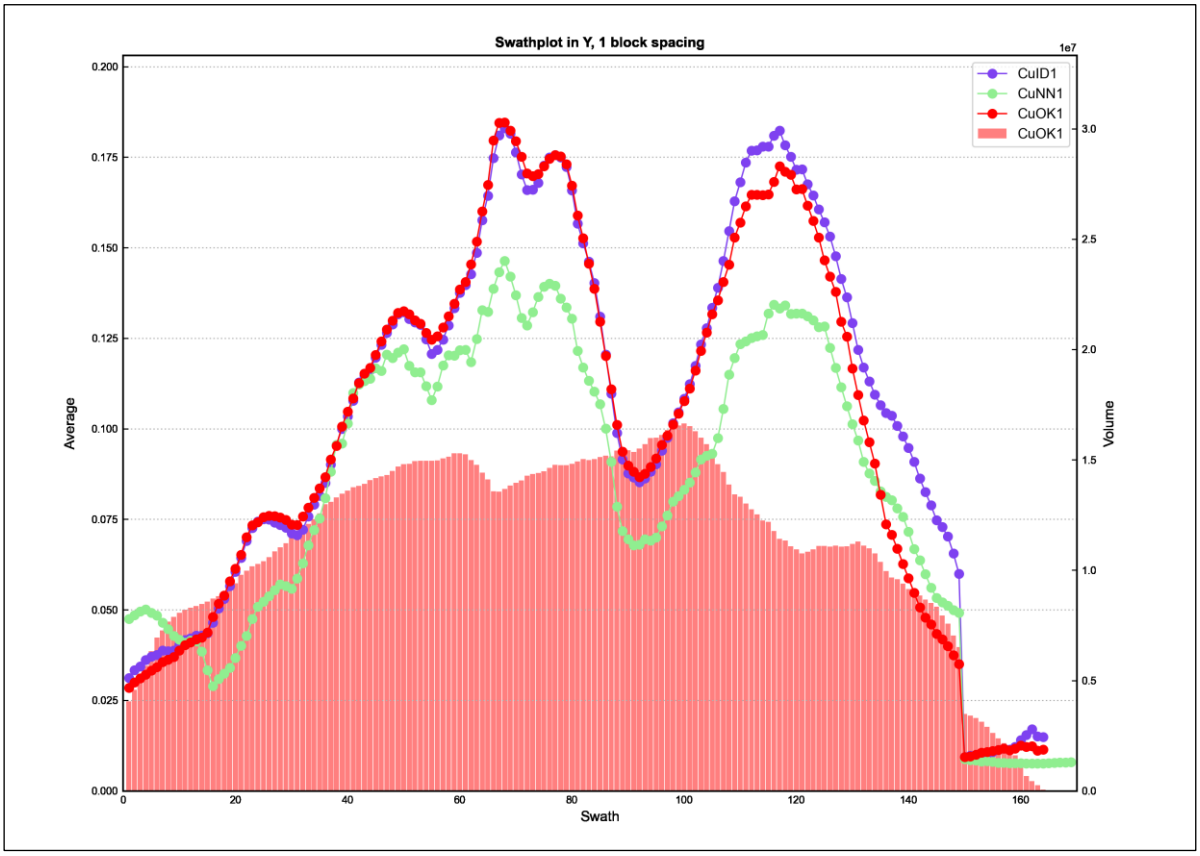

Source: Red Pennant

Figure 14-7: Copper Elevations Swathplot Example

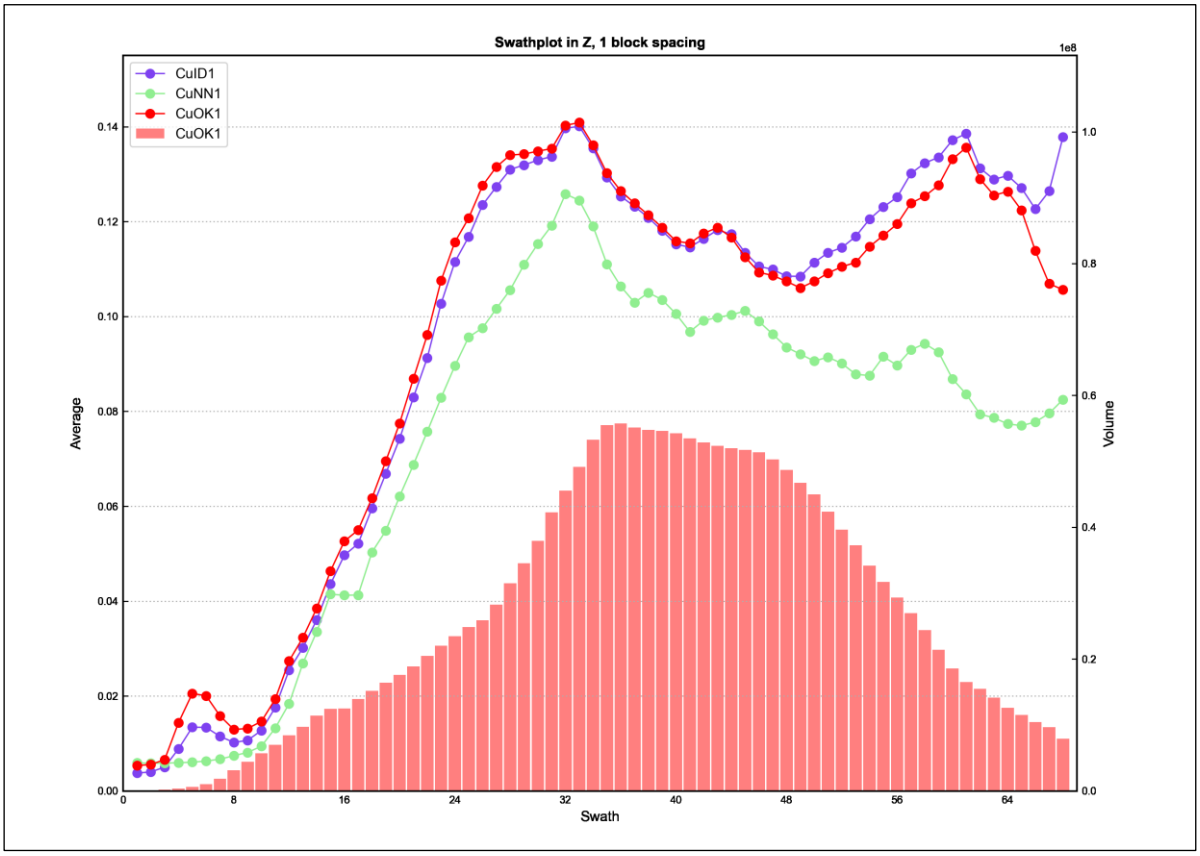

Source: Red Pennant

Figure 14-8: Copper Kriged Block Estimates and Drill Data West-East Section Y+6,359,930 (50 m wide)

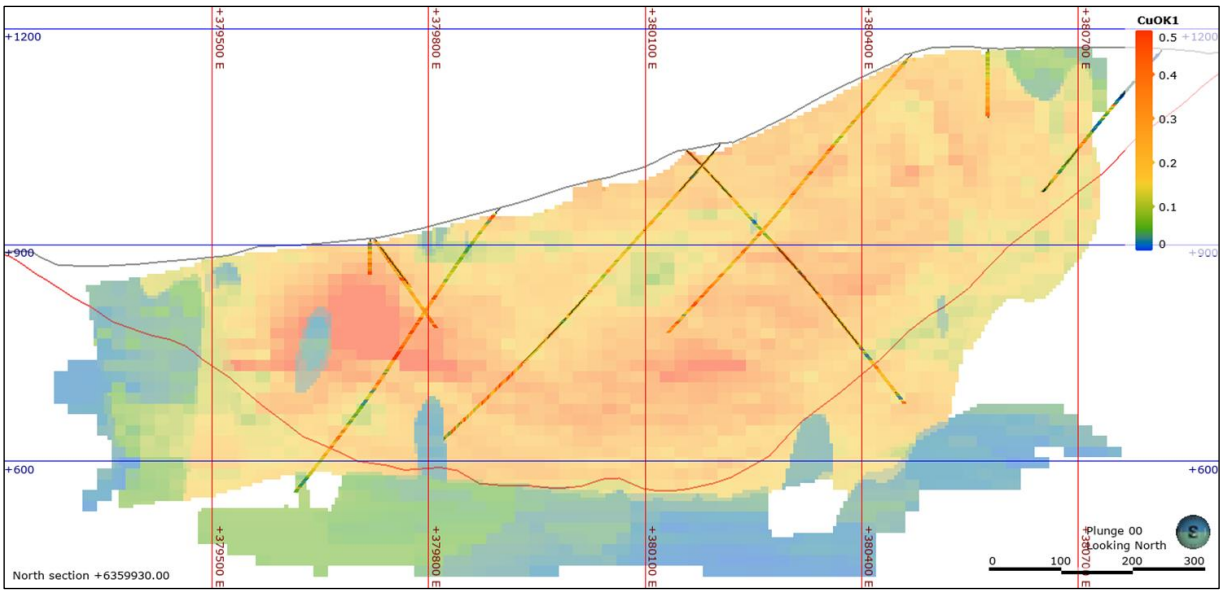

Source: Red Pennant

Figure 14-9: Gold Kriged Block Estimates and Drill Data West-East Section Y+6,359,930

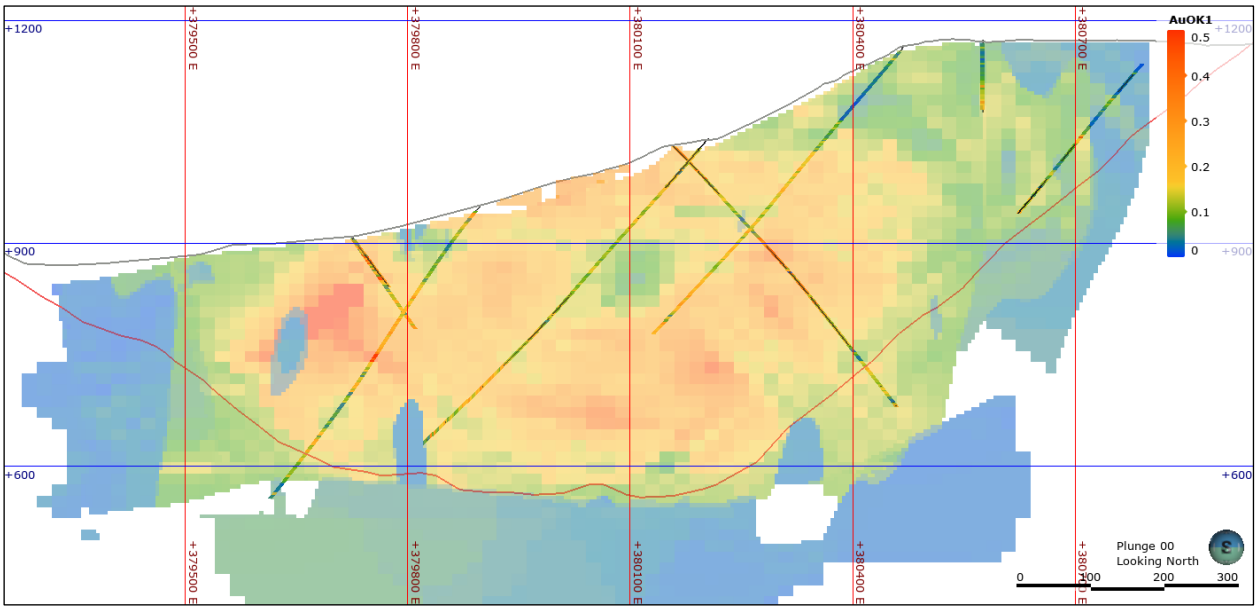

Source: Red Pennant

Figure 14-10: Copper Kriged Block Estimates and Drill Data Paramount-Liard NNW-SSE Section (X+379,872 Y+6,360,170 Looking to 060, 50 m wide)

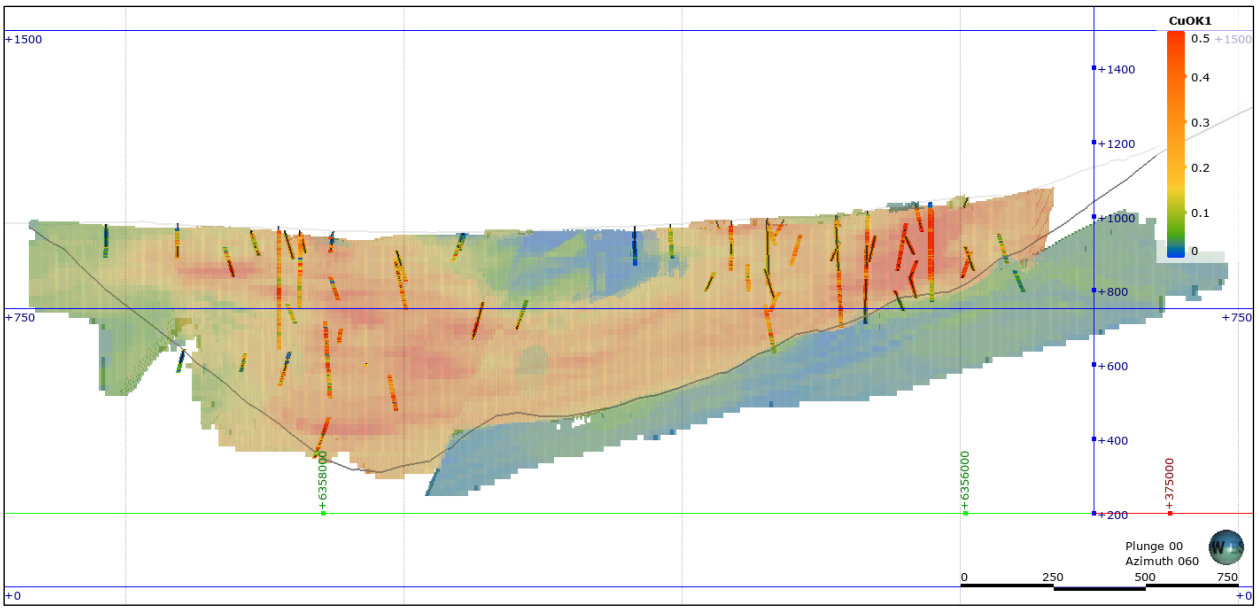

Source: Red Pennant

Figure 14-11: Molybdenum Kriged Block Estimates and Drilled Data Paramount-Liard NNW-SSE Section (X+379,872 Y+6,360,170 Looking to 060)

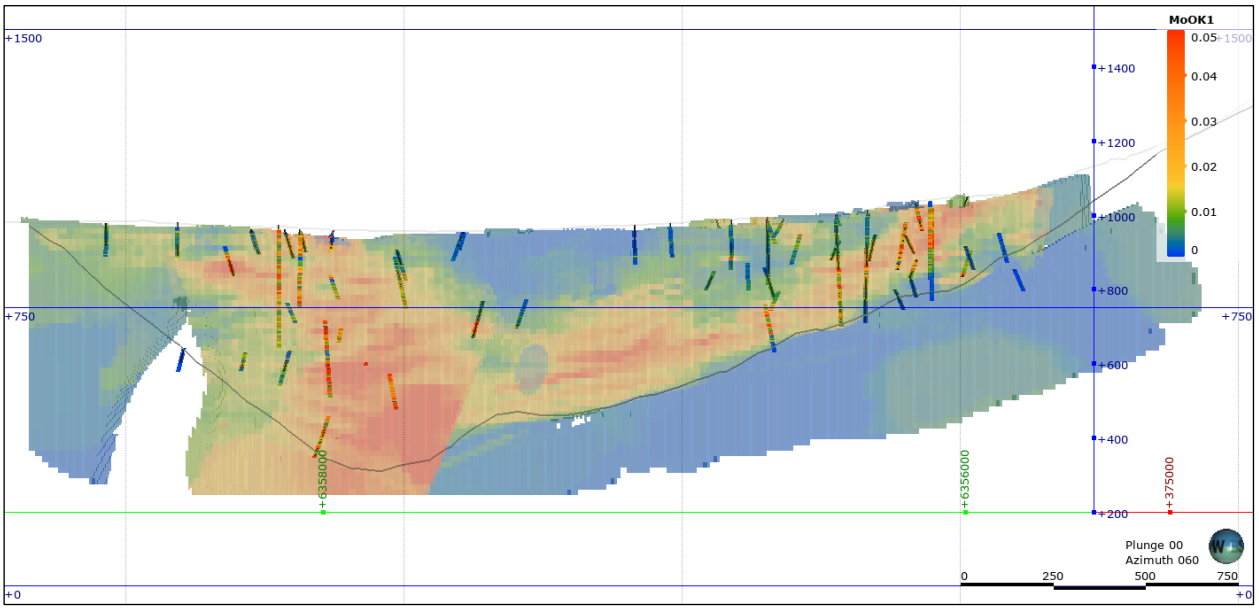

Source: Red Pennant

Figure 14-12: Grade Tonnage Comparison for Copper Block Estimates for the Current Estimates and Previous 2018 and 2011 Estimates

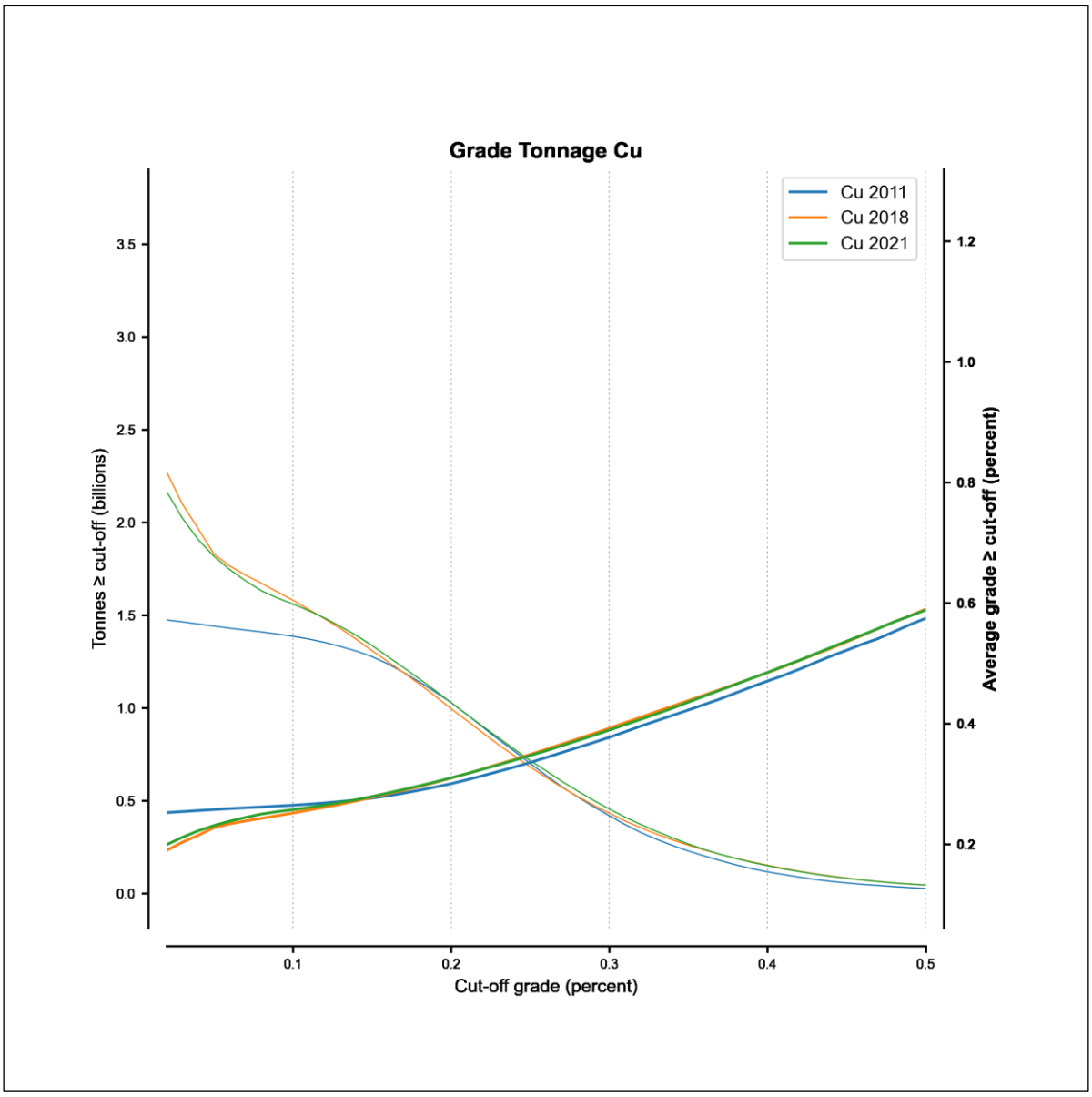

Source: Red Pennant

Figure 14-13: Grade Tonnage Comparison for Gold Block Estimates for the Current Estimates and Previous 2018 and 2011 Estimates

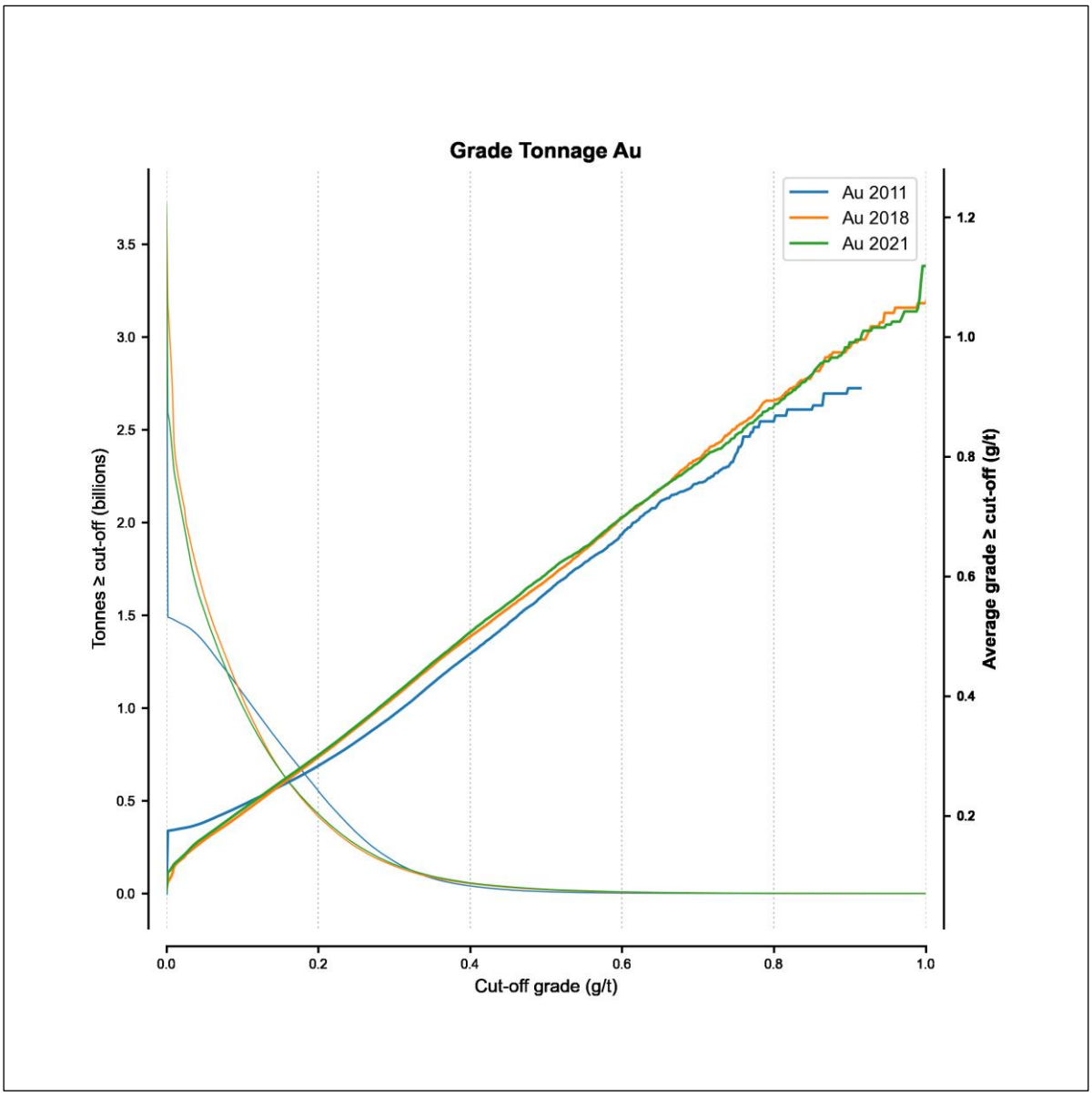

Source: Red Pennant

Figure 14-14: Grade Tonnage Comparison for Molybdenum Block Estimates for the Current Estimates and Previous 2018 and 2011 Estimates.

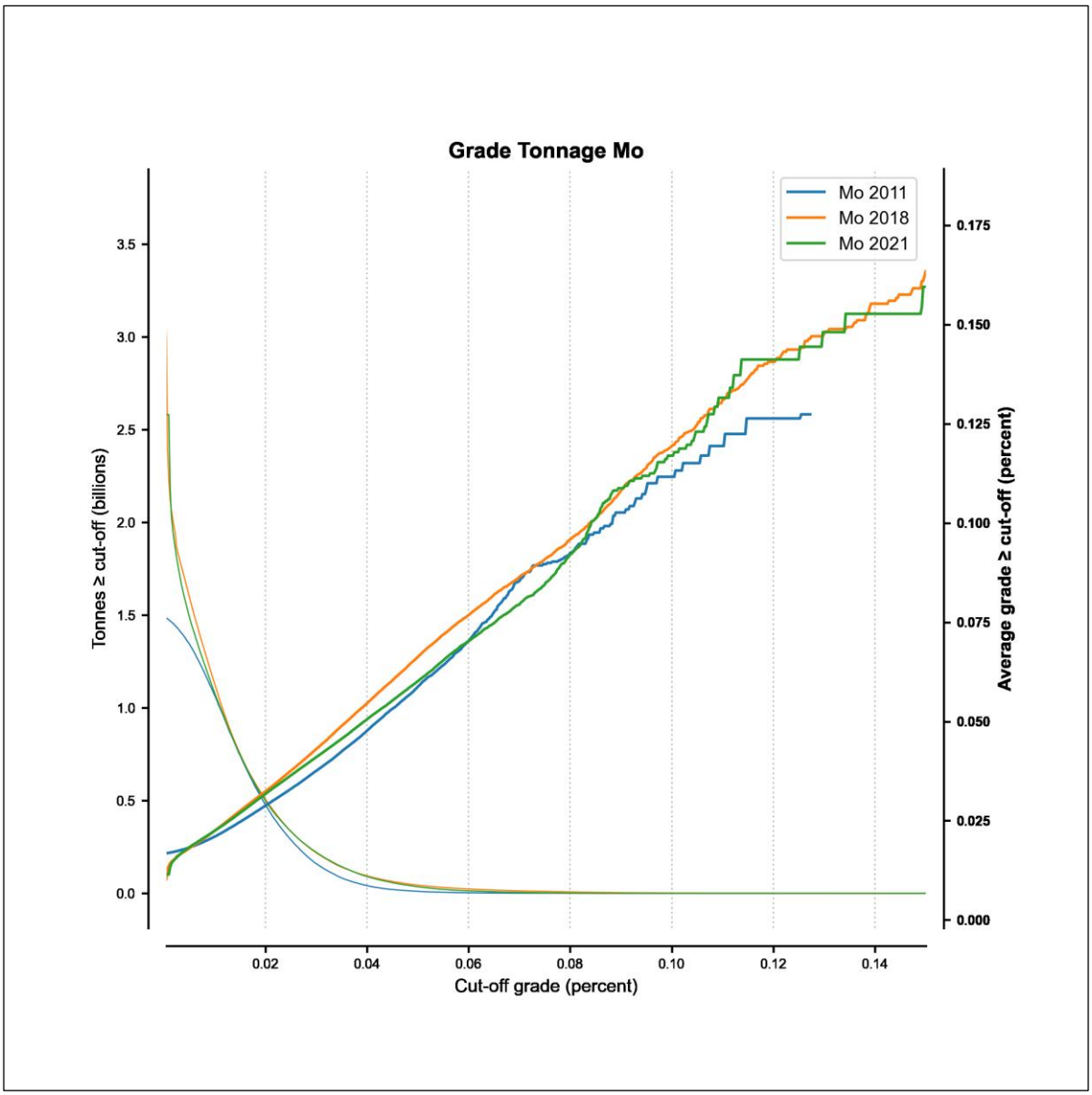

Source: Red Pennant

Figure 14-15: Grade Tonnage Comparison for Silver Block Estimates for the Current Estimates and Previous 2018 and 2011 Estimates

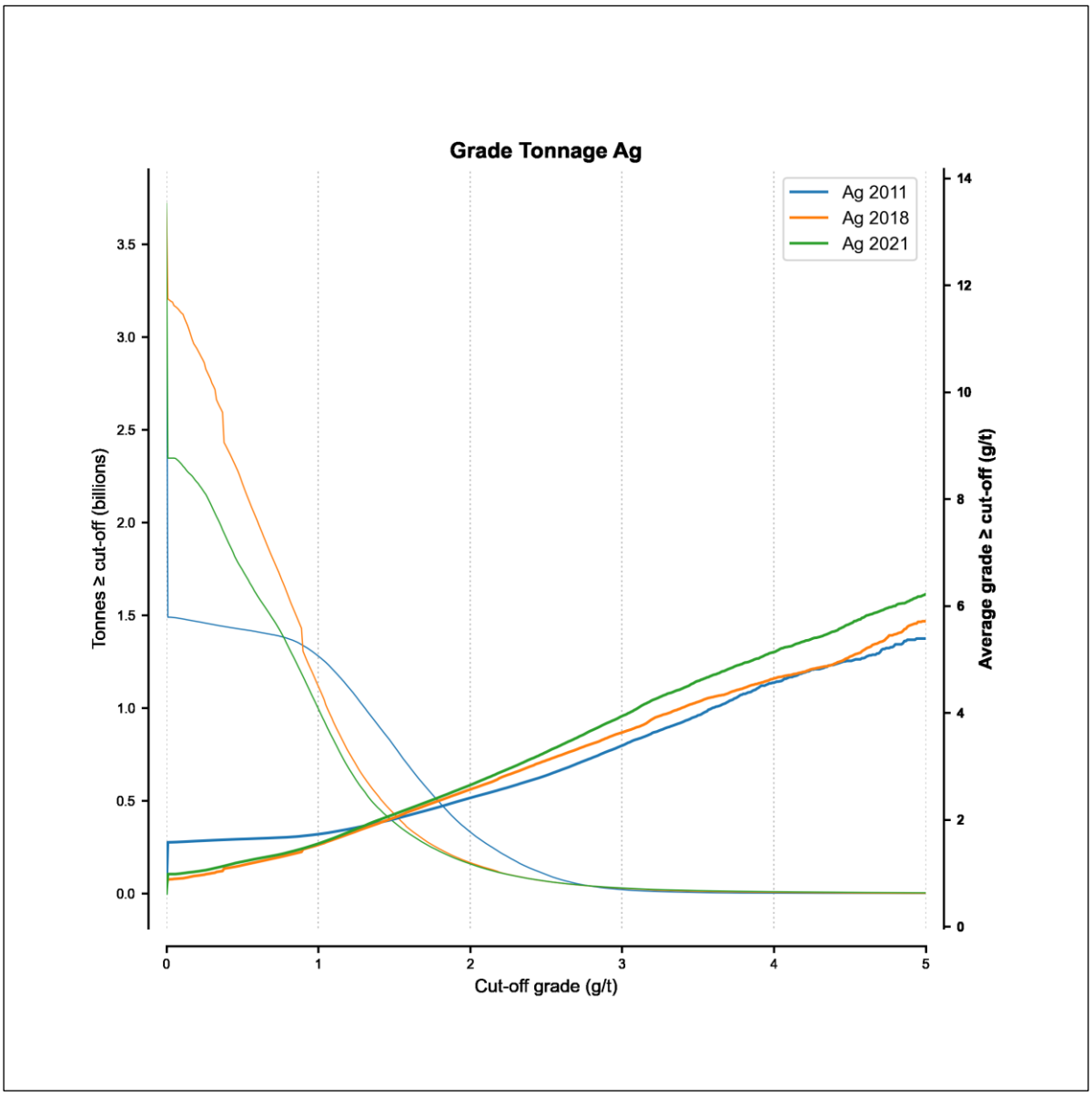

Source: Red Pennant

The validations indicated the block model estimates are reasonable.

14.10 Classification of Mineral Resources

The Kriging Slope of Regression was generated during the estimation and is a measure of confidence related to distance from data in the context of the spatial uncertainty (corresponding with the variogram models). The copper Kriging Slope of Regression was used as the main driver of uncertainty.

Measured, Indicated, and Inferred Mineral Resources were classified using the parameters outlined in Table 14-10.

Table 14-10: Confidence Classification Criteria

Categories	Average Distance to Estimation Composites	Slope of Regression
Measured	<48 m	> 0.85
Indicated	48<128 m	0.6 - 0.85
Inferred	128-500 m	0.05 – 0.6

The extents of measured, indicated, and inferred mineral resources within the conceptual pit are illustrated in Figure 14-16 to Figure 14-18, inclusive.

Figure 14-16: View of Measured Mineral Resource Looking East

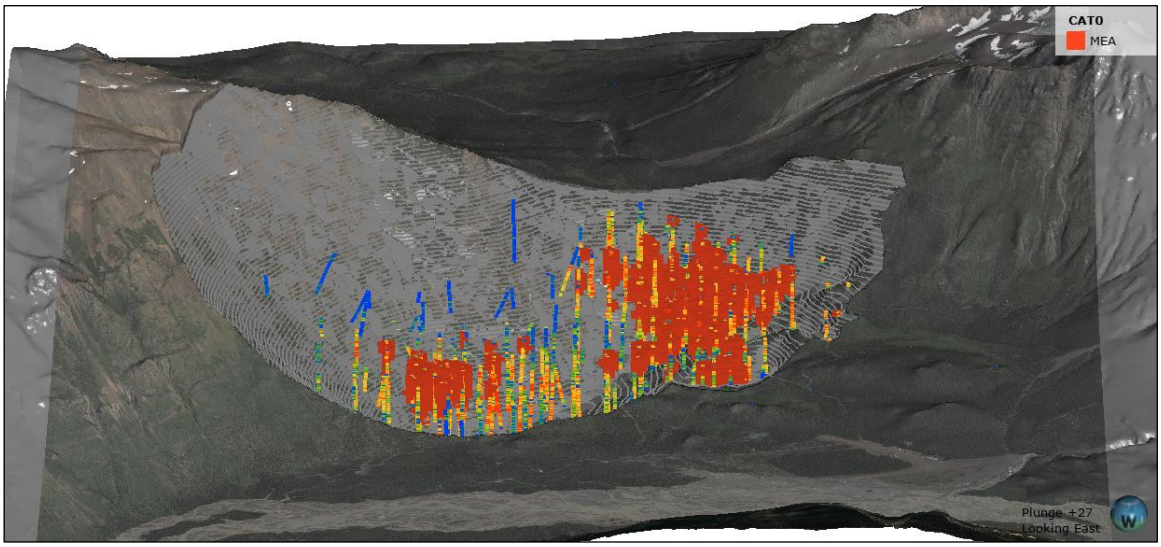

Source: Red Pennant

Figure 14-17: View of Measured & Indicated Mineral Resources Looking East

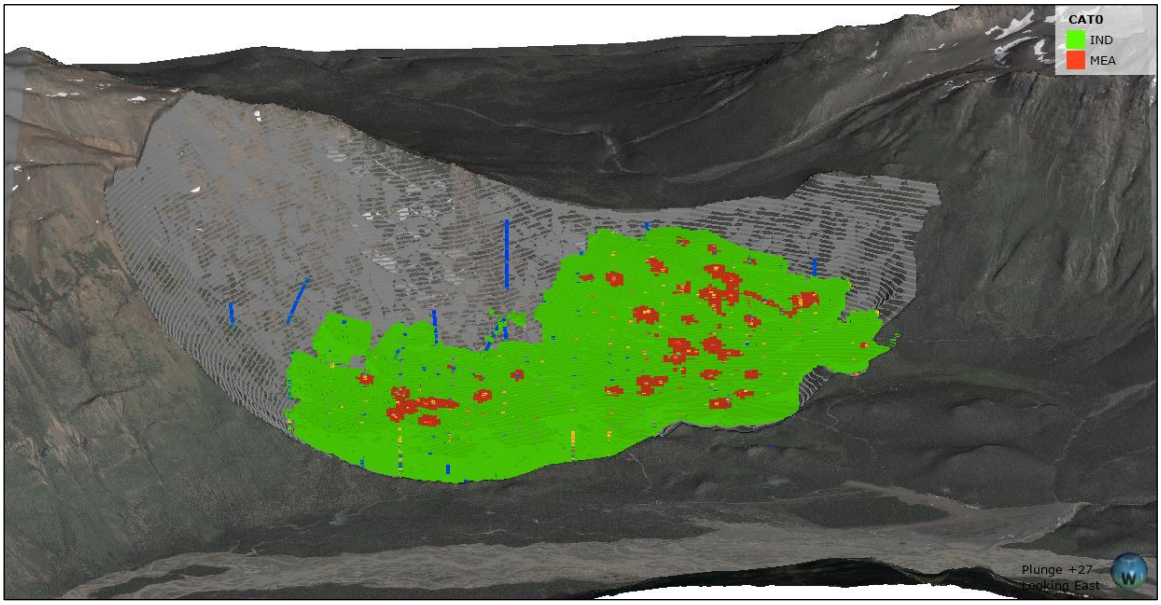

Source: Red Pennant

Figure 14-18: View of Measured, Indicated & Inferred Mineral Resources Looking East

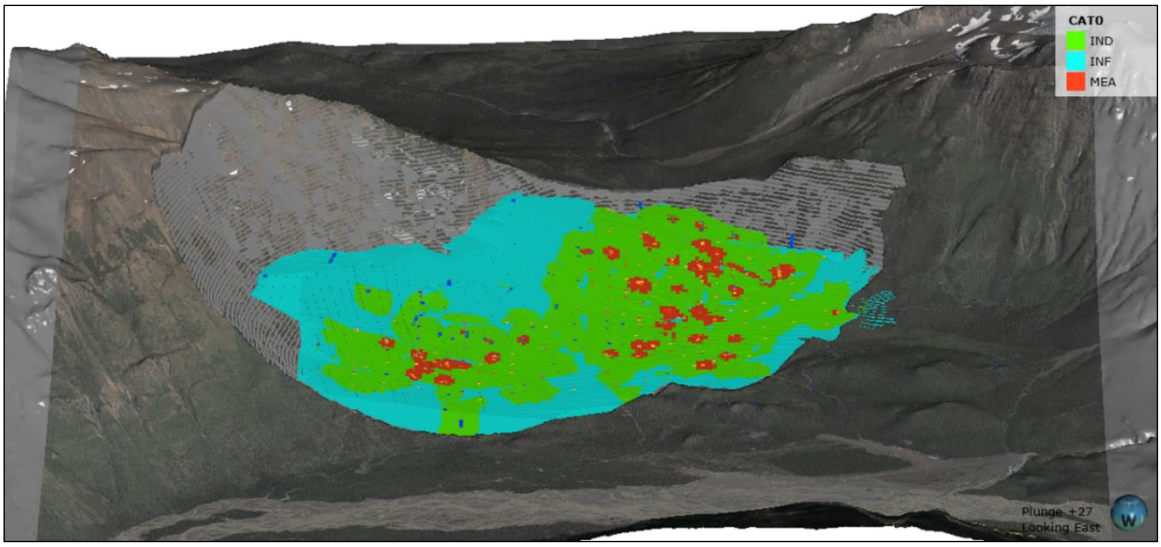

Source: Red Pennant

14.11 Reasonable Prospects of Eventual Economic Extraction

Mineral Resources were constrained using a conceptual ultimate pit shell based on the input parameters listed in Table 14-11. These values were used to calculate a block-by-block net smelter return (NSR) for copper and molybdenum concentrates. The parameters and pit shell are the same as the pit shell used to constrain the mineral resources in 2018.

Table 14-11: Conceptual Pit Shell Input Parameters

	Units	Values
Metal Prices		
Copper	US$/lb	3.00
Molybdenum	US$/lb	10.00
Gold	US$/oz	1,200.00
Silver	US$/oz	20.00
Mill Feed Rate		
Tonnes per annum	Mt	47.5
Financial Analysis Assumptions		
Discount rate	%	8.0
Exchange rate	$CAD/$US	1.20
Copper Concentrate		
Copper concentrate grade	%	28.00
Copper recovery	%	90.00*
Molybdenum Concentrate		
Molybdenum concentrate grade	%	50.00
Molybdenum recovery	%	85.00*
Unit Costs		
Processing and general and administrative costs	US$/t	4.31
Mining cost	US$/t	1.95
Pit Slopes Whittle		
All units (overall slope angle) (OSA)	degrees	40 to 44

14.12 Resource Sensitivity to Cut-off

The tonnage and grade sensitivities at different cut-off (NSR) values are illustrated in Figure 14-19 and Figure 14-20, for measured and indicated mineral resources and in Figure 14-21 and Figure 14-22, for inferred mineral resources within the conceptual resource pit shell.

Figure 14-19: Measured and Indicated Cu, Mo Grade and Tonnage Trends at Different NSR Cut-offs

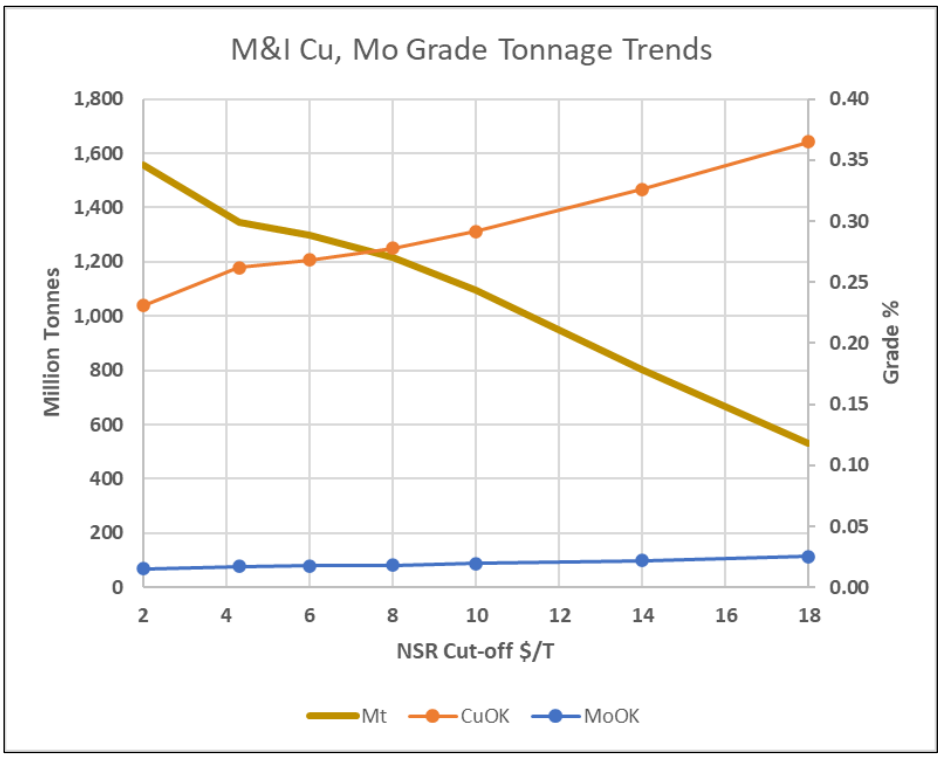

Source: Red Pennant

Figure 14-20: Measured and Indicated Au, Ag Grade and Tonnage Trends at Different NSR Cut-offs

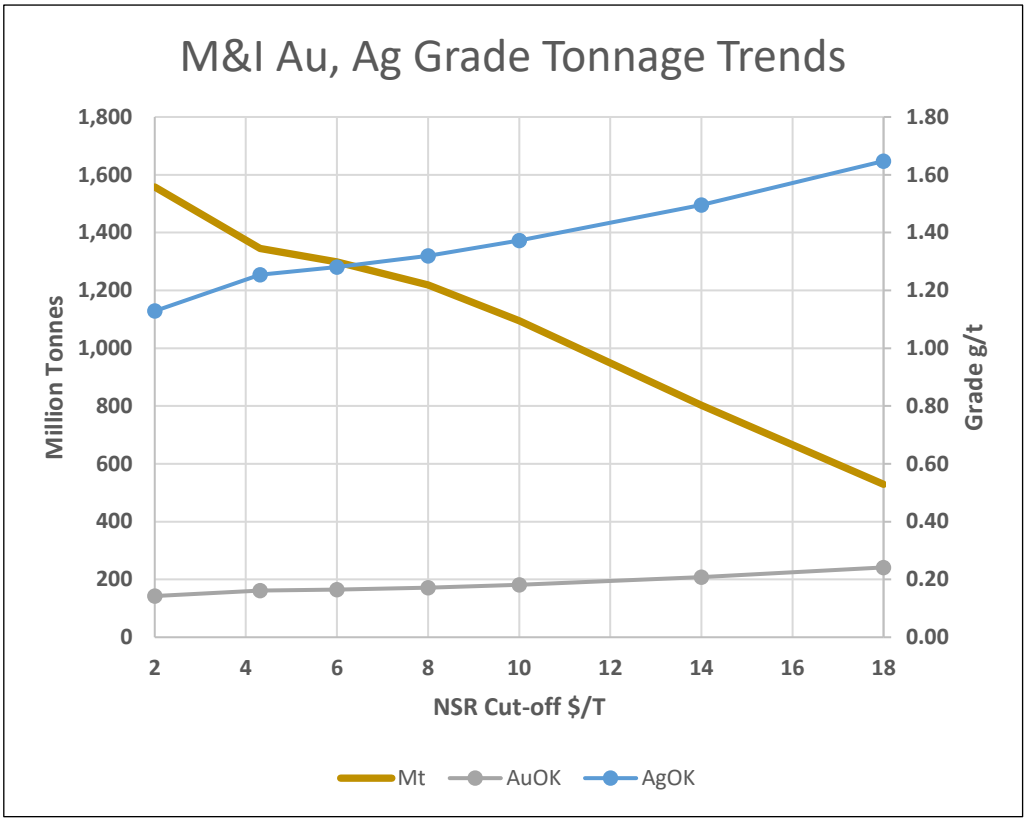

Source: Red Pennant

Figure 14-21: Inferred Material Cu, Mo Grade and Tonnage Trends at Different NSR Cut-offs

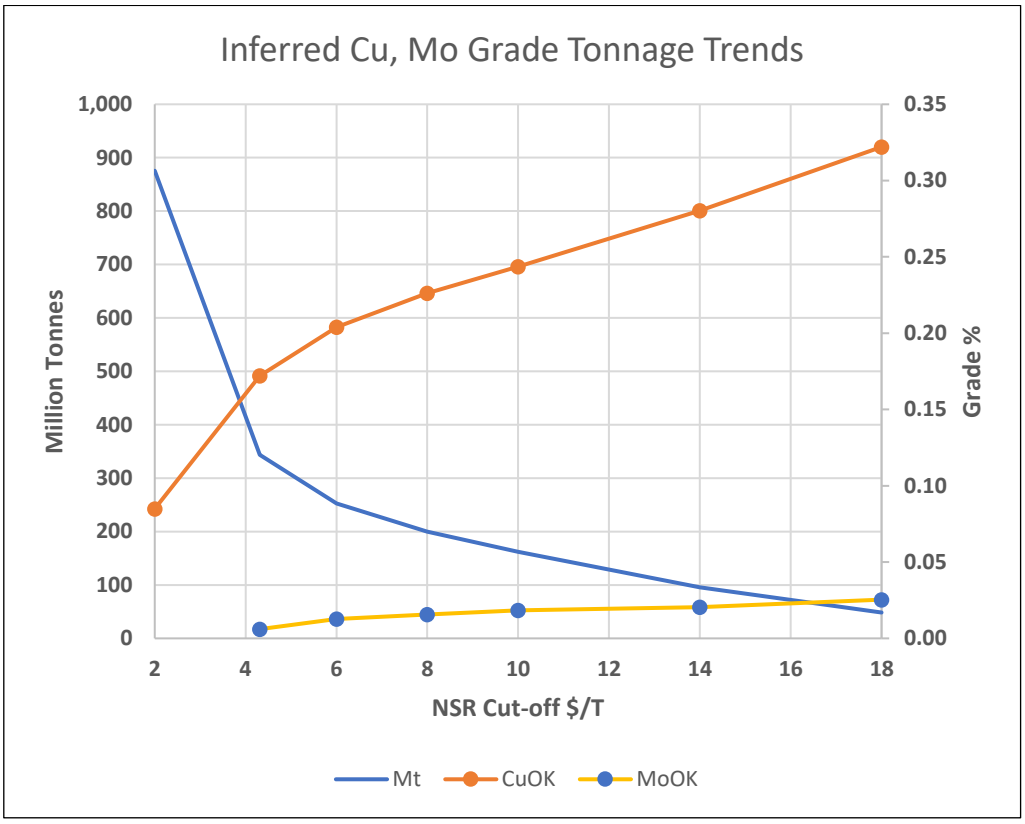

Source: Red Pennant

Figure 14-22: Inferred Material Au, Ag Grade and Tonnage Trends at Different NSR Cut-offs

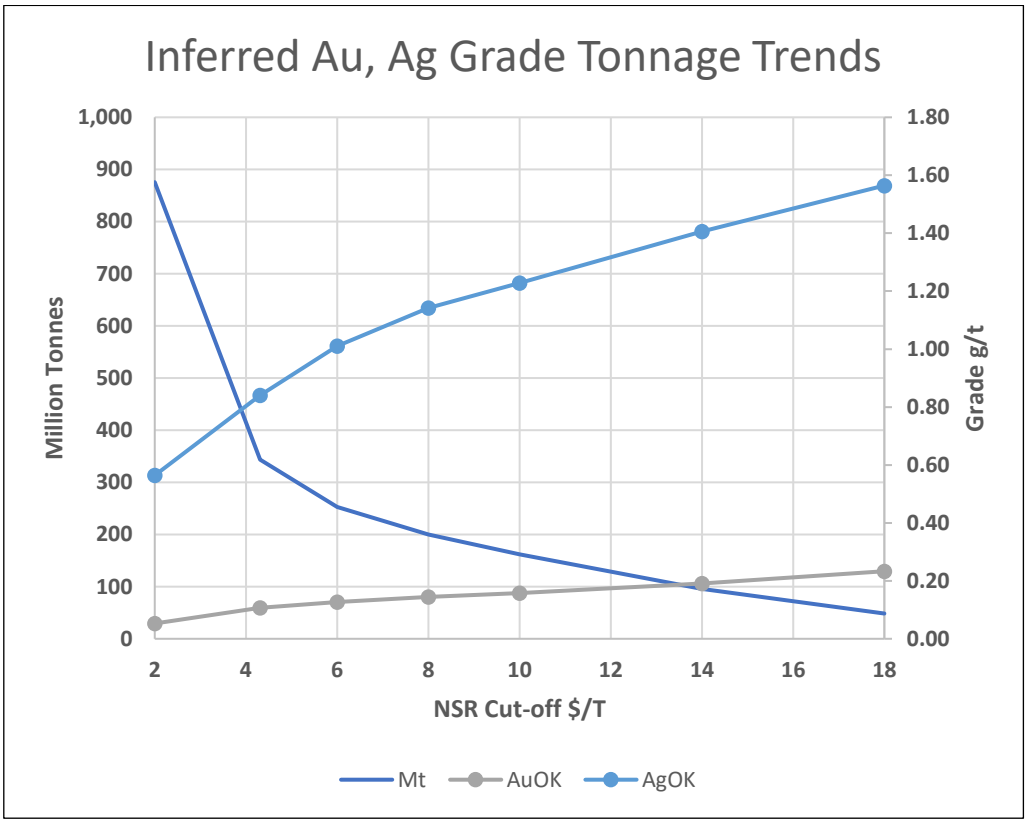

Source: Red Pennant

14.13 Mineral Resource Statement

The Mineral Resource was estimated in January 2021 and constrained within an optimized ultimate pit shell and are summarized in Table 14-12.

Table 14-12: Mineral Resource Statement

		Average Value				Material Content			
	Mass	Cu	Au	Mo	Ag	Cu	Au	Mo	Ag
Category	Mt	%	g/t	%	g/t	million lb	million t. oz	million lb	million t. oz
Measured	176	0.32	0.22	0.018	1.46	1,262	1.28	71	8.26
Indicated	1,169	0.25	0.15	0.017	1.22	6,503	5.69	440	46.00
Total M&I	**1,346**	**0.26**	**0.16**	0.017	**1.25**	**7,764**	**6.97**	**511**	**54.25**
Inferred	344	0.17	0.11	0.013	0.84	1,303	1.18	96	9.28

Notes:

Mt=millions of tonnes, Cu=copper, Au=gold, Mo=molybdenum, Ag=silver, Mlbs.=millions of pounds, Mozs.=millions of ounces.

Notes: Mineral Resources are reported using the 2014 CIM Definition Standards.

The QP for the estimate is Mr. Michael F O'Brien, P.Geo., Red Pennant Resources Geoscience. Mineral Resources have an effective date of 15 January 2021.

Mineral Resources are reported within a conceptual constraining pit shell that includes the following input parameters: $3/lb Cu, $10/lb Mo, $1,200/oz Au, $20/oz Ag, mining cost of CA$1.95/t mined, processing cost of CA$4.94/t processed and pit slope angles that vary from 40–44º. Metal recoveries; Cu 86.6%, Au 73%, Mo 58.8%, Ag 48.3%.

Mineral Resources are reported using a net smelter return cut-off of US$4.31/t, and a Cdn$ to US$ exchange rate of 1.20. Metal prices are in $US.

Tonnes are metric tonnes, with copper and molybdenum grades as percentages, and gold and silver grades as gram per tonne units. Copper and molybdenum metal content is reported in pounds and gold and silver content is reported in troy ounces.

Totals may not sum due to rounding.

14.14 Factors That May Affect the Mineral Resource Estimate

Areas of uncertainty that may materially impact the Mineral Resource estimates include:

- Changes to long-term metal price assumptions;
- Changes in local interpretations of mineralization geometry, fault geometry and continuity of mineralized zones;
- Changes to the net smelter return used to constrain the estimates;
- Changes to the regression equation used to fill in missing gold and silver values;
- Changes to metallurgical recovery assumptions;
- Changes to the input assumptions used to derive the conceptual open pit outlines used to constrain the estimate;

- Changes to resource classification approach;
- Variations in geotechnical, hydrogeological and mining assumptions;
- Changes to environmental, permitting and social license assumptions.

14.15 Comments on Section 14.0

The QP believes that the Mineral Resources have been estimated using good industry practice and conform to the 2014 CIM Definition Standards. Mineral Resources are constrained by reasonable open pit mining assumptions.

There are no other known environmental, legal, title, taxation, socioeconomic, marketing, political or other relevant factors that would materially affect the estimation of Mineral Resources that are not discussed in this Report.

15.0 MINERAL RESERVE ESTIMATES

This section is not relevant for this Report.

16.0 MINING METHODS

This section is not relevant for this Report.

17.0 RECOVERY METHODS

This section is not relevant for this Report.

18.0 PROJECT INFRASTRUCTURE

This section is not relevant for this Report.

19.0 MARKET STUDIES AND CONTRACTS

This section is not relevant for this Report.

20.0 ENVIRONMENTAL STUDIES, PERMITTING AND SOCIAL OR COMMUNITY IMPACT

This section is not relevant for this Report.

21.0 CAPITAL AND OPERATING COSTS

This section is not relevant for this Report.

22.0 ECONOMIC ANALYSIS

This section is not relevant for this Report.

23.0 ADJACENT PROPERTIES

There are no material adjacent properties.

24.0 OTHER RELEVANT DATA AND INFORMATION

This section is not relevant for this Report.

25.0 INTERPRETATION AND CONCLUSIONS

25.1 Introduction

Based on the review of all relevant data, reports and previous metallurgical test work programs, the QPs for this Report provided the following interpretations and conclusions:

25.2 Mineral Tenure, Surface Rights, Water Rights, Royalties and Agreements

Information provided by Copper Fox and available through Mineral Titles Online (BC) regarding the mineral tenure over the Project area supports that the Schaft Creek JV has a valid title that is sufficient to support estimation of Mineral Resources.

To the extent known, there are no other significant factors and risks that may affect access, title, or the right or ability to perform work on the Project that are not discussed in this Report.

25.3 Geology and Mineralization

The Schaft Creek deposit is classified as calc-alkalic porphyry copper-gold molybdenum style mineralization.

The extensive work since the early 1960s has informed a good understanding of the regional setting, lithologies, and the geological, structural, and alteration controls on mineralization and is sufficient to support estimation of Mineral Resources.

The Schaft Creek Project covers an extensive porphyry complex that extends over approximately 15 km including the Schaft Creek deposit and the Discovery Zone. The limits of the mineralization in the Schaft Creek deposit have not been delineated and remain open at depth, along strike, and to the east. Drilling (four drill holes) on the Discovery Zone located 1.2 km along strike of the Schaft Creek deposit intersected porphyry style copper-molybdenum-gold-silver mineralization over significant widths, the limits of which have not been delineated. Geological mapping/sampling, soil, stream sediment and silt sampling and geophysics surveys have identified several targets along strike of the Schaft Creek deposit that indicate potential for additional zones of porphyry copper-gold mineralization within the complex.

25.4 Exploration, Drilling, and Analytical Data

The exploration programs completed on the Schaft Creek deposit, the Discovery Zone, and regionally are appropriate for this style of the deposit/mineralization.

The sampling methods used in the various programs were reviewed and found to be acceptable for Mineral Resource estimation. Sample preparation, analysis, and security measures were consistent with industry standards at the time the sampling was conducted.

The quantity and quality of the lithological, geotechnical, drill collar, and down-hole survey data collected during the drilling programs are sufficient to support Mineral Resource estimation. The sampling intervals are adequate for porphyry style mineralization. Sampling is representative of the grade variations within the deposit.

The QA/QC review completed by the Schaft Creek JV in 2017 and reviewed for this Report demonstrated that the silver analytical results from the 1980s Teck drilling programs are not acceptable to support estimation.

A number of drilling programs have been completed on the Schaft Creek deposit over a long period of time with different sampling protocols and budgetary constraints. Consequently, many samples from the early campaigns were not assayed for gold and silver. Re-sampling programs and re-analytical programs have been completed where possible. Sample intervals with missing gold and silver values have been estimated using a regression curve based on known gold and silver correlation with copper assay data.

QA/QC programs on drilling programs, included blanks, duplicates, and standard reference material sample insertion rates, are within industry-accepted standards to adequately address precision, accuracy, and contamination. The QA/QC programs have not detected any material sample biases.

The data verification completed for this Report concluded that the data supports the geological interpretations and is of sufficient quality to support the Mineral Resource estimation.

25.5 Metallurgical Test Work

A number of metallurgical test work programs were completed on mineralization for the Schaft Creek deposit and were found to be appropriate for porphyry-style copper mineralization.

Samples selected for testing during the early phases of the Project were representative of the various styles of mineralization. These samples were selected mainly from the Liard Zone with the objective of representing the first five years of mining. The majority of the test work selected head grades higher than the expected average grade for the deposit and are informative but not representative for the deposit. Later programs included test work on samples from the Paramount Zone.

The metallurgical test results from previous test programs indicate that the mineralization responded well to the conventional flotation concentration, which are widely used to process the mineralization from porphyry copper deposits. On average, the concentrate produced is expected to contain higher than 28% Cu. The data from G&T and PRA show that on average, at the primary grind size of 80% passing 146 µm, 86.7% of the copper reported to the copper concentrate at a grade of 29.9% Cu. The gold, silver, and molybdenum recoveries to the concentrate were 74.7%, 56.9%, and 73.7%, respectively. The copper, gold, and molybdenum recoveries appear to relate to their respective head grades.

The molybdenum and copper separation from the copper-molybdenum bulk concentrate shows that a separate molybdenum concentrate can be produced. However, the copper content may be higher than the penalty level outlined by most molybdenum smelters. Further tests to reduce copper content by hydrometallurgical treatments should be conducted. The test work also shows that the molybdenum

concentrate contains an elevated rhenium level. It is possible that the rhenium may be recoverable if the smelter chosen to treat the molybdenum is equipped with a rhenium recovery system.

Multi-element assays on the bulk concentrates generated from the locked cycle tests showed that on average, the impurities of the copper concentrates produced from the mineralization should not attract smelting penalties.

The test work indicates that the mineral samples tested are very resistant to SAG and ball mill grinding. More energy efficient comminution circuits should be assessed.

Further test work is required to optimize the process conditions, verify metallurgical performances, and improve comminution circuit energy efficiency.

25.6 Mineral Resource Estimates

The Mineral Resource estimation conforms to industry best practice and is reported using the 2019 CIM Definition Standards.

Re-classification of current Inferred and Indicated resources to a higher confidence resource classification would provide a higher confidence level for the deposit. Expansion of the resource base by drilling interpreted extensions of the mineralization contained within the constraining pit is expected to have a high probability of success.

Factors that could affect the estimates include changes to long-term metal price assumptions; changes in local interpretations of mineralization geometry, fault geometry and continuity of mineralized zones; changes to the net smelter return used to constrain the estimates; changes to the regression equation used to fill in missing gold and silver values; changes to metallurgical recovery assumptions; changes to the input assumptions used to derive the conceptual open pit outlines used to constrain the estimate; variations in geotechnical, hydrogeological, and mining assumptions; and changes to environmental, permitting, and social license assumptions.

25.7 Conclusions

Based on the input parameters and the project data, the Mineral Resources show reasonable prospects of eventual economic extraction. The limits of the mineralization in the Schaft Creek deposit have not been established.

Exploration has located significant zones of porphyry style mineralization along strike of the Schaft Creek deposit. Additional exploration is warranted.

26.0 RECOMMENDATIONS

The updated geological model completed by the Schaft Creek JV and Resource Estimate presented in this Report, have provided several opportunities to advance the Schaft Creek Project. It is recommended that a combined geotechnical and geometallurgical drilling program be completed. The results of this program, which if successful, could have a significant impact on a future mine plan and milling/infrastructure design for the project.

The recommended program is designed to allow many of the proposed drill holes to be utilized for the proposed geotechnical and geometallurgical program and contribute additional geological/ mineralogical data. The location of the proposed drill holes and specific parameters for each program would be established by the Schaft Creek JV.

26.1 Geology

The recommended drilling program would provide additional information that could inform a higher level of confidence in the geological model for the Schaft Creek deposit. The drill program would provide additional data on distribution of copper species, controls on mineralization, alteration patterns, and overall average metal grades in these areas of the Schaft Creek deposit.

26.1.1 Geological and Geotechnical Drilling

The recommended geological drilling is estimated to be 7,300 m. With a unit cost of $620 per m all-included, the total cost is estimated at $4.5 million. These proposed drill holes would increase the quality of the geological model and resource confidence, investigate potential extension to the mineralization, and provide additional information on the mineralogy and metal grades in these areas of the Schaft Creek deposit. As well, these drill holes would be used to collect geotechnical information to investigate opportunities to increase pit slope angles with the objective of reducing the Life of Mine strip ratio.

26.2 Metallurgical Test Work

Tetra Tech recommends further metallurgical test work focused on the four geometallurgical domains within the Schaft Creek deposit to further investigate the geometallurgical variability and throughput assumptions for each geometallurgical domain. The parameters of the test work should be designed to optimize process conditions and update metallurgical performances. The test work should include the following:

- The sample selection for the proposed test work should include consideration for expected average Life of Mine head grades as well as expected average head grades for the first 5-year and 10-year mine plans. The test work should include a range of expected head grades within each geometallurgical domain on either side of the Life of Mine average grade as set out in the Resource Estimate included in this Report.

- Additional metallurgical response evaluations should be conducted to further investigate mineral liberation, copper mineral species, and metallurgical response for each geometallurgical domain to update the process flowsheet. The cost of the test work is estimated to be $200,000.
- Bench scale test work to further investigate the metallurgical performance of samples representing geometallurgical domains and expected mill feeds from each domain in the initial five- and 10-year mill feeds, based on the updated mine plan. The cost of the test work is estimated to be $100,000.
- The test work should focus on obtaining addition information on comminution parameters for each geometallurgical domain to determine if a more energy efficient, higher throughput circuit design is possible. The cost of the test work is estimated to be $100,000.
- Mineralogical investigation from previous test work indicates that rhenium occurs as discrete particles associated with molybdenite. The test work should include further copper-molybdenum separation tests to assess the potential additional value of rhenium in the molybdenum concentrate. The cost of this evaluation is estimated to be $60,000.

27.0 REFERENCES

27.1 General

Tetra Tech Inc. 2013. Copper Fox Metals Inc. Technical Report & Appendices – Feasibility Study Schaft Creek Project, BC, Canada. NI 43-101 Feasibility Study prepared for Copper Fox Metals Inc. January 23, 2013.

27.2 Geology

Ash, C., Macdonald, R.W.J., Stinson, P.K., Fraser, T.M., Read, P.R., Pustka, J.F., Nelson, K.J., Ardan, K.M., Friedman, R.M., and Lefebure, D.V., 1997: Geology and Mineral Occurrences of the Tatogga Lake Area, Northwestern British Columbia (104G/9E & 16SE, 104H/12NW & 13SW): British Columbia Ministry of Energy and Mines, Open File Map 1997-3, scale 1:50,000.

Bailey, L., Heppe, K., Jutras, G., Takaichi, M., Stock, L., Beckman, S., and Hollis, L., 2014: Assessment Report on Drilling, Geological, and Geochemical Work Conducted During 2013 at the Schaft Creek Copper-Molybdenum-Gold Porphyry Project, Liard Mining Division, British Columbia, Canada.

Bailey, L., Takaichi, M., Heppe, K., Jutras, G., Stock, L., and Beckman, S., 2015: Technical Report on Geological Work Conducted During 2014 at the Schaft Creek Copper-Molybdenum-Gold Porphyry Deposit, Liard Mining Division, British Columbia, Canada.

Bailey, L., Jutras, G., Rae, S., Medig, K., Redman, N., Stock, L., Takaichi, M., Heppe, K., Howe, B., and Beckman, S., 2016: Assessment Report on the Schaft Creek Porphyry Copper-Gold-Molybdenum Deposit.

Betmanis, A.I., 1978: Report on the Geology (Including Prospector's Report) of the LaCasse and Schaft Claims, Schaft Creek Property, Liard Mining Division, B.C.: report from Teck Corporation; B.C. Ministry of Energy, Mines and Petroleum Resources, Assessment Report no. 6939, 33 p and 2 maps at 1:5000 scale.

Bradford, J., 2006: 2006 Geological and Geochemical Report on the Schaft Creek North Property, Northwestern British Columbia.: report for Paget Resources Corporation; B.C. Ministry of Energy, Mines, and Petroleum Resources, Assessment Report no. 28848, 12 p.

Brown, D.A., Gunning, M.H., and Greig, C.J., 1996: The Stikine Project: Geology of Western Telegraph Creek Map Area, Northwestern British Columbia: British Columbia Geological Survey, Bulletin 95, 182 p.

Canadian Institute of Mining, Metallurgy and Petroleum (CIM), 2003: Estimation of Mineral Resources and Mineral Reserves, Best Practice Guidelines: Canadian Institute of Mining, Metallurgy and Petroleum, November 23, 2003, http://www.cim.org/committees/estimation2003.pdf.

Canadian Institute of Mining, Metallurgy and Petroleum (CIM), 2014: CIM Standards for Mineral Resources and Mineral Reserves, Definitions and Guidelines: Canadian Institute of Mining, Metallurgy and Petroleum, May 2014.

Canadian Securities Administrators (CSA), 2011: National Instrument 43-101, Standards of Disclosure for Mineral Projects: Canadian Securities Administrators.

Caron, M.E., Carter, G., and McGuigan, P.J., 2012. Progress Report – 2011 Exploration Program for the Schaft Creek Property, Schaft Creek, Northwestern British Columbia. Prepared by Cambria Geosciences Inc. April 2012, 77 pages, July 13, 2010.

Greig, C.J., 2009: 2008 Geochemical Program, Schaft Creek North Property, Liard Mining Division, BC.: report for C.J. Greig and B.J. Kreft; BC Ministry of Energy, Mines, and Petroleum Resources, Assessment Report no. 30682, 59 p.

Halle, S., Dilles, J.H., and Tosdal, R.M., 2015: Footprints: Hydrothermal Alteration and Geochemical Dispersion Around Porphyry Copper Deposits: Society of Economic Geologists, SEG Newsletter, no 100, January 2015.

LeBoutillier, N. G., 2013: The Schaft Creek Project, British Columbia Canada, A Petrographic, Qemscan and Geochemical Study of Selected Diamond Drill Holes: Report for Copper Fox Metals Inc. 886 p.

Morrison, R., and Karrei, L., 2012: Technical Report and Resource Estimate on the Schaft Creek Cu-Au-Mo-Ag Project, BC, Canada: Tetra Tech Wardrop report for Copper Fox Metals Inc, 325 p.

Teck Resources Ltd.2018. Schaft Creek Resource Estimation Report. January 2018

27.3 Metallurgy

Cominco Engineering Services Ltd (CESL), 2007. Schaft Creek Bench Test Report. August 24, 2007

Contract Support Services, 2007. JK Simulation - SABC Circuit - 65,000 dmtpd at P80 100 microns. Apr 04, 2007

Contract Support Services, 2008. JK Simulation - SABC Circuit - 100,000 dmtpd at P80 150 microns. Apr 06, 2008

Contract Support Services, 2010. JK Simulation - SABC Circuit - 120,000 dmtpd at P80 150 microns. Mar 19, 2010

Contract Support Services, 2012. JK Simulation - SABC Circuit – 130000 dmtpd at P80 150 microns. Nov 27, 2012

Contract Support Services, 2012. JK Simulation-SABC Circuit - 120000 dmtpd at P80 150 microns. Jan 13, 2012

G&T Metallurgical Services Ltd, 2008. Advanced Flowsheet Development Studies. Project No. KM2136. Jun 20, 2008

G&T Metallurgical Services Ltd, 2008. Flotation Responses of three Ore Sources. Project No. KM2050. Jan 09, 2008

G&T Metallurgical Services Ltd, 2009. Pilot Plant Testing Schaft Creek Deposits. Project No. KM2292. Nov 24, 2009

G&T Metallurgical Services Ltd, 2010. Advanced Flowsheet Development Studies. Project No. KM2291. Mar 12, 2010

G&T Metallurgical Services Ltd, 2012. Metallurgical Assessment of Schaft Creek Ores. Project No. KM3149. Jan 12, 2012

G&T Metallurgical Services Ltd, 2015. Schaft Creek Comminution Program. Project No. KM3149. Sept 22, 2015

Hazen Research. Inc (Hazen), 2007. Comminution Testing. Project No. 10515. February 15, 2007

HYYPPA Engineering, LLC (HEL), 2007. Schaft Creek Metallurgical Update, incl PRA Reports and Hazen Report. Sep 06, 2007

Polysius Research Centre (Polysius), 2008. High-Pressure Grinding Tests on Copper/Gold/Molybdenum Ore from the Schaft Creek Project. Project No. 2337 3326. October 02, 2008

Process Research Associates Ltd, 2004. Acid Base Accounting Test Report. Project No. 0409111. Dec 14, 2004

Process Research Associates Ltd, 2004. Metallurgical Validation Tests on Selected Drill Hole Core Samples. Project No. 0402903. Aug 25, 2004

Process Research Associates Ltd, 2005. Metallurgical Tests on Selected Drill Core Samples. Project No. 0502002. Oct 21, 2005

Samuel Engineering, Inc., 2008. Preliminary Feasibility Study on the Development of the Schaft Creek Project Located in Northwest British Columbia, Canada. September 15, 2008

Schaft Creek JV Schaft Creek 2015 GeoMet Program - Findings
December 14th, 2015

28.0 CERTIFICATES AND CONSENTS OF QUALIFIED PERSONS

CERTIFICATE OF QUALIFIED PERSON

I, Hassan Ghaffari, M.A.Sc., P.Eng., do hereby certify:

- I am a Director of Metallurgy with Tetra Tech Canada Inc. with a business address at Suite 1000, 10th Floor, 885 Dunsmuir Street, Vancouver, BC, V6C 1N5.
- This certificate applies to the technical report entitled "Copper Fox Metals Inc. Resource Estimate Update for the Schaft Creek Property, British Columbia, Canada", with an effective date of January 15, 2021 (the "Technical Report").
- I am a graduate of the University of Tehran (M.A.Sc., Mining Engineering, 1990) and the University of British Columbia (M.A.Sc., Mineral Process Engineering, 2004).
- I am a member in good standing of the Engineers and Geoscientists British Columbia (#30408).
- My relevant experience includes 30 years of experience in mining and mineral processing plant operation, engineering, project studies and management of various types of mineral processing, including hydrometallurgical mineral processing for porphyry mineral deposits.
- I am a "Qualified Person" for the purposes of National Instrument 43-101 Standards of Disclosure for Mineral Projects (NI 43-101) for those sections of the Technical Report that I am responsible for preparing.
- I conducted a personal inspection of the Schaft Creek property on September 22, 2010 and inspected the overall project site, including site access roads.
- I am responsible for Sections 1.0 (except 1.2 and 1.3), 2.0, 15.0, 16.0, 17.0, 18.0, 19.0, 20.0, 21.0, 22.0, 24.0, 25.1, 25.7, 26.0 (except 26.1 and 26.2) and 27.1 of the Technical Report.
- I am independent of Copper Fox Metals Inc. as Independence is defined by Section 1.5 of NI 43-101.
- I have had involvement with the Schaft Creek property that is the subject of the Technical Report, in acting as a Qualified Person for the "Feasibility Study on the Schaft Creek Project, BC, Canada (the "Technical Report") with an effective date of January 23, 2013.
- I have read NI 43-101 and the sections of the Technical Report that I am responsible for have been prepared in compliance with NI 43-101.
- As of the date of this certificate, to the best of my knowledge, information and belief, the section of the Technical Report that I am responsible for contain all scientific and technical information that is required to be disclosed to make the technical report not misleading.

Signed and dated this 6th day of May, 2021

"signed and stamped"

Hassan Ghaffari, M.A.Sc., P.Eng.
Director of Metallurgy
Tetra Tech Canada Inc.

CERTIFICATE OF QUALIFIED PERSON

I, Jianhui (John) Huang, Ph.D., P.Eng., do hereby certify:

- I am a Senior Metallurgist with Tetra Tech Canada Inc. with a business address at Suite 1000, 10th Floor, 885 Dunsmuir Street, Vancouver, British Columbia, V6C 1N5.
- This certificate applies to the technical report entitled "Mineral Resource Estimate Update for the Schaft Creek Property, British Columbia, Canada", with an effective date of January 15, 2021 (the "Technical Report").
- I am a graduate of North-East University, China (B.Eng., 1982), Beijing General Research Institute for Non-ferrous Metals, China (M.Eng., 1988), and Birmingham University, United Kingdom (Ph.D., 2000).
- I am a member in good standing of the Engineers and Geoscientists British Columbia (#30898).
- My relevant experience includes over 34 years involvement in mineral processing for base metal ores, gold and silver ores, and rare metal ores, and mineral processing plant operation and engineering including hydrometallurgical mineral processing for porphyry mineral deposits.
- I am a "Qualified Person" for purposes of National Instrument 43-101 Standards of Disclosure for Mineral Projects (NI 43-101) for those sections of the Technical Report that I am responsible for preparing.
- I conducted a personal inspection of the Schaft Creek property on August 9, 2010 and reviewed drill cores and overall project site, including the potential processing plant site.
- I am responsible for Sections 1.3, 13.0, 25.5, 26.2, and 27.3 (for matters related to metallurgy and process of the Technical Report).
- I am independent of Copper Fox Metals Inc. as Independence is defined by Section 1.5 of NI 43-101.
- I have had involvement with the Schaft Creek property that is the subject of the Technical Report, in acting as a Qualified Person for the "Feasibility Study on the Schaft Creek Project, BC, Canada" (the "Technical Report") with an effective date of January 23, 2013.
- I have read NI 43-101 and the sections of the Technical Report that I am responsible for have been prepared in compliance with NI 43-101.
- As of the date of this certificate, to the best of my knowledge, information and belief, the section of the Technical Report that I am responsible for contain all scientific and technical information that is required to be disclosed to make the technical report not misleading.

Signed and dated this 6th day of May, 2021

"signed and stamped"

Jianhui (John) Huang, Ph.D., P.Eng.
Senior Metallurgist
Tetra Tech Canada Inc.

CERTIFICATE OF QUALIFIED PERSON

I, Michael F. O'Brien, P.Geo., do hereby certify:

- I am an independent consultant and director of Red Pennant Communications Corp. a British Columbia Corporation, with a business address at 81-1380 Pinetree Way, Coquitlam, BC, V3E 3S6.
- This certificate applies to the technical report entitled "Mineral Resource Estimate Update for the Schaft Creek Property, British Columbia, Canada", with an effective date of January 15, 2021 (the "Technical Report").
- I am a graduate of the University of Natal, (B.Sc. Hons. Geology, 1978) and the University of the Witwatersrand (M.Sc. Engineering, 2002).
- I am a member in good standing of Engineers and Geoscientists British Columbia (#41338).
- I am a member in good standing of the South African Council for Natural Scientific Professions (South Africa, 400295/87). My relevant experience is 36 years of experience in operations, mineral project assessment and I have the experience relevant to Mineral Resource estimation of metal deposits. I have estimated Mineral Resources for greenstone-hosted gold, diatreme complex epithermal gold deposits, porphyry copper-gold, volcanogenic massive sulphide deposits and shear zone-hosted deposits. I am a "Qualified Person" for the purposes of National Instrument 43-101 (the "Instrument").
- My recent personal inspection of the Property was on October 30, 2020 and reviewed drill cores and the general layout of the camp and topography.
- I am responsible for Sections 1.2, 3.0, 4.0, 5.0, 6.0, 7.0, 8.0, 9.0, 10.0, 11.0, 12.0, 14.0, 23.0, 25.2, 25.3, 25.4, 25.6, 26.1, and 27.2 (for matters related to geology and resource estimate of the Technical Report).
- I am independent of Copper Fox Metals Inc. as Independence is defined by Section 1.5 of NI 43-101.
- I have read NI 43-101 and the sections of the Technical Report that I am responsible for have been prepared in compliance with NI 43-101.
- As of the date of this certificate, to the best of my knowledge, information and belief, the section of the Technical Report that I am responsible for contain all scientific and technical information that is required to be disclosed to make the technical report not misleading.

Signed and dated this 6th day of May, 2021

"signed and stamped"

Michael F. O'Brien, P.Geo.
Owner
Red Pennant Geoscience Ltd.

CONSENT OF QUALIFIED PERSONS

I, **Hassan Ghaffari, M.A.Sc., P.Eng.,** consent to the public filing of the technical report titled "**RESOURCE ESTIMATE UPDATE FOR THE SCHAFT CREEK PROPERTY, BRITISH COLUMBIA, CANADA**" with the effective date of January 15, 2021 by Copper Fox Metals Inc. I certify that I have read the News Release dated March 22, 2021 filed by Copper Fox Metals Inc. and any other News Releases relating to the report that fairly and accurately represents the information in the Sections of the Technical Report for which I am responsible.

Dated this 6th day of May 2021

"Signed and Sealed"

Hassan Ghaffari, M.A.Sc., P.Eng.
B.C. Registration No. 30408

I, **Jianhui (John) Huang, Ph.D., P.Eng.**, consent to the public filing of the technical report titled "**RESOURCE ESTIMATE UPDATE FOR THE SCHAFT CREEK PROPERTY, BRITISH COLUMBIA, CANADA**" with the effective date of January 15, 2021 by Copper Fox Metals Inc. I certify that I have read the News Release dated March 22, 2021 filed by Copper Fox Metals Inc. and any other News Releases relating to the report that fairly and accurately represents the information in the Sections of the Technical Report for which I am responsible.

Dated this 6th day of May 2021

"Signed and Sealed"

Jianhui (John) Huang, Ph.D., P.Eng.
B.C. Registration No. 30898

I, **Michael F. O'Brien, P.Geo.**, consent to the public filing of the technical report titled "**RESOURCE ESTIMATE UPDATE FOR THE SCHAFT CREEK PROPERTY, BRITISH COLUMBIA, CANADA**" with the effective date of January 15, 2021 by Copper Fox Metals Inc. I certify that I have read the News Release dated March 22, 2021 filed by Copper Fox Metals Inc. and any other News Releases relating to the report that fairly and accurately represents the information in the Sections of the Technical Report for which I am responsible.

Dated this 6th day of May 2021

"Signed and Sealed"

Michael F. O'Brien, P.Geo.
B.C. Registration No. 41338